Exploring the role of TRIM27 and TRIM32 in autophagy

Juncal García García

A dissertation of the degree of Philosophiae Doctor

UiT- The Arctic University of Norway

Faculty of Health Science

Department of Medical Biology

Molecular Cancer Research Group

February 2021

Table of Contents

Summary

Tripartite motif family proteins (TRIMs) are a wide family of E3 ligases involved in the control of several cellular processes such as intracellular signaling, innate immunity, transcription, cell cycle regulation and carcinogenesis. In recent years, some members of this family have been found to have a role in autophagy.

The central theme of this thesis is the role of two TRIM proteins in selective autophagy. I joined this project born from a screen of 22 different TRIM proteins using the double-tag assay, which represented the 11 TRIM family subgroups. The goal of this screen was to identify candidates with a potential role in autophagy, alleging that their presence in the lysosome linked them somehow with the autophagy process. From our screen, TRIM27 and TRIM32 were identified as new potential autophagic substrates, and we decided to further investigate their role in autophagy.

We found that TRIM27 has an effect in starvation-induced autophagy and associates with core autophagy proteins and the autophagy receptors p62/SQSTM1 and NBR1. Furthermore, TRIM27 interacts directly with and ubiquitylates p62/SQSTM1. We established TRIM27 KO cells, which showed high expression levels of the lysosomal protein LAMP2 and formation of big LAMP2 rings in the cytosol.. TRIM27 is proposed to act as an oncogene. In line with this, we identify TRIM27 mRNA levels to be strongly upregulated in cancer tissue from breast cancer patients. Intriguingly, we found the protein level of TRIM27 in various breast cancer cell lines to be inversely correlated with LAMP2 and LC3B expression. This suggests a potential role of TRIM27 in autophagy in certain types of breast cancer.

We also examined the autophagic role of TRIM32, including two mutant variants of TRIM32 that are associated with Limb-Girdle-Muscular-Dystrophy 2H (LGMD2H) or Bardet-Biedl-Syndrome 11 (BBS11), respectively. First, we found that TRIM32 is directed to autophagic degradation by p62/SQSTM1, but also act as a regulator of p62/SQSTM1 autophagic activity. This formed a feedback loop that was controlled by the direct interaction and ubiquitylation of p62/SQSTM1 by TRIM32. Interestingly, the TRIM32 mutant implicated in the muscular dystrophy disease LGMD2H failed to ubiquitylate p62/SQSTM1. Next, we further studied the role of TRIM32 towards the other proteins in the SLRfamily of autophagy receptors. We found that TRIM32 interacts and ubiquitylates the autophagy receptor NDP52, stabilizes the phosphorylated form of the autophagy regulator TBK1 and facilitates mitophagy. Lastly, we studied how TRIM32 auto-ubiquitylation regulates its activity and stability. We found that TRIM32 contains a PEST sequence, which exposure seems to be regulated by ubiquitylation and acetylation. This was a novel finding since to date, no PEST sequence has been identified in TRIM proteins. Taken together, these findings highlight the pivotal role of TRIM27 and TRIM32 as regulators of selective autophagy.

“En resumen: toda obra grande es el fruto de la paciencia y de la perseverancia, combinadas con una atención orientada tenazmente durante meses y aun años hacia un objeto particular.”

“In summary, all great work is the fruit of patience and perseverance, combined with tenacious concentration on a subject over a period of months or years.”

Reglas y consejos sobre investigación científica,1899

Santiago Ramón y Cajal

Acknowledgments

Throughout these 4 years of PhD and the writing of this dissertation, I have received a great deal of support and assistance.

I wish to show my immense gratitude to my supervisor, Eva Sjøttem. As I always say, she has been my guardian angel in this journey, and I could not have asked for a better supervisor. She has always been there for me, helped me grow at both a professional and personal level, and encouraged me when my motivation was running low. She is also one of the most inspiring women I know.

I would also like to thank my co-supervisors Trond Lamark and Terje Johansen. Thank you for the hospitality, constant input and ideas. I came to Tromsø without any knowledge on autophagy, and I have learned so much from you both. Thank you, Trond, for reading and giving input in the writing of this work.

I am deeply indebted to Pradip Bhujabal and Katrine Overå, with whom I have worked hand in hand in this project, and have helped so much. Special thanks to Jack Bruun, who helped me carry out the difficult task of understanding Mass Spectrometry results.

I wish to express my gratitude to all the lab members of the MCRG. In particular, to Hanne Brenne, who has been a big help and support during this project, and who shares my love for running and a good Ponceau staining. Thank you to Gry Evjen, who has always given me a hand when I needed it, especially when trying to improve my Norwegian skills. I would like to thank Mireia Nager, whom I have learned so much, not only in the lab, but who also gave me a different way to see the world (Gràcies per tot Mireia). Many thanks to Nikoline Rasmussen, her patience and quiet temperament make of her a great colleague and fantastic friend. Thanks also to Anthimi Palara, who always has a smile and made sure our office was filled with the Christmas spirit every single year. Thank you as well to Thanasis Kournoutis, who has been the last to come but brings such joy to the lab. Many thanks to the rest of the lab members who have contributed to make me feel at home and comfortable in my workplace.

I would also thank my friend Álvaro Martinez, who deserves an award for the most patient person in the world, and who has accompanied me since the first day of this journey. His support through memes has been priceless. Special thanks to Nathalie Krauth and Maria Perez, who came to visit me in Tromsø, and have shown me their support in this project. Many thanks to my friend Linda Field, who has supported me in this journey all the way from California.

I also wish to thank my family, my parents and my two siblings Blanca and Pablo. I could not have completed this project without their support and love. Special thanks to my mother, who has kept herself close and supportive, even in the distance. I would also like to thank my cousin Andrea, who obtained her PhD before me and who has always been a source of inspiration and support. I would also like to thank my grandmother Balbina, who has always encouraged me to get a higher education. I would also like to thank all my extended family for their support during these 4 years.

Finally yet importantly, and even though he did not want to be in this section, I would like to thank Christian Andreassen for his patience, love and encouragement. I met him halfway on this journey and he has been a great support.

List of papers

Paper I

TRIM27 is an autophagy substrate implicated in autophagy induction and regulation of LAMP2

Garcia, J.G., Overå, K.S., Knutsen, E., Bhujabal, Z., Evjen, G., Lamark, T., Johansen, T., Sjøttem, E.

Manuscript

Paper II

TRIM32, but not its muscular dystrophy-associated mutant, positively regulates and is targeted to autophagic degradation by p62/SQSTM1.

Overå, K.S., Garcia, J.G., Bhujabal, Z., Jain, A., Øvervatn, A., Larsen, K.B., Deretic, V., Johansen, T., Lamark, T., and Sjøttem, E. (2019).

J. Cell Science. PMID 31828304.

Paper III

TRIM32 – a putative regulator of NDP52 mediated selective autophagy

Garcia, J.G., Bhujabal, Z., Overå, K.S., Sjøttem, E.

Manuscript

Paper IV

Generation of the short TRIM32 isoform is regulated by Lys 247 acetylation and a PEST sequence

Garcia-Garcia J., Overå, K.S., Khan, W., Sjøttem, E.

PLOS One. In revision.

Abbreviations

Abi2	Abl interactor 2
Ago2	Protein argonaute 2
ALS	Amyotrophic lateral sclerosis
AKT	AKT8 virus oncogene cellular homolog
AMBRA1	Activating molecule in BECN1-regulated autophagy protein 1
AMPK	AMP-activated protein kinase
ATG	Autophagy related
ATP	Adenosine triphosphate
BBS11	Bardet Biedl syndrome 11
BNIP3	BCL2 and adenovirus E1B 19 kDa-interacting protein 3
BRAF	V-raf murine sarcoma viral oncogene homolog B1
CCCP	Carbonyl cyanide m-chlorophenylhydrazone
CMA	Chaperone- mediated autophagy
CC	Coiled-Coil
EGFR	Epidermal Growth Factor Receptor
EMT	Epithelial-to-mesenchymal transition
ER	Endoplasmic reticulum
FGFR1	Ectopic type 1 FGF receptor
FIP200	Focal adhesion kinase family interaction protein of 200 kDa
FKBP8	FK506-bidning protein 8
FUNDC1	FUN14 domain-containing protein 1
GABARAP	aminobutyric acid receptor-associated protein
Gal8	Galectin8
GLUT1	Glucose transporter 1
HP	Hydrophobic pocket
Hsc70	Heat shock-cognate protein of 70 kDa
IDP	Intrinsically disordered proteins
IDR	Intrinsically disordered regions
IFN	Interferon
IRF3	Interferon regulatory factor 3
KEAP1	Kelch-like ECH-associated protein 1
KIR	KEAP1 interacting region

LAMP2	Lysosomal-associated membrane-2 protein
LDS	LIR docking site
LGMD2H	Limb girdle muscular dystrophy 2H
LIR	LC3 interacting region
LMP	Lysosomal membrane protein
MAGE-L2	Melanoma antigen L2
MAVS	Mitochondrial antiviral signaling protein
mTOR	Mammalian target of rapamycin
Mtb	*Mycobacterium tuberculosis*
MYC	Myelocytomatosis oncogene cellular homolog
NAP1	Nucleosome assembly protein 1
NBR1	Neighbor of BRCA1 gene 1
NDP52	Nuclear dot protein-52
NDRG2	Myc-repressed gene N-myc downstream-regulated gene 2
NES	Nuclear export signal
NFκB	NFκB Nuclear factor kappa light chain enhancer of activated B cells
NLS	Nuclear localization signal
NOD2	Nucleotide-binding oligomerization domain-containing protein 2
NRF2	NF-E2-related factor 2
OMM	Mitochondrial outer membrane
OPTN	Optineurin
PB1	Phox and Bem1
PDCD10	Programmed cell death protein 10
PE	Phosphatidylethanolamine
PHD	Plant homeodomain
PI3K	Phosphatidylinositol 3-kinase
PI3P	Phosphatidylinositol 3-phosphate
PIASy	Protein inhibitor of activated STATy
PINK1	PTEN-induced kinase 1
PML	Promyelocytic leukemia
PTEN	Phosphatase and Tensin Homolog deleted on Chromosome 10
PTM	Post-translational modification
RARα	Retinoic acid receptor alpha

RB1	Retinoblastoma protein 1
RING	Really interesting new gene
ROS	Reactive Oxigen Species
SAR	Selective autophagy receptors
SINTBAD	Similar to NAP1 TBK1 Adaptor
SKICH	SKIP carboxyl homology
SLR	Sequestosome-1-like receptors
SNARE	Soluble n-ethylmaleimide-sensitive factor-attachment protein receptors
SQSTM1	Sequestosome-1
STAT3	Signal transducer and activator of transcription 3
STING	Stimulator of IFN genes
SUMO	Small ubiquitin-like modifier
TAK	TGF β-activated kinase
TAX1BP1	Human T-cell leukemia virus type 1 binding protein 1
TBK1	TANK-binding kinase 1
TLR	Toll like receptor
TNFα	Tumor necrosis factor α
TRIF	TIR domain-containing adaptor molecule 1
TRIM	Tripartite motif
UBA	Ubiquitin-associated domain
UBZ	Ubiquitin binding zinc finger
UDS	UIM docking site
UIM	Ubiquitin-interacting motif
ULK1	Unc-51-like kinase 1
UPS	Ubiquitin proteasome system
USP	Ubiquitin carboxyl-terminal hydrolase
VPS34	Vacular protein sorting 32
WIPI	WD-repeat protein interacting with phosphoinositides
ZZ	ZZ-type zinc finger domain

Introduction

Planet earth can be a hostile place, where organisms of all sorts are in a constant fight for survival. Evolution has provided cells the ability to improve the quality of those survival mechanisms, arriving to very high complex networks that work coordinately to try to ensure the continuity of the species. At a cellular level, eukaryote cells have developed a high degree of complexity in order to maintain homeostasis.

Introduction to the Ubiquitin/Proteasome (UPS) system

Synthesis and clearance of functional proteins regulate their availability within the cell, adapting the protein pool to the cellular needs. Thus, protein degradation is a crucial element in the maintenance of cellular homeostasis. In addition to the level, also the functionality of cellular proteins are continuously checked. For this purpose, the cell has several mechanism that work together to ensure the quality and functionality of the synthetized proteins. The protein quality control system of the cell monitors the complete life cycle of a protein at the different steps of its synthesis, acting as a surveillance mechanism (Pohl and Dikic 2019). From the very first stages of protein translation, there are cellular components in charge of controlling the quality of mRNA and their nascent protein products, so in case of mistakes they do not continue further of the synthesis chain (Dikic 2017). Furthermore, chaperons help on the protein folding process, as well as detecting misfolded proteins and send them for degradations if the efforts for correct folding fails (Saibil 2013). The cell is in constant battle in order to maintain its homeostasis, which leads to a constant control of protein concentration, as well as remodeling, repair or elimination of those proteins that became damaged. If the cell is not able to degrade those proteins at a certain moment, they can also be sequestered in special compartments until the cell is able to proceed to their degradation (Sontag, Samant, and Frydman 2017) . Such a crucial process for the cell's well-being is tightly regulated in a spatially and timely manner through two main systems: the ubiquitin-proteasome system (UPS) and the lysosomal-mediated proteolysis (hereafter autophagy) (Figure 1). Around 80-90% of proteins are degraded through the UPS system whereas the remaining 10-20% are degraded by the lysosomal-mediated proteolysis. In general, small short-lived proteins are the main substrates for the proteasome, while long-lived proteins and bigger structures such as protein aggregates or whole organelles are mainly degraded by autophagy (Kleiger and Mayor 2014; Ding et al.

2014). However, these two systems are highly interconnected, thus, different degradation patterns can be observed depending on the cellular conditions.

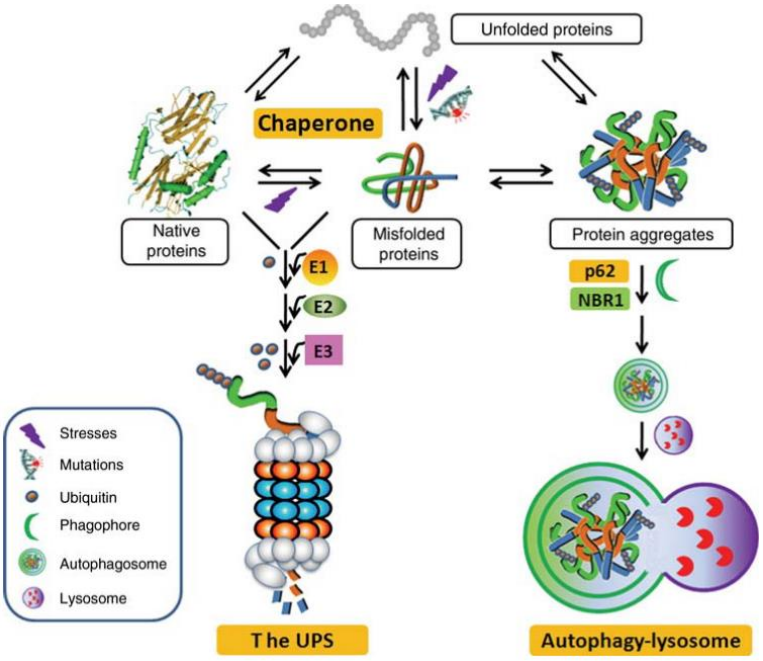

Figure 1. Protein quality control of eukaryotic cells. Chaperones facilitate the folding of nascent polypeptides and refolding of misfolded proteins. The UPS degrades both misfolded/damaged proteins and excess native proteins in the cell. The autophagy-lysosomal pathway removes protein aggregates formed by the misfolded proteins that have escaped from the surveillance of chaperones and the UPS. (X. Wang and Su 2010)

The ubiquitin-proteasome system consists in a well-defined network of components which act together to tag proteins for degradation. The main tag is a 76 amino acid globular protein called ubiquitin (Yu and Matouschek 2017). Targeted proteins are conjugated to ubiquitin by the mediation of three sequential reactions (Figure 2). The first reaction is the activation of ubiquitin by E1 enzymes, which is the only step of the process that requires ATP. The second members of the cascade are E2 enzymes, which conjugate ubiquitin for its delivery to the next step. The third and last reaction is mediated by E3 ligases that make possible the binding of the activated ubiquitin to the target molecule (Oh, Akopian, and Rape 2018). According to current knowledge, in the human genome there are two E1 enzymes genes, 40 E2 genes and around 600 E3 ligase genes (Celebi et al. 2020) . Thus, while E1 and E2 enzymes are highly conserved and in most cases do not present much specificity, whereas E3 ligases are in charge of recognizing the substrate, which makes them the main regulator of ubiquitylation.

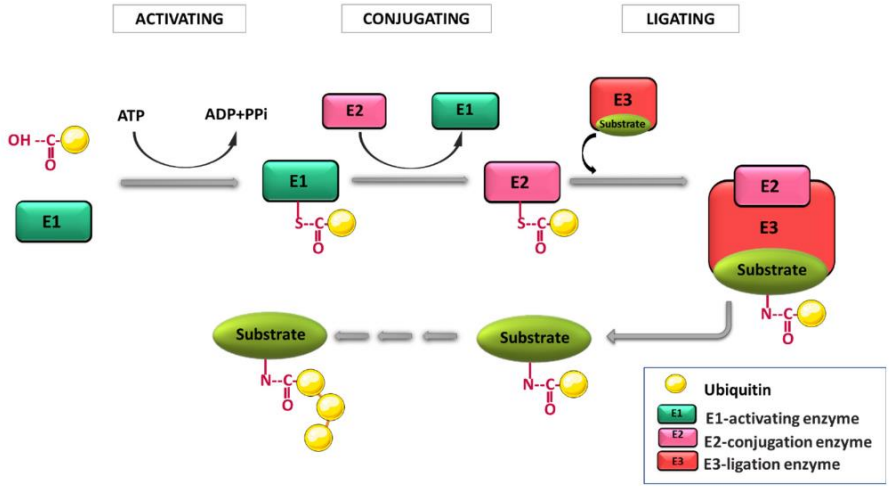

Figure 2. Enzymatic reaction of ubiquitylation. For activation of the ubiquitylation process, E1 enzyme makes a thioester bond with the ubiquitin molecule, and the required energy is supplied by the hydrolysis of ATP. In the conjugation step, the ubiquitin on the E1 enzyme is transferred to the E2 enzyme. Finally, the substrate–E3 enzyme bond is involved, and the C-terminal of the ubiquitin molecule makes a covalent bond with the substrate. (Celebi et al. 2020)

Ubiquitylation consists in the covalent binding of an ubiquitin molecule to a protein. The most common type of ubiquitylation is called canonical ubiquitylation and is defined by the formation of an isopetide bond between a lysine residue of the target protein and the C-terminal glycine 76 of an ubiquitin molecule (mono- ubiquitylation) (Kleiger and Mayor 2014). Other molecules of ubiquitin can then be attached to that mono-ubiquitin in eight potential sites: M1, K6, K11, K27, K29, K33, K48 and K63, which originate different linkages of polyubiquitin chains (poly- ubiquitylation). In addition, there may exist branched linkage types (Dikic 2017), and other ubiquitin-like proteins may also be conjugated to ubiquitin, such is the case of SUMO or NEDD8 molecules (Swatek and Komander 2016). Overall, this provides a wide range of combinations referred as “ubiquitin code” that is essential in directing the cellular fate of the ubiquitylated protein. Ubiquitin as a post-translational modification (PTM) that plays a role in many cellular processes such as DNA repair response, cell cycle regulation, autophagy, cellular differentiation and cell-mediated immunity (Yu and Matouschek 2017; Kwon and Ciechanover 2017).

The established ubiquitin modification shown to label proteins for degradation by the UPS is the addition of K48-linked chains. Ubiquitylated proteins tagged for degradation by the UPS are transported to the 26S proteasome, more commonly called “the proteasome” (Figure 3). The 26S proteasome is a barrel-shaped proteolytic organelle formed by the 20S central catalytic complex and two 19S complexes that function as a lid (Bard et al. 2018). The degradation and recycling of proteins occurs in the 20S central subunit, whereas the 19S

complexes regulate the binding to cargo-loaded shuttling proteins, deubiquitylate the substrates and channel them into the inner core of the proteasome (Budenholzer et al. 2017).

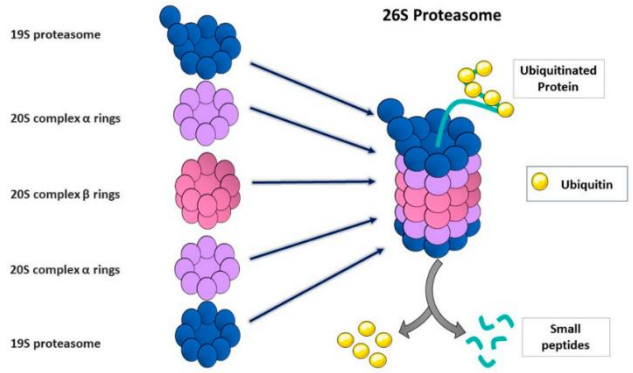

Figure 3. Structure of proteasome and degradation of ubiquitylated substrates. The 26S proteasome has a multicomplex structure that is composed of a 19S regulatory units and a 20S catalytic core unit. In the 19S regulatory complex, the ubiquitinated proteins are unfolded, and ubiquitin tags are separated from the protein by deubiquitinase enzymes. Consequently, the unfolded polypeptide chain is delivered to the 20S catalytic core complex where they are degraded into small peptides. (Celebi et al. 2020)

Ubiquitylation: A full world beyond protein degradation

In the beginning, ubiquitin was identified merely as a tag for degradation, however in the last decades evidences have shown that ubiquitin has other important roles beyond tagging a protein for degradation in the proteasome. Ubiquitylation is a reversible modification that shows a high level of specificity, this makes the ubiquitin-dependent signaling very rapid and dynamic (Jia Liu et al. 2015). Therefore, it is not surprising that ubiquitylation as a signaling mechanism is involved in numerous cellular processes that require a quick switch. Among those processes can be found chromatin architecture, gene-specific transcription, DNA repair, protein quality control at the translational level, protein transport, control of signal transduction and cellular defense against pathogens (Oh, Akopian, and Rape 2018).

Histones can be modified by the addition of one or more molecules of ubiquitin. Depending on the type of linkage, the outcome can lead to different consequences in controlling gene expression, DNA methylation or DNA repair (Meas and Mao 2015). Interestingly, de-ubiquitinases (DUBs) work doing the opposite roles of E3 ligases, removing ubiquitin from previously ubiquitylated proteins (Wilkinson 2009). At first, it was thought that the only role of the dynamic between E3 ligases and DUBs was merely counteract each other's actions. However, it has been shown that these two enzymes acting in direct opposition can generate a more complex signaling output. An example of this mechanism has been shown during the

process of mitophagy (autophagy of mitochondria), when an activation of the E3 ligase PARKIN and an inhibition of the counteracting USP30 take place simultaneously. This leads to a rapid tagging of defective mitochondria with a dense ubiquitin signal that will lead to its prompt degradation. (Cunningham et al. 2015) Therefore, it is not uncommon to find E3 ligases and DUBs forming part of the same complexes, which highlights the importance of reversibility in ubiquitin signaling (Harrigan et al. 2018).

Ubiquitin signaling is also able to act as a quality control at the translational level. E3 ligases are present next to the ribosomes to ensure the quality of the proteins being synthesized (Grumati and Dikic 2018). There are proteins that are attached to ribosomes such as E3 listerin, which binds stalled ribosomes (Shao, Von der Malsburg, and Hegde 2013). In addition, there are E3 ligases that cooperate with chaperones that detect misfolded or mislocalized proteins, or by the binding of an E3 ligase to a degron (degenerated motif of a misfolded polypeptide) (Davey and Morgan 2016). All these mechanism will lead the low quality proteins to degradation before they accumulate and disturb the homeostasis of the cell. Once the proteins are correctly synthesized, ubiquitin-signaling also contributes to control their transport and delivery to their programmed destination. Ubiquitylation is a modification that can show high spatial precision, which can impose directionality onto signaling cascades. A good example of the effect of ubiquitylation in protein trafficking is the internalization of EGFR for its inactivation (Levkowitz et al. 1998). Ubiquitin has also a crucial role in the defense of the cell against pathogens. Both bacteria and viruses have developed mechanism to highjack the ubiquitylation system in order to not be detected and proceed to infection (Zong et al. 2021).

Autophagy: The phagophore's turn

The term and idea of autophagy came to life by a Belgium scientist called Christian de Duve, who firstly described lysosomes as a new cellular organelle, and later on the degradation of cytoplasmic material in these lytic compartments. He defined this process as autophagy, which means self-eating in Greek (Ohsumi 2014). However, the lack of methodology to continue the research in the role of autophagy and its mechanistic lead to a delay in the field. In the late 1990, many new methods in molecular biology made possible to decipher the insights of this degradation pathway. In the last 20 years, there has been an outbreak of discoveries and knowledge surrounding autophagy. Starting with the discovery of the autophagy related proteins by Yoshinori Ohsimi, which lead him to a Nobel Prize in Medicine in 2016, to the

description of the LC3-interactiong region (LIR) motif and autophagy receptors (Kirkin 2020; Zimmermann et al. 2016; Johansen and Lamark 2020). All these achievements have allowed us to understand better, how the cell maintains its homeostasis through a very complex equilibrium between synthesis and degradation.

Even though the concept of autophagy is simple, cytoplasmic material delivered to the lysosomes for its degradation, the way and reasons why that cytoplasmic material ends up in the lytic compartment is much more complex and still to date not fully understood. There are three described types of autophagy: microautophagy, chaperon-mediated autophagy (CMA), and macroautophagy (Figure 4).

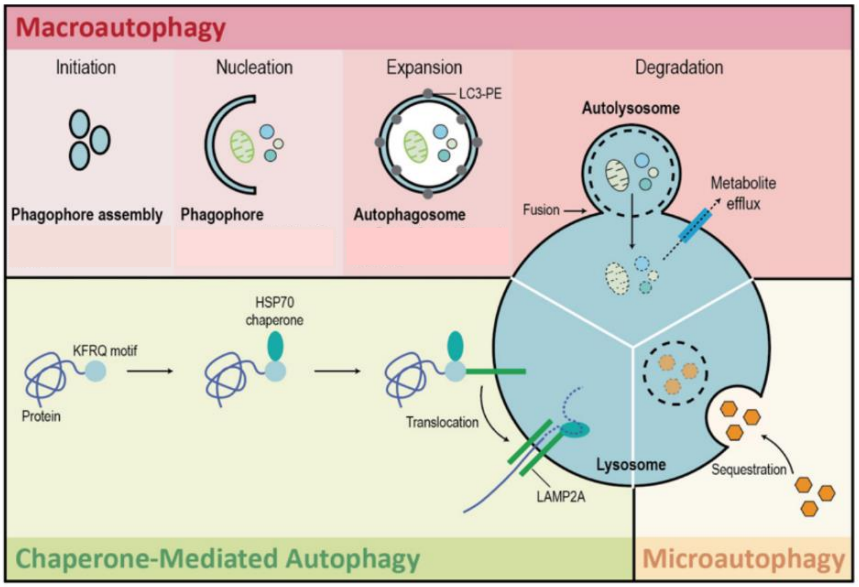

Figure 4. Types of autophagy. There are three types of autophagy: macroautophagy, microautophagy, and chaperone-mediated autophagy. Macroautophagy is a type of autophagy that delivers cellular contents to the lysosome via the formation of double-membrane structures called autophagosomes, which then fuse with lysosomes. Microautophagy facilitates the direct uptake and breakdown of cytosolic cargo by lysosomes. Chaperone-mediated autophagy refers to the chaperone-dependent targeting of specific cytosolic proteins to lysosomes for proteolysis. (Ho et al. 2019)

Microautophagy is defined by the sequestration of cytoplasmic material directly into the lysosome or endosomes through an invagination of the membrane that eventually pitches off into the lumen (Li, Li, and Bao 2012; Mejlvang et al. 2018). During CMA, which only happens in mammals, proteins that expose a pentapeptide signature motif (KFERQ) are recognized by heat shock 70 kDa protein 8 (HSPA8/HSC70), which in turn binds to the lysosomal-associated membrane protein LAMP 2A (LAMP2A) that translocates the protein directly into the lysosome (Kaushik and Cuervo 2018). By definition, CMA is a selective mechanism, and microautophagy can also be defined as selective until a certain extent, since it seems that the

cell selects which proteins are going to be delivered to the lysosome. The best-characterized autophagy pathway is macroautophagy, which is commonly called autophagy. The main feature of this form of autophagy is the engulfment of cellular material by a double-membrane structure called phagophore. The phagophore then is transported through microtubules and eventually fused with lysosomes, which will degrade the delivered substrates through the action of lysosomal hydrolases. This process can be non-selective, the so-called bulk-autophagy, or selective, which is called selective autophagy. At first, it was thought that macroautophagy was merely a response for nutrient depravation, which leaded to the degradation of any cellular material accessible in the cell in order to provide molecular building blocks while no nutrients were available. However, growing evidences show that not only this form of autophagy can be highly selective, but that there are many stimuli that can activate this cellular mechanism (L Galluzzi et al. 2017).

The main steps of the autophagic pathways are initiation, nucleation of the phagophore, membrane expansion/elongation, maturation and fusion (Figure 5). The proteins involved in the regulation of autophagy are called ATG proteins (autophagy-related genes). Despite the fact that there are more than 40 of those ATG proteins, which all play a role in autophagy, there are 17 conserved ATG proteins that are essential and sufficient to make the autophagic process possible. This subset of essential ATG is called the "core autophagy machinery". These ATG proteins are recruited to the site of autophagosome formation and act in a sequential manner in order to fully form a closed autophagosome that will eventually fuse with a lysosome for the degradation of its content (Melia, Lystad, and Simonsen 2020). The ATG proteins were firstly described in yeast. However, autophagy seems to be a conserved mechanism among eukaryotes, therefore, many ATG present in yeast have their counterparts in mammals (Reggiori and Klionsky 2013). As expected, a higher degree of complexity is added to higher eukaryotes, adding new regulators and mediators to this process.

The autophagy process starts at the Endoplasmatic Reticumul (ER) by the unbedding of a cup shaped-membrane leading to the formation of a pre-autophagosome or omegasome (Hurley and Young 2017). Under normal conditions, autophagy is mainly controlled by nutrient availability and the metabolic needs of the cell. The status of threonine-serine kinase ULK1 is the main determinant of autophagy activation, due to its position as the most upstream kinase within the autophagy core machinery. The two main regulators of this kinase are AMP-activated protein kinase (AMPK) and mTORC1, which directly phosphorylate ULK1. On one side, AMPK activity positively regulates autophagy, whereas mTORC1 inhibits autophagy under

nutrient-rich conditions (Alers et al. 2012). Starvation and rapamycin treatment are sufficient to activate autophagy via mTORC1, which has been reported to have a regulatory role not only in initiation of autophagy but also in nucleation, elongation and fusion of autophagosome to lysosomes (Dossou and Basu 2019). Starvation induced autophagy is initiated by the activation of ULK1 via mTORC1 inhibition, which leads to the phosphorylation of ULK1. The ULK1 complex formed by ULK1/2, ATG13, FIP200 and ATG101 is rapidly recruited to this developing membrane. Next, the class III lipid kinase complex I formed VPS34, VPS15, ATG14 and Beclin 1, is recruited. Beclin 1 is then phosphorylated by ULK1, which leads to Beclin 1 transforming phosphoatidylinositol-2-phosphate into phosphatidylinositol-3-phosphatase (PtdIns3P) (Russell et al. 2013). The increasing of the levels of PtdIns3P in the pre-autophagosome leads to the recruitment of WD-repeat protein interacting with phosphoinositides (WIPI) proteins. There are four members of this family (from WIPI1 to WIPI4), which act as a bridge between PdIns3P production and ATG8 proteins lipidation (Proikas-Cezanne et al. 2015). The ATG8 family in mammals consists of at least 6 proteins (LC3A, B, and C, GABARAP, GABARAP-L1 and L2), all of which hereafter referred as ATG8 proteins. Pro-LC3 is the LC3 fresh form coming from translation, which is cleaved by ATG4 and deacetylated by SIRT proteins, forming LC3-I. Then WIPI2 recruits the ATG12-ATG5-ATG16L complex, which catalyzes the conjugation of LC3-II into the expanding autophagy membrane. The lipidation of LC3 molecules and elongation of the membrane leads to the closure of the autophagosome, which then becomes a mature autophagosome. This autophagosome can either fuse with late endosomes to form amphisomes, which later fuse with lyososmes, or directly fuse with a lysosome. The fusion product of an autophahosome and a lysosome is called autolysosome. The supply of lipids to form this autophagosome is mediated by ATG9, through ATG9 vesicles, which come from membrane reservoirs like Golgi apparatus (Matoba et al. 2020; Gómez-Sánchez et al. 2018). This autophagosome will be transported via microtube tracks towards the lysosomes, which are commonly found in the perinuclear region of the cell (Johnson et al. 2016). This transport is possible thank to small GTPase Rab7, which links autophagosome to microtubule motors through FYVE and coiled-coil domain containing 1 (FYCO1) (Pankiv, Alemu, et al. 2010). There are other proteins involved in the transport of autophagosome along the microtubules, however, their mechanism is still poorly understood. Once in close proximity, the autophagosomes fuse with a lysosome via a Rab GTPases, which localize in specific membranes and recruit tethering complexes that act as bridges to bring the autophagosome and lysosomes together. On the other side, these tethering complexes help membrane-tethering complexes and soluble N-ethylmaleimide-sensitive factor attachment

protein receptors, commonly known as SNAREs proteins, to physically drive the fusion of opposing lipid bilayers (Nair and Klionsky 2011). Once the fusion has taken place, the cargo delivered to the lysosome will be degraded (Nakamura and Yoshimori 2017). Despite the exact mechanism of which autophagosome formation and who contributes to this process is not fully understood, it is becoming clear that all intracellular compartment contribute in different degrees.

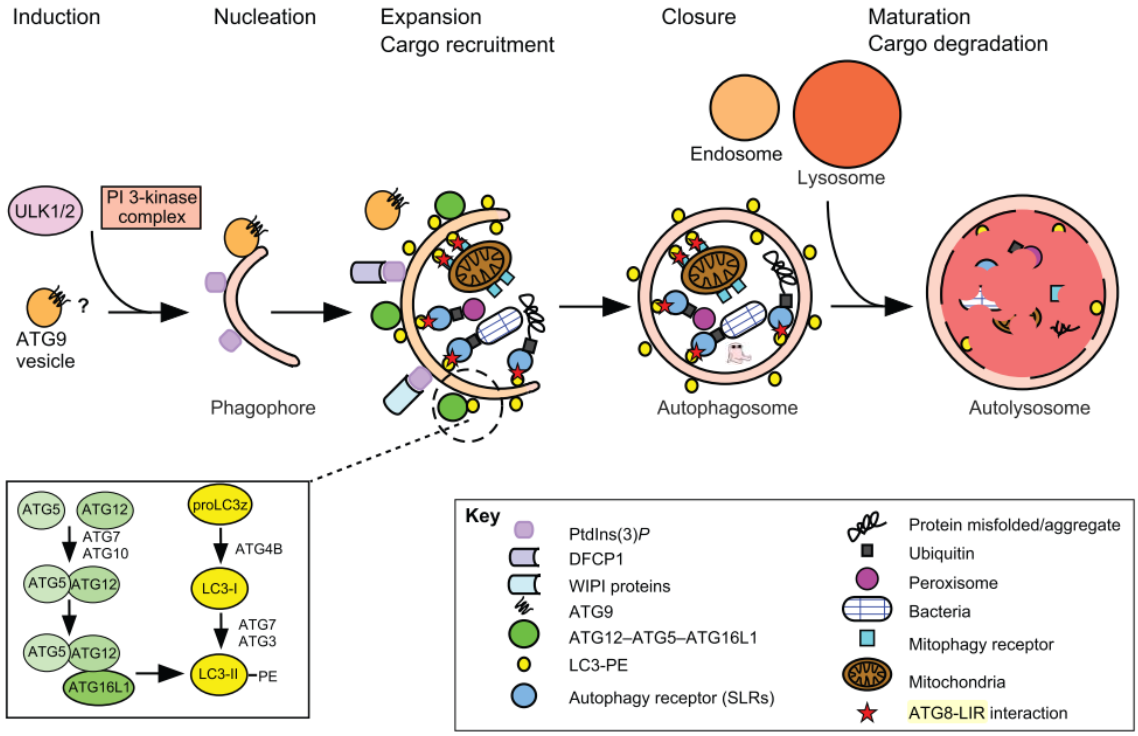

Figure 5. Overview of selective autophagy in mammalian cells. The main steps of autophagy are initiation, nucleation, expansion cargo recruitment, closure, maturation and cargo degradation.

In this context, autophagy is shown to be non-selective, trying to degrade any available cytosolic molecules to obtain nutrients. However, autophagy has also been shown to behave in a selective manner, regulating the degradation of big cellular structures such as organelles, nuclear components, the proteasome, protein aggregates or invading pathogens. In this context, autophagy has a much more complex role than being a response to scarcity, and depending on the stresses that the cell has to face, it works as a powerful cytoprotective mechanism (Zaffagnini and Martens 2016).

Selective autophagy: Entering the world of LIRs

In contrast to bulk-autophagy, selective autophagy can have different substrates that are selected for degradation under certain conditions, which vary depending on the stress or stimuli that the cell receives (Lamark, Svenning, and Johansen 2017). In the last years, there has been an outbreak surrounding this type of autophagy (Kirkin 2020). Selective autophagy is classified into "-phagies", describing the organelle or structure that is targeted for degradation: for example, pexophagy is the autophagic degradation of peroxisomes (Germain and Kim 2020), ER-phagy refers to the autophagic degradation of the ER (Nakatogawa and Ohsumi 2020), mitophagy involves autophagy of mitochondria (Swerdlow and Wilkins 2020), aggrephagy refers to the degradation of protein aggregates (Lamark and Johansen 2012), and so forth. The list of types of autophagy is growing and it is likely to expand even further in the years to come (Kirkin and Rogov 2019). The main interaction to control selective autophagy is by the interaction of ATG8s with LC3-interacting motifs, the so-called LIRs (Birgisdottir, Lamark, and Johansen 2013). The core consensus sequence of a LIR is [W/F/Y]xx[L/I/V], where negatively charged amino acids are commonly found in the middle of the sequence (x) (Birna Birgisdottir et al. 2019; Lamark, Svenning, and Johansen 2017). The LIR motif forms an extended B-sheet positioned in a crevice formed by the N-terminal arm and the ubiquitin-like domain of the ATG8. The LIR is bound to hydrophobic pockets HP1 and HP2 in the ATG8s (Birgisdottir, Lamark, and Johansen 2013; Sora et al. 2020). The LIRs that follow this definite pattern are called canonical LIR motifs, which is the case for the majority of found functional LIRs. However, non-canonical LIRs have also been described, which interestingly show more restricted binding preference relative to ATG8 family members (Rogov et al. 2014). Intriguingly, it seems that LIRs-containing proteins can bind other elements of the autophagic core machinery through their LIR motifs than ATG8 proteins, as is the case of the binding of ATG19 to ATG5 via its LIR motif, forming an axis with the ATG12-ATG5-ATG16 complex. The binding of ATG19 to either ATG5 or ATG8 through its LIR motif seems to be mutually exclusive, suggesting a hierarchy of binding events that might ensure the directionality of reactions in the process of autophagosome formation (Fracchiolla, Sawa-Makarska, and Martenshttps 2017). This novel finding adds another function to LIRs, which seems to be beyond their binding of ATG8s.

ATG8 proteins act as adaptors or scaffold for recruitment of LIR-containing proteins to both surfaces of the growing phagophore (Johansen and Lamark 2020). This way they serve four main functions in autophagy: First, they act as membrane scaffolding of LIR-containing

core autophagy components of the ULK1/2 complex, class III PI3K complex I, the ATG4B protease processing ATG8s (Rasmussen et al. 2017), and ATG12-ATG5 to the rim and outer surface of the phagophore. Secondly, there is a LIR-dependent attachment of Selective autophagy receptors (SARs) to the inner surface of the pagophore. Third, help in the fusion of autophagosome and fourth assisting transport of autophagosomes to the lysosomes. Interestingly, ATG8 are not necessary for autophagosome formation, but essential for autophagosome-lysosome fusion. Their removal causes smaller autophagosomes, as well as slower initiation of the formation of those, leading to a very inefficient autophagic flux (T. N. Nguyen et al. 2016). Among the human ATG8 proteins, LC3s seem to be highly involved in elongation of the phagophore membrane, whereas the GABARAP subfamily is essential for autophagosome maturation (Jacquet et al. 2020). It is still not clear what the exact role of the different ATG8s are. They seem to add redundancy to the system, since there are cargos that can be recognized by more than one receptor. However, there are receptors that show a preference for certain members of the ATG8 proteins. This is the case of NDP52, which show a much stronger binding towards LC3C (von Muhlinen et al. 2012). The preference of receptors to different forms of ATG8s proteins suggests that the diversity adds both redundancy and specificity to the autophagic process (Wirth et al. 2019).

Intriguingly, it seems that LIRs-containing proteins can bind other elements of the autophagic core machinery through their LIR motifs than ATG8 proteins, adding additional functionality to LIRs. It has been suggested that this is a way to ensure the directionality of reactions. In addition, ATG8 can also bind other proteins through their non-LIR motif. A decade ago a study suggested a possible interaction between a large range of protein interacting with ATG8 independently of their LIR docking site (LDS) (Behrends et al. 2010), however, there are still only a few examples describing such an interaction. The recently described ubiquitin-binding motif (UIM) shows a LIR-independent interaction of the ATG8 proteins through the UIM-docking side (UDS). These two biding surfaces are well separated, which enable simultaneous biding. This was observed in *Arabidopsis*, where ATG8 binds RPN10 through on the UDS and DSK2 through its LDS (Marshall et al. 2019).

Autophagy receptors: The big guardians

How the cell selects the cargo to be degraded and in which conditions that happens leads to a very complex network of pathways that work together to maintain the homoeostasis of the cell. The big guardians of this process are the so-called autophagy receptors (SARs) (Johansen and Lamark 2020). Not all act at the same time or in the same conditions. They show a certain degree of redundancy, helping resolving emergencies for the cell even in the absence of one or more SARs. The most known autophagy receptors are: p62/SQSTM1, NBR1, TAX1BP1, Optineurin and NDP52 (Calcoco2), which all together are called SLRs (SQSTM1-like receptors) (Fig X). However, in the past years there has been an increase in the number of proteins that can also act as autophagy receptors, such as TRIM family proteins (see sections bellow) or organelle-bound receptors (Jia et al. 2018) (Zaffagnini and Martens 2016). This suggest that the cell has many resources to ensure the proper clearance of damaged elements.

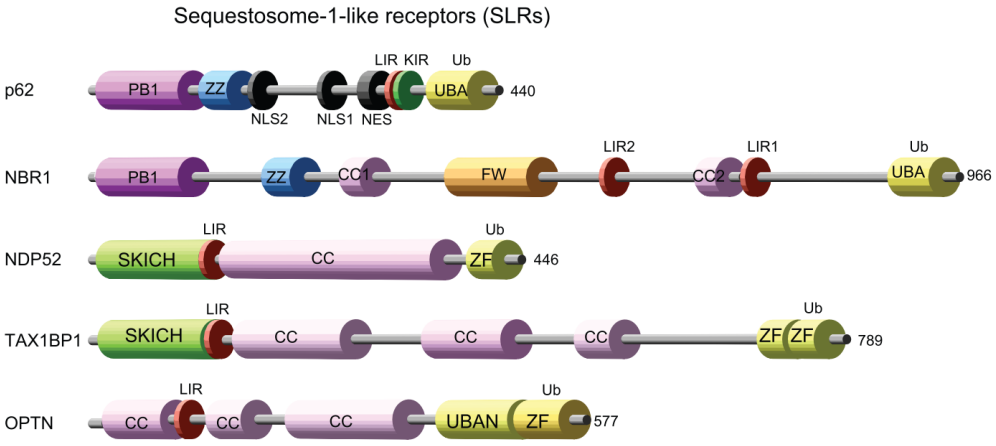

Figure 6. Domain architecture of selective autophagy cargo receptors SLRs. The sequestosome-1-like receptors (SLRs) constitute of p62, NBR1, NDP52, TAX1BP1 and OPTN (optineurin) in mammals. (Birgisdottir et al., 2013)

The SLRs are typically degraded in the lysosome, where they end up after binding the cargo and forming autophagosome, or by being imbedded directly to the lysosome by microautophagy (Mejlvang et al. 2018). Some of them such Optineurin can also be degraded by the proteasome (Wild et al. 2011). The description of the SLRs and their mechanistic have helped establishing the characteristics that are needed to qualify as an autophagy receptor. The essential characteristics of a *bona fide* autophagic receptor are: first, SARs have a LIR motif that binds to the ATG8s lipidated to the inner surface of the phagophore. Secondly, they are able to bind the cargo directly or through ha labelling protein such ubiquitin, and third they are degraded together with their cargo (Lamark, Svenning, and Johansen 2017).

P62: the pioneer

The most well-known and firstly discovered autophagy receptor is called p62/SQSTM1 (Atg19 in yeast) (Bjørkøy et al. 2005). The p62 domain architecture consists in an N-terminal headed by self-interacting PB1 domain, followed by ZZ-type zinc finger domain (ZZ), two nuclear localization signals (NLS), a nuclear export signal (NS), a LIR motif, and a KEAP1-interacting region (KIR) (Lamark, Svenning, and Johansen 2017) (Figure 7). In the C-terminal shows an ubiquitin associated UBA domain (Pankiv et al. 2007; Pankiv, Lamark, et al. 2010). The PB1 domain mediates p62 polymerization and binds other PB1-domain containing proteins, while the UBA domain binds the ubiquitylated substrates, showing preference for K63-linked polyubiquitin chains (Lamark et al. 2003).

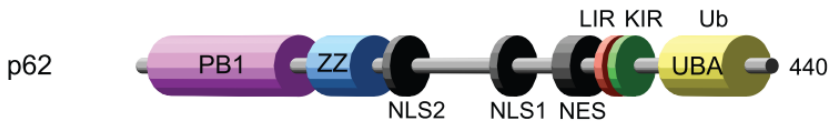

Figure 7. Domains of p62. P62 is a 440 amino acid protein containing a PB1 domain (PB1), a ZZ-type zink finger domain (ZZ), two nuclear localization signals 1 and 2 (NLS1 and NLS2), a nuclear export signal (NES), an LC3- interacting region (LIR), a Keap interacting region (KIR), and an ubiquitin-associated domain (UBA). (Birgisdottir, Lamark, and Johansen 2013)

Even though p62 commonly binds ubiquitylated substrates and leads them to degradation, this *bona fide* autophagy receptor can also bring to degradation non- ubiquitylated cargos (Lamark, Svenning, and Johansen 2017). The regulation of p62 occurs both in the transcriptional and translational level. NRF2 is an important regulator of p62 levels, and its translocation to the nucleus leads to a rapid increase in the levels of p62 transcription (Katsuragi, Ichimura, and Komatsu 2016). Post-transcriptional modifications (PTMs) are the main responsible of p62 regulation after its transcription, which form a complex network of modifications that control the functionality of this autophagy receptor. Among those PTMs are found phosphorylation and ubiquitylation (Lamark, Svenning, and Johansen 2017). A strong recruitment of p62 occurs when the cell faces high levels of oxidative stress or a high accumulation of protein aggregates (Cohen-Kaplan et al. 2016). The homopolydimerization of p62, via its PB1 domain, leads to long polymeric chains forming helical filaments (Jakobi et al. 2020). These polymeric chains mixed with ubiquitin chains often undergoing phase separation, leading to the formation of droples. This condensates form a network surrounding the selected cargo (Sun et al. 2018).

Besides p62 pivotal role in autophagy, this autophagic receptor has several roles in several cellular signaling pathways involved in cellular survival and growth. The roles of p62 have been found to be important in a variety of cancers (Ning and Wang 2018). The over expression of p62 has been described in many studies, and elevated levels of p62 expression is associated with poor prognosis (Ruan et al. 2018). Selective autophagy is one of the mechanisms through which p62 dysregulation leads to advantageous growth for cancer cells (D. Nguyen et al. 2019). P62 also activates pro-survival signaling and gene expression, as well as stabilization of a set of pro-metastatic mRNAs (Ségal-Bendirdjian et al. 2014).

NDP52: The pathogens' enemy

Another well-known SLR is NDP52, which is also called Calcoco2 (calcium binding and coiled-coil domain 2) (Von Muhlinen et al. 2010). This autophagy receptor is a member of the nuclear dots (NDs) and it is formed by a SKICH domain at the amino terminus, followed by a LIR motif, a coiled-coil domain in the central region, and a Ubiquitin binding zinc finger (UBZ) in the carboxyl terminus (T. Fu et al. 2018; Fan et al. 2020) (Figure 8). The finger motifs contain the binding domain for ubiquitin, mediating the important role of this receptor in ubiquitin-mediated protein degradation (Xie et al. 2015).

Figure 8. Structure of NDP52. NDP52 contains 446 amino acid, including the domains of SKICH, LC3-interaction region (LIR), COILED-COIL (CC), and UBZ. UBZ domain interacts with Ub, identifies and binds autophagy substrates. LIR domain interacts with LC3 and assists substrate anchoring to autophagosome membranes. From (Birna Birgisdottir et al. 2019)

NDP52 is tightly linked to innate immunity and has a crucial role in the degradation of invading pathogens (xenophagy) (Von Muhlinen et al. 2010). On one side, NDP52 targets bacteria to the nascent autophagosome by binding ubiquitin coated bacteria and ATG8 through its LIR motif, leading to the delivery of the tagged bacteria to the forming autophagosome (von Muhlinen et al. 2012). On the other side, NDP52 promotes autophagosome maturation by interacting with ATG8 through a distinct LC3-interacting region and the motor protein MYOSIN VI (Verlhac, Viret, and Faure 2015). NDP52 recognizes and targets ubiquitin coated *Salmonella* for degradation by binding via its SKICH domain the adaptor proteins Nap1 and Sintbad, which recruit TBK1 (Thurston et al. 2009). At the same time, TBK1 regulates the

autophagic functions of NDP52 by phosphorylating its SKICH domain (Heo et al. 2015). Moreover, NDP52 forms a trimeric complex with FIP200 and NAP1, which promotes the progression of antibacterial autophagy (Ravenhill et al. 2019). Furthermore, NDP52 interacts with Galectin-8 (Gal8), a cytosolic lectin that acts as a danger receptor, binding host glycans exposed on damaged *Salmonella*-containg vacuoles. NDP52 contains a Galectin-8 interacting region between the coiled-coil and UBZ domains. Therefore Gal8 activates NDP52-mediated xenophagy by detecting complex glycans that are not commonly present in the cellular cytosol, acting as a monitor of endo-lysosomal integrity (Thurston et al. 2012).

Another important role of NDP52 is the mediation of clearance of mitochondria (mitophagy) (Vainshtein and Grumati 2020). It has been shown that NDP52 is recruited to the mitochondria by the internal mitochondrial protein PTEN-induced kinas 1, commonly known as PINK1 (Lazarou et al. 2015). Once there, NDP52 associates with the ULK1 complex by its interaction with FIP200 (Ravenhill et al. 2019), interaction that is necessary for NDP52-induced mitophagy (Shi et al. 2020). The association of NDP52 with FIP200 is facilitated by TBK1, which is able to induce autophagy in the absence of LC3 (Vargas et al. 2019). In this context, the ULK1 complex activation mediated by NDP52 is independent of AMPK and mTOR activity.

Moreover, NDP52 mediates the degradation of other proteins involved in miRNA regulation, genomic stability and immune signaling. NDP52 mediates the degradation of retrotransposon RNA, DICER and protein argonaute 2 (Ago2) in the miRNA level (Gibbings et al. 2012). NDP52 sends to degradation the retrotransposon RNA, acting as a physiological buffer against genetic variegation (Guo et al. 2014). Furthermore, NDP52 deals with the degradation of mitochondrial antiviral signaling protein (MAVS), involved in Type I Inteferon signaling. (S. Jin et al. 2017). Another contribution of NDP52 to the regulation of the immune response is by mediating the degradation of the signaling adaptor protein TUR domain containing adaptor molecule 1 (TRIF) and Myeloid differentiation primary response protein MyD88 (MyD88), which are both implicated in Toll-like receptor (TLR) signaling (Inomata et al. 2012). Mutations found in NDP52 have been linked to Crohn disease, characterized by a chronic inflammation of the gastrointestinal tract. In this disease, NDP52 has been suggested to have a role in controlling NFKB signaling downstream of the toll-like receptor pathway, which is crucial in inflammatory signaling (Till et al. 2013).

Mitophagy: recycling big energy factories

Mitochondria are double-membrane organelles that constantly supply the cell with energy in form of ATP by the oxidation of fatty acids and pyruvate in the electron transport chain (Raimundo et al. 2017). Mitochondria have a bacterial origin, and even though the exact origin is unknown, it is clear that at some point in time an eukaryote cell integrated a bacterium as an organelle, stablishing a relationship of endosymbiosis (Zachar and Gergely Boza 2020). Through the years, mitochondria has not become only the powerhouse of the cell, but it has also developed an essential role in many other cellular functions such as production of reactive species (ROS), apoptosis, necrosis, autophagy, stress regulation, production of lipids and carbohydrates, Ca2+ storage and innate immunity (Murphy 2009; Nieminen 2003; Lorenzo Galluzzi et al. 2012).

Mitochondria are exposed to constant threats to their integrity and functionality, especially from the oxidative stress coming from the electron transport chain and production of ROS (Lorenzo Galluzzi et al. 2012). The protection of the fitness of this organelle is formed by a sophisticated system that acts both at the mitochondrial and cellular level. The mitochondria's first response to stress is through the action of antioxidants, DNA repair, protein folding and degradation (Scheibye-Knudsen et al. 2015). Moreover, fusion and fission of mitochondria also contribute to dilute and segregate damaged mitochondria respectively, acting as another layer of quality control (Eisner, Picard, and Hajnóczky 2018). On the other side, the autophagy machinery is able to target damaged mitochondria and lead them to degradation in the lysosomes. This process of engulfment and removal of mitochondria is called mitophagy, which acts as an important quality control of mitochondria at a cellular level (Wilkins et al. 2021). However, it is important to acknowledge that mitophagy is not limited to the removal of damaged mitochondria. This mechanism of selective autophagy is actually a natural mechanism that the cell has to control the amount of mitochondria that is present in the cytosol (Onishi et al. 2021). A good example of this mechanism under normal conditions is the removal of mitochondria on erythrocytes during their maturation (Mortensen et al. 2010). As the main responsible of transporting oxygen along the human body, erythrocytes have to get rid of the mitochondria they contain during their maturation process, so oxygen can be exclusively transported instead of partially consumed by the electron transport chain of mitochondria.

Mitophagy in yeast occurs through a protein present in the mitochondrial outer membrane (OMM) called ATG32, which acts as a mitophagy-specific autophagy receptor

(Okamoto, Kondo-Okamoto, and Ohsumi 2009). Upon nitrogen starvation or stationary growth, the expression of ATG32 is induced at the transcriptional level, which leads to higher level of this ATG protein in the OMM. Then, ATG32 binds ATG11, which works as an adaptor protein for selective types of autophagy, recruiting other ATG proteins that will promote autophagosome formation (Kanki et al. 2009). ATG32's activity seems to be regulated via different modifications and actions of regulators, diversifying the control of this mechanism.

In mammals, mitophagy seems to be a more sophisticated process and the signals that activate it are different to the ones in yeast (Madruga, Maestro, and Martínez 2021). Among the stressors that lead to activation of mitophagy, disruption of mitochondrial membrane potential seems to be one of the most potent triggers (S. M. Jin and Youle 2013). A proton-selective ionophore, called CCCP, causes mitochondrial depolarization and accumulation of mitophagy receptors on the OMM (Figure 9). Because of its powerful effect on mitochondria, CCCP is one of the most widely used activators of mitophagy *in vitro* (Yoo and Jung 2018). The recognition of target mitochondria to be degraded occurs through two main mechanism in mammals, by the direct interaction of LC3 with its receptors and by LC3 adapters, which can occur in an ubiquitylation-dependent and independent manner (Swerdlow and Wilkins 2020). There are several receptors suggested to mediate the elimination of mitochondrial under both physiological and pathological conditions. Among those receptors are BNIP3 and NIX, FUNDC1, BCL2L13 (mammalian functional counterpart of yeast ATG32), and FKBP8 (Bhujabal et al. 2017) (Figure 10).

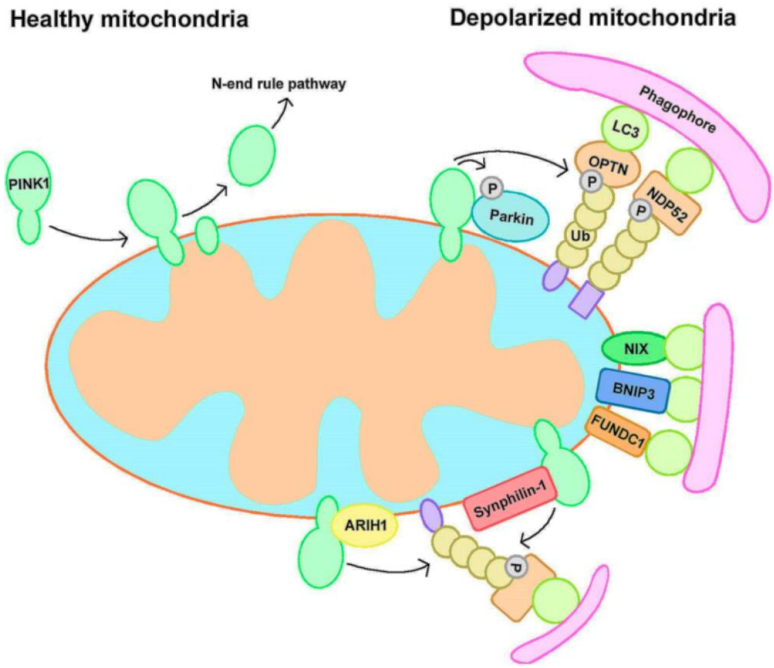

Figure 9. Mitophagy produced by depolarization of mitochondria. From (Jia Liu et al. 2019) Mitophagy can be divided into Parkin-dependent or independent pathways. Under normal conditions, PINK1 localizes to mitochondria and is translocated to the mitochondrial inner membrane (MIM), where it is cleaved and subsequently degraded. However, when mitochondria become depolarized, PINK1 accumulates at the outer mitochondrial membrane (OMM) and recruits Parkin. Activated Parkin leads to the ubiquitination of substrates and the recruitment of autophagy receptors to initiate mitophagy. In addition, Parkin-independent mitophagy includes receptor-mediated and ubiquitin ligase-mediated mitophagy.

PTEN-induced putative kinase 1 (PINK1) and Parkin form an essential axis for the control of induction and control of mitophagy. Under normal conditions, PINK1 is continuously being degraded by the proteasome. A damage in the mitochondria, such membrane depolarization, reduced the cleavage of PINK, which consequently accumulates in the mitochondrial outer membrane (OMM). The accumulated PINK1 become them autophosphorylated and activated, consequently phosphorylating ubiquitin and leading to recruitment of Parkin. As an E3 ligase, Parkin poly ubiquitylates its substrates and leads them to degradation. The degradation of such substrates eventually induces mitochondrial fission and mitophagy (Geisler et al. 2010). The SLRs, which in the case of mitochondria act as adapters, are recruited to the K63-linked polyubiquitylated substrates on the mitochondria. Then those SLRs recruit the necessary machinery for autophagosome formation surrounding those mitochondria and bring them to degradation. The two most important SLRs implicated in ubiquitin dependent mitophagy are OPTN and NDP52 (Lazarou et al. 2015). The kinase Tank-binding kinase 1 (TBK1) becomes activated by OPTN and promotes mitophagy through the phosphorylation of OPTN and NDP52. Interestingly, PINK1 is also able to recruit OPTN and NDP52 independently of the action of Parkin (Lazarou et al. 2015). Damaged mitochondria can also be recognized by autophagy receptors in an ubiquitin-independent manner. This is the case of the recruitment of p62 by mitochondrial protein CHDH (choline dehydrogenase), leading to the formation of the CHDH-p62-LC3 complex, which promotes mitophagy (Park et al. 2014). Moreover, there are also mitochondrial proteins such as BNIP3, NIX and FUNDC1, that can act as receptors (Onishi et al. 2021) (Figure 10). FK506-bidning protein 8 (FKBP8) is located in the OMM and leads to mitophagy by its interaction with LC3A. An additional point of regulation of mitophagy by FKBP8 is its localization. This mitochondrial protein migrates to the ER under stress conditions, and the inability to do so leads to an activation of mitophagy (Bhujabal et al. 2017).

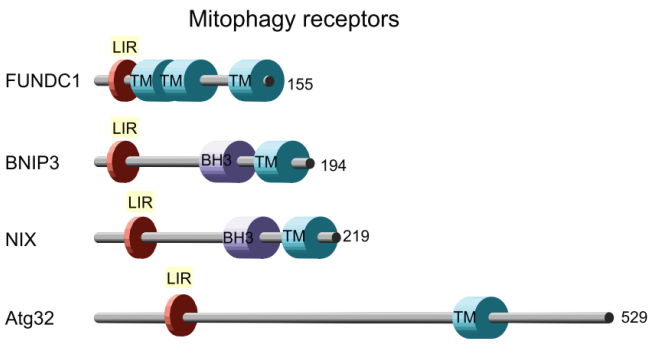

Figure 10. Most studied Mitophagy receptors. FUNDC1, BNIP3, NIX mammalian autophagy receptors and ATG32, receptor in charge of mitophagy in yeast.

The regulation of the amount and fitness of such an important organelle as the mitochondria is crucial for the well-being of the cell, therefore it is not surprising that a dysfunction in mitophagy is linked to many pathological conditions. Mitophagy seems to be implicated in several diseases, including Parkinson's disease, Alzheimer's disease, Huntington's disease, Amyotrophic lateral sclerosis (ALS), cancer, cardiovascular diseases and atherosclerosis. (Rottenberg and Hoek 2021)

The lysosomes and LAMPs: at the acidic edge

The lysosomes are cellular organelles that constitute the main degradative compartment of the cell (Davidson and Vander Heiden 2017). However, it has been reported that lysosomes are involved in several cellular processes besides degradation of the delivered cellular material such as cholesterol homeostasis, plasma membrane repair, bone and tissue remodeling, defense against pathogens, cell death and cell signaling (Saftig and Klumperman 2009). The substrates are delivered to the lysosome via endocytosis, phagocytosis or autophagy (Tancini et al. 2020). There are two essential groups of proteins in lysosomes: soluble lysosomal hydrolases and integral lysosomal membrane proteins (LMPs). Lysosomal hydrolases are delivered to the lysosomes from the Golgi and require a pH between 4.5-5.5 to become active, which allows the cell to be protected from the action of those hydrolases in unwanted locations (Parenti, Medina, and Ballabio 2021). The acidic pH of the lumen of lysosomes is achieved and maintained by an H+-ATPase (Johnson et al. 2016). LMPs are mainly found in the lysosomal limiting membrane, where they perform diverse functions, including acidification of the lysosomal lumen, protein import from the cytosol, membrane fusion and transport of degradation products to the cytoplasm (Saftig and Klumperman 2009). Some of the most abundant LMPs are the lysosome associated membrane proteins (LAMPs), which are glycosylated proteins commonly found in the membrane of the lysosomes. There are 5 different types of LAMPs, which are unequally expressed along tissues, suggesting a diversification of functions. The most abundant and best studied are LAMP-1 and LAMP-2 (Alessandrini, Pezzè, and Ciribilli 2017). These two LAMPs present a similar length and 37% amino acid sequence homology. Their structure consists in a highly glycosylated luminal region, a transmembrane region and a short C-terminal cytosolic domain. LAMP-1 or LAMP-2 deficient mice are viable and fertile, which suggest that they might have similar functions or those functions partially overlap (E.-L. Eskelinen 2006).

Whereas LAMP-1 presents only one transcript, LAMP-2 has three different splicing isoforms: LAMP-2A, LAMP-2B, and LAMP-2C. Mutations in LAMP-2 lead to Danon disease, a multisystem disorder that presents skeletal myopathy, cognitive defects and visual problems (Rowland et al. 2016). However, recent findings point towards LAMP-2B as the main responsible of this disease (Myerowitz, Puertollano, and Raben 2021). LAMP-2A is one of the essential components of CMA, taking the selected proteins into the lysosome for degradation (Kaushik and Cuervo 2018). LAMP-2B is involved in macroautophagy, mediating the autophagosome-lysosome fusion, through its binding to ATG14 and VAMP8 (Chi et al. 2018). LAMP-2C acts as an inhibitor of CMA and mediates the autophagy of nucleic acids by binding RNA and DNA (Fujiwara et al. 2015). Due to the difference in expression among different cell types and not a high degree of homology among them, it seems clear that LAMPs have diversified their functions to fulfill different needs in different tissues (Alessandrini, Pezzè, and Ciribilli 2017).

Lysosomes have a crucial role in cellular homeostasis, and the dysfunction of this organelle is involved in several diseases. Defects in genes encoding lysosomal proteins lead to lysosomal storage diseases (Platt 2018). Moreover, the impairment of lysosomal function has also been reported in other more common pathologies, including inflammatory and autoimmune disorders, cancer, neurodegenerative diseases and metabolic diseases (Reddy Bonam, Wang, and Muller 2019).

Even though they LAMP2 is a widely used lyosomal marker, its mechanism of action and its implication in cancer is still poorly understood. LAMP2 plays a role in the support of early cancer progression, helping cancer cells surviving in acidic enviroments (Mogami et al. 2013). Moreover, LAMP2 is highly expressed in poorly expressed in several cancer, where reduced expression of LAMP2 has been associated with a loss of migration and invasion capabilities (Koukourakis et al. 2015). LAMP2A isoform has shown increased expression in breast tumor tissue, and its inhibition results in sensitibilization of tumor cells to radioation and doxorubicin therapy (Saha 2012).

Crosstalk of UPS and autophagy

For many years and due to the lack of research in autophagy, the degradation pathways of UPS and autophagy were perceived as two separate cellular mechanisms that acted in parallel of each other without interacting. UPS was in charged of small short-lived proteins mainly for

mediating cellular responses through protein pool control, whereas autophagy was responsible for the degradation of large and long-lived proteins or organelles (Ji and Kwon 2017). Proteasomal degradation took place in the cytosol, whereas degradation via autophagy took place in the lysosomes. Furthermore, proteasomal degradation associated with degradation of proteins, providing temporal control of proteins such as cell cycle regulators (Kravtsova-Ivantsiv and Ciechanover 2012). On the contrary, autophagy was perceived merely as a cellular response to starvation. However, it is becoming more clear that these two pathways are not only linked by several common players, but also stablish a network of crosstalk and cooperation (Nam et al. 2017).

The most relevant common denominator shared by UPS and autophagy is the molecule of ubiquitin. The current model defends that the nature of poly-ubiquitin chains determines the mode of degradation. UPS has a preference for K48-linked chains, while autophagy has a predilection for K63-linked chains, organelles and mono-ubiquitylated substrates (Grice and Nathan 2016). Sharing such an essential player in both pathways and due to their pivotal role in maintaining cellular homeostasis, it is imperative that these two degradation mechanism crosstalk and regulate each other. Autophagy is activated when the proteasome is already working at full capacity. However, the proteasome seems not to be able to take over when autophagy is inhibited, due to the proteasomes limitations in the size of the proteins is able to degrade (Wurzer et al. 2015). One of the suggested regulators of this phenomenon is the master tumor repressor p53, which upon UPS inhibition, accumulates, leading to an activation of AMPK and inhibition of mTOR1 (Horn and Vousden 2007). UPS and autophagy have another point of interplay in the degradation of the proteasome, a type of autophagy called proteaphagy (Enenkel et al. 2020). Interestingly, certain conditions, such as muscle atrophy in fasting requires both mechanisms (J. Zhao et al. 2007), indicating the complementary relationship between the two degradation pathways. Hence, these two mechanism of degradation have a compensatory and complementary relationship, ensuring in most cases a win in the battle for homeostasis.

TRIM proteins, as E3 ligases, are linked to the UPS. Growing evidences show their crucial role in autophagy (Michael A Mandell, Saha, and Thompson 2020). Thus, they also become common denominators of both pathways. TRIM proteins have a great contribution in misfolded proteins clearance, facilitating their degradation through both the UPS and autophagy (Boise et al. 2020), which I will go in further detail in the section dedicated to TRIM proteins in autophagy. Moreover, TRIM proteins not only act as E3, ligases. TRIM27 or TRIM19, which

both have SUMOylation ligase activity, which may also regulate the degradation of proteins (Chu and Yang 2011).

Phase separation: a new layer of complexity and regulation

The primer idea of an organelle is a structure surrounded by a double-membrane. However, this idea has been left behind by the discovery of biomolecular condensates in a cellular context (Dignon, Best, and Mittal 2020). The formation of these membraneless organelles by liquid-liquid phase separation (LLPS) adds another layer of complexity and dynamism to many cellular processes. Phase separation involves demixing of a homogenous liquid solution of macromolecules into two phases that coexist, a dense phase that is enriched and a dilute phase that is depleted for specific macromolecules (Boeynaems et al. 2018). This phase allows rapid and dynamic exchange of components of the condensate with the surrounding environment. The viability of these phase separates is possible due to multivalent interactions that often include folded globular domains, intrinsically disordered proteins (IDPs) or intrinsically disordered regions (IDR) and/or RNA or DNA scaffolds (Yoshizawa et al. 2020). Among all those elements, they can be categorized into two groups depending on their role in the formation of phase separates: stickers and spacers. Stickers are those macromolecules that engage in reversible non-covalent intra or intermolecular interactions, leading to physical crosslinks, thus, they "stick" to another macromolecule. On the contrary, spacers are found between stickers, and even though they are not directly involved in the crosslink, they can influence the assembly of linked molecules (Choi, Holehouse, and Pappu 2020). Even though the better known is the liquid-liquid phase separation, membraneless organelles can be in the form of different phase separations such hydro-gel or liquid-solid separation. This seem to be the case of p62 bodies in the liver cell line huh-1, where p62 forms gel-like droplets, which work as platform for autophagosome formation (Kageyama et al. 2020).

The membraneless compartments can be found both in the cytosol and the nucleus. The presence of the so-called bodies have been known for years, but a lack of methodology to analyze them made it difficult to fully describe their nature. Arising evidences suggest that nuclear structures such as promyelocytic leukemia (PML) bodies, Cajal bodies, SUMO bodies, NEAT bodies, histone locus bodies, or the mitotic spindle are indeed biomolecular condensates that participate in nuclear organization and regulation (Zimber, Nguyen, and Gespach 2004). Promyelocytic leukemia (PML) bodies are present in the nucleus, where they have an important

role in the regulation of chromatin dynamics (Corpet et al. 2020), and in the cytoplasm, commonly linked to the ER and mitochondria (Carracedo, Ito, and Pandolfi 2011). PML bodies undergo phase separation, stablishing a dynamic network between their components (Yoshizawa et al. 2020). Interestingly, the major mediator of the structure of these bodies is TRIM19, which also known as PML. TRIM19 has ubiquitin and SUMO E3 ligase activity that contribute to the formation and maintenance of their structures by the interaction with scaffolding proteins (Corpet et al. 2020).

Since this is a spontaneous reaction, the question of how the cell is able to control phase separation of cellular components rapidly arises. It has been reported that PTMs such as phosphorylation, ubiquitylation, arginine methylation and sumoylation can act as cellular switches controlling phase separation (Hofweber and Dormann 2019; Owen and Shewmaker 2019). Interestingly, many proteins commonly involved in phase separation show in their sequence many residues targeted by PTMs. Another control point of phase separations seems to be controlling the concentration and distribution of the elements participating in the process. Thus, the cell is able to shuttle phase separation prone elements in and out of the nucleus or other cellular compartments to control the formation of the biomolecular condesate (Boeynaems et al. 2018).

The role of ubiquitin in phase-separation: The infrastructure of the cross-talkers

Liquid-liquid phase separation (LLPS) has emerges as an additional player in the spatiotemporal regulation of quality control in the cell. This control mechanism seems to be for several structures ubiquitin dependent (Lei, Wu, and Winklhofer 2020). LLPS provides a transient and dynamic compartmentalization of several cellular processes, such as autophagy (Banani et al. 2017). The autophagic receptor p62 plays a key role in protein quality control. Growing evidences show that p62 is able to perform this function undergoing phase separation. Polymerization of p62 increases its affinity to polyubiquitin-linked cargo and LC3B, while dimeric p62 shuttles ubiquitylated proteins to the proteasome (Wurzer et al. 2015). Additionally, mono-ubiquitin of p62 has been observed to inhibit phase separation, likely due to its interference in the binding of the UBA domain with the cargo. Inhibition or impairment of the proteasome leads to a lower abundance of mono-ubiquitin, and in consequence a higher number of ubiquitylated substrates (Berkamp, Mostafavi, and Sachse 2020). In this context,

p62 is called by those ubiquitylated substrates, which promotes p62 condensation and subsequent autophagosomal degradation (Figure 11). In the past years, it has been suggested that p62 also undergos a further step of phase separation, forming a gel-like structure (Kageyama et al. 2021). However, this theory is still in its initial stages.

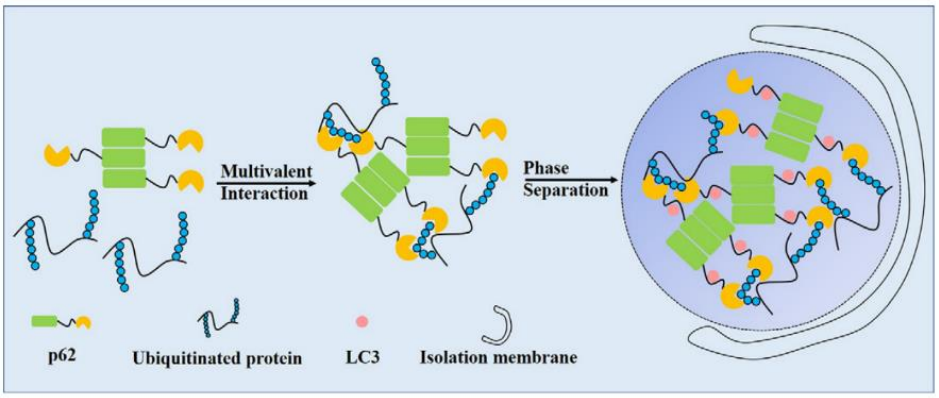

Figure 11. **Poly-ubiquitin chain-induced p62 phase separation drives autophagic cargo segregation.** Polyubiquitin chain-induced p62 phase separation drives autophagic cargo segregation. p62 proteins form oligomers through the PB1 domain (green part) and bind ubiquitin through the UBA domain (yellow part). Both domains facilitate multivalent interactions. When protein concentrations reach a threshold, liquid–liquid phase separation occurs to form p62 bodies. Other client proteins, such as LC3 and Keap1, are also recruited to p62 bodies. p62 bodies are then degraded by autophagy. cation–piFrom (Sun et al. 2020)

This ability to quickly form these condensates provides an efficient way of sequestering and processing cellular material destined to be degraded. Hence, ubiquitin seems to be not only the major common denominator between UPS and autophagy, but it also controls the compensatory mechanisms between these two pathways.

TRIMs: a family of E3 ligases

Tripartite motif family proteins (TRIMs) are a wide family of proteins involved in the control of several cellular processes such as intracellular signaling, innate immunity, transcription, cell cycle regulation, autophagy and carcinogenesis (Boise et al. 2020; M A Mandell et al. 2014; Watanabe and Hatakeyama 2017). To date, there are more than 80 distinct protein members in the TRIM family. The vast majority of those TRIMs present E3 ligase activity since they contain a RING finger-domain, with a few exceptions such as TRIM16 or TRIM20, which lack this domain but still has the ubiquitin binding activity (Michael A Mandell, Saha, and Thompson 2020). Individual TRIM proteins have also showed functions of SUMOlyation and NEDDylation of themselves or their interacting partners (Chu and Yang 2011; Noguchi et al.

2011). Those TRIMs defined as E3 ligases are characterized by the presence of tripartite motif RBCC domain. The RBCC domain contains in the N-terminal one RING-finger domain, one or two B-boxes (B1/B2) and a coiled-coil (CC) domain (Reymond et al. 2001). The B-box together with the coiled-coil domain mediate protein-protein interactions. The coiled-coil domain is the responsible of TRIM hetero- and homodimerization, crucial for many TRIM proteins that require dimerization to be catalytically active (Koliopoulos et al. 2016). In addition, most TRIMs also present domains at the C-terminus, which gives them specificity for their target proteins (Ikeda and Inoue 2012). Based on the composition of the C-terminus domain and domain organization, TRIMs can be classified in 12 subfamilies (I-XI). (Figure 12) The C-terminus domains present in TRIM proteins are: COS domain, fibronectin type III repeat (FNIII), SPRY domain, PRY domain, PHD domain, bromodomain (BROMO), filamin-type IG domain (FIL), NHL domain, Meprin and TRAF-homology domain (MATH), ADP-ribosylation factor family domain (ARF), transmembrane region (TM) and acid-rich (Watanabe and Hatakeyama 2017; Michael A Mandell, Saha, and Thompson 2020).

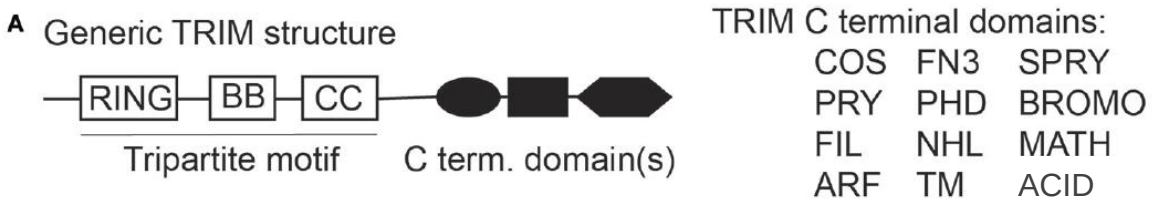

Figure 12. Generic structure of Tripartite motif (TRIM) proteins and subfamilies. (Michael A Mandell, Saha, and Thompson 2020)

TRIMs expression is found down or upregulated in numerous cancers (Shigetsugu Hatakeyama 2011). In general, a significant decrease of TRIM expression suggests a tumor suppressive role, whereas a significant overexpression suggest an oncogenic role. To date, the TRIMs that have been associated to cancer are TRIMs 11, 14, 24, 25 ,27, 28, 29, 33, 37, 44, and 59 (Michael A Mandell, Saha, and Thompson 2020). This list is likely to grow in the following years, and the general rule of thumb of the effect by decreased/increased expression might change overtime if more versatile roles of TRIM in cancer are discovered.

Over the years, there has been found an association of TRIM genes with chromosomal translocations, leading many times to the contribution to oncogenesis. One of the most known is the translocation between TRIM19 gene (PML) on chromosome 15 and the retinoic acid receptor alpha (RARα) gene located on chromosome 17 (Cambiaghi et al. 2012). This

translocation is associated with acute promylocytic leukemia, and acts by repressing genes associated with retinoic acid signaling (Corpet et al. 2020). Moreover, the RET genes on chromosome 10 has been found in translocations with several TRIM genes, including TRIM24, TRIM27 and TRIM33 (Crawford, Johnston, and Irvine 2018). TRIM24 has been found translocated with RET gene in papillary thyroid cancer (Santoro and Carlomagno 2013), with BRAF gene in melanoma (Hutchinson et al. 2013) and lung cancer (Nakaoku et al. 2014), and with FGFR1 gene in myeloproliferative syndrome (Belloni et al. 2005). All these fusion proteins lead to the upregulation of activity of the RET, BRAF or FGFR1 kinases, resulting in the activation of multiple pro-survival signaling. The fusion of these genes with TRIM proteins lead to a gain-of-function that has profound effects in oncogenesis.

Some TRIMs are involved in the regulation of pathways seminal to cancer stemness, including STAT signaling, AKT signaling, NANG-Sox2-Oct3/4 networks, and pathways related to epithelial mesenchymal transition (EMT). (reviewed by (Jaworska et al. 2020)), suggesting a TRIM-dependent contribution to cancer stemness. TRIM28 is reported to maintain Oct-3/4-Sox-NANOG expression in breast cancer cells (Czerwińska, Mazurek, and Wiznerowicz 2017), whereas TRIM24 enhances STATS3-mediate transcriptional activation, leading to cancer stemness in glioblastoma (Lv et al. 2017). In addition, TRIM14, TRIM24 and TRIM27 have been reported to mediate AKT signaling, enhancing EMT (Eberhardt et al. 2020). In contrast, TRIM16 has been found to be a negative regulator of stemness in breast (Yao, J. Xu, T. Tian, T. Fu, X. Wang, W. 2016) and ovarian cancer cells (H. Tan et al. 2017). A deeper description, as well as more TRIMs involved in stem cells cell-renewal abilities is likely to arise in the following years. Autophagy plays a pivotal role in cancer stemness through its contribution in cellular homeostasis and longevity (Chang 2020). Autophagic regulation is a very prominent feature of TRIMs, so it would be unsurprising that the effect of this family of proteins on autophagy lead to effects in cancer stemness.

The tumor suppressor protein p53 has a central role in the regulation of genomic stability by inducing cell cycle arrest and apoptosis if extensive cellular DNA damage occurs (Horn and Vousden 2007). The interaction between TRIM proteins and p53 has been extensively described (reviewed in). TRIMs 11, 21, 24, 25, 28, 29, 31, 32, 39, and 59 are found to negatively regulate p53 by directly ubiquitinating p53, leading to its proteasomal degradation in the cytoplasm.

Breast cancer is the most common malignancy in women worldwide, and it is curable in the 70-80% of the cases if it is diagnosed in its early stages (Harbeck et al. 2019). To date,

there are 15 TRIM proteins associated to breast cancer. The expression of TRIMs 13, 21 and 62 was found decreased, whereas the expression of TRIMs 11, 24, 37, 44 and 59 was found increased (Michael A Mandell, Saha, and Thompson 2020). Decreased levels of TRIM13 expression was associated with worse distance metastasis free survival, diseases specific survival, metastatic relapse free survival ad relapse free survival (W. X. Chen et al. 2019). The decreased expression of TRIM21 correlates with poor overall survival in breast cancer patients (Vicenzi et al. 2019). Up-regulation of TRIM11 has been suggested to act through AKT/GLUT1 signaling pathway in breast cancer (Song et al. 2019), while up-regulation of TRIM24 and TRIM37 have been linked to histone modifications in breast cancer (Tsai et al. 2010; Bhatnagar et al. 2014). Elevated levels of TRIM32 and TRIM44 were associated with effects in the NFKB pathway in breast cancer (Kawabata et al. 2017; T. T. Zhao et al. 2018). Moreover, TRIM59 is found up-regulated in metastatic breast cancer, where it is observed to mediate the p62-selective degradation of tumor suppressor PDCD10 (P. Tan et al. 2018), highlighting the role of a TRIM protein acting on autophagy in breast cancer.

TRIMS in autophagy: the newcomers

TRIM proteins play several roles in autophagy, acting at different levels of regulation both as regulators and effectors (Michael A Mandell, Saha, and Thompson 2020) (Figure 13). Some TRIMs regulate autophagy at the mRNA levels by affecting the transcription of autophagy genes. Good examples of this phenomenon is TRIM59, which negatively regulate the expression of Becn1 mRNA or TRIM37, which acts as a suppressor of autophagy by inhibiting the activation and nuclear translocation of the pro-autophagy transcription factor TFEB (W. Wang et al. 2018; Han et al. 2018). In addition, TRIM16 promotes the expression of p62 by driving Nrf2 activation under conditions of oxidative stress (Kumar Jena et al. 2018). Other TRIMs can act as transcriptional regulators, as is the case of TRIM28. This TRIM is also known as KAP1 and represses the expression of miRNAs that target autophagy factors such as ULK1, Becn1 and Atg12 (Czerwińska, Mazurek, and Wiznerowicz 2017). Interestingly, TRIM65 promotes autophagy by preventing miRNA-based down-regulation of ATG7 (X. Pan et al. 2019).

Certain TRIM proteins seem to be involved in the regulation of autophagy through the regulation of upstream signals such as mTOR and AMPK pathways, as well as STING/TAK1 pathway. TRIM37 interacts directly with mTOR complex components and promotes assembly

of active mTOR complexes to the lyososome. Interestingly, TRIM37 deficient cells show high rates of autophagy flux, becoming “autophagy addicted”, leading to cell death if autophagy is inhibited (W. Wang et al. 2018). TRIM proteins also regulate AMPK and its ability to induce autophagy. TRIM28 ubiquitylates the AMPKα1 subunit, leading it to degradation, thus repressing autophagy. Pro-cancer kinase TAK1 is involved in the regulation of AMPK activity. Interestingly, TRIMs 5 and 8 activate this kinase, whereas TRIM38 inhibits it (Pertel et al. 2011; Hu et al. 2014). On the other hand, another essential pathway for the control of autophagy is STING-TBK1 signaling axis. Several TRIMs are involved in the regulation of these pathways through interaction of different players of this pathway. STING is found in the ER membrane in an inactive state, and it becomes activated in response to cytosolic DNA detection, that leads to the recruitment of TBK1. The activation of the STING-TBK1 complex re-localizes to the ER-intermediate compartment and activates transcription factor IRF3 (Kimura et al. 2015). TRIM56 and TRIM32 catalyze the formation of K63-linked polyubiquin chain of STING (Tsuchida et al. 2010; Wu et al. 2020). TRIM27 promotes the proteasomal degradation of TBK1 (Zheng et al. 2015). TRIM23 is a unique TRIM that contains an ARF domain, which interacts with TBK1 and is implicated in TRIM23-mediated autophagy (Sparrer et al. 2017). It is likely that more TRIMs are able to regulate autophagy by acting on TBK1. In addition, TRIM16 has an important role in lysophagy through its binding to Galectin-3. Upon invasion of mycobacterium, the vacuoles that contain them (endosomes and eventually lysosomes) can experience membrane damage, which can eventually release the invading bacteria into the cytosol. Galectin-3 detects the glycans exposed by the damaged membrane, which presence is unusual in the cytosol. Then Galectin-3 recruits TRIM16, which in turn serves as a platform for autophagic initiation factors (Chauhan et al. 2016).

Some TRIMs are able to directly interact with the conserved core autophagy machinery, thus modulating autophagy. Some TRIMs, such as TRIM5α, 6, 16, 17, 20, 22, 49 and 55, act as a platform through the assembling of ULK1 and Beclin 1. This regulatory complex has been name TRIMosome, which regulates selective autophagy (Nicely reviewed in (Kimura et al. 2015)). TRIM 5α, 6, 17, 22 and 49 interact with ULK1 and Beclin 1. TRIM5α also interacts with ATG14L1 and AMBRA1, which are both interactors of the Beclin 1 complex . Other TRIMs that interact with ULK1 and/ or Beclin 1 complexes are TRIM 13, 16, 20, 21, 28, 32, and 50. In general, the action of these TRIMs lead to an induction of autophagy. However, there are TRIMs such TRIM17 that interacts with ULK1 and Beclin 1 and inhibits autophagosome formation (Michael A. Mandell et al. 2016). TRIM 6, 16, and 20 also form protein complexes

with ATG16L1, and TRIM5α co-immunoprecipitates with ATG5, however, their effect of ATG8 lipidation and autophagosome membrane elongation has not been elucidated yet. Interestingly, there are some TRIMs that are able to modulate autophagy through its non-E3 ligase activity. A good example is TRIM20, which lacks a RING domain but can still assemble active autophagy initiation complexes. TRIM28 is able to SUMOylate Hvps34, enhancing the PI3 kinase activity of Beclin 1 complex (Czerwińska, Mazurek, and Wiznerowicz 2017). In addition, TRIM32 promotes the activity of ULK1 complex through the generation of unattached K63-linked poly-ubiquitin chains (Di Rienzo, Piacentini, and Fimia 2019). It would not be surprising that other TRIMs can modulate autophagy through their SUMO or NEEDylation activities, as well as interaction with the autophagy machinery that does not require their E3 ligase action.

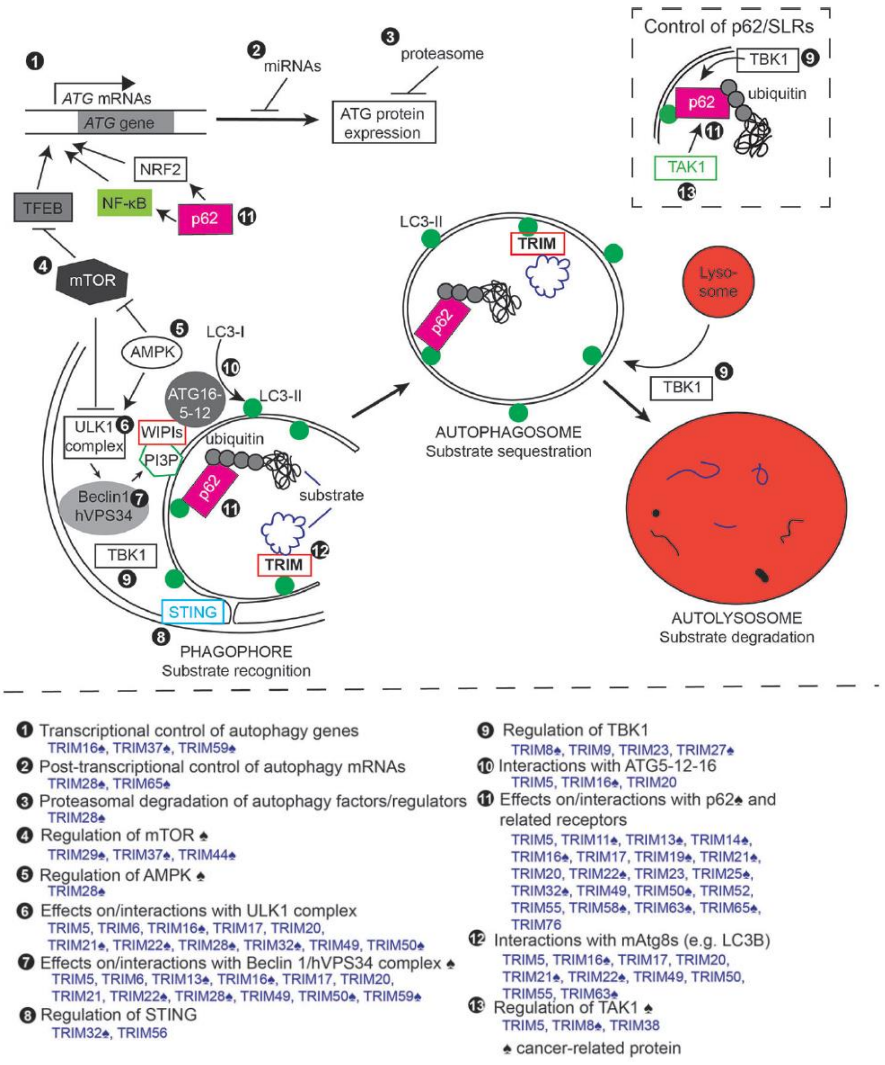

Figure 13. Roles of TRIM proteins in autophagy to date. Schematic of different steps/stages of the autophagy pathway by TRIM proteins (top). Summary of TRIM actions in autophagy (bottom). ♠ Symbol indicates proteins with reported cancer relevance. (Rottenberg and Hoek 2021)

The vast majority of TRIMs contain a RING domain that acts as an E3 ligase, therefore, the idea that TRIMs tag substrates for being recognized by autophagy receptors is one of the first one that comes to mind. However, such TRIM-mediated autophagy has not been well-described yet. A study suggested that TRIM21 ubiquitylates kinase IKKβ, facilitating its degradation by autophagy (Niida, Tanaka, and Kamitani 2010). Some TRIMs actually seem to act as autophagy receptors themselves, binding the substrate while recruiting the autophagic machinery (Kimura, Mandell, and Deretic 2016). TRIM5 acts as an autophagy receptor during viral infection. TRIM5α contains two LIR motifs that directly binds ATG8 proteins, while it has a SPRY domain in its C-terminal that can bind the autophagic substrates (Michael A Mandell et al. 2015). There are other TRIMs that are able to bind ATG8s (Rienzo et al. 2020). It is likely that more TRIMs can act as autophagy receptors themselves upon certain stress or stimuli that the cells face. Typically, autophagy receptors end being degraded in the lysosomes together with their targeted proteins (Johansen and Lamark 2020). To date, several TRIMs has been reported to be degraded by autophagy (found in lyosomes): TRIM 5α, 13, 16, 20, 21, 23, 27, 31, 32, 45, 50, and 56 (Nicely reviewed in (S Hatakeyama 2017) and (Michael A Mandell, Saha, and Thompson 2020)).

Due to its multifunctional nature, the mechanisms that the cells have to control p62 action is tightly regulated and are not completely elucidated. In the last years, TRIM proteins have emerged as key regulators of p62. Many TRIMs have been shown to interact with p62 or to colocalize with p62 in cellular structures (Reviewed in Michael A Mandell et al., 2020). One of the main functions of p62 is the organization and sequestration of ubiquitylated proteins into cytoplasmic punctate structures called p62 bodies, which have liquid droplet-like properties. It is suggested that these structures may act as a platform for p62-mediated signaling, concentrating and leading cellular waste to degradation (Zaffagnini et al. 2018). To date, 14 TRIMs have been linked to the regulation of the formation and clearance of these structures. A subgroup formed by TRIM 5, 16, 17, 32, 50, 52, and 58 seem to increase the abundance of p62 bodies, whereas TRIM 14, 19, 21, 22, 25, 65, and 76 have the opposite effect (Kimura, Mandell, and Deretic 2016; J. A. Pan et al. 2016; Kumar Jena et al. 2018; Kehl et al. 2019; Overå et al. 2019). In contrast, TRIM16 is required for the formation of p62 bodies in the same circumstances (Kumar Jena et al. 2018). TRIMs have also been suggested to modulate p62 activity via the control of its phosphorylation status (Michael A Mandell, Saha, and Thompson 2020). Another mechanism TRIM proteins have to control p62 dynamics is by their action on

Nrf2. TRIM21 negative regulates Nrf2-directed cytoprotective antioxidant response of p62 (Bartolini et al. 2018).

All these examples of the regulation of autophagy by TRIM proteins show the high specificity of this family of E3 ligases. Interestingly, no TRIM homologs have been identified in yeast, which is well-studied autophagy model organism. Thus, TRIM proteins might add complexity to the mammalian autophagy system, being able to regulate more specific degradation processes (Michael A Mandell, Saha, and Thompson 2020).

TRIM27 and its known roles

TRIM27 is an E3 ligase also known as Ret finger protein (RFP protein), which was firstly described as a fusion protein with the tyrosine kinase domain of the c-RET proto-oncogene originated by DNA rearrangement (Hasegawa et al. 1996). This 58-kDa protein is part of the largest subclass on the TRIM protein family of proteins, class-IV. TRIM27 can be found both in the cytoplasm and the nucleus of the cells, depending on the cell type (G. Tezel et al. 1999). TRIM27 expression is found in all human tissues, however, it is significantly higher in male germ cells (Zhuang et al. 2016). TRIM27 structure consists in a N-terminal formed by a RING domain, that confers the E3 ligase activity as well as SUMOylation (Chu and Yang 2011), followed by a B-box and a coiled-coil domain, which are in charge of oligomerization. In the C-terminal TRIM27 contains a PRY followed by an SPRY domain (Figure 14). TRIM27 contains in the coiled-coil region a nuclear export (NES) sequence that allows shuttling between the nucleus and the cytoplasm (Harbers et al. 2001).

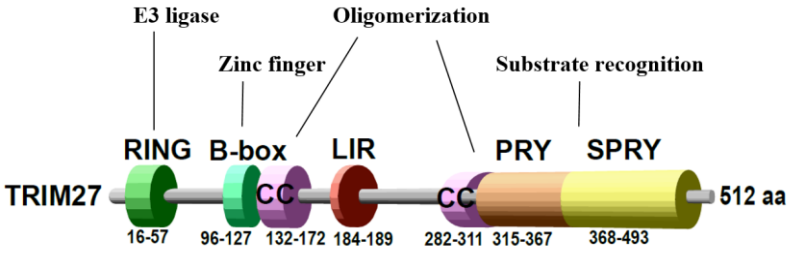

Figure 14. TRIM27 structure. A RING-finger domain, a B-box, two coiled-coil domains, a LIR motif in between the coiled coil domains, followed by a PRY and SPRY domains in its C-terminal form TRIM27.

TRIM27 is involved in the regulation of several cellular processes such as immunity, apoptosis, cell growth, proliferation, transcriptional regulation, tumorigenesis and endosomal

recycling (Nie et al. 2016; Zoumpoulidou et al. 2012; Y. Liu et al. 2014; Zhuang et al. 2016). TRIM27 is reported to have several roles in host defense against pathogens. TRIM27 acts as a host restriction factor during mycobacterial infection, enhancing immune-inflammatory response and cell apoptosis (J Wang et al. 2016). Interestingly, TRIM27 is found downregulated in *mycobacterium tuberculosis* (Mtb) patients compared to latent and healthy subjects, suggesting that TRIM27 might play a role in response to Mtb infection (Y. Chen et al. 2017). In addition, TRIM27 has been identified as a degradation target of Herpes Simple Virus 1 ICP0 (Conwell et al. 2015), and together with USP7 negatively modulates antiviral type I Interferon (INF) signaling (Cai et al. 2018). Additionally, TRIM27 is linked to the regulation of NfKB pathway by mediating the degradation of nucleotide-binding oligomerization domain-containing protein 2 (NOD2) (Zurek et al. 2012). TRIM27 plays a role in endosomal recycling when it is in complex with USP7 and MAGE-L2. This complex regulates the activity of the WASH/retromer-mediated endosomal recycling through its ubiquitylation status (Hao et al. 2015).

TRIM27 has been identified as an oncogene, highly expressed in various cancer types such as breast cancer (Xing et al. 2020). TRIM27 promotes proliferation mainly through its nuclear function, participating in transcriptional regulation complexes (Horio et al. 2012; Iwakoshi et al. 2012; Tsukamoto et al. 2009; G. G. Tezel et al. 2009; Nie et al. 2016; H. X. Zhang et al. 2018; Y. Zhang et al. 2018). It has also been proposed to be involved in cell migration and invasion (Y. Zhang et al. 2018). TRIM27 acts as a transcription repressor through interactions with myocardin related transcription factor B (MRTFB) (Kato et al. 2014), retinoblastoma susceptibility gene (RB1) (Zoumpoulidou et al. 2012), and enhanced of polycomb (EPC) (Shimono et al. 2000). TRIM27 also mediates the IL-6-induced activation of STAT3 via a retromer-dependent pathway, leading to inflammation associated cancer development (H. X. Zhang et al. 2018). Moreover, a recent study suggests that TRIM27 plays a role in the Hippo-BIRC5 axis in gastric cancer, a crucial pathway in regulating tissue homeostasis and organ growth (Y. Yao et al. 2020).

TRIM27 is involved in the regulation of apoptosis via ubiquitylation of PTEN, which inhibits its phosphorylation activity and does not allow the PTEN-dependent activation of TRAIL expression (Lee et al. 2013). PI3K/AKT pathway plays an important role in cancer progression through its involvement in cellular metabolism. (Q. Wang, Chen, and Hay 2017) Growing evidences show that TRIM27 regulates the action of this pathway through different mechanisms. On one side, TRIM27 has been shown to activate p-AKT in colorectal cancer (Y.

Zhang et al. 2018). In addition, TRIM27 controls PTEN activity, which suppresses the activation of AKT via PTEN on esophageal squamous cell carcinoma (ESCC) (L. Ma et al. 2019). Furthermore, PTEN/AKT axis has been shown as a target in suppressing glycolysis activity in cancer cells under hypoxic conditions (F. Chen et al. 2015), which represents a link between TRIM27 and glycolysis metabolism.

TRIM27 has been associated with several human diseases such as Parkinson's disease (Y. Liu et al. 2014), immune disorders and cancer (Watanabe and Hatakeyama 2017). TRIM27 expression levels have been found upregulated in a variety of human cancers, including breast, endometrial, lung and colon cancer (Xing et al. 2020; Tsukamoto et al. 2009; S. Liu et al. 2020; Zoumpoulidou et al. 2012). Altogether, the important role of TRIM27 in cancer development and metastasis seems evident, however, the mechanistic through which TRIM27 acts is not fully elucidated yet.

TRIM32 and TRIM32-related diseases

TRIM32 is a part of the TRIM family proteins subgroup C-VII. This group is characterized by the presence of NHL (NCL-1, HT2A and LIN-41) motifs in its C-terminal (Figure 15). TRIM32 contains six NHL repeats, which mediate protein-protein interaction (Slack and Ruvkun 1998). Of note, NHL domains have a positively charged top surface, which is able to bind RNA (Loedige et al. 2013). This suggests that TRIM-NHL family play a role as miRNA regulators (Tocchini and Ciosk 2015). The B-box and the RING domain cooperate to specify TRIM32 subcellular localization (Lazzari and Meroni 2016). Additionally, the B-box of TRIM32 is responsible for its oligomerization, which is necessary for its catalytic activity (Koliopoulos et al. 2016). TRIM32 undergoes auto-ubiquitylation in presence of E2 enzymes belonging to the D and E subfamilies (Napolitano et al. 2011). Due to the ability of TRIM32 to work with several UBE2 enzymes, its catalytic activity leads to several possibilities of ubiquitin chains on the substrates. TRIM32 is able to tag both K48, mainly implicated in proteasomal degradation (Grice and Nathan 2016), and K63, which is strongly implicated in immune signaling and autophagy (Erpapazoglou, Walker, and Haguenauer-Tsapis 2014). Hence, TRIM32 leads the ubiquitylated proteins to different fates.

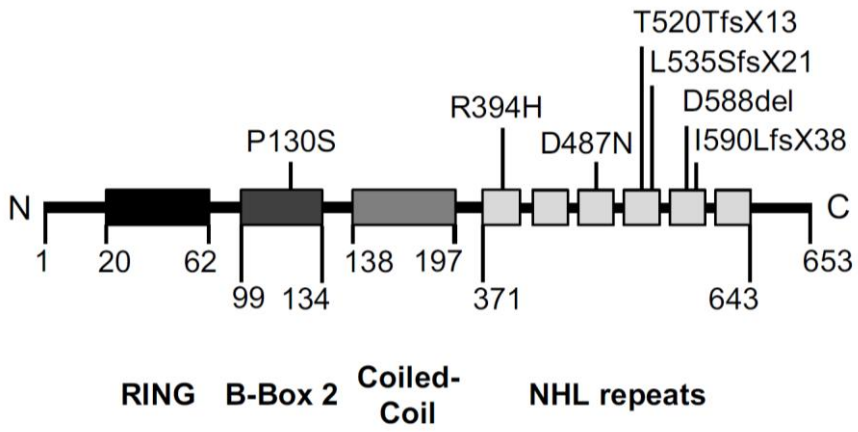

Figure 15. TRIM32 structure and diseases-related mutations. TRIM32 is formed by the RBCC motif characteristic of the TRIM protein family, followed by 6 NHL domains. A point mutation in the B-box (P130S) causes BBS11, and the six marked mutations of the NHL cause LGMD2H. From (Lazzari and Meroni 2016)

TRIM32 expression is detectable in all cells of the body, with high expression levels in the brain and heart (Frosk et al. 2002). Among the identified substrates of TRIM32, there are many muscular-relevant proteins such as actin, α-actinin, desmin, tropomyosin, suggesting that TRIM32 has an important role in muscle homestosasis (Cohen et al., 2009; Kudryashova et al., 2005). Other TRIM32 substrates are cell cycle regulators such as c-Myc, MYCN and p53 (Lazzari and Meroni 2016). In addition other proteins that become substrates of TRIM32 are the cytoplasmic enzyme NDRG2 (Mokhonova et al. 2015), the RARα nuclear receptor (Sato et al. 2011), the PB1 viral RNA polymerase and the innate immunity adaptor STING (J. Zhang et al. 2012).

As mentioned, TRIM32 has a large number of substrates that are tagged for protein degradation, therefore it comes as no surprise that the impairment of the degradation of some of those substrates leads to several human pathologies. E3 ligases play an essential role in muscular physiology, especially in muscular atrophy (Sandri 2013). Genetic mutations in the NHL domains of TRIM32 cause the muscle disorder Limb Girdle Muscular 4 Dystrophy 2H (LGMD2H), which is associated with impaired auto-oligomerization and self-ubiquitylation, and reduced TRIM32 expression level (Zhao et al., 2019, Locke et al., 2009). TRIM32 is associated with this muscular disease through seven mutations in the NHL domain: D487N, R394H, V591M, D588del, T520TfsX13, L535SfsX21 and I590LfsX38 (Figure 15). LGMD2H caused by TRIM32 mutations is a form of autosomal recessive muscular dystrophy. LGMD2H patients present a wide range of symptoms, ranging from no apparent muscular impairment to severe muscle weakness (Lazzari et al. 2019). Conversely, a missense-mutation (P130S) in the B-Box domain results in the disease Bardet-Biedl syndrome 11 (BBS11), which has a

pleiotropic phenotype (Chiang et al., 2006). BBS11 is characterized by obesity, retinal degradation, genito-urinary tract malformations, and cognitive impairment (Chiang et al. 2006). Interestingly, BBS11 patients do not show any muscle alterations, highlighting the functionality differences between the B-box and NHL domains of TRIM32. A mouse TRIM32 model created by (Kudryashova et al. 2009) found that muscular dystrophy caused by TRIM32 mutations involves both neurogenic and myogenic characteristics. This same group produced a Knock-In (KI) mouse model with the LGMD2H mutation D487N. Interestingly, this mutation destabilizes the protein, which leads to its degradation, resulting in the same phenotype as TRIM32 mice (Kudryashova et al. 2011). Further studies by this group with the TRIM32 null mice showed that even though TRIM32 plays a key role in muscle regrowth after atrophy, it is not necessary to trigger muscle atrophy (Kudryashova, Kramerova, and Spencer 2012). Even though the pathological mechanism of TRIM32 that leads to LGMD2H is still unclear, several studies suggest that the loss of E3 ligase activity and/or interaction properties of TRIM32 are involved in the pathogenesis of this disease.

Several proteins involved in tumorgenesis are found among TRIM32 substrates (Lazzari and Meroni 2016). Depending on the context and the targeted protein, TRIM32 acts as an oncogene or a tumor suppressor. TRIM32 expression has been found increased in colorectal cancer, lung cancer, hepatocellular carcinoma and head and neck squamous cell carcinoma (Lazzari and Meroni 2016; T. T. Zhao et al. 2018; Ju Liu et al. 2014). On one side, TRIM32 regulates p-53-mediated cellular stress responses. In response to stress, the tumor suppressor p53 induces the expression of TRIM32. Consequently, TRIM32 interacts and sends p53 to degradation, creating a feedback loop that regulates the activity of p53 (Ju Liu et al. 2014). Moreover, TRIM32 is responsible for the degradation of tumor suppressor Abl interactor 2 (Abi2), promoting cell proliferation, transformation and metastasis (Kano et al. 2008). Additionally, TRIM32 has been shown to positively mediate TNF-induced apoptosis via proteasomal degradation of the anti-apoptotic factor XIAP (Ryu et al. 2011). TRIM32 also regulates UVB-induced keratinocyte apoptosis through induction of NFkB by the degradation of its inhibitor Piasy (Albor et al. 2006). Furthermore, TRIM32 supports MYCN degradation, promoting asymmetric cell division in neuroblastoma cells (Izumi and Kaneko 2014). A recent study found that TRIM32 interacts and degrades the transcription factor Gli1, which is involved in sonic hedgejog (SHH) signaling (M. Wang et al. 2020). This pathway is involved in neurogenesis during development and its dysregulation often leads to tumorgenesis. In this

context, TRIM32 acts as a tumor suppressor. All these roles of TRIM32 in different cellular pathways show its prominent implication in cancer development.

Moreover, it has also been shown that TRIM32 activates ULK1 via the autophagy cofactor AMBRA 1, facilitating autophagy in muscle cells upon atrophy induction (Di Rienzo, Piacentini, and Fimia 2019). Importantly, the LGMD2H disease mutant of TRIM32 was unable to associate with ULK1 and induce autophagy (Di Rienzo, Piacentini, and Fimia 2019). These findings suggest that TRIM32 is involved in the regulation of autophagy in muscle cells.

Aim of the study

This project was born from a screen of 22 different TRIM proteins using the double-tag assay, which represented the 11 TRIM family subgroups. The goal of this screen was to identify candidates with a potential role in autophagy, alleging that their presence in the lysosome liked them somehow with the autophagy process. Previous studies have already recognized some TRIM proteins as regulators and receptors in selective autophagy. Our hypothesis was that within the 80 members of the TRIM family, there are additional TRIM proteins that are degraded by autophagy and might potentially function as autophagy receptors or regulators. From the screen, TRIM27, TRIM32 and TRIM45 were identified as new potential autophagic substrates. We decided to further investigate the roles of TRIM27 and TRIM32 in autophagy, to try to test our hypothesis.

The following aims were defined to test this hypothesis:

1. Identify if these TRIM proteins are autophagy substrates
2. Identify which part of the core autophagy machinery is mediating their autophagic degradation
3. Identify if these TRIM proteins have characteristics as autophagy receptors
4. Identify if these TRIM proteins have any specific role in autophagy

Summary of papers

Paper I

TRIM27 is an autophagy substrate implicated in autophagy induction and regulation of LAMP2

Garcia, J.G., Overå, K.S., Bhujabal, Z., Knutsen, E., Evjen, G., Lamark, T., Johansen, T., Sjøttem, E.

Manuscript

In this study, we investigated the role of TRIM27 in autophagy. Firstly, we identified TRIM27 as an autophagic substrate, which degradation was depended on ATG7 and the SLRs family of autophagy receptors. We mapped a LIR domain in its coiled coil region with specificity towards LC3C and GABARAP. Establishment of HEK293 FlpIn TRIM27 KO cells showed that TRIM27 has an effect in starvation-induced autophagy. Reconstitution of the TRIM27 KO cells with EGFP-TRIM27 showed that TRIM27 associates with core autophagy proteins and the SLRs p62 and NBR1. Furthermore, TRIM27 interacts directly with and ubiquitylates p62. Interestingly, the TRIM27 KO cells displayed high levels of LAMP2 expression, forming big LAMP rings in the cytosol of the cells. TRIM27 is described as an oncogene, and we found TRIM27 mRNA levels to be strongly upregulated in cancer tissue from breast cancer patients, as well and in various breast cancer cell lines. Intriguingly, TRIM27 expression seems to be inversely correlated with LAMP2 and LC3B expression in the analyzed cell lines, linking TRIM27 to the regulation of autophagy in breast cancer cell lines Thus, these cell lines are potentially a model system to identify the roles of TRIM27 in autophagy in breast cancer and its implication in the pathology of this cancer.

Paper II

TRIM32, but not its muscular dystrophy-associated mutant, positively regulates and is targeted to autophagic degradation by p62/SQSTM1.

Overå, K.S., Garcia, J.G., Bhujabal, Z., Jain, A., Øvervatn, A., Larsen, K.B., Deretic, V., Johansen, T., Lamark, T., and Sjøttem, E. (2019).

J. Cell Science. PMID 31828304.

In this first study on TRIM32, we identified TRIM32 as an autophagic substrate. TRIM32 degradation was mediated the Sequestrome-like receptor p62 in an ATG7 dependent pathway. We showthat TRIM32 directly interacts and ubiquitylates p62on lysine residues involved in the

regulation of p62 activity. This forms a feedback loop between TRIM32 and p62. Interestingly, the TRIM32 mutant implicated in the muscular dystrophy disease LGMD2H was not able to undergo autophagic degradation and failed to ubiquitylate p62. In contrast, the BBS11 disease mutant strongly facilitated p62 ubiquitylation, sequestration and degradation. These findings pointed to a dual role of TRIM32 in autophagy, as a cargo and a regulator of p62. Notably, the LGMD2H mutation phenotype suggests thatdysfunctional TRIM32-mediated regulation of p62 may represent one of the pathological mechanisms of this disease.

Paper III

TRIM32 – a putative regulator of NDP52 mediated selective autophagy

Garcia, J.G., Bhujabal, Z., Overå, K.S., Sjøttem, E.

Manuscript

In paper III, we further studied the role of TRIM32 towards the other SLRs, which we identified in paper II as putative mediatorss of TRIM32 degradation by autophagy. In this study, we show that TRIM32 downregulates the protein levels of all SLR proteins. Focusing on NDP52, we show that TRIM32 interacts directly with and ubiquitylates NDP52. On the other side, NDP52 was able to direct autophagic degradation of TRIM32. NDP52 is important for recruiting ULK1 and the autophagic machinery to damaged mitochondria. We show that reintroduction of TRIM32 in TRIM32 KO cells leads to ULK1 stabilisation, and increased phosphorylation of the autophagic regulator TBK1. Conversely, the LGMD2H mutated version of TRIM32 does not affect NDP52 and ULK1 expression, or facilitate TBK1 autophosphorylation. Finally, we show that mitophagy is impaired in TRIM32 KO cells compared to normal cells and TRIM32 KO cells reconstituted with TRIM32. Thus, TRIM32 seems to be a regulator of NDP52, ULK1 and TBK1, which together may facilitate selective degradation of mitochondria.

Paper IV

Generation of the short TRIM32 isoform is regulated by Lys 247 acetylation and a PEST sequence

Garcia-Garcia J., Overå, K.S., Khan, W., Sjøttem, E.

PLOS One. In revision.

In paper IV, derived from our findings in paper II, we studied how TRIM32 auto-ubiquitylation regulates its activity and stability. TRIM32 has two variants, a full-length protein and a truncated protein. However, the mechanism regulating these two isoforms is poorly understood. In this third study, we found that TRIM32 contains a PEST sequence located in the unstructured

region between the coiled coil domain and the NHL repeats. This PEST sequence directs the cleavage of TRIM32, resulting in a cleaved protein similar to the short isoform. Furthermore, we found that the exposure of this PEST sequence seems to be regulated by ubiquitylation and acetylation of the lysines K50, K247 and K401. The produced short isoform is catalytic inactive, suggesting a dominant negative role. This was a novel finding since to date, no PEST sequence had been identified in TRIM proteins.

Discussion

The central theme of this thesis is the role of two TRIM proteins in selective autophagy. I joined this project born from a screen of 22 different TRIM proteins using the double-tag assay, which represented the 11 TRIM family subgroups. The goal of this screen was to identify candidates with a potential role in autophagy, alleging that their presence in the lysosome linked them somehow with the autophagy process. The knowledge surrounding the role of TRIM proteins in autophagy has increased in the recent years. TRIM proteins show several links to autophagy, and one of them is the function as autophagy receptors. Previous studies have already recognized TRIM5α, TRIM13, TRIM16, TRIM20, TRIM21 and TRIM63 as regulators and receptors in selective autophagy (Kimura, Mandell, and Deretic 2016). From our screen, TRIM27, TRIM32 and TRIM45 were identified as new potential autophagic substrates. We decided to further investigate the roles of TRIM27 and TRIM32 in autophagy, and our findings are presented in the following papers. In paper I, we investigated the role of TRIM27 in autophagy, finding that TRIM27 has an effect in starvation-induced autophagy and associates with core autophagy proteins and the SLRs p62 and NBR1. Furthermore, TRIM27 interacts and ubiquitylates p62/SQSTM1 (hereafter p62). TRIM27 KO cells show high levels of LAMP2 expression, forming big LAMP rings in the cytosol of the cells. Furthermore, we found TRIM27 mRNA levels to be strongly upregulated in cancer tissue from breast cancer patients, as well and in various breast cancer cell lines. Intriguingly, TRIM27 expression seems to be inversely correlated with LAMP2 expression in the analyzed cell lines. In paper II, we examined the autophagic role of TRIM32 including two TRIM32 mutations associated with two different diseases. In this first study on TRIM32, we found that TRIM32 is directed to autophagic degradation by p62, but also a regulator of p62 autophagic activity. This formed feedback loop was controlled by the direct interaction and ubiquitylation of p62 by TRIM32. Interestingly, the TRIM32 mutant implicated in the muscular dystrophy disease LGMD2H failed to ubiquitylate p62. In paper III, we further studied the role of TRIM32 towards the other SLRs. In this study, we found that TRIM32 interacts and ubiquitylates the autophagy receptor NDP52, stabilizes the phosphorylated form of TBK1 and facilitates mitophagy. In paper IV, derivate from our findings in paper II, we studied how TRIM32 auto-ubiquitylation regulates its activity and stability. In this third study, we found that TRIM32 contains a PEST sequence, which exposure seems to be regulated by ubiquitylation and acetylation of the lysines K50, K247 and K401. This was a novel finding since to date, no PEST sequence had been identified in TRIM proteins.

Taken together, these findings highlight the pivotal role of TRIM proteins as regulators of autophagy.

Exploring the role of TRIM27 in autophagy

We hypothesized that the presence of TRIM27 in the lysosomes using the double-tag assay could be an indicative of this TRIM protein playing a role in regulation of autophagy. TRIM27 is part of the same subclass as TRIM5α, a well-recognized TRIM that acts as an autophagy receptor upon viral infection (Keown et al. 2018). We could not help but wonder if TRIM27 might act in a similar manner. In an attempt to answer this question, we tried to further investigate how TRIM27 ended up in the lysosomes. Flow cytometry assays using HEK293 FlpIn cells with inducible expression of EGFP-TRIM27 (Larsen et al. 2010) showed that TRIM27 could be degraded by both the proteasomal and the autophagic pathway, having the proteasome as the main degradation pathway both under normal and starved conditions (data not shown). Many TRIM proteins have a role and interact with the autophagy machinery under very specific circumstances, such as oxidative stress or invasion of pathogens (Kumar Jena et al. 2018; Sparrer et al. 2017). Therefore, TRIM27 might not have an active role in basal conditions, but it is plausible that another type of stimuli leads to the activation of TRIM27 autophagic function, thus ending up in the lysosomes. In this study, we show that TRIM27 autophagic degradation is mediated by the SLRs family of autophagy receptors in an ATG7 dependent pathway, pointing to selective autophagy being responsible for TRIM27 degradation.

It is recently shown that the only transmembrane autophagy protein ATG9 plays an important role in the nucleation of the autophagosome (Sawa-Makarska et al. 2020). ATG9 vesicles traffics from Golgi to endosomes in a ULK1-dependent manner under stress conditions (Young et al. 2006), and ULK1 phosphorylation regulates trafficking of ATG9 under autophagy-inducing conditions (Zhou et al. 2017). In this work, we show that depletion of ATG9 leads to increased levels of TRIM27. Further, TRIM27 seems to be modified in the ATG9 KO cells, resulting in a slower migrating band visualized by Western blotting. Moreover, certain EGFP-TRIM27 bodies co-localized with ATG9 in the reconstituted HEK293 FlpIn EGFP-TRIM27 cell line. Interestingly, the autophagy receptors p62 and NBR1 also displayed increased protein levels in the ATG9 KO cells, and occurred as slower migration bands on the Western blot gels. This clearly points to TRIM27 as an autophagy substrate similarly as NBR1 and p62. In contrast, the autophagy receptor NDP52 did not display aberrant mobility in the ATG9 KO cell

extract, even if its protein level were slightly increased. Protein levels of lipidated LC3B were decreased in the ATG9 KO cells. This is in line with recent reports describing that ATG9 vesicles recruit the autophagy machinery and establish membrane contact sites with membrane donor compartments. ATG2 mediates transfer of lipids from donor membrane to the autophagosome formation sites, leading to PIP3 formation and ATG8 lipidation. Hence, lipidation of LC3 is dependent on ATG9 vesicles (Sawa-Makarska et al. 2020). Interestingly, we observed decreased levels of LC3B dots in the HEK293 FlpIn TRIM27 KO cell lines, indicative of reduced LC3B lipidation in these cells. Seeing that some autophagy related proteins such as the autophagy receptors p62 and NBR1 are modified upon ATG9 depletion, raise the question if ATG9 vesicles contain more than lipids. There is the possibility that ATG9 vesicles contain protein modifiers such as phosphatases or de-ubiquitinases (DUBs), which are able to modify TRIM27, p62 or NBR1. The impairment in the delivery of those modifiers could explain the slower migrating bands we have observed. Another plausible scenario is that ATG9 depletion inhibits the degradation of certain autophagy-related proteins and consequently they accumulate. This accumulation of non-degraded proteins may recruit E3 ligases and kinases that modify them. The role that ATG9 plays in promoting these changes in TRIM27, p62 and NBR1 is a question that would be interesting to address in future experiments.

In this study, we found that TRIM7 interacts with p62 *in vitro* and co-precipitates and co-localizes with p62 in cells. However, interaction of TRIM27 with NDP52 was only seen by GST-pull down assays, which does not represent the real environment of the cell. However, we also observed that NDP52 mediated TRIM27 degradation in Penta KO cells reconstituted with NDP52. These results suggest that NDP52 may have a connection with TRIM27. NDP52 is a big player in xenophagy, detecting invading pathogens and bringing them do degradation (Verlhac, Viret, and Faure 2015). NDP52 interacts specifically with LC3C via a so-called CLIR motif, and this interaction was proposed to be crucial for innate immunity since cells lacking either protein was not able to protect their cytoplasm against *Salmonella* (von Muhlinen et al. 2012). We found that TRIM27 contains a LIR motif in between its coiled-coil domain. Intriguingly, our results show that the TRIM27 LIR motif also has a preference for LC3C. This may suggest, even though very preliminary, a potential collaboration of TRIM27 and NDP52, linked to LC3C by their LIR motifs. Previous studies on TRIM27 highlight its strong ties to immune signaling regulation (Conwell et al. 2015; Zurek et al. 2012; J Wang et al. 2016). Therefore, these findings may suggest that TRIM27 represents a link between innate immunity and selective autophagy.

In pursuance of getting a better understanding on the role of TRIM27 in selective autophagy, we produced a TRIM27 knock-out cell line in HEK293 FlpIn T-Rex cells with CRISPR-Cas9 technology (Ran et al. 2013), and re-constituted it with EGFP-TRIM27 and EGFP only. EGFP-TRIM27 was very efficiently expressed in the reconstituted cells, hence we used only 100 ng of Tetracycline or Doxycycline to obtain an expression level close to the endogenous expression level of TRIM27. EGFP-TRIM27 seems to be very prone to aggregation, a characteristic we did not observe for f.ex.TRIM32 which expression was re-constituted in HEK293 FlpIn TRIM32 KO cells. . This fact suggested that TRIM27 overexpression produces high levels of ubiquitin, leading to high aggregation. This matter has been a big concern for us over the development of this project, since autophagy is responsible for clearing ubiquitylated protein aggregates in the cell (Lamark and Johansen 2012). The HEK293 FlpIn cell line, TRIM27 KO and reconstituted cell lines stained with different antibodies detecting autophagy related proteins shed some light on this concern. On one side, TRIM27 co-localized with members of the autophagy initiation complex, such as ATG9, ATG13 and ULK1. Moreover, we also found co-localization with the autophagy receptors p62 and NBR1. This raised the question if this co-localization happened to be unspecific and due to the TRIM27 aggregation tendency. For that, we also stained with antibodies against various marker proteins such as LC3B (autophagosome), GM130 (Golgi),Calreticulin (ER), FK2 (Ubiquitin) and UPS7 (recognized TRIM27 interactor). Interestingly, TRIM27 did not co-localize with LC3B more than in a few dots, suggesting that not all autophagy-related proteins were present in the TRIM27 aggregates. Furthermore, TRIM27 was not found in proximity to the Golgi marker GM130 and the ER marker Calreticulin, which was in line with the literature on the cytoplasmic and nuclear localization of TRIM27 (Harbers et al. 2001). In addition, TRIM27 did co-localize with UPS7, which is a well-known interaction partner, as well as ubiquitin (Zaman et al. 2013). These two positive controls indicated that the localization of reconstituted EGFP-TRIM27 is close to the localization of endogenous TRIM27. Unfortunately, this could not be verified by immunostaining of endogenous TRIM27, since we could not find any TRIM27 antibody that worked in immunostaining.

Importantly, our MS analysis of immunoprecipitated EGFP-TRIM27 identified co-precipitation of several autophagy related proteins, among them ATG7, TBK1, LAMP2, p62, NBR1, NDP52 and TAX1BP1. The association of TRIM27 structures with all SLRs further supported our hypothesis that the SLRs mediate TRIM27 degradation. Likewise, the co-precipitation of TRIM27 with ATG7 and LAMP2 also highlighted a link between TRIM27 and autophagy.

Previously, TRIM27 in shown to induce TBK1 degradation via K48-linked ubiquitylation at Lys251 and Lys372 promoted by Siglec1 in interferon type I mediated antiviral innate immune response (Zheng et al. 2015). This supports our finding of TBK1 as one of the potential TRIM27 interactors in the MS analysis. However, we were not able to detect any effect of TRIM27 on TBK1 levels, in neither basal nor starved conditions. This can be explained by the fact that TRIM27 mediated degradation of TBK1 only happens upon stimulation of the antiviral immune system. However, we observed that TRIM27 protein levels in HeLa TBK1 KO cells were stabilized compared to normal HeLa cells (data not shown). This may suggest that TBK1 regulates the protein levels of TRIM27. Due to the pivotal role of TBK1 in autophagy, this is a novel finding that would be worth exploring further.

Surprisingly, we identified LAMP2 as a TRIM27 interaction partner. LAMP2 is a highly glycosylated protein decorating the luminal surface of lysosomal membranes (E. L. Eskelinen, Tanaka, and Saftig 2003). It is an important regulator of maturation of autophagosomes, and LAMP2 deficiencies leads to accumulation of autophagosomes (Saftig, Beertsen, and Eskelinen 2008). Depletion of TRIM27 either by genetic KO, or by TRIM27 siRNA treatments, resulted in accumulation of LAMP2 protein levels, and the formation of large LAMP2 rings in HEK293 FlpIn cells. The large LAMP2 rings were often localized in the perinuclear region, in close proximity with TRIM27 bodies and mitochondria. Whether LAMP2 accumulation as such leads to formation of large lysosomes, or whether these large LAMP2 rings indicate that TRIM27 is implicated in the regulation of lysosome biogenesis, is an interesting question to address in further studies. However, we clearly show that TRIM27 deficiency results in accumulation of LAMP2. This accumulation can be due to impaired degradation of LAMP2 in TRIM27 KO cells, since TRIM27 is an E3 ligase that directs proteins to degradation by ubiquitylation. Alternatively, it can be due to increased expression of LAMP2 at the transcriptional level.

TRIM27 has been proposed as a oncogene promoting cell proliferation (Zurek et al. 2012), as well as cell migration by activating EMT (Y. Zhang et al. 2018). In this study, HEK293 FlpIn TRIM27 KO cells showed an enhanced proliferation rate compared to normal HEK293 FlpIn cells. This is partially in contradiction with the general literature, proposing that TRIM27 facilitates cell proliferation (Y. Yao et al. 2020; Zoumpoulidou et al. 2012; Y. Ma et al. 2016). This may suggest that the effect of TRIM27 on cell proliferation is dependent on the specific cancer cell type. On the contrary, the migration capacity of HEK293 FlpIn TRIM27 KO cells was decreased compared to normal HEK293 FlpIn cells or the TRIM27 KO cells reconstituted with EGFP-TRIM27. This is in line with other studies studies suggesting a role of TRIM27 in

EMT (Y. Zhang et al. 2018). Therefore, the reconstituted HEK293 FlpIn TRIM27 KO EGFP-TRIM27 cells seem to be a realiable source that mimic the function of endogenous TRIM27.

Interestingly, we found LAMP2 expression to be upregulated in the breast cancer cell lines displaying no or very low expression levels of TRIM27. This correlates well with our analyses in HEK293 cells, suggesting that loss of TRIM27 leads to enhanced LAMP2 expression. LAMP2 plays a role in the support of early cancer progression, helping cancer cells surviving in acidic enviroments (Mogami et al. 2013). LAMP2 is highly expressed in several cancers, where reduced expression of LAMP2 has been associated with a loss of migration and invasion capabilities (Koukourakis et al. 2015). LAMP2A isoform has shown increased expression in breast tumor tissue, and its inhibition results in sensitation of tumor cells to radioation and doxorubicin therapy (Saha 2012). Autophagy helps cancer cells to survive under nutrient and oxygen stress (Filomeni, De Zio, and Cecconi 2015). TRIM27 seems to facilitate starvation induced autophagy. Hence, this can be one mechanism that TRIM27 uses to facilitate growth of cancer cells. Collectively, these results point to TRIM27 as a putative regulator of autophagy, and that one of its oncogenic features is to facilitate the autophagy process in cancer cells. Moveover, breast cancer cell lines with various expression levels of TRIM27 represent promising model systems for further revealing the molecular mechanisms of TRIM27 in autophagy and cancer.

TRIM32 as an autophagic substrate and its role in autophagy

After identifying the presence of TRIM32 in the lysosome both under normal and starvation conditions, the first question that raised was how it ended up in the lytic compartment. In order to answer this broad question, we firstly investigated who was in charge of the degradation of TRIM32. BafA1 and MG-132 are widely used lysosomal and proteasomal inhibitors respectively. The effect of these two inhibitors on the levels of TRIM32 showed that both pathways mediate the degradation of TRIM32. Proteasomal degradation of TRIM32 showed to be the main degradative pathway under normal conditions, whereas autophagy was equally implicated in the degradation of TRIM32 under starving conditions. These results suggest a potential link of TRIM32 in autophagy. Later we found that the degradation of TRIM32 was dependent on ATG7 and the SLRs. The main SLRs responsible for bringing TRIM32 to the lysosomes were the autophagy receptors, p62 and NDP52. Moreover, we found a direct interaction and ubiquitylation of those SLRs by TRIM32. Moreover, we show that NBR1 seems also to mediate TRIM32 autophagy degradation, however, we have not proven any interaction.

It has been reported that TRIM32 interacts with the autophagy receptor TAX1BP1 (Yang et al. 2017). However, our results did not show a TAX1BP1-dependent degradation of TRIM32 (data not shown), meaning that TAX1BP1 is associated with TRIM32 but does not mediate its degradation by autophagy. This difference might be due to this interaction being cell-type specific, in our study we used Hela cells, while Yang et al. 2017 used HEK293 cells. Nonetheless, we cannot exclude OPTN and TAXBP1 as potential mediators of TRIM32 autophagic degradation just yet, since we used an over-expression system and more experiments are needed to rule them out.

The lipidation of LC3-I to LC3-II is a widely used autophagy marker, using the number of LC3-II in the cell as the number of autophagosomes formed (Yoshii and Mizushima 2017). Another commonly used marker to evaluate autophagy is p62, which binds LC3 and is degraded in the lysosome (Pankiv et al. 2007). Our results showed co-localization of TRIM32 with LC3B and p62. TRIM32 ablation showed a reduction of the formation of p62 dots compared to TRIM32 WT. Of note, the inhibition of autophagosome degradation also increases the amount of LC3-II and p62 (Bjørkøy et al. 2005; Tanida et al. 2005). Thus, the amount of LC3-II and p62 in the cell might not accurately represent the degradation of autophagosomes, since it does not allow us to distinguish if the observed effect is due to the induction of autophagy or its inhibition. Moreover, it has been shown that LC3B-II is also localized in non-autophagic structures not associated with the lysosome, commonly due to overexpression of the protein by transient transfection or the formation of aggregates (Kuma, Matsui, and Mizushima 2007). To try to answer this question, we analyzed the protein levels of both the SLRs and LCB in TRIM32 KO cells. The cells lacking TRIM32 display higher expression of all SLRs (p62, NBR1, NDP52, Optineurin and TAX1BP1), and this effect is recovered when reconstituting with myc-TRIM32^{WT}. We analyzed the mRNA levels of these SLRs in the TRIM32 KO, which shows no change on the transcriptional level of the SLRs, meaning that the changes in the expression of the SLRs are due to TRIM32 effects on their degradation rather than their synthesis. Moreover, the analysis of the expression of the SLRs and LC3 on TRIM32 KO cells in starvation conditions followed by a treatment with BafA1 and MG132 did not show a difference between TRIM32 KO and WT, suggesting that TRIM32 ablation does not have an effect on global autophagy. Of note, in paper II we show that reintroducing NDP52 or NBR1 in Penta KO cells facilitates TRIM32 degradation. This suggest that at least to date, three SLRs mediate autophagic degradation of TRIM32, and that their action seems to be independent of each other.

Taken together, these results suggests that TRIM32 autophagic degradation is mediated by selective autophagy.

We observed co-localization of LC3 and TRIM32, thus we wondered if TRIM32 could work as an autophagy receptor itself. In order to try to answer this question, we evaluated the interaction between TRIM32 and the six human ATG8s. Our results showed affinity of TRIM32 towards LC3A, LC3C, GABARAP and GABARAP-L1, while displaying a weak affinity towards LC3B and GABARAP-L2. Our inability finding a LIR motif within TRIM32 by the use of different strategies lead us to think that the interaction of TRIM32 and the mentioned ATG8s was mediated in a non-LIR dependent manner. The autophagy protein RPN10 of *Arabidopsis* contains a UIM-docking site (UDS) that is able to bind ATG8s proteins (Marshall et al. 2019). In the case of TRIM32, where we did not find a UIM motif either, the interaction with ATG8s does not seem to be mediated by one linear motif. Instead, it is likely that this interaction is carried out through several regions of TRIM32. Nevertheless, this interaction could be interesting to investigate further to see whether it has a role in autophagy. Importantly, ATG8s have roles outside autophagy (Lorenzo Galluzzi and Green 2019), therefore, it is plausible that TRIM32 and ATG8s might cooperate together in a non-LIR fashion to perform a function that is not related to autophagy.

TRIM32 and TRIM32-related diseases on p62

To continue to investigate the association between TRIM32 and p62, we analyzed the interaction between these two proteins. Our results showed that TRIM32 interacts with p62 both *in vitro* and in cells. However, the absence of p62 still leaded to TRIM32 RedOnly dots, meaning that p62 is not the only SLR in charge of TRIM32 degradation. Importantly, TRIM32 KO showed lower levels and an impaired turnover of p62, which were recovered by re-introduction of myc-TRIM32. In paper II, we show how TRIM32 ubiquitylates p62, and that ubiquitylation is lost upon TRIM32 ablation or by the use of the deubiquitinase USP2. Catalytically inactive TRIM32^{C44S} also showed the inability to ubiquitylate p62, indicating that TRIM32 E3 ligase activity is in charge of mediating this ubiquitylation reaction.

Genetic mutations in the NHL domains of TRIM32 cause the muscle disorder Limb Girdle Muscular Dystrophy 2H (LGMD2H), whereas a missense-mutation (P130S) in the B-Box domain results in the disease Bardet-Biedl syndrome 11 (BBS11) (Chiang et al., 2006). These two diseases, despite being affected by mutations on the same gene, lead to two completely

different phenotypes. LGMD2H is associated with different degrees of muscle atrophy (Zhao et al., 2019, Locke et al., 2009), whereas BBS11 has a pleiotropic phenotype that shows no effects in muscular homeostasis (Chiang et al., 2006). TRIM32 is associated with this muscular disease through seven mutations in the NHL domain (Saccone et al. 2008; Cossée et al. 2009), however in this study we have focused on the most common, D487N mutation. In order to investigate if these mutations had an effect on the degradation of TRIM32 by autophagy, we reconstituted TRIM32 KO cells with both mutants $TRIM32^{D487N}$ and $TRIM^{P130S}$. The LGMD2H mutant show a very similar phenotype to the one observed in TRIM32 KO cells, characterized by the inability to ubiquitintate p62. Interestingly, $TRIM32^{D487N}$ is able to bind to p62, but does not shows any catalytically activity. As expected, $TRIM32^{D487N}$ is not able to auto-ubiquitylate itself either, due to its catalytically inactive form. These findings are in line with previous studies, where a Knock In mouse model with the LGMD2H mutation D487N shows the same phenotype as the TRIM32 null mice due to the destabilization of the protein and subsequent degradation (Kudryashova et al. 2011). On the contrary, the BBS11 mutant shows the opposite effect. $TRIM32^{P130S}$ is not only able to successfully ubiquitylate p62, but it shows a higher association with the autophagy receptor. Moreover, $TRIM32^{P130S}$ also displays a higher TRIM32 RedOnly dot formation upon starvation in comparison to $TRIM32^{WT}$, suggesting that this mutation in the B-Box may lead to higher autophagic degradation of TRIM32.

TRIM32 requieres oligomerization to be catalytically active, which is provided by its RING domain. The B-Box helps in the oligomerization but it has been shown dispensable (Lazzari et al. 2019). Other TRIM proteins have been reported that their B-Box can confer E3 ligase activity, such is the case of TRIM16 (Bell et al. 2012). However, a recent study showed that this does not seem to be the case of TRIM32 (Lazzari et al. 2019). In the case of TRIM16, this E3 ligase lacks a RING domain but contain two B-Boxes, one of them being structurally similar to a RING domain, and the dimerization of both may resemble to an actual RING domain, thus conferring E3 ligase catalytic activity (Bell et al. 2012). This does not apply to TRIM32 due to their differences in structure, where TRIM32 only contains one B-Box, which does not resemble to a RING domain. The RING domain of TRIM32 is necessary for association with E2 enzymes, whereas the B-Box is not (Napolitano et al. 2011). However, we cannot rule out that the B-Box might determine the topology of the ubiquitin chain together with E2. It has been shown that deletion of the B-Box in TRIM32 and point mutations C100/C103A leads to a slightly higher efficiency in the building of polyubiquitin chains activity due to the closer

proximity of the RING and NHL domains. This suggests that the B-Box might acts as a spacer for modulating TRIM32 processivity (Lazzari et al. 2019). Both the RING domain and B-Box mediate TRIM32 localization. The absence of the RING domain leads to larger aggregates dispersed throughout the cytoplasm, while ablation of the B-Box, leads to less aggregates/cytoplasmic bodies. Interestingly, these RINGless or B-Boxless mutants retain the ability to self-associate (Lazzari et al. 2019). This suggest that these two domains might mediate TRIM32 subcellular localization by the interaction with other proteins, ultimately controlling TRIM32 enzymatic activity since it is a way to regulate the availability of active TRIM32 in cells.

The phenotype of BBS11 has little similarity to the one from LGMD2H. The B-Box of TRIM32 mediates TRIM32 localization, eventually regulating its availability within the cell and therefore its function. Moreover, TRIM32 B-Box might be a regulator of the RING domain catalytic activity by bringing the enzymatic pocket closer to its substrate, which could explain why in our results, P130S shows a higher localization of TRIM32 with p62 (its substrate) and thus, it shows a higher turnover of p62 and a stronger tendency to form TRIM32 RedOnly dots. The symptoms observed in BBS11 patients might be a consequence of the higher efficiency on E3 ligase activity by this point mutation, and its modulation of its localization, eventually impeding or dysregulating the binding of TRIM32 to some of its substrates, which are involved in many cellular processes, leading to a multisystem phenotype.

P62 is commonly organized in flexible polymers where its PB1 domain constitute a helical scaffold. These scaffolds form filaments that are able to bind LC3 and the addition of long ubiquitin chains induces disassembly and shortening of these filaments (Ciuffa et al. 2015). Therefore, it is suggested that p62 forms a highly structured but flexible assembly that provides a large molecular scaffold for the nascent autophagosome, while being able to accommodate the selected cargo (Jakobi et al. 2020). Interestingly, dimerization and ubiquitylation of p62 are incompatible with each other due to the occlusion of the ubiquitin binding sites when dimerized (Isogai et al. 2011). E2 enzymes are in charge of transporting the activated ubiquitin to the E3 ligases, which bind the ubiquitin to the substrate. Nevertheless, E2 enzymes are also able to directly ubiquitylate, which might be a way for the cell to have even more diversity in the control of the pattern of ubiquitylation (Stewart et al. 2016). To date, the two E2 enzymes UBE2D2 and UBE2D3 have been reported to be able to interact and mediate p62 ubiquitylation. The interaction between the E2 enzymes and p62 occurs via the EIR region of p62, which results in ubiquitylation at nine lysine residues, which among those we can find K157 and K295 (Peng

et al. 2017). This poly-ubiquitylation of p62 relieves the inhibition of the UBA domain in the p62 dimer, allowing binding and tethering of ubiquitylated cargo to the ATG8s conjugated to the phagophore (Peng et al. 2017). In an attempt to identify the exacts sides where TRIM32 ubiquitylates p62, we performed an MS analysis with both the $TRIM32^{WT}$ and the TRIM32 disease mutants $TRIM32^{D487N}$ and $TRIM32^{P130S}$. The $TRIM^{D478N}$ mutant was used as a negative control, since it is not able to ubiquitylate p62. Our results showed that p62 was potentially ubiquitylated on two lysines, K157 and K295. Unfortunately, we were unable to map the exact lysines that TRIM32 was able to ubiquitylate in cells, indicating that TRIM32 might ubiquinate p62 in several sites. It would be worth continuing the mapping to find the sites of TRIM32-mediated ubiquitylation of p62. Nonetheless, we did get some interesting observations. Our results showed TRIM32 mono-ubiquitylate p62, potentially on several residues. This mono-ubiquitylation seems to enhance p62 body formation and p62-mediated autophagy. Interestingly, $TRIM32^{D478N}$ was not able to carry out the mono-ubiquitylation of p62, however still shows interaction with p62. This is in line with other studies were this mutant of TRIM32 failed to promote mono-ubiquitylation but still bond dysbindin and its respective E2 enzyme (Locke et al. 2009). TRIM32 has been shown to interact with ULK1 and Piasy, however, this interaction is inhibited by $TRIM32^{D478N}$ (Albor et al. 2006; Di Rienzo, Piacentini, and Fimia 2019). Therefore, the binding site of TRIM32 and p62 is in a different localization than the one between TRIM32 and either ULK1 or Piasy. Among TRIM32 targets, there are many proteins involved in muscle function regulation. The fact that $TRIM32^{D478N}$, which causes LGMD2H, is able to interact with the substrate but not attach an ubiquitin molecule to it might partially lead to the pathology of this disease. The clear phenotype difference between these two diseases suggests the pivotal role of NHL domains in muscle tissue. NHL domains are in charge of protein-protein interaction, thus mutations on those may lead to an effect on the ability to ubiquitylate its substrates and/or auto-ubiquitylation. Interestingly, mutations in NHL domains (D478N) lead to an impairment of TRIM32 catalytic activity, suggesting that NHL domain may also partially regulate this function.

TRIM32, NDP52 and mitophagy

In paper II we show that the degradation of TRIM32 is mediated by p62, but the reconstitution of Penta KO cells with p62 does not completely recover $TRIM32^{WT}$ levels of RedOnly dots. This leads us to think that other SLRs are involved in TRIM32 autophagic degradation. In paper III we show that NDP52 also mediates the autophagic degradation of TRIM32. We also show

the interaction between NDP52 and TRIM32 both *in vitro* and in cells. Moreover, NDP52 levels considerable decrease in TRIM32 KO cells, while its trascription levels are unaffected, suggesting that TRIM32 contributes to autophagic degradation of this receptor. As the case of p62, TRIM32 is also able to ubiquitylate NDP52. Interestingly, both $TRIM32^{WT}$ and the disease mutants $TRIM32^{PS130S}$ and $TRIM32^{D487N}$ equally bind NDP52 *in vitro* and all co-localized with NDP52 in certain dots under normal conditions. Conversely, inhibition of lysosomes by BafA1 produced the accumulation of NDP52 dots. In this context, the co-localizaiton of NDP52 with $TRIM32^{D487N}$ is much lower compared to $TRIM32^{WT}$ and $TRIM32^{PS130S}$. These results suggest that the NDP52 interaction with TRIM32 is independent of TRIM32 catalytic activity.

NDP52 has an important role in the clearance of mitochondria (Vainshtein and Grumati 2020), where it is recruited by PINK1 (Lazarou et al. 2015). Then, NDP52 associates with the ULK1 complex by its interaction with FIP200 (Ravenhill et al. 2019). NDP52-induced mitophagy requires the interaction of NDP52 and FIP200, since this interaction promotes FIP200 membrane binding capacity (Shi et al. 2020). Interestingly, TBK1 is able to induce autophagy in the absence of LC3 (Vargas et al. 2019). We then wondered if TRIM32 might affect the ability of NDP52 to induce mitophagy. For this purpose, we used the double-tag assay on the transmembrane region of the mitochondria protein OMP25 (OMP25TM) (mCherry-EGFP-OMP25TM) as a way to monitor mitophagy, while overexpressing the mitophagy receptor FKBP8 together with its corresponding ATG8 protein and LC3A (Bhujabal et al. 2017). Our results show that TRIM32 ablation reduces the levels of mitophagy compared to HEK293 FlpIn cells, and reintroduction of myc-TRIM32 completely restores the mitophagy activity. Intriguingly, we found ULK1 expression to be upregulated in HEK293 FlpIn TRIM32 KO cells reconstituted with myc-$TRIM32^{WT}$ compared to TRIM32 KO cells. The BBS11 disease mutant $TRIM32^{PS130S}$ displays a similar ULK1 expression level as $TRIM32^{WT}$, whereas $TRIM32^{D487}$ resembles to the TRIM32 KO cells. At this point we wonder if TRIM32 ubiquitylates ULK1, however, our results do not show a difference on the ubiquitylation status of ULK1 either in the TRIM32 KO cells, or reconstituted with TRIM32 both wildtype and mutants. These results suggest that TRIM32 promotes higher levels of ULK1 and this effect depends on TRIM32 E3 ligase activity, but TRIM32 does not mediate the ubiquitylation of ULK1. These results are in line with another study that found that ULK1 is not a direct substrate of TRIM32 (Di Rienzo, Piacentini, and Fimia 2019).

TBK1 kinase plays a dual role in the initiation of mitophagy. This kinase facilitates the interaction of NDP52 and FIP200, a member of the ULK1 complex. Meanwhile, TBK1

associates with the autophagy receptors OPTN, NDP52 and p62, which will recruit the core autophagy machinery and proceed to the formation of the autophagosome. TBK1 becomes activated by the ubiquitin chain binding of OPTN, and in response TBK1 phosphorilates OPTN in the position S177, which promotes OPTN ATG8 recruitment, and in position S473 and S513, which promotes ubiquitin chain binding, TBK1 activation and OPTN retention and efficient mitophagy in vivo (Heo et al. 2015). This creates a self-reinforcing positive feedback mechanism to ensure efficient mitophagy. TBK1 enrichment of the mitochondrial membrane induces the autophosphorylation of TBK1 in position S172. HEK293 FlpIn TRIM32 KO cells show low levels of S172 phosphorylated TBK1, and reconstitution of the KO cells with $TRIM32^{WT}$, $TRIM32^{PS130S}$ or $TRIM32^{D487N}$ lead to increased levels of phosphorylation. This suggest that TRIM32 effect on TBK1 phosphotylation in position S172 is not mediated by its catalytic activity.

To sum up, TRIM32 seems to induce NDP52-mediated autophagy. In this context, the ULK1 complex activation mediated by NDP52 is independent of AMPK and mTOR activity. A previous study shows TRIM32 localized to the mitochondria, further supporting the possibility of TRIM32 playing a role in mediating or regulation mitophagy (J. Zhang et al. 2012). Moreover, TRIM32 interacts with AMBRA1, a mitophagic receptor and a positive regulator of ULK1 activity. It has been reported that AMBRA1 promotes mitophagy by the action of the E3 ligase HUWE1 that acts as an inducing factor (Strappazzon et al. 2020). Moreover, AMBRA1 is able to promote mitophagy in a PINK1/PARKIN- dependent and independent manner (Van Humbeeck, Cornelissen, and Vandenberghe 2011). It would be interesting to further investigate the regulation of both ULK1 and TBK1 by TRIM32 in relation to autophagy. AMBRA1 could be one possible mediator of this regulation. It would also be worth exploring if TRIM32 interacts and has a similar effect in other autophagic receptors. We have described the direct effect that TRIM32 has on p62. Interestingly, this autophagic receptor is also able to mediate mitophagy (Geisler et al. 2010), therefore, we cannot rule out the possibility that TRIM32 has also a regulatory effect on p62-mediated mitophagy. Of note, NDP52 shows a preference for LC3C (von Muhlinen et al. 2012). In paper I we show the high affinity that TRIM32 presents for LC3C, an interaction that seem to be non-LIR dependent. The fact that these two proteins show a preference for LC3C could be a hint of a possible regulation of the autophagosome formation by the action of TRIM32 and NDP52 towards LC3C during mitophagy.

TRIM32 short isoform and its regulation

There are two variants of TRIM32 protein in humans. The main variant, and the one that we have described in paper I and II, is a 653 amino acid protein. Meanwhile, the second variant is formed by only 172 animo acid and lacks the NHL-repeats and the unstructured region between RCC and the NHL-domain (ensemble.org and Uniprot.org Q13049). In paper I and II, we show insights on the function of the long variant of TRIM32 and its role in selective autophagy. TRIM32 requires auto-ubiquitylation and oligomerization to become catalytically active (Overå et al. 2019). However, how this auto-ubiquitylation takes places is not fully understood yet. In order to try to answer this question, we perfomed a Mass spectrometry analysis (MS) of $TRIM32^{WT}$, $TRIM32^{D487N}$, $TRIM32^{P130S}$ to identify which lysine residues in TRIM32 are targeted for auto-ubiquitylation. By the comparison of both $TRIM32^{WT}$ and $TRIM32^{P130S}$, which are both catalytically active, to the catalytically inactive $TRIM32^{D487N}$, we obtained several hints. One on side, $TRIM32^{D487N}$ did not display any ubiquitylated lysine, which was expected from results shown in our previous study (Overå et al. 2019). On the other side, $TRIM32^{WT}$ and $TRIM32^{P130S}$ shown two ubiquitylated peptides in K50 and K401. Additionally, peptides with acetylation on lysine K247 were identified in the TRIM32 disease mutants' precipitates. From these results, we decided to produce plasmids containing mutations of the identified lysines to arginine and analyze their behavior. Peculiarly, the double mutation EGFP-$TRIM32^{K247R/K401R}$ resulted in a partially cleaved protein (mix of cleaved and non-cleaved protein), while the triple mutation EGFP-$TRIM32^{K50R/K247R/K401R}$ leaded to a complete cleavage of TRIM32. The size of this protein was around 20 kDa (excluding the tag), which resembles to the short variant of TRIM32. Intriguingly, this cleaved protein is more prompt to form aggregates near the Golgi, while the full-length TRIM32 isoform is located throughout the cytoplasm as previously described in other studies (Kawaguchi et al. 2017). The short TRIM32 variant should be transcribed with a 3' UTR, which is not recognized so far. Therefore, this short isoform might be the results of post-translational modifications on the long-length TRIM32 variant, which is something that occurs in other proteins (Jianhui Wang et al. 2012). In an attempt to complete this puzzle, and since the use of the deubiquitinase USP2 did not produced any cleavage in TRIM32, we wondered if acetylation on position K247 could be the trigger for this short form of TRIM32. The replacement of the described lysines to glumatine (Q) in order to mimic acetylation, acetylation mimicking in position K247 completely inhibited the cleavage. This restored long-length TRIM32 by K247 acetylation displayed a similar localization as the previously analyzed $TRIM32^{WT}$. To check if autophagy degradation of TRIM32 was affected by these PTM on the lysine residues K50, K247 and K401, we performed

a double-tag assay on the various TRIM32 lysine mutation constructs. This assay showed that the cleaved protein and TRIM32$^{K50R/K247Q/K401R}$ were not able to form any RedOnly dots. The mCherry-EYFP-TRIM32K$^{247R/K401R}$ and mCherry-EYFP-TRIM32^{K247Q} constructs formed RedOnly dots, but to a lesser extent than mCherry-EYFP-TRIM32WT. This suggests that PTMs on the lysine residues K50, K247 and K401 regulate autophagic degradation of TRIM32, and all of them are needed for normal degradation of TRIM32 by autophagy. Thus, the acetylation of TRIM32 on its position K247 seems to be play a pivotal role on its stability. Then we wondered if TRIM32 encodes specific sequences that are exposed to proteolytic cleavage, such as PEST sequences. By the use of the PEST perdiction tool from EMBOSS, we obtained a putative PEST sequence located between amino acid 248 and 270 of TRIM32. Intriguingly, this sequence is located accurately adjacent to lysine K247. A partial ablation of this PEST sequence in TRIM32$^{K50R/K247R/K401R}$ lead to an inhibition of the cleavage, while not compromising the stability of TRIM32 in TRIM32^{WT}. The TRIM32$^{K50R/K247R/K401R}$, which is cleaved, and TRIM32$^{K50R/K247Q/K401R}$, which is full-length, do not display auto-ubiquitylation activity. While, TRIM32^{WT} with a partial deleted PEST sequence and the TRIM32^{K247Q} are both able to auto-ubiquitylate. As we demonstrated in paper II, TRIM32 degradation is mediated by both proteasomal and lysosomal pathways. We did try to pinpoint the pathway implicated in PEST-mediated cleavage of TRIM32, however, we did not find it. Taken together, this shows the importance of lysines K50, K247 and K401 on TRIM32 activity, since the lack of them leads to a catalytic inactive form of TRIM32. It also highlights the critical role that acetylation plays as a post-transcriptional modification, since in the case of TRIM32 we suspect that acetylation prevents the exposure of the PEST sequence to proteolytic enzymes. It would be interesting to investigate how this cleavage of TRIM32 to produce a short isoform occurs, as well as its function in a cellular context.

Methodological considerations

In order to assess of the role of TRIM32 and TRIM27 in selective autophagy we have performed several molecular biology methods, which can be found in the materials and methods section of each paper. Here I discuss the limitations of some of these techniques, as well as the strategies we have used to trouble-shoot and minimize the impact of the flaws of each method.

Double tag assay

A double-tag assay is characterized by tagging a desired protein with fluorescence tags, such as EGFP and mCherry, in order to be able to follow up its presence in the different compartments of the cell, particularly discriminating between the lysosomes and the cytosol. The GFP tag is acid- sensitive while the mCherry tag is acid-insensitive. The GFP tag becomes unstable and degraded in the lysosomes, leading to RedOnly dots (Hundeshagen et al. 2011). In our study, we used this assay to investigate if TRIM32 and TRIM27 were substrates for autophagic degradation. We also used this method to monitor the degradation dynamics of p62 in TRIM32 KO cells, as a way to monitor autophagic flux. This assay is a very useful tool to investigate if the tagged proteins are localized in the lysosome, since the presence of these proteins in the lytic compartment suggests that they may be degraded by the autophagy pathway. However, this tool has main setbacks. One is that it require over-expression of the protein under study, another is that the tag might affect the tagged proteins functionality or their ability to undergo autophagic degradation. Therefore, the observed puncta structures might not mimic endogenous protein. Hence, double-tag assays were only used as an initial screening method in our system, and the interesting findings investigated further by other methods.

In vitro GST pull down essay

GST-pulldown assay was used as a screening tool for identifying the interaction between TRIM27 and TRIM32 with members of the ATG8 proteins, as well as the autophagic receptors p62 and NDP52. This *in vitro* method is a suitable for examining direct interaction and estimate the extent of the affinity between the studied proteins. However, the accuracy of the results obtained in this assay are questionable. The fact that it is performed in vitro leads to an artificial environment far from the one found in cells. Both false positive and false negatives can be generated, leading to physiologically irrelevant data. In cells, proteins are folded and undergo

post-translational modification that produce a functional protein as a final product. *In vitro* translation can produce incorrect folding due to the lack of machinery necessary for this purpose. This might lead to incorrectly folded proteins, which leads to a false positive or negative that is physiologically irrelevant. In addition, proteins showing interaction *in vitro* may never encounter each other inside the cell due to their localization, which can also lead to a false positive. On the contrary, the proteins that require a post-translational modification to interact with others might show a negative result, leading to a false negative. In this study, *in vitro* GST pulldown was used in combination with methods performed in cells, such as immunoprecipitation and immunostaining, proving the interaction at a cellular level.

CRISPR/Cas9 technology

The CRISPR/Cas9 techonology was used in this study to generate TRIM27 and TRIM32 KO cell lines. CRISPR stands for Clustered Regularly Interspaced Short Palindromic Repeats and are part of the microbial adaptive immune system (Ran et al. 2013). First, we produced specific guide RNA sequences targeting the gene of interest early in exon 1 by using bioinformatics tools from Feng Zhang group (Ran et al. 2013), and cloned them into a plasmid expressing Cas9. The enzyme Cas9 cuts double-stranded DNA after recognition of the protospacer adjacent motif (PAM) sequence and binding of guide RNA with its specific target gene sequence (in our case TRIM27 and TRIM32 respectively). Then mammalian DNA repair system non-homologous end joining (NHEJ) or homology directed repair (HDR) repair the DNA, likely leading to a missing of the targeted gene. The guide RNA is normally around 20 nucleotides long. There is the possibility that the guide RNA binds non-targeted genes, leading to off-target effects (Y. Fu et al. 2013). Off-target mutations may cause genomic instability and disruption of otherwise normal genes. In order to identify if the phenotype in due to knock out of the gene of interest, or an off-target effect, several methods can be used: A) validation of the phenotype in more than one KO clone. B) re-introduction of the KO gene into the KO clone and verify that the phenotype is reversed to WT, C) sequence the genome of the KO cells, either by complete genome sequencing or sequence the regions of the genome that have closest similarity to the guide RNA, which are more exposed to off-target effects. In the case of TRIM32 KO, we verified them by A and C. However, in the case of TRIM27 KO, we only managed to obtain one reliable KO clone, thus only verifying by C. We did obtain an alternative KO that showed possible off-target effects. This KO cell seemed displayed a proteolytic activity leading to cut of GFP-tagged proteins, showing a diffuse GFP signal, which really compromised

the reliability of the results. We tried to solve this throwback by additionally using siRNA to prove that the observed effect was due to the KO or KD of TRIM27. The results obtained by either reconstituting the TRIM27 KO cells as well as the use of siRNA show similar results, giving us confidence that the results obtained were a product of the effect of TRIM27 and not off-side effects produced by the technology.

Stable cell lines

The FlpIn T-REX system was used to generate cell lines that stably express TRIM27 and TRIM32 and its mutants. The T-Rex system consists in the use of the regulatory element from *E. Coli* Tn10-encoded tetracycline (Tet) resistance operon (Hillen and Berens 1994). The tetracycline regulation in the T-Rex system is based on the binding of tetracycline to the Tet repression and de-repression of the promoter controlling expression of the gene of interest (F. Yao et al. 1998). Even though desired, an induced expression by this system that leads to the same expression levels as the endogenous protein is rare. The promoter used in the FlpIn system is thepowerful CMV promoter, which activity might not resemble to the endogenous promoter for TRIM27 and TRIM32. This is a very delicate issue in the case of the study of autophagy, since excessive amounts of proteins condensate in the cytoplasm can active this process in an unspecific manner. This was our biggest concern in the case of TRIM27, which was easily overexpressed when induced with tetracycline. We troubleshoot this issue by performing tetracyclinetitration, leading to induction with very low concentration of tetracycline. In the HEK293 FlpIn TRIM32 Kos cells we failed to generate reconstituted cell-lines via the FlpIn system.. In a second attempt to re-constitute the TRIM32 KO cells, we decided to use Lentivirus, which was finally successful. The expression of TRIM27 and TRIM32 was never exactly as the endogenous levels, however, we believe that our results are a reflection of the role of these two TRIM proteins in the cell.

Transfections and ubiquitin assays

Transient transfection is a powerful and fast method to analyze the localization and activity of proteins in the cell without the need of producing stable expressing cell lines. However, the temporality and abundance of the studied protein might not be mimicking the real cellular environment. In all papers in this study, we perform the transfection of a variety of plasmids to

cells mentioned in the materials and methods section of each paper. Even though being a fast and simple method, the big flaw is the effect of over-expression of proteins. Similar to the concerns of the double-tag assay, the plasmids commonly contain a tag attached to the studied protein that can interfere with the functionality of the protein. Moreover, overexpression of a protein can lead to false interactions and localizations that do not represent the endogenous behavior of the protein. We started performing ubiquitylation assays co-expressing tagged ubiquitin together with p62. However, we noticed that the use of ubiquitin alone induced ubiquitylation of p62. This is in line with previous studies, which showed that overexpression of ubiquitin activated autophagy in a p62-dependent fashion (Peng et al. 2017). Moreover, in the case of the overexpression of p62, high amounts of this protein has shown to form aggregates (Pankiv et al. 2007), an effect that can be incorrectly attributed to the knock-out of the TRIM proteins, when in reality is an off-side effect due to p62 nature.

Western Blotting as a quantitative method

In our study, the detection and measurement of protein variations in the cell was measured mainly through Western blot. This well-described method has been used for many years in the biology and biochemistry fields (Mahmood and Yang 2012). Even though this method shows a very high sensitivity and it is able to measure very low protein concentrations, using it as a quantitative method has its risks for several reasons. Western blotting is a multi-step method were all steps are crucial for proper results. This means that many mistakes can happen along the process. The loading of an equal protein concentration is considered a key factor to ensure reliability. Transfer can be done unequally along the membrane, so a good loading shown in a housekeeping gene does not ensure reliability. This is why in our study we have always used Ponceau to check the quality of the transfer of proteins from the gel to the membrane. In addition, housekeeping genes such as PCNA, Actin or GAPDH have been used as loading controls. The high concentrations of these housekeeping genes in comparison to the proteins we want to analyzed is also worth raising doubts. The detection of some proteins, for example TRIM27 and TRIM32, require a high protein loading to ensure being visible when developing the membrane. However, the amount of housekeeping proteins in those samples are in general high, which could potentially lead to misleading loading appreciation due to overexposure. Therefore, in our experiments we have always tried to keep the loading to the minimum in order to minimize this effect.

Use of antibodies in immunoblotting, immunoprecipitation and confocal microscopy

Throughout this study, we have made an extensive use of antibodies for the experiments involving immunoblotting, immunoprecipitation and immunostaining. Antibodies are an essential tool in biomedical research, which in most cases with high specificity towards their targets. Broadly used antibodies, such as the one for p62, show a high degree of specificity and are reliable sources for analyzing the dynamics of the targeted proteins. However, some antibodies might bind to other proteins, leading to unspecific signal. This has been a challenge for us, since the TRIM27 antibody, even though showing specificity towards TRIM27, also bind an unidentified protein present in the serum of the cellular growing media. We made this early discovery when we saw a higher and thick band only in full medium treated cells compared to the ones treated with HBSS. Moreover, TRIM27 antibody did not work properly on immunostaining. We solved this problem using stable cell lines.

In addition, we used immunoprecipitation for analyzing the association of TRIM27 and TRIM32 with other proteins. Mass spectrometry is a powerful tool to identify possible interaction partners, however, the immoprecipitation procedure might not reflect the real situation inside the cell. The preparation of the samples involve the lysis of the cells prior to incubating them with the GFP/MYC-trap. This leads to an artificial environment where cells that do not interact in normal conditions might co-precipitate together due to their proximity.

References

Albor, Amador, Sally El-Hizawi, Elizabeth J. Horn, Melanie Laederich, Patrick Frosk, Klaus Wrogemann, and Molly Kulesz-Martin. 2006. “The Interaction of Piasy with Trim32, an E3-Ubiquitin Ligase Mutated in Limb-Girdle Muscular Dystrophy Type 2H, Promotes Piasy Degradation and Regulates UVB-Induced Keratinocyte Apoptosis through NFκB.” *Journal of Biological Chemistry* 281 (35): 25850–66. https://doi.org/10.1074/jbc.M601655200.

Alers, Sebastian, Antje S Löffler, Sebastian Wesselborg, and Björn Stork. 2012. “Role of AMPK-MTOR-Ulk1/2 in the Regulation of Autophagy: Cross Talk, Shortcuts, and Feedbacks.” https://doi.org/10.1128/MCB.06159-11.

Alessandrini, Federica, Laura Pezzè, and Yari Ciribilli. 2017. “LAMPs: Shedding Light on Cancer Biology.” *Seminars in Oncology*. W.B. Saunders. https://doi.org/10.1053/j.seminoncol.2017.10.013.

Banani, Salman F., Hyun O. Lee, Anthony A. Hyman, and Michael K. Rosen. 2017. “Biomolecular Condensates: Organizers of Cellular Biochemistry.” *Nature Reviews Molecular Cell Biology*. Nature Publishing Group. https://doi.org/10.1038/nrm.2017.7.

Bard, Jared A M, Ellen A Goodall, Eric R Greene, Erik Jonsson, Ken C Dong, and Andreas Martin. 2018. “Structure and Function of the 26S Proteasome.” https://doi.org/10.1146/annurev-biochem.

Bartolini, Desirée, Katiuscia Dallaglio, Pierangelo Torquato, Marta Piroddi, and Francesco Galli. 2018. “Nrf2-P62 Autophagy Pathway and Its Response to Oxidative Stress in Hepatocellular Carcinoma.” *Translational Research*. Mosby Inc. https://doi.org/10.1016/j.trsl.2017.11.007.

Behrends, Christian, Mathew E Sowa, Steven P Gygi, and & J Wade Harper. 2010. “Network Organization of the Human Autophagy System.” https://doi.org/10.1038/nature09204.

Bell, Jessica L., Alena Malyukova, Jessica K. Holien, Jessica Koach, Michael W. Parker, Maria Kavallaris, Glenn M. Marshall, and Belamy B. Cheung. 2012. “TRIM16 Acts as an E3 Ubiquitin Ligase and Can Heterodimerize with Other TRIM Family Members.” *PLoS ONE* 7 (5): 37470. https://doi.org/10.1371/journal.pone.0037470.

Belloni, Elena, Maurizio Trubia, Patrizia Gasparini, Carla Micucci, Cinzia Tapinassi, Stefano Confalonieri, Paolo Nuciforo, et al. 2005. “8p11 Myeloproliferative Syndrome with a Novel t(7;8) Translocation Leading to Fusion of TheFGFR1 AndTIF1 Genes.” *Genes, Chromosomes and Cancer* 42 (3): 320–25. https://doi.org/10.1002/gcc.20144.

Berkamp, Sabrina, Siavash Mostafavi, and Carsten Sachse. 2020. “Structure and Function of P62/SQSTM1 in the Emerging Framework of Phase Separation.” *The FEBS Journal*, December, febs.15672. https://doi.org/10.1111/febs.15672.

Bhatnagar, Sanchita, Claude Gazin, Lynn Chamberlain, Jianhong Ou, Xiaochun Zhu, Jogender S Tushir, Ching-Man Virbasius, et al. 2014. “TRIM37 Is a New Histone H2A Ubiquitin Ligase and Breast Cancer Oncoprotein.” *Nature* 516. https://doi.org/10.1038/nature13955.

Bhujabal, Zambarlal, Åsa B Birgisdottir, Eva Sjøttem, Hanne B Brenne, Aud Øvervatn, Sabrina Habisov, Vladimir Kirkin, Trond Lamark, and Terje Johansen. 2017. “FKBP8 Recruits LC3A to Mediate Parkin-independent Mitophagy.” *EMBO Reports* 18 (6): 947–61. https://doi.org/10.15252/embr.201643147.

Birgisdottir, Åsa B, Trond Lamark, and Terje Johansen. 2013. “The LIR Motif-Crucial for Selective Autophagy.” https://doi.org/10.1242/jcs.126128.

Birna Birgisdottir, Åsa, Stephane Mouilleron, Zambarlal Bhujabal, Martina Wirth, Eva Sjøttem, Gry Evjen, Wenxin Zhang, et al. 2019. “Members of the Autophagy Class III Phosphatidylinositol 3-Kinase Complex I Interact with GABARAP and GABARAPL1 via LIR Motifs.” https://doi.org/10.1080/15548627.2019.1581009.

Bjørkøy, Geir, Trond Lamark, Andreas Brech, Heidi Outzen, Maria Perander, Aud Øvervatn, Harald

Stenmark, and Terje Johansen. 2005. “P62/SQSTM1 Forms Protein Aggregates Degraded by Autophagy and Has a Protective Effect on Huntingtin-Induced Cell Death.” *The Journal of Cell Biology* 171 (4): 603–14. https://doi.org/10.1083/jcb.200507002.

Boeynaems, Steven, Simon Alberti, Nicolas L Fawzi, Tanja Mittag, Magdalini Polymenidou, Frederic Rousseau, Joost Schymkowitz, et al. 2018. “Protein Phase Separation: A New Phase in Cell Biology.” *Trends Cell Biol*. https://doi.org/10.1016/j.tcb.2018.02.004.

Boise, Lawrence H, Arun Upadhyay, Elodie Lafont, Yang Li, Liang Chen, Litian Zhang, Lukman O Afolabi, and Xiaochun Wan. 2020. “Emerging Roles of Tripartite Motif-Containing Family Proteins (TRIMs) in Eliminating Misfolded Proteins.” *Frontiers in Cell and Developmental Biology*. https://doi.org/10.3389/fcell.2020.00802.

Budenholzer, Lauren, Chin Leng Cheng, Yanjie Li, and Mark Hochstrasser. 2017. “Proteasome Structure and Assembly.” *Journal of Molecular Biology*. https://doi.org/10.1016/j.jmb.2017.05.027.

Cai, J, H Y Chen, S J Peng, J L Meng, Y Wang, Y Zhou, X P Qian, et al. 2018. “USP7-TRIM27 Axis Negatively Modulates Antiviral Type I IFN Signaling.” *FASEB J* 32 (10): 5238–49. https://doi.org/10.1096/fj.201700473RR.

Cambiaghi, V, V Giuliani, S Lombardi, C Marinelli, F Toffalorio, and P G Pelicci. 2012. “TRIM Proteins in Cancer.” *Adv Exp Med Biol* 770: 77–91. https://doi.org/10.1007/978-1-4614-5398-7_6.

Carracedo, Arkaitz, Keisuke Ito, and Pier Paolo Pandolfi. 2011. “The Nuclear Bodies inside out: PML Conquers the Cytoplasm.” *Current Opinion in Cell Biology*. Curr Opin Cell Biol. https://doi.org/10.1016/j.ceb.2011.03.011.

Celebi, Gizem, Hale Kesim, Ebru Ozer, and Ozlem Kutlu. 2020. “Molecular Sciences The Effect of Dysfunctional Ubiquitin Enzymes in the Pathogenesis of Most Common Diseases.” *International Journal of Molecular Sciences*. https://doi.org/10.3390/ijms21176335.

Chang, Natasha C. 2020. “Autophagy and Stem Cells: Self-Eating for Self-Renewal.” *Frontiers in Cell and Developmental Biology*. Frontiers Media S.A. https://doi.org/10.3389/fcell.2020.00138.

Chauhan, Santosh, Suresh Kumar, Ashish Jain, Marisa Ponpuak, Michal H. Mudd, Tomonori Kimura, Seong Won Choi, et al. 2016. “TRIMs and Galectins Globally Cooperate and TRIM16 and Galectin-3 Co-Direct Autophagy in Endomembrane Damage Homeostasis.” *Developmental Cell* 39 (1): 13–27. https://doi.org/10.1016/j.devcel.2016.08.003.

Chen, Fenglin, Mingkai Zhuang, Canmei Zhong, Jun Peng, Xiaozhong Wang, Jianying Li, Zhixin Chen, and Yuehong Huang. 2015. “Baicalein Reverses Hypoxia-Induced 5-FU Resistance in Gastric Cancer AGS Cells through Suppression of Glycolysis and the PTEN/Akt/HIF-1α Signaling Pathway.” *Oncology Reports* 33 (1): 457–63. https://doi.org/10.3892/or.2014.3550.

Chen, Wei Xian, Lin Cheng, Ling Yun Xu, Qi Qian, and Yu Lan Zhu. 2019. “Bioinformatics Analysis of Prognostic Value of TRIM13 Gene in Breast Cancer.” *Bioscience Reports* 39 (3). https://doi.org/10.1042/BSR20190285.

Chen, Y, S Cao, Y Sun, and C Li. 2017. “Gene Expression Profiling of the TRIM Protein Family Reveals Potential Biomarkers for Indicating Tuberculosis Status.” *Microb Pathog*. https://doi.org/10.1016/j.micpath.2017.12.008.

Chi, Congwu, Andrea Leonard, Walter E Knight, Kevin M Beussman, Yuanbiao Zhao, Yingqiong Cao, Pilar Londono, et al. 2018. “LAMP-2B Regulates Human Cardiomyocyte Function by Mediating Autophagosome-Lysosome Fusion.” *PNAS* 116 (2). https://doi.org/10.1073/pnas.1808618116.

Chiang, Annie P, John S Beck, Hsan-Jan Yen, Marwan K Tayeh, Todd E Scheetz, Ruth E Swiderski, Darryl Y Nishimura, et al. 2006. “Homozygosity Mapping with SNP Arrays Identifies TRIM32, an E3 Ubiquitin Ligase, as a Bardet-Biedl Syndrome Gene (BBS11).” www.pnas.orgcgidoi10.1073pnas.0600158103.

Choi, Jeong-Mo, Alex S. Holehouse, and Rohit V. Pappu. 2020. “Physical Principles Underlying the

Complex Biology of Intracellular Phase Transitions." *Annual Review of Biophysics* 49 (1): 107–33. https://doi.org/10.1146/annurev-biophys-121219-081629.

Chu, Y, and X Yang. 2011. "SUMO E3 Ligase Activity of TRIM Proteins." *Oncogene* 30 (9): 1108–16. https://doi.org/10.1038/onc.2010.462.

Ciuffa, Rodolfo, Trond Lamark, Terje Johansen, and Carsten Sachse Correspondence. 2015. "The Selective Autophagy Receptor P62 Forms a Flexible Filamentous Helical Scaffold." *CellReports* 11: 748–58. https://doi.org/10.1016/j.celrep.2015.03.062.

Cohen-Kaplan, Victoria, Ido Livneh, Noa Avni, Bertrand Fabre, Tamar Ziv, Yong Tae Kwon, and Aaron Ciechanover. 2016. "P62- and Ubiquitin-Dependent Stress-Induced Autophagy of the Mammalian 26S Proteasome." *Proceedings of the National Academy of Sciences of the United States of America* 113 (47): E7490–99. https://doi.org/10.1073/pnas.1615455113.

Cohen, Shenhav, Jeffrey J. Brault, Steven P. Gygi, David J. Glass, David M. Valenzuela, Carlos Gartner, Esther Latres, and Alfred L. Goldberg. 2009. "During Muscle Atrophy, Thick, but Not Thin, Filament Components Are Degraded by MuRF1-Dependent Ubiquitylation." *Journal of Cell Biology* 185 (6): 1083–95. https://doi.org/10.1083/jcb.200901052.

Conwell, S E, A E White, J W Harper, and D M Knipe. 2015. "Identification of TRIM27 as a Novel Degradation Target of Herpes Simplex Virus 1 ICP0." *J Virol* 89 (1): 220–29. https://doi.org/10.1128/JVI.02635-14.

Corpet, Armelle, Constance Kleijwegt, Simon Roubille, Franceline Juillard, Karine Jacquet, Pascale Texier, and Patrick Lomonte. 2020. "SURVEY AND SUMMARY PML Nuclear Bodies and Chromatin Dynamics: Catch Me If You Can!" *Nucleic Acids Research* 48 (21): 11890–912. https://doi.org/10.1093/nar/gkaa828.

Cossée, Mireille, Clotilde Lagier-Tourenne, Claire Seguela, Michel Mohr, France Leturcq, Hulya Gundesli, Jamel Chelly, Christine Tranchant, Michel Koenig, and Jean Louis Mandel. 2009. "Use of SNP Array Analysis to Identify a Novel TRIM32 Mutation in Limb-Girdle Muscular Dystrophy Type 2H." *Neuromuscular Disorders* 19 (4): 255–60. https://doi.org/10.1016/j.nmd.2009.02.003.

Crawford, L J, C K Johnston, and A E Irvine. 2018. "TRIM Proteins in Blood Cancers." *J Cell Commun Signal* 12 (1): 21–29. https://doi.org/10.1007/s12079-017-0423-5.

Cunningham, Christian N., Joshua M. Baughman, Lilian Phu, Joy S. Tea, Christine Yu, Mary Coons, Donald S. Kirkpatrick, Baris Bingol, and Jacob E. Corn. 2015. "USP30 and Parkin Homeostatically Regulate Atypical Ubiquitin Chains on Mitochondria." *Nature Cell Biology* 17 (2): 160–69. https://doi.org/10.1038/ncb3097.

Czerwińska, Patrycja, Sylwia Mazurek, and Maciej Wiznerowicz. 2017. "The Complexity of TRIM28 Contribution to Cancer." *Journal of Biomedical Science*. BioMed Central Ltd. https://doi.org/10.1186/s12929-017-0374-4.

Davey, Norman E., and David O. Morgan. 2016. "Building a Regulatory Network with Short Linear Sequence Motifs: Lessons from the Degrons of the Anaphase-Promoting Complex." *Molecular Cell*. Cell Press. https://doi.org/10.1016/j.molcel.2016.09.006.

Davidson, Shawn M, and Matthew G Vander Heiden. 2017. "Critical Functions of the Lysosome in Cancer Biology." *Annu. Rev. Pharmacol. Toxicol* 57: 481–507. https://doi.org/10.1146/annurev-pharmtox-010715-103101.

Dignon, Gregory L., Robert B. Best, and Jeetain Mittal. 2020. "Biomolecular Phase Separation: From Molecular Driving Forces to Macroscopic Properties." *Annual Review of Physical Chemistry* 71 (1): 53–75. https://doi.org/10.1146/annurev-physchem-071819-113553.

Dikic, Ivan. 2017. "Proteasomal and Autophagic Degradation Systems." *The Annual Review of Biochemestry*. https://doi.org/10.1146/annurev-biochem.

Ding, F, H Xiao, M Wang, X Xie, and F Hu. 2014. "The Role of the Ubiquitin-Proteasome Pathway in Cancer Development and Treatment." *Front Biosci (Landmark Ed)* 19: 886–95.

https://doi.org/10.2741/4254.

Dossou, Akpedje S, and Alakananda Basu. 2019. “Cancers The Emerging Roles of MTORC1 in Macromanaging Autophagy.” *Cancers*. https://doi.org/10.3390/cancers11101422.

Eberhardt, Wolfgang, Kristina Haeussler, Usman Nasrullah, and Josef Pfeilschifter. 2020. “Molecular Sciences Multifaceted Roles of TRIM Proteins in Colorectal Carcinoma.” *International Journal of Meolcular Sciences*. https://doi.org/10.3390/ijms21207532.

Eisner, Verónica, Martin Picard, and György Hajnóczky. 2018. “Mitochondrial Dynamics in Adaptive and Maladaptive Cellular Stress Responses.” *Nature Cell Biology*. Nature Publishing Group. https://doi.org/10.1038/s41556-018-0133-0.

Enenkel, Cordula, Eyal Gur, Jeroen Roelofs, Shay Ben Aroya, and Ofri Karmon. 2020. “Spatial Organization of Proteasome Aggregates in the Regulation of Proteasome Homeostasis.” *Frontiers in Molecular Biosciences | Www.Frontiersin.Org* 1: 150. https://doi.org/10.3389/fmolb.2019.00150.

Erpapazoglou, Zoi, Olivier Walker, and Rosine Haguenauer-Tsapis. 2014. “Versatile Roles of K63-Linked Ubiquitin Chains in Trafficking.” *Cells* 3: 1027–88. https://doi.org/10.3390/cells3041027.

Eskelinen, Eeva-Liisa. 2006. “Roles of LAMP-1 and LAMP-2 in Lysosome Biogenesis and Autophagy.” *Molecular Aspects of Medicine* 27: 495–502. https://doi.org/10.1016/j.mam.2006.08.005.

Eskelinen, Eeva Liisa, Yoshitaka Tanaka, and Paul Saftig. 2003. “At the Acidic Edge: Emerging Functions for Lysosomal Membrane Proteins.” *Trends in Cell Biology*. Elsevier Ltd. https://doi.org/10.1016/S0962-8924(03)00005-9.

Fan, Shuangqi, Keke Wu, Mengpo Zhao, Erpeng Zhu, Shengming Ma, Yuming Chen, Hongxing Ding, Lin Yi, Mingqiu Zhao, and Jinding Chen. 2020. “Molecular Sciences The Role of Autophagy and Autophagy Receptor NDP52 in Microbial Infections.” *International Journal of Molecular Sciences*. https://doi.org/10.3390/ijms21062008.

Filomeni, G., D. De Zio, and F. Cecconi. 2015. “Oxidative Stress and Autophagy: The Clash between Damage and Metabolic Needs.” *Cell Death and Differentiation*. Nature Publishing Group. https://doi.org/10.1038/cdd.2014.150.

Fracchiolla, Dorotea, Justyna Sawa-Makarska, and Sascha Martenshttps. 2017. “Beyond Atg8 Binding: The Role of AIM/LIR Motifs in Autophagy.” https://doi.org/10.1080/15548627.2016.1277311.

Frosk, Patrick, Tracey Weiler, Edward Nylen, Thangirala Sudha, Cheryl R. Greenberg, Kenneth Morgan, T. Mary Fujiwara, and Klaus Wrogemann. 2002. “Limb-Girdle Muscular Dystrophy Type 2H Associated with Mutation in TRIM32, a Putative E3-Ubiquitin-Ligase Gene.” *American Journal of Human Genetics* 70 (3): 663–72. https://doi.org/10.1086/339083.

Fu, Tao, Jianping Liu, Yingli Wang, Xingqiao Xie, Shichen Hu, and Lifeng Pan. 2018. “Mechanistic Insights into the Interactions of NAP1 with the SKICH Domains of NDP52 and TAX1BP1.” *PNAS*. https://doi.org/10.1073/pnas.1811421115.

Fu, Yanfang, Jennifer A. Foden, Cyd Khayter, Morgan L. Maeder, Deepak Reyon, J. Keith Joung, and Jeffry D. Sander. 2013. “High-Frequency off-Target Mutagenesis Induced by CRISPR-Cas Nucleases in Human Cells.” *Nature Biotechnology* 31 (9): 822–26. https://doi.org/10.1038/nbt.2623.

Fujiwara, Yuuki, Katsunori Hase, Keiji Wada, and Tomohiro Kabuta. 2015. “An RNautophagy/DNautophagy Receptor, LAMP2C, Possesses an Arginine-Rich Motif That Mediates RNA/DNA-Binding.” *Biochemical and Biophysical Research Communications* 460 (2): 281–86. https://doi.org/10.1016/j.bbrc.2015.03.025.

Galluzzi, L, E H Baehrecke, A Ballabio, P Boya, J M Bravo-San Pedro, F Cecconi, A M Choi, et al. 2017. “Molecular Definitions of Autophagy and Related Processes.” *EMBO J* 36 (13): 1811–36. https://doi.org/10.15252/embj.201796697.

Galluzzi, Lorenzo, and Douglas R. Green. 2019. “Autophagy-Independent Functions of the Autophagy Machinery.” *Cell*. Cell Press. https://doi.org/10.1016/j.cell.2019.05.026.

Galluzzi, Lorenzo, Oliver Kepp, Christina Trojel-Hansen, and Guido Kroemer. 2012. “Mitochondrial Control of Cellular Life, Stress, and Death.” *Circulation Research*. https://doi.org/10.1161/CIRCRESAHA.112.268946.

Geisler, Sven, Kira M. Holmström, Diana Skujat, Fabienne C. Fiesel, Oliver C. Rothfuss, Philipp J. Kahle, and Wolfdieter Springer. 2010. “PINK1/Parkin-Mediated Mitophagy Is Dependent on VDAC1 and P62/SQSTM1.” *Nature Cell Biology* 12 (2): 119–31. https://doi.org/10.1038/ncb2012.

Germain, Kyla, and Peter K Kim. 2020. “Molecular Sciences Pexophagy: A Model for Selective Autophagy.” *International Journal of Molecular Sciences*. https://doi.org/10.3390/ijms21020578.

Gibbings, Derrick, Serge Mostowy, Florence Jay, Yannick Schwab, Pascale Cossart, and Olivier Voinnet. 2012. “Selective Autophagy Degrades DICER and AGO2 and Regulates MiRNA Activity.” *Nature Cell Biology* 14 (12): 1314–21. https://doi.org/10.1038/ncb2611.

Gómez-Sánchez, Rubén, Jaqueline Rose, Rodrigo Guimarães, Muriel Mari, Daniel Papinski, Ester Rieter, Willie J. Geerts, et al. 2018. “Atg9 Establishes Atg2-Dependent Contact Sites between the Endoplasmic Reticulum and Phagophores.” *Journal of Cell Biology* 217 (8): 2743–63. https://doi.org/10.1083/jcb.201710116.

Grice, Guinevere L, and James A Nathan. 2016. “The Recognition of Ubiquitinated Proteins by the Proteasome.” *Cellular and Molecular Life Sciences*. https://doi.org/10.1007/s00018-016-2255-5.

Grumati, Paolo, and Ivan Dikic. 2018. “Ubiquitin Signaling and Autophagy.” *Journal of Biological Chemistry*. American Society for Biochemistry and Molecular Biology Inc. https://doi.org/10.1074/jbc.TM117.000117.

Guo, Huishan, Maneka Chitiprolu, David Gagnon, Lingrui Meng, Carol Perez-Iratxeta, Diane Lagace, and Derrick Gibbings. 2014. “Autophagy Supports Genomic Stability by Degrading Retrotransposon RNA.” *Nature Communications* 5. https://doi.org/10.1038/ncomms6276.

Han, Tianyu, Meng Guo, Mingxi Gan, Bentong Yu, Xiaoli Tian, and Jian-Bin Wang. 2018. “TRIM59 Regulates Autophagy through Modulating Both the Transcription and the Ubiquitination of BECN1.” https://doi.org/10.1080/15548627.2018.1491493.

Hao, Y H, M D Fountain Jr., K Fon Tacer, F Xia, W Bi, S H Kang, A Patel, et al. 2015. “USP7 Acts as a Molecular Rheostat to Promote WASH-Dependent Endosomal Protein Recycling and Is Mutated in a Human Neurodevelopmental Disorder.” *Mol Cell* 59 (6): 956–69. https://doi.org/10.1016/j.molcel.2015.07.033.

Harbeck, Nadia, Frédérique Penault-Llorca, Javier Cortes, Michael Gnant, Nehmat Houssami, Philip Poortmans, Kathryn Ruddy, Janice Tsang, and Fatima Cardoso. 2019. “Breast Cancer.” *Nature Reviews Disease Primers* 5 (1): 1–31. https://doi.org/10.1038/s41572-019-0111-2.

Harbers, M, T Nomura, S Ohno, and S Ishii. 2001. “Intracellular Localization of the Ret Finger Protein Depends on a Functional Nuclear Export Signal and Protein Kinase C Activation.” *J Biol Chem* 276 (51): 48596–607. https://doi.org/10.1074/jbc.M108077200.

Harrigan, Jeanine A., Xavier Jacq, Niall M. Martin, and Stephen P. Jackson. 2018. “Deubiquitylating Enzymes and Drug Discovery: Emerging Opportunities.” *Nature Reviews Drug Discovery*. Nature Publishing Group. https://doi.org/10.1038/nrd.2017.152.

Hasegawa, N, T Iwashita, N Asai, H Murakami, Y Iwata, T Isomura, H Goto, T Hayakawa, and M Takahashi. 1996. “A RING Finger Motif Regulates Transforming Activity of the Rfp/Ret Fusion Gene.” *Biochem Biophys Res Commun* 225 (2): 627–31. https://doi.org/10.1006/bbrc.1996.1221.

Hatakeyama, S. 2017. “TRIM Family Proteins: Roles in Autophagy, Immunity, and Carcinogenesis.” *Trends Biochem Sci* 42 (4): 297–311. https://doi.org/10.1016/j.tibs.2017.01.002.

Hatakeyama, Shigetsugu. 2011. “TRIM Proteins and Cancer.” *Nat Rev Cancer* 11 (11): 792–804. https://doi.org/10.1038/nrc3139.

Heo, Jin Mi, Alban Ordureau, Joao A. Paulo, Jesse Rinehart, and J. Wade Harper. 2015. “The PINK1-PARKIN Mitochondrial Ubiquitylation Pathway Drives a Program of OPTN/NDP52 Recruitment and TBK1 Activation to Promote Mitophagy.” *Molecular Cell* 60 (1): 7–20. https://doi.org/10.1016/j.molcel.2015.08.016.

Hillen, Wolfgang, and Christian Berens. 1994. “Mechanisms Underlying Expression of Tn10 Encoded Tetracycline Resistance.” *Annual Review of Microbiology*. Annual Reviews Inc. https://doi.org/10.1146/annurev.mi.48.100194.002021.

Ho, Matthew, Ashish Patel, Cathal Hanley, Adam Murphy, Tara McSweeney, Li Zhang, Amanda McCann, Peter Gorman, and Giada Bianchi. 2019. “Exploiting Autophagy in Multiple Myeloma.” *Journal of Cancer Metastasis and Treatment* 5 (70). https://doi.org/10.20517/2394-4722.2019.25.

Hofweber, Mario, and Dorothee Dormann. 2019. “Friend or Foe-Post-Translational Modifications as Regulators of Phase Separation and RNP Granule Dynamics.” *Journal of Biological Chemistry*. American Society for Biochemistry and Molecular Biology Inc. https://doi.org/10.1074/jbc.TM118.001189.

Horio, M, T Kato, S Mii, A Enomoto, M Asai, N Asai, Y Murakumo, K Shibata, F Kikkawa, and M Takahashi. 2012. “Expression of RET Finger Protein Predicts Chemoresistance in Epithelial Ovarian Cancer.” *Cancer Med* 1 (2): 218–29. https://doi.org/10.1002/cam4.32.

Horn, H. F., and K. H. Vousden. 2007. “Coping with Stress: Multiple Ways to Activate P53.” *Oncogene*. Nature Publishing Group. https://doi.org/10.1038/sj.onc.1210263.

Hu, Ming Ming, Qing Yang, Jing Zhang, Shi Meng Liu, Yu Zhang, Heng Lin, Zhe Fu Huang, et al. 2014. “TRIM38 Inhibits TNFα- and IL-1β-Triggered NF-KB Activation by Mediating Lysosome-Dependent Degradation of TAB2/3.” *Proceedings of the National Academy of Sciences of the United States of America* 111 (4): 1509–14. https://doi.org/10.1073/pnas.1318227111.

Humbeeck, Cindy Van, Tom Cornelissen, and Wim Vandenberghe. 2011. “Ambra1: A Parkin-Binding Protein Involved in Mitophagy.” *Autophagy*. Taylor and Francis Inc. https://doi.org/10.4161/auto.7.12.17893.

Hundeshagen, Phillip, Anne Hamacher-Brady, Roland Eils, and Nathan R. Brady. 2011. “Concurrent Detection of Autolysosome Formation and Lysosomal Degradation by Flow Cytometry in a High-Content Screen for Inducers of Autophagy.” *BMC Biology* 9 (1): 38. https://doi.org/10.1186/1741-7007-9-38.

Hurley, James H., and Lindsey N. Young. 2017. “Mechanisms of Autophagy Initiation.” *Annual Review of Biochemistry* 86 (June): 225–44. https://doi.org/10.1146/annurev-biochem-061516-044820.

Hutchinson, Katherine E, Doron Lipson, Philip J Stephens, Geoff Otto, Brian D Lehmann, Pamela L Lyle, Cindy L Vnencak-Jones, et al. 2013. “Human Cancer Biology BRAF Fusions Define a Distinct Molecular Subset of Melanomas with Potential Sensitivity to MEK Inhibition.” *Clinical Cancer Research Clin Cancer Res* 19 (24). https://doi.org/10.1158/1078-0432.CCR-13-1746.

Ikeda, K, and S Inoue. 2012. “TRIM Proteins as RING Finger E3 Ubiquitin Ligases.” *Adv Exp Med Biol* 770: 27–37. https://doi.org/10.1007/978-1-4614-5398-7_3.

Inomata, Megumi, Shumpei Niida, Ken-Ichiro Shibata, and Takeshi Into. 2012. “Regulation of Toll-like Receptor Signaling by NDP52-Mediated Selective Autophagy Is Normally Inactivated by A20.” *Cellular and Molecular Life Sciences*. https://doi.org/10.1007/s00018-011-0819-y.

Isogai, Shin, Daichi Morimoto, Kyohei Arita, Satoru Unzai, Takeshi Tenno, Jun Hasegawa, Yu Shin Sou, et al. 2011. “Crystal Structure of the Ubiquitin-Associated (UBA) Domain of P62 and Its Interaction with Ubiquitin.” *Journal of Biological Chemistry* 286 (36): 31864–74. https://doi.org/10.1074/jbc.M111.259630.

Iwakoshi, A, Y Murakumo, T Kato, A Kitamura, S Mii, S Saito, Y Yatabe, and M Takahashi. 2012.

"RET Finger Protein Expression Is Associated with Prognosis in Lung Cancer with Epidermal Growth Factor Receptor Mutations." *Pathol Int* 62 (5): 324–30. https://doi.org/10.1111/j.1440-1827.2012.02797.x.

Izumi, Hideki, and Yasuhiko Kaneko. 2014. "Trim32 Facilitates Degradation of MYCN on Spindle Poles and Induces Asymmetric Cell Division in Human Neuroblastoma Cells." *Cancer Research* 74 (19): 5620–30. https://doi.org/10.1158/0008-5472.CAN-14-0169.

Jacquet, Marine, Michaël Guittaut, Annick Fraichard, and Gilles Despouy. 2020. "The Functions of Atg8-Family Proteins in Autophagy and Cancer: Linked or Unrelated?" https://doi.org/10.1080/15548627.2020.1749367.

Jakobi, Arjen J., Stefan T. Huber, Simon A. Mortensen, Sebastian W. Schultz, Anthimi Palara, Tanja Kuhm, Birendra Kumar Shrestha, et al. 2020. "Structural Basis of P62/SQSTM1 Helical Filaments and Their Role in Cellular Cargo Uptake." *Nature Communications* 11 (December): 1–15. https://doi.org/10.1038/s41467-020-14343-8.

Jaworska, Anna Maria, Nikola Agata Wlodarczyk, Andrzej Mackiewicz, and Patrycja Czerwinska. 2020. "The Role of TRIM Family Proteins in the Regulation of Cancer Stem Cell Self-Renewal." *Stem Cells*. Wiley-Blackwell. https://doi.org/10.1002/stem.3109.

Ji, C H, and Y T Kwon. 2017. "Crosstalk and Interplay between the Ubiquitin-Proteasome System and Autophagy." *Mol Cells* 40 (7): 441–49. https://doi.org/10.14348/molcells.2017.0115.

Jia, Jingyue, Yakubu Princely Abudu, Aurore Claude-Taupin, Yuexi Gu, Suresh Kumar, Won Choi, Ryan Peters, et al. 2018. "Galectins Control MTOR and AMPK in Response to Lysosomal Damage to Induce Autophagy." https://doi.org/10.1080/15548627.2018.1505155.

Jin, Seok Min, and Richard J. Youle. 2013. "The Accumulation of Misfolded Proteins in the Mitochondrial Matrix Is Sensed by PINK1 to Induce PARK2/Parkin-Mediated Mitophagy of Polarized Mitochondria." *Autophagy* 9 (11): 1750–57. https://doi.org/10.4161/auto.26122.

Jin, Shouheng, Shuo Tian, Tianhao Duan, Yaoxing Wu, and Jun Cui Correspondence. 2017. "Tetherin Suppresses Type I Interferon Signaling by Targeting MAVS for NDP52-Mediated Selective Autophagic Degradation in Human Cells." *Molecular Cell* 68: 308-322.e4. https://doi.org/10.1016/j.molcel.2017.09.005.

Johansen, Terje, and Trond Lamark. 2020. "Selective Autophagy: ATG8 Family Proteins, LIR Motifs and Cargo Receptors." *Journal of Molecular Biology*. https://doi.org/10.1016/j.jmb.2019.07.016.

Johnson, Danielle E., Philip Ostrowski, Valentin Jaumouillé, and Sergio Grinstein. 2016. "The Position of Lysosomes within the Cell Determines Their Luminal PH." *Journal of Cell Biology* 212 (6): 677–92. https://doi.org/10.1083/jcb.201507112.

Kageyama, Shun, Sigurdur Runar Gudmundsson, Yu Shin Sou, Yoshinobu Ichimura, Naoki Tamura, Saiko Kazuno, Takashi Ueno, et al. 2021. "P62/SQSTM1-Droplet Serves as a Platform for Autophagosome Formation and Anti-Oxidative Stress Response." *Nature Communications* 12 (1): 1–16. https://doi.org/10.1038/s41467-020-20185-1.

Kageyama, Shun, Sigurdur Runar Gudmundsson, Yu-Shin Sou, Yoshinobu Ichimura, Naoki Tamura, Saiko Kazuno, Takashi Ueno, et al. 2020. "Serves as a Platform for Autophagosome Formation and Anti-Oxidative Stress Response." *Nature Communications*. https://doi.org/10.1038/s41467-020-20185-1.

Kanki, Tomotake, Ke Wang, Yang Cao, Misuzu Baba, and Daniel J. Klionsky. 2009. "Atg32 Is a Mitochondrial Protein That Confers Selectivity during Mitophagy." *Developmental Cell* 17 (1): 98–109. https://doi.org/10.1016/j.devcel.2009.06.014.

Kano, Satoshi, Naoto Miyajima, Satoshi Fukuda, and Shigetsugu Hatakeyama. 2008. "Tripartite Motif Protein 32 Facilitates Cell Growth and Migration via Degradation of Abl-Interactor 2." *Cancer Research* 68 (14): 5572–80. https://doi.org/10.1158/0008-5472.CAN-07-6231.

Kato, T, A Enomoto, T Watanabe, H Haga, S Ishida, Y Kondo, K Furukawa, et al. 2014.

"TRIM27/MRTF-B-Dependent Integrin Beta1 Expression Defines Leading Cells in Cancer Cell Collectives." *Cell Rep* 7 (4): 1156–67. https://doi.org/10.1016/j.celrep.2014.03.068.

Katsuragi, Yoshinori, Yoshinobu Ichimura, and Masaaki Komatsu. 2016. "Regulation of the Keap1–Nrf2 Pathway by P62/SQSTM1." *Current Opinion in Toxicology*. Elsevier B.V. https://doi.org/10.1016/j.cotox.2016.09.005.

Kaushik, Susmita, and Ana Maria Cuervo. 2018. "The Coming of Age of Chaperone-Mediated Autophagy." *Nature Reviews Molecular Cell Biology*. Nature Publishing Group. https://doi.org/10.1038/s41580-018-0001-6.

Kawabata, Hidetaka, Kotaro Azuma, Kazuhiro Ikeda, Ikuko Sugitani, Keiichi Kinowaki, Takeshi Fujii, Akihiko Osaki, Toshiaki Saeki, Kuniko Horie-Inoue, and Satoshi Inoue. 2017. "TRIM44 Is a Poor Prognostic Factor for Breast Cancer Patients as a Modulator of NF-KB Signaling." *International Journal of Molecular Sciences Article*. https://doi.org/10.3390/ijms18091931.

Kawaguchi, Yuki, Masato Taoka, Takahiro Takekiyo, Takamasa Uekita, Ikuo Shoji, Naomi Hachiya, and Tohru Ichimura. 2017. "TRIM32-Cytoplasmic-Body Formation Is an ATP-Consuming Process Stimulated by HSP70 in Cells." Edited by Michael Sherman. *PLOS ONE* 12 (1): e0169436. https://doi.org/10.1371/journal.pone.0169436.

Kehl, Stephanie R, Brandy-Lee A Soos, Bhaskar Saha, Seong Won Choi, Anthony W Herren, Terje Johansen, and Michael A Mandell. 2019. "<scp>TAK</Scp> 1 Converts Sequestosome 1/P62 from an Autophagy Receptor to a Signaling Platform." *EMBO Reports* 20 (9): e46238. https://doi.org/10.15252/embr.201846238.

Keown, Jeremy R., Moyra M. Black, Aaron Ferron, Melvyn Yap, Michael J. Barnett, F. Grant Pearce, Jonathan P. Stoye, and David C. Goldstone. 2018. "A Helical LC3-Interacting Region Mediates the Interaction between the Retroviral Restriction Factor Trim5 and Mammalian Autophagy-Related ATG8 Proteins." *Journal of Biological Chemistry* 293 (47): 18378–86. https://doi.org/10.1074/jbc.RA118.004202.

Kimura, T, A Jain, S W Choi, M A Mandell, K Schroder, T Johansen, and V Deretic. 2015. "TRIM-Mediated Precision Autophagy Targets Cytoplasmic Regulators of Innate Immunity." *J Cell Biol* 210 (6): 973–89. https://doi.org/10.1083/jcb.201503023.

Kimura, T, M Mandell, and V Deretic. 2016. "Precision Autophagy Directed by Receptor Regulators - Emerging Examples within the TRIM Family." *J Cell Sci* 129 (5): 881–91. https://doi.org/10.1242/jcs.163758.

Kirkin, Vladimir. 2020. "History of the Selective Autophagy Research: How Did It Begin and Where Does It Stand Today?" Journal of Molecular Biology. 2020. https://doi.org/10.1016/j.jmb.2019.05.010.

Kirkin, Vladimir, and Vladimir V. Rogov. 2019. "A Diversity of Selective Autophagy Receptors Determines the Specificity of the Autophagy Pathway." *Molecular Cell*. Cell Press. https://doi.org/10.1016/j.molcel.2019.09.005.

Kleiger, G, and T Mayor. 2014. "Perilous Journey: A Tour of the Ubiquitin-Proteasome System." *Trends Cell Biol* 24 (6): 352–59. https://doi.org/10.1016/j.tcb.2013.12.003.

Koliopoulos, Marios G, Diego Esposito, Evangelos Christodoulou, Ian A Taylor, and Katrin Rittinger. 2016. "Functional Role of TRIM E3 Ligase Oligomerization and Regulation of Catalytic Activity." *The EMBO Journal* 35: 1204–18. https://doi.org/10.15252/embj.201593741.

Koukourakis, Michael I., Dimitra Kalamida, Achilleas Mitrakas, Stamatia Pouliliou, Sofia Kalamida, Efthimios Sivridis, and Alexandra Giatromanolaki. 2015. "Intensified Autophagy Compromises the Efficacy of Radiotherapy against Prostate Cancer." *Biochemical and Biophysical Research Communications* 461 (2): 268–74. https://doi.org/10.1016/j.bbrc.2015.04.014.

Kravtsova-Ivantsiv, Yelena, and Aaron Ciechanover. 2012. "Non-Canonical Ubiquitin-Based Signals for Proteasomal Degradation." *Journal of Cell Science* 125 (3): 539–48.

https://doi.org/10.1242/jcs.093567.

Kudryashova, Elena, Irina Kramerova, and Melissa J Spencer. 2012. “Satellite Cell Senescence Underlies Myopathy in a Mouse Model of Limb-Girdle Muscular Dystrophy 2H.” *The Journal of Clinical Investigation* 122. https://doi.org/10.1172/JCI59581.

Kudryashova, Elena, Dmitri Kudryashov, Irina Kramerova, and Melissa J. Spencer. 2005. “Trim32 Is a Ubiquitin Ligase Mutated in Limb Girdle Muscular Dystrophy Type 2H That Binds to Skeletal Muscle Myosin and Ubiquitinates Actin.” *Journal of Molecular Biology* 354 (2): 413–24. https://doi.org/10.1016/j.jmb.2005.09.068.

Kudryashova, Elena, Arie Struyk, Ekaterina Mokhonova, Stephen C. Cannon, and Melissa J. Spencer. 2011. “The Common Missense Mutation D489N in TRIM32 Causing Limb Girdle Muscular Dystrophy 2H Leads to Loss of the Mutated Protein in Knock-in Mice Resulting in a Trim32-Null Phenotype.” *Human Molecular Genetics* 20 (20): 3925–32. https://doi.org/10.1093/hmg/ddr311.

Kudryashova, Elena, Jun Wu, Leif A. Havton, and Melissa J. Spencer. 2009. “Deficiency of the E3 Ubiquitin Ligase TRIM32 in Mice Leads to a Myopathy with a Neurogenic Component.” *Human Molecular Genetics* 18 (7): 1353–67. https://doi.org/10.1093/hmg/ddp036.

Kuma, Akiko, Makoto Matsui, and Noboru Mizushima. 2007. “LC3, an Autophagosome Marker, Can Be Incorporated into Protein Aggregates Independent of Autophagy: Caution in the Interpretation of LC3 Localization.” *Autophagy* 3 (4): 323–28. https://doi.org/10.4161/auto.4012.

Kumar Jena, Kautilya, Srinivasa Prasad Kolapalli, Subhash Mehto, Parej Nath, Biswajit Das, Pradyumna Kumar Sahoo, Abdul Ahad, et al. 2018. “TRIM16 Controls Assembly and Degradation of Protein Aggregates by Modulating the P62-NRF2 Axis and Autophagy.” *The EMBO Journal*, 98358. https://doi.org/10.15252/embj.201798358.

Kwon, Y T, and A Ciechanover. 2017. “The Ubiquitin Code in the Ubiquitin-Proteasome System and Autophagy.” *Trends Biochem Sci* 42 (11): 873–86. https://doi.org/10.1016/j.tibs.2017.09.002.

Lamark, Trond, and Terje Johansen. 2012. “Aggrephagy: Selective Disposal of Protein Aggregates by Macroautophagy.” *International Journal of Cell Biology* 2012. https://doi.org/10.1155/2012/736905.

Lamark, Trond, Maria Perander, Heidi Outzen, Kurt Kristiansen, Aud Øvervatn, Espen Michaelsen, Geir Bjørkøy, and Terje Johansen. 2003. “Interaction Codes within the Family of Mammalian Phox and Bem1p Domain-Containing Proteins.” *Journal of Biological Chemistry* 278: 34568–81. https://doi.org/10.1074/jbc.M303221200.

Lamark, Trond, Steingrim Svenning, and Terje Johansen. 2017. “Regulation of Selective Autophagy: The P62/SQSTM1 Paradigm.” *Essays in Biochemistry*. Portland Press Ltd. https://doi.org/10.1042/EBC20170035.

Larsen, Kenneth Bowitz, Trond Lamark, Aud Øvervatn, Ingvill Harneshaug, Terje Johansen, and Geir Bjørkøy. 2010. “A Reporter Cell System to Monitor Autophagy Based on P62/SQSTM1.” *Autophagy* 6 (6): 784–93. https://doi.org/10.4161/auto.6.6.12510.

Lazarou, Michael, Danielle A. Sliter, Lesley A. Kane, Shireen A. Sarraf, Chunxin Wang, Jonathon L. Burman, Dionisia P. Sideris, Adam I. Fogel, and Richard J. Youle. 2015. “The Ubiquitin Kinase PINK1 Recruits Autophagy Receptors to Induce Mitophagy.” *Nature* 524 (7565): 309–14. https://doi.org/10.1038/nature14893.

Lazzari, Elisa, Medhat S El-Halawany, Matteo De March, Floriana Valentino, Francesco Cantatore, Chiara Migliore, Silvia Onesti, and Germana Meroni. 2019. “Analysis of the Zn-Binding Domains of TRIM32, the E3 Ubiquitin Ligase Mutated in Limb Girdle Muscular Dystrophy 2H.” https://doi.org/10.3390/cells8030254.

Lazzari, Elisa, and Germana Meroni. 2016. “TRIM32 Ubiquitin E3 Ligase, One Enzyme for Several Pathologies: From Muscular Dystrophy to Tumours.” *International Journal of Biochemistry and Cell Biology*. Elsevier Ltd. https://doi.org/10.1016/j.biocel.2016.07.023.

Lee, James T., Jing Shan, Jiayun Zhong, Muyang Li, Brenda Zhou, Amanda Zhou, Ramon Parsons, and Wei Gu. 2013. “RFP-Mediated Ubiquitination of PTEN Modulates Its Effect on AKT Activation.” *Cell Research* 23 (4): 552–64. https://doi.org/10.1038/cr.2013.27.

Lei, Linlin, Zhixiao Wu, and Konstanze F. Winklhofer. 2020. “Protein Quality Control by the Proteasome and Autophagy: A Regulatory Role of Ubiquitin and Liquid-Liquid Phase Separation.” *Matrix Biology*. https://doi.org/10.1016/j.matbio.2020.11.003.

Levkowitz, Gil, Hadassa Waterman, Eli Zamir, Zvi Kam, Shlomo Oved, Wallace Y Langdon, Laura Beguinot, Benjamin Geiger, and Yosef Yarden. 1998. “C-Cbl/Sli-1 Regulates Endocytic Sorting and Ubiquitination of the Epidermal Growth Factor Receptor.” www.genesdev.org.

Li, Wen Wen, Jian Li, and Jin Ku Bao. 2012. “Microautophagy: Lesser-Known Self-Eating.” *Cellular and Molecular Life Sciences*. Cell Mol Life Sci. https://doi.org/10.1007/s00018-011-0865-5.

Liu, Jia, Weijin Liu, Ruolin Li, and Hui Yang. 2019. “Mitophagy in Parkinson’s Disease: From Pathogenesis to Treatment.” *Cells* 8 (7): 712. https://doi.org/10.3390/cells8070712.

Liu, Jia, Shavali Shaik, Xiangpeng Dai, Qiong Wu, Xiuxia Zhou, Zhiwei Wang, and Wenyi Wei. 2015. “Targeting the Ubiquitin Pathway for Cancer Treatment.” *Biochimica et Biophysica Acta - Reviews on Cancer*. Elsevier. https://doi.org/10.1016/j.bbcan.2014.11.005.

Liu, Ju, C Zhang, X L Wang, P Ly, V Belyi, Z Y Xu-Monette, K H Young, W Hu, and Z Feng. 2014. “E3 Ubiquitin Ligase TRIM32 Negatively Regulates Tumor Suppressor P53 to Promote Tumorigenesis.” *Cell Death and Differentiation* 21: 1792–1804. https://doi.org/10.1038/cdd.2014.121.

Liu, Shiyuan, Ying Tian, Ying Zheng, Yao Cheng, Danjie Zhang, Jiantao Jiang, and Shaomin Li. 2020. “TRIM27 Acts as an Oncogene and Regulates Cell Proliferation and Metastasis in Non-Small Cell Lung Cancer through SIX3-β-Catenin Signaling.” *Aging* 12 (24): 25564–80. https://doi.org/10.18632/aging.104163.

Liu, Y, M Zhu, L Lin, X Fan, Z Piao, and X Jiang. 2014. “Deficiency of Trim27 Protects Dopaminergic Neurons from Apoptosis in the Neurotoxin Model of Parkinson’s Disease.” *Brain Res* 1588: 17–24. https://doi.org/10.1016/j.brainres.2014.09.018.

Locke, Matthew, Caroline L Tinsley, Matthew A Benson, and Derek J Blake. 2009. “TRIM32 Is an E3 Ubiquitin Ligase for Dysbindin.” *Human Molecular Genetics*. https://doi.org/10.1093/hmg/ddp167.

Loedige, Inga, Dimos Gaidatzis, Ragna Sack, Gunter Meister, and Witold Filipowicz. 2013. “The Mammalian TRIM-NHL Protein TRIM71/LIN-41 Is a Repressor of MRNA Function.” *Nucleic Acids Research* 41 (1): 518–32. https://doi.org/10.1093/nar/gks1032.

Lv, Deguan, Yanxin Li, Weiwei Zhang, Angel A. Alvarez, Lina Song, Jianming Tang, Wei Qiang Gao, Bo Hu, Shi Yuan Cheng, and Haizhong Feng. 2017. “TRIM24 Is an Oncogenic Transcriptional Co-Activator of STAT3 in Glioblastoma.” *Nature Communications* 8 (1): 1–13. https://doi.org/10.1038/s41467-017-01731-w.

Ma, Liang, Ninghua Yao, Ping Chen, and Zhixiang Zhuang. 2019. “TRIM27 Promotes the Development of Esophagus Cancer via Regulating PTEN/AKT Signaling Pathway.” *Cancer Cell International*. https://doi.org/10.1186/s12935-019-0998-4.

Ma, Y, Z Wei, R C Bast Jr., Z Wang, Y Li, M Gao, Y Liu, et al. 2016. “Downregulation of TRIM27 Expression Inhibits the Proliferation of Ovarian Cancer Cells in Vitro and in Vivo.” *Lab Invest* 96 (1): 37–48. https://doi.org/10.1038/labinvest.2015.132.

Madruga, Enrique, Inés Maestro, and Ana Martínez. 2021. “Molecular Sciences Mitophagy Modulation, a New Player in the Race against ALS.” https://doi.org/10.3390/ijms22020740.

Mahmood, Tahrin, and Ping Chang Yang. 2012. “Western Blot: Technique, Theory, and Trouble Shooting.” *North American Journal of Medical Sciences* 4 (9): 429–34. https://doi.org/10.4103/1947-2714.100998.

Mandell, M A, A Jain, J Arko-Mensah, S Chauhan, T Kimura, C Dinkins, G Silvestri, et al. 2014. “TRIM Proteins Regulate Autophagy and Can Target Autophagic Substrates by Direct Recognition.” *Dev Cell* 30 (4): 394–409. https://doi.org/10.1016/j.devcel.2014.06.013.

Mandell, Michael A., Ashish Jain, Suresh Kumar, Moriah J. Castleman, Tahira Anwar, Eeva Liisa Eskelinen, Terje Johansen, Rytis Prekeris, and Vojo Deretic. 2016. “TRIM17 Contributes to Autophagy of Midbodies While Actively Sparing Other Targets from Degradation.” *Journal of Cell Science* 129 (19): 3562–73. https://doi.org/10.1242/jcs.190017.

Mandell, Michael A, Tomonori Kimura, Ashish Jain, Terje Johansen, and Vojo Deretic. 2015. “TRIM Proteins Regulate Autophagy: TRIM5 Is a Selective Autophagy Receptor Mediating HIV-1 Restriction.” https://doi.org/10.4161/15548627.2014.984278.

Mandell, Michael A, Bhaskar Saha, and Todd A Thompson. 2020. “The Tripartite Nexus: Autophagy, Cancer, and Tripartite Motif-Containing Protein Family Members.” *Frontier in Pharmacology*. https://doi.org/10.3389/fphar.2020.00308.

Marshall, Richard S, Zhihua Hua, Sujina Mali, Fionn Mcloughlin, and Richard D Vierstra. 2019. “ATG8-Binding UIM Proteins Define a New Class of Autophagy Adaptors and Receptors.” *Cell* 177: 766-781.e24. https://doi.org/10.1016/j.cell.2019.02.009.

Matoba, Kazuaki, Tetsuya Kotani, Akihisa Tsutsumi, Takuma Tsuji, Takaharu Mori, Daisuke Noshiro, Yuji Sugita, et al. 2020. “Atg9 Is a Lipid Scramblase That Mediates Autophagosomal Membrane Expansion.” *Nature Structural and Molecular Biology* 27 (12): 1185–93. https://doi.org/10.1038/s41594-020-00518-w.

Meas, Rithy, and Peng Mao. 2015. “Histone Ubiquitylation and Its Roles in Transcription and DNA Damage Response.” *DNA Repair*. Elsevier B.V. https://doi.org/10.1016/j.dnarep.2015.09.016.

Mejlvang, Jakob, Hallvard Olsvik, Steingrim Svenning, Jack Ansgar Bruun, Yakubu Princely Abudu, Kenneth Bowitz Larsen, Andreas Brech, et al. 2018. “Starvation Induces Rapid Degradation of Selective Autophagy Receptors by Endosomal Microautophagy.” *Journal of Cell Biology* 217 (10): 3640–55. https://doi.org/10.1083/JCB.201711002.

Melia, Thomas J., Alf H. Lystad, and Anne Simonsen. 2020. “Autophagosome Biogenesis: From Membrane Growth to Closure.” *Journal of Cell Biology*. Rockefeller University Press. https://doi.org/10.1083/JCB.202002085.

Mogami, Tae, Naho Yokota, Mikiko Asai-Sato, Roppei Yamada, Shiro Koizume, Yuji Sakuma, Mitsuyo Yoshihara, et al. 2013. “Annexin A4 Is Involved in Proliferation, Chemo-Resistance and Migration and Invasion in Ovarian Clear Cell Adenocarcinoma Cells.” Edited by Guan Xin-Yuan. *PLoS ONE* 8 (11): e80359. https://doi.org/10.1371/journal.pone.0080359.

Mokhonova, Ekaterina I, Nuraly K Avliyakulov, Irina Kramerova, Elena Kudryashova, Michael J Haykinson, and Melissa J Spencer. 2015. “The E3 Ubiquitin Ligase TRIM32 Regulates Myoblast Proliferation by Controlling Turnover of NDRG2.” https://doi.org/10.1093/hmg/ddv049.

Mortensen, M., D. J.P. Ferguson, M. Edelmann, B. Kessler, K. J. Morten, M. Komatsu, and A. K. Simon. 2010. “Loss of Autophagy in Erythroid Cells Leads to Defective Removal of Mitochondria and Severe Anemia in Vivo.” *Proceedings of the National Academy of Sciences of the United States of America* 107 (2): 832–37. https://doi.org/10.1073/pnas.0913170107.

Muhlinen, Natalia von, Masato Akutsu, Benjamin J. Ravenhill, Ágnes Foeglein, Stuart Bloor, Trevor J. Rutherford, Stefan M.V. Freund, David Komander, and Felix Randow. 2012. “LC3C, Bound Selectively by a Noncanonical LIR Motif in NDP52, Is Required for Antibacterial Autophagy.” *Molecular Cell* 48 (3): 329–42. https://doi.org/10.1016/j.molcel.2012.08.024.

Muhlinen, Natalia Von, Teresa Thurston, Grigory Ryzhako, Stuart Bloor, and Felix Randow. 2010. “NDP52, a Novel Autophagy Receptor for Ubiquitin-Decorated Cytosolic Bacteria.” https://doi.org/10.4161/auto.6.2.11118.

Murphy, Michael P. 2009. “How Mitochondria Produce Reactive Oxygen Species.” *Biochemical*

Journal. Portland Press Ltd. https://doi.org/10.1042/BJ20081386.

Myerowitz, Rachel, Rosa Puertollano, and Nina Raben. 2021. "Impaired Autophagy: The Collateral Damage of Lysosomal Storage Disorders." *EBioMedicine*. Elsevier B.V. https://doi.org/10.1016/j.ebiom.2020.103166.

Nair, Usha, and Daniel J. Klionsky. 2011. "Autophagosome Biogenesis Requires SNAREs." *Autophagy*. Taylor and Francis Inc. https://doi.org/10.4161/auto.7.12.18001.

Nakamura, Shuhei, and Tamotsu Yoshimori. 2017. "New Insights into Autophagosome-Lysosome Fusion." https://doi.org/10.1242/jcs.196352.

Nakaoku, Takashi, Koji Tsuta, Hitoshi Ichikawa, Kouya Shiraishi, Hiromi Sakamoto, Masato Enari, Koh Furuta, et al. 2014. "Human Cancer Biology Druggable Oncogene Fusions in Invasive Mucinous Lung Adenocarcinoma." *Clin Cancer Res* 20 (12). https://doi.org/10.1158/1078-0432.CCR-14-0107.

Nakatogawa, Hitoshi, and Yoshinori Ohsumi. 2020. "Review Autophagic Degradation of the Endoplasmic Reticulum." *Japan Academy*. https://doi.org/10.2183/pjab.96.001.

Nam, Taewook, Jong Hyun Han, Sushil Devkota, and Han Woong Lee. 2017. "Emerging Paradigm of Crosstalk between Autophagy and the Ubiquitin-Proteasome System." *Molecules and Cells*. Korean Society for Molecular and Cellular Biology. https://doi.org/10.14348/molcells.2017.0226.

Napolitano, Luisa M., Ellis G. Jaffray, Ronald T. Hay, and Germana Meroni. 2011. "Functional Interactions between Ubiquitin E2 Enzymes and TRIM Proteins." *Biochemical Journal* 434 (2): 309–19. https://doi.org/10.1042/BJ20101487.

Nguyen, Duy, Shabnam Shaid, Olesya Vakhrusheva, Sebastian E. Koschade, Kevin Klann, Marlyn Thölken, Fatima Baker, et al. 2019. "Loss of the Selective Autophagy Receptor P62 Impairs Murine Myeloid Leukemia Progression and Mitophagy." *Blood* 133 (2): 168–79. https://doi.org/10.1182/blood-2018-02-833475.

Nguyen, Thanh Ngoc, Benjamin Scott Padman, Joanne Usher, Viola Oorschot, Georg Ramm, and Michael Lazarou. 2016. "Atg8 Family LC3/GAB ARAP Proteins Are Crucial for Autophagosome-Lysosome Fusion but Not Autophagosome Formation during PINK1/Parkin Mitophagy and Starvation." *Journal of Cell Biology* 215 (6): 857–74. https://doi.org/10.1083/jcb.201607039.

Nie, D, D Zhang, J Dai, M Zhang, X Zhao, W Xu, Z Chen, L Wang, Z Wang, and Z Qiao. 2016. "Nicotine Induced Murine Spermatozoa Apoptosis via Up-Regulation of Deubiquitinated RIP1 by Trim27 Promoter Hypomethylation." *Biol Reprod* 94 (2): 31. https://doi.org/10.1095/biolreprod.115.131656.

Nieminen, Anna Liisa. 2003. "Apoptosis and Necrosis in Health and Disease: Role of Mitochondria." *International Review of Cytology* 224: 29–55. https://doi.org/10.1016/S0074-7696(05)24002-0.

Niida, Motoko, Makoto Tanaka, and Tetsu Kamitani. 2010. "Downregulation of Active IKKβ by Ro52-Mediated Autophagy." *Mol Immunol* 47 (14): 2378–87. https://doi.org/10.1016/j.molimm.2010.05.004.

Ning, Shunbin, and Ling Wang. 2018. "The Multifunctional Protein P62 and Its Mechanistic Roles in Cancers." *Current Cancer Drug Targets* 19 (6): 468–78. https://doi.org/10.2174/1568009618666181016164920.

Noguchi, Keita, Fumihiko Okumura, Norihiko Takahashi, Akihiko Kataoka, Toshiya Kamiyama, Satoru Todo, and Shigetsugu Hatakeyama. 2011. "TRIM40 Promotes Neddylation of IKKg and Is Downregulated in Gastrointestinal Cancers." *Carcinogenesis* 32 (7): 995–1004. https://doi.org/10.1093/carcin/bgr068.

Oh, Eugene, David Akopian, and Michael Rape. 2018. "Principles of Ubiquitin- Dependent Signaling." *Annual Review of Cell and Developmental Biology*. Annual Reviews Inc. https://doi.org/10.1146/annurev-cellbio-100617-062802.

Ohsumi, Yoshinori. 2014. “Historical Landmarks of Autophagy Research.” *Cell Research*. Nature Publishing Group. https://doi.org/10.1038/cr.2013.169.

Okamoto, Koji, Noriko Kondo-Okamoto, and Yoshinori Ohsumi. 2009. “Mitochondria-Anchored Receptor Atg32 Mediates Degradation of Mitochondria via Selective Autophagy.” *Developmental Cell* 17 (1): 87–97. https://doi.org/10.1016/j.devcel.2009.06.013.

Onishi, Mashun, Koji Yamano, Miyuki Sato, Noriyuki Matsuda, and Koji Okamoto. 2021. “Molecular Mechanisms and Physiological Functions of Mitophagy.” *The EMBO Journal*, January, e104705. https://doi.org/10.15252/embj.2020104705.

Overå, Katrine Stange, Juncal Garcia-Garcia, Zambarlal Bhujabal, Ashish Jain, Aud Øvervatn, Kenneth Bowitz Larsen, Vojo Deretic, Terje Johansen, Trond Lamark, and Eva Sjøttem. 2019. “TRIM32, but Not Its Muscular Dystrophy-Associated Mutant, Positively Regulates and Is Targeted to Autophagic Degradation by P62/SQSTM1.” *Journal of Cell Science* 132 (23). https://doi.org/10.1242/jcs.236596.

Owen, Izzy, and Frank Shewmaker. 2019. “The Role of Post-Translational Modifications in the Phase Transitions of Intrinsically Disordered Proteins.” *International Journal of Molecular Sciences*. MDPI AG. https://doi.org/10.3390/ijms20215501.

Pan, Ji An, Yu Sun, Ya Ping Jiang, Alex J. Bott, Nadia Jaber, Zhixun Dou, Bin Yang, et al. 2016. “TRIM21 Ubiquitylates SQSTM1/P62 and Suppresses Protein Sequestration to Regulate Redox Homeostasis.” *Molecular Cell* 61 (5): 720–33. https://doi.org/10.1016/j.molcel.2016.02.007.

Pan, Xufeng, Yong Chen, Yuzhou Shen, and Jicheng Tantai. 2019. “Knockdown of TRIM65 Inhibits Autophagy and Cisplatin Resistance in A549/DDP Cells by Regulating MiR-138-5p/ATG7.” *Cell Death and Disease* 10 (6): 1–11. https://doi.org/10.1038/s41419-019-1660-8.

Pankiv, Serhiy, Endalkachew A. Alemu, Andreas Brech, Jack Ansgar Bruun, Trond Lamark, Aud Øvervatn, Geir Bjørkøy, and Terje Johansen. 2010. “FYCO1 Is a Rab7 Effector That Binds to LC3 and PI3P to Mediate Microtubule plus End - Directed Vesicle Transport.” *Journal of Cell Biology* 188 (2): 253–69. https://doi.org/10.1083/jcb.200907015.

Pankiv, Serhiy, Terje Høyvarde Clausen, Trond Lamark, Andreas Brech, Jack Ansgar Bruun, Heidi Outzen, Aud Øvervatn, Geir Bjørkøy, and Terje Johansen. 2007. “P62/SQSTM1 Binds Directly to Atg8/LC3 to Facilitate Degradation of Ubiquitinated Protein Aggregates by Autophagy[S].” *Journal of Biological Chemistry* 282 (33): 24131–45. https://doi.org/10.1074/jbc.M702824200.

Pankiv, Serhiy, Trond Lamark, Jack Ansgar Bruun, Aud Øvervatn, Geir Bjørkøy, and Terje Johansen. 2010. “Nucleocytoplasmic Shuttling of P62/SQSTM1 and Its Role in Recruitment of Nuclear Polyubiquitinated Proteins to Promyelocytic Leukemia Bodies.” *Journal of Biological Chemistry* 285 (8): 5941–53. https://doi.org/10.1074/jbc.M109.039925.

Parenti, Giancarlo, Diego L Medina, and Andrea Ballabio. 2021. “The Rapidly Evolving View of Lysosomal Storage Diseases.” *EMBO Molecular Medicine* 13 (2): e12836. https://doi.org/10.15252/emmm.202012836.

Park, Sungwoo, Seon Guk Choi, Seung Min Yoo, Jin H. Son, and Yong Keun Jung. 2014. “Choline Dehydrogenase Interacts with SQSTM1/P62 to Recruit LC3 and Stimulate Mitophagy.” *Autophagy* 10 (11): 1906–20. https://doi.org/10.4161/auto.32177.

Peng, Hong, Jiao Yang, Guangyi Li, Qing You, Wen Han, Tianrang Li, Daming Gao, et al. 2017. “Ubiquitylation of P62/Sequestosome1 Activates Its Autophagy Receptor Function and Controls Selective Autophagy upon Ubiquitin Stress.” *Cell Research* 27 (5): 657–74. https://doi.org/10.1038/cr.2017.40.

Pertel, Thomas, Stéphane Hausmann, Damien Morger, Sara Züger, Jessica Guerra, Josefina Lascano, Christian Reinhard, et al. 2011. “TRIM5 Is an Innate Immune Sensor for the Retrovirus Capsid Lattice.” *Nature* 472 (7343): 361–65. https://doi.org/10.1038/nature09976.

Platt, Frances M. 2018. “Emptying the Stores: Lysosomal Diseases and Therapeutic Strategies.”

https://doi.org/10.1038/nrd.2017.214.

Pohl, Christian, and Ivan Dikic. 2019. “Cellular Quality Control by the Ubiquitin-Proteasome System and Autophagy.” *Science*. American Association for the Advancement of Science. https://doi.org/10.1126/science.aax3769.

Proikas-Cezanne, Tassula, Zsuzsanna Takacs, Pierre Dönnes, and Oliver Kohlbacher. 2015. “WIPI Proteins: Essential PtdIns3P Effectors at the Nascent Autophagosome.” *Journal of Cell Science*. Company of Biologists Ltd. https://doi.org/10.1242/jcs.146258.

Raimundo, Nuno, Henna Tyynismaa, Marc Germain, Kiran Todkar, and Hema S Ilamathi. 2017. “Mitochondria and Lysosomes: Discovering Bonds.” *Frontiers in Cell and Developmental Biology | Www.Frontiersin.Org* 5: 106. https://doi.org/10.3389/fcell.2017.00106.

Ran, F. Ann, Patrick D. Hsu, Jason Wright, Vineeta Agarwala, David A. Scott, and Feng Zhang. 2013. “Genome Engineering Using the CRISPR-Cas9 System.” *Nature Protocols* 8 (11): 2281–2308. https://doi.org/10.1038/nprot.2013.143.

Rasmussen, Mads Skytte, Stéphane Mouilleron, Birendra Kumar Shrestha, Martina Wirth, Rebecca Lee, Kenneth Bowitz Larsen, Yakubu Abudu Princely, Nicola O’reilly, Eva Sjøttem, and Sharon A Toozehttps. 2017. “ATG4B Contains a C-Terminal LIR Motif Important for Binding and Efficient Cleavage of Mammalian Orthologs of Yeast Atg8.” https://doi.org/10.1080/15548627.2017.1287651.

Ravenhill, Benjamin J., Keith B. Boyle, Natalia von Muhlinen, Cara J. Ellison, Glenn R. Masson, Elsje G. Otten, Agnes Foeglein, Roger Williams, and Felix Randow. 2019. “The Cargo Receptor NDP52 Initiates Selective Autophagy by Recruiting the ULK Complex to Cytosol-Invading Bacteria.” *Molecular Cell* 74 (2): 320-329.e6. https://doi.org/10.1016/j.molcel.2019.01.041.

Reddy Bonam, Srinivasa, Fengjuan Wang, and Sylviane Muller. 2019. “Lysosomes as a Therapeutic Target.” *Nature Reviews Drug Discovery* 18: 923–48. https://doi.org/10.1038/s41573-019-0036-1.

Reggiori, Fulvio, and Daniel J Klionsky. 2013. “Autophagic Processes in Yeast: Mechanism, Machinery and Regulation.” https://doi.org/10.1534/genetics.112.149013.

Reymond, Alexandre, Germana Meroni, Anna Fantozzi, Giuseppe Merla, Stefano Cairo, Lucilla Luzi, Daniela Riganelli, et al. 2001. “The Tripartite Motif Family Identifies Cell Compartments.” *EMBO Journal* 20 (9): 2140–51. https://doi.org/10.1093/emboj/20.9.2140.

Rienzo, Martina Di, Mauro Piacentini, and Gian Maria Fimia. 2019. “A TRIM32-AMBRA1-ULK1 Complex Initiates the Autophagy Response in Atrophic Muscle Cells.” *Autophagy* 15 (9): 1674–76. https://doi.org/10.1080/15548627.2019.1635385.

Rienzo, Martina Di, Alessandra Romagnoli, Manuela Antonioli, • Mauro Piacentini, and Gian Maria Fimia. 2020. “TRIM Proteins in Autophagy: Selective Sensors in Cell Damage and Innate Immune Responses.” *Cell Death & Differentiation* 27: 887–902. https://doi.org/10.1038/s41418-020-0495-2.

Rogov, Vladimir, Volker Dötsch, Terje Johansen, and Vladimir Kirkin. 2014. “Interactions between Autophagy Receptors and Ubiquitin-like Proteins Form the Molecular Basis for Selective Autophagy.” *Molecular Cell*. Mol Cell. https://doi.org/10.1016/j.molcel.2013.12.014.

Rottenberg, Hagai, and Jan B Hoek. 2021. “Cells The Mitochondrial Permeability Transition: Nexus of Aging, Disease and Longevity.” https://doi.org/10.3390/cells10010079.

Rowland, Teisha J, Mary E Sweet, Luisa Mestroni, and Matthew R G Taylor. 2016. “Danon Disease-Dysregulation of Autophagy in a Multisystem Disorder with Cardiomyopathy.” https://doi.org/10.1242/jcs.184770.

Ruan, Haihua, Jingyue Xu, Lingling Wang, Zhenyu Zhao, Lingqin Kong, Bei Lan, and Xichuan Li. 2018. “The Prognostic Value of P62 in Solid Tumor Patients: A Metaanalysis.” *Oncotarget* 9 (3): 4258–66. https://doi.org/10.18632/oncotarget.23101.

Russell, Ryan C., Ye Tian, Haixin Yuan, Hyun Woo Park, Yu Yun Chang, Joungmok Kim, Haerin Kim, Thomas P. Neufeld, Andrew Dillin, and Kun Liang Guan. 2013. "ULK1 Induces Autophagy by Phosphorylating Beclin-1 and Activating VPS34 Lipid Kinase." *Nature Cell Biology* 15 (7): 741–50. https://doi.org/10.1038/ncb2757.

Ryu, Yeung Sook, Younglang Lee, Keun Woo Lee, Chae Young Hwang, Jin Soo Maeng, Jeong Hoon Kim, Yeon Soo Seo, Kwan Hee You, Byeongwoon Song, and Ki Sun Kwon. 2011. "TRIM32 Protein Sensitizes Cells to Tumor Necrosis Factor (TNFα)-Induced Apoptosis via Its RING Domain-Dependent E3 Ligase Activity against X-Linked Inhibitor of Apoptosis (XIAP)." *Journal of Biological Chemistry* 286 (29): 25729–38. https://doi.org/10.1074/jbc.M111.241893.

Saccone, Valentina, Michela Palmieri, Luigia Passamano, Giulio Piluso, Germana Meroni, Luisa Politano, and Vincenzo Nigro. 2008. "Mutations That Impair Interaction Properties of TRIM32 Associated with Limb-Girdle Muscular Dystrophy 2H." *Human Mutation* 29 (2): 240–47. https://doi.org/10.1002/humu.20633.

Saftig, Paul, Wouter Beertsen, and Eeva Liisa Eskelinen. 2008. "LAMP-2: A Control Step Fot Phagosome and Autophagosome Maturation." *Autophagy* 4 (4): 510–12. https://doi.org/10.4161/auto.5724.

Saftig, Paul, and Judith Klumperman. 2009. "Lysosome Biogenesis and Lysosomal Membrane Proteins: Trafficking Meets Function." https://doi.org/10.1038/nrm2745.

Saha, Tapas. 2012. "LAMP2A Overexpression in Breast Tumors Promotes Cancer Cell Survival via Chaperone-Mediated Autophagy." *Autophagy* 8 (11): 1643–56. https://doi.org/10.4161/auto.21654.

Saibil, Helen. 2013. "Chaperone Machines for Protein Folding, Unfolding and Disaggregation Europe PMC Funders Group." *Nat Rev Mol Cell Biol* 14 (10): 630–42. https://doi.org/10.1038/nrm3658.

Sandri, Marco. 2013. "Protein Breakdown in Muscle Wasting: Role of Autophagy-Lysosome and Ubiquitin-Proteasome." *International Journal of Biochemistry and Cell Biology*. Elsevier Ltd. https://doi.org/10.1016/j.biocel.2013.04.023.

Santoro, Massimo, and Francesca Carlomagno. 2013. "Central Role of RET in Thyroid Cancer." *Cold Spring Harbor Perspectives in Biology* 5 (12). https://doi.org/10.1101/cshperspect.a009233.

Sato, Tomonobu, Fumihiko Okumura, Satoshi Kano, Takeshi Kondo, Tadashi Ariga, and Shigetsugu Hatakeyama. 2011. "TRIM32 Promotes Neural Differentiation through Retinoic Acid Receptor-Mediated Transcription." *Journal of Cell Science* 124 (20): 3492–3502. https://doi.org/10.1242/jcs.088799.

Sawa-Makarska, Justyna, Verena Baumann, Nicolas Coudevylle, Sören von Bülow, Veronika Nogellova, Christine Abert, Martina Schuschnig, Martin Graef, Gerhard Hummer, and Sascha Martens. 2020. "Reconstitution of Autophagosome Nucleation Defines Atg9 Vesicles as Seeds for Membrane Formation." *Science* 369 (6508). https://doi.org/10.1126/SCIENCE.AAZ7714.

Scheibye-Knudsen, Morten, Evandro F Fang, Deborah L Croteau, David M Wilson Iii, and Vilhelm A Bohr. 2015. "Protecting the Mitochondrial Powerhouse." *Trends Cell Biol*. https://doi.org/10.1016/j.tcb.2014.11.002.

Ségal-Bendirdjian, Evelyne, Mario P Tschan, Josy Reiffers, and Mojgan Djavaheri-Mergny. 2014. "Pro-Survival Role of P62 during Granulocytic Differentiation of Acute Myeloid Leukemia Cells." *Molecular & Cellular Oncology* 1 (4): e970066. https://doi.org/10.4161/23723548.2014.970066.

Shao, Sichen, Karina Von der Malsburg, and Ramanujan S. Hegde. 2013. "Listerin-Dependent Nascent Protein Ubiquitination Relies on Ribosome Subunit Dissociation." *Molecular Cell* 50 (5): 637–48. https://doi.org/10.1016/j.molcel.2013.04.015.

Shi, Xiaoshan, Chunmei Chang, Adam L. Yokom, Liv E. Jensen, and James H. Hurley. 2020. "The Autophagy Adaptor Ndp52 and the Fip200 Coiled-Coil Allosterically Activate Ulk1 Complex Membrane Recruitment." *ELife* 9 (August): 1–20. https://doi.org/10.7554/ELIFE.59099.

Shimono, Y, H Murakami, Y Hasegawa, and M Takahashi. 2000. “RET Finger Protein Is a Transcriptional Repressor and Interacts with Enhancer of Polycomb That Has Dual Transcriptional Functions.” *J Biol Chem* 275 (50): 39411–19. https://doi.org/10.1074/jbc.M006585200.

Slack, Frank J., and Gary Ruvkun. 1998. “A Novel Repeat Domain That Is Often Associated with RING Finger and B-Box Motifs.” *Trends in Biochemical Sciences* 23 (12): 474–75. https://doi.org/10.1016/S0968-0004(98)01299-7.

Song, WenBo, Zheng Wang, Xiang Gu, ALi Wang, XiaoJun Chen, Hui Miao, JunFeng Chu, and Ye Tian. 2019. “TRIM11 Promotes Proliferation and Glycolysis of Breast Cancer Cells via Targeting AKT/GLUT1 Pathway.” *OncoTargets and Therapy* 12 (June): 4975–84. https://doi.org/10.2147/OTT.S207723.

Sontag, Emily Mitchell, Rahul S Samant, and Judith Frydman. 2017. “Mechanisms and Functions of Spatial Protein Quality Control.” https://doi.org/10.1146/annurev-biochem.

Sora, Valentina, Mukesh Kumar, Emiliano Maiani, Matteo Lambrughi, Matteo Tiberti, and Elena Papaleo. 2020. “Structure and Dynamics in the ATG8 Family From Experimental to Computational Techniques.” *Frontiers in Cell and Developmental Biology*. Frontiers Media S.A. https://doi.org/10.3389/fcell.2020.00420.

Sparrer, Konstantin M.J., Sebastian Gableske, Matthew A. Zurenski, Zachary M. Parker, Florian Full, Gavin J. Baumgart, Jiro Kato, et al. 2017. “TRIM23 Mediates Virus-Induced Autophagy via Activation of TBK1.” *Nature Microbiology* 2 (11): 1543–57. https://doi.org/10.1038/s41564-017-0017-2.

Stewart, Mikaela D, Tobias Ritterhoff, Rachel E Klevit, and Peter S Brzovic. 2016. “E2 Enzymes: More than Just Middle Men.” *Cell Research* 26: 423–40. https://doi.org/10.1038/cr.2016.35.

Strappazzon, Flavie, Anthea Di Rita, Angelo Peschiaroli, Pier Paolo Leoncini, Franco Locatelli, Gerry Melino, and Francesco Cecconi. 2020. “HUWE1 Controls MCL1 Stability to Unleash AMBRA1-Induced Mitophagy.” *Cell Death & Differentiation* 27: 1155–68. https://doi.org/10.1038/s41418-019-0404-8.

Sun, Daxiao, Rongbo Wu, Pilong Li, and Li Yu. 2020. “Phase Separation in Regulation of Aggrephagy.” *Journal of Molecular Biology*. Academic Press. https://doi.org/10.1016/j.jmb.2019.06.026.

Sun, Daxiao, Rongbo Wu, Jingxiang Zheng, Pilong Li, and Li Yu. 2018. “Polyubiquitin Chain-Induced P62 Phase Separation Drives Autophagic Cargo Segregation.” *Cell Research* 28 (4): 405–15. https://doi.org/10.1038/s41422-018-0017-7.

Swatek, Kirby N., and David Komander. 2016. “Ubiquitin Modifications.” *Cell Research*. Nature Publishing Group. https://doi.org/10.1038/cr.2016.39.

Swerdlow, Natalie S, and Heather M Wilkins. 2020. “Molecular Sciences Mitophagy and the Brain.” *International Journal of Molecular Sciences*. https://doi.org/10.3390/ijms21249661.

Tan, Hongwei, Jin Qi, Guanghua Chu, and Zhaoyang Liu. 2017. “Tripartite Motif 16 Inhibits the Migration and Invasion in Ovarian Cancer Cells.” *Oncology Research* 25 (4): 551–58. https://doi.org/10.3727/096504016X14758370595285.

Tan, Peng, Youqiong Ye, Lian He Id, Jiansheng Xie, Ji Jing Id, Guolin Ma Id, Hongming Pan, Leng Hanid, Weidong Han, and Yubin Zhouid. 2018. “TRIM59 Promotes Breast Cancer Motility by Suppressing P62-Selective Autophagic Degradation of PDCD10.” https://doi.org/10.1371/journal.pbio.3000051.

Tancini, Brunella, Sandra Buratta, Federica Delo, Krizia Sagini, Elisabetta Chiaradia, Roberto Maria Pellegrino, Carla Emiliani, and Lorena Urbanelli. 2020. “Membranes Lysosomal Exocytosis: The Extracellular Role of an Intracellular Organelle.” *Membranes* 10 (406). https://doi.org/10.3390/membranes10120406.

Tanida, Isei, Naoko Minematsu-Ikeguchi, Takashi Ueno, and Eiki Kominami. 2005. “Lysosomal Turnover, but Not a Cellular Level, of Endogenous LC3 Is a Marker for Autophagy.” *Autophagy*

1 (2): 84–91. https://doi.org/10.4161/auto.1.2.1697.

Tezel, G G, A Uner, I Yildiz, G Guler, and M Takahashi. 2009. “RET Finger Protein Expression in Invasive Breast Carcinoma: Relationship between RFP and ErbB2 Expression.” *Pathol Res Pract* 205 (6): 403–8. https://doi.org/10.1016/j.prp.2008.12.014.

Tezel, G, T Nagasaka, N Iwahashi, N Asai, T Iwashita, K Sakata, and M Takahashi. 1999. “Different Nuclear/Cytoplasmic Distributions of RET Finger Protein in Different Cell Types.” *Pathol Int* 49 (10): 881–86. https://doi.org/10.1046/j.1440-1827.1999.00957.x.

Thurston, Teresa L.M., Michal P. Wandel, Natalia Von Muhlinen, Ágnes Foeglein, and Felix Randow. 2012. “Galectin 8 Targets Damaged Vesicles for Autophagy to Defend Cells against Bacterial Invasion.” *Nature* 482 (7385): 414–18. https://doi.org/10.1038/nature10744.

Thurston, Teresa L M, Grigory Ryzhakov, Stuart Bloor, Natalia Von Muhlinen, and Felix Randow. 2009. “The TBK1 Adaptor and Autophagy Receptor NDP52 Restricts the Proliferation of Ubiquitin-Coated Bacteria.” *Nature Immunology*. https://doi.org/10.1038/ni.1800.

Till, Andreas, Simone Lipinski, David Ellinghaus, Gabriele Mayr, Suresh Subramani, Philip Rosenstiel, and Andre Franke. 2013. “Autophagy Receptor CALCOCO2/NDP52 Takes Center Stage in Crohn Disease.” https://doi.org/10.4161/auto.25483.

Tocchini, Cristina, and Rafal Ciosk. 2015. “TRIM-NHL Proteins in Development and Disease.” *Seminars in Cell and Developmental Biology* 47–48 (December): 52–59. https://doi.org/10.1016/j.semcdb.2015.10.017.

Tsai, Wen-Wei, Zhanxin Wang, Teresa T Yiu, Kadir C Akdemir, Weiya Xia, Stefan Winter, Cheng-Yu Tsai, et al. 2010. “TRIM24 Links a Non-Canonical Histone Signature to Breast Cancer.” *Nature*. https://doi.org/10.1038/nature09542.

Tsuchida, Tetsuo, Jian Zou, Tatsuya Saitoh, Himanshu Kumar, Takayuki Abe, Yoshiharu Matsuura, Taro Kawai, and Shizuo Akira. 2010. “The Ubiquitin Ligase TRIM56 Regulates Innate Immune Responses to Intracellular Double-Stranded DNA.” *Immunity* 33 (5): 765–76. https://doi.org/10.1016/j.immuni.2010.10.013.

Tsukamoto, H, T Kato, A Enomoto, N Nakamura, Y Shimono, M Jijiwa, N Asai, et al. 2009. “Expression of Ret Finger Protein Correlates with Outcomes in Endometrial Cancer.” *Cancer Sci* 100 (10): 1895–1901. https://doi.org/10.1111/j.1349-7006.2009.01278.x.

Vainshtein, Anna, and Paolo Grumati. 2020. “Cells Selective Autophagy by Close Encounters of the Ubiquitin Kind.” *Cells*. https://doi.org/10.3390/cells9112349.

Vargas, Jose Norberto S., Chunxin Wang, Eric Bunker, Ling Hao, Dragan Maric, Giampietro Schiavo, Felix Randow, and Richard J. Youle. 2019. “Spatiotemporal Control of ULK1 Activation by NDP52 and TBK1 during Selective Autophagy.” *Molecular Cell* 74 (2): 347-362.e6. https://doi.org/10.1016/j.molcel.2019.02.010.

Verlhac, Pauline, Christophe Viret, and Mathias Faure. 2015. “Dual Function of CALCOCO2/NDP52 during Xenophagy.” *Autophagy* 11 (6): 965–66. https://doi.org/10.1080/15548627.2015.1046672.

Vicenzi, Elisa, San Raffaele, David E Levy, Jan Terje Andersen, Stian Foss, Maria Bottermann, Alexandra Jonsson, Inger Sandlie, and Leo C James. 2019. “TRIM21-From Intracellular Immunity to Therapy.” *Frontiers in Immunology | Www.Frontiersin.Org* 1: 2049. https://doi.org/10.3389/fimmu.2019.02049.

Wang, J, J L Teng, D Zhao, P Ge, B Li, P C Woo, and C H Liu. 2016. “The Ubiquitin Ligase TRIM27 Functions as a Host Restriction Factor Antagonized by Mycobacterium Tuberculosis PtpA during Mycobacterial Infection.” *Sci Rep* 6: 34827. https://doi.org/10.1038/srep34827.

Wang, Jianhui, Wei Zhang, Zanhua Yi, Shiyang Wang, and Zongdong Li. 2012. “Identification of a Thrombin Cleavage Site and a Short Form of ADAMTS-18.” *Biochemical and Biophysical Research Communications* 419 (4): 692–97. https://doi.org/10.1016/j.bbrc.2012.02.081.

Wang, Minglei, Wenqin Luo, Yu Zhang, Rong Yang, Xuefeng Li, Yanjing Guo, Chenlu Zhang, Ru Yang, and Wei Qiang Gao. 2020. “Trim32 Suppresses Cerebellar Development and Tumorigenesis by Degrading Gli1/Sonic Hedgehog Signaling.” *Cell Death and Differentiation* 27 (4): 1286–99. https://doi.org/10.1038/s41418-019-0415-5.

Wang, Qi, Xinyu Chen, and Nissim Hay. 2017. “Akt as a Target for Cancer Therapy: More Is Not Always Better (Lessons from Studies in Mice).” *British Journal of Cancer* 117 (2): 159–63. https://doi.org/10.1038/bjc.2017.153.

Wang, Wei, Zhijie Xia, Jean Claude Farré, and Suresh Subramani. 2018. “TRIM37 Deficiency Induces Autophagy through Deregulating the MTORC1-TFEB Axis.” *Autophagy* 14 (9): 1574–85. https://doi.org/10.1080/15548627.2018.1463120.

Watanabe, M, and S Hatakeyama. 2017. “TRIM Proteins and Diseases.” *J Biochem* 161 (2): 135–44. https://doi.org/10.1093/jb/mvw087.

Wild, Philipp, Hesso Farhan, David G. McEwan, Sebastian Wagner, Vladimir V. Rogov, Nathan R. Brady, Benjamin Richter, et al. 2011. “Phosphorylation of the Autophagy Receptor Optineurin Restricts Salmonella Growth.” *Science* 333 (6039): 228–33. https://doi.org/10.1126/science.1205405.

Wilkins, Heather M, Russell H Swerdlow, Konstantinos Palikaras, P Hemachandra Reddy, and Michael Tran. 2021. “Defective Autophagy and Mitophagy in Aging and Alzheimer’s Disease.” https://doi.org/10.3389/fnins.2020.612757.

Wilkinson, Keith D. 2009. “DUBs at a Glance.” *Journal of Cell Science* 122 (14): 2325–29. https://doi.org/10.1242/jcs.041046.

Wirth, Martina, Wenxin Zhang, Minoo Razi, Lynet Nyoni, Dhira Joshi, Nicola O’reilly, Terje Johansen, Sharon A Tooze, and Stéphane Mouilleron. 2019. “Molecular Determinants Regulating Selective Binding of Autophagy Adapters and Receptors to ATG8 Proteins.” *Nature Communications*. https://doi.org/10.1038/s41467-019-10059-6.

Wu, Siyu, Junsheng Zhang, Qian Xue, Jing Liu, Bingzhong Huang, Zhuoliang He, Jianni Huang, et al. 2020. “Duck TRIM32 Functions in IFN-β Signaling Against the Infection of H5N6 Highly Pathogenic Avian Influenza Virus.” *Frontiers in Immunology* 11 (February). https://doi.org/10.3389/fimmu.2020.00377.

Wurzer, Bettina, Gabriele Zaffagnini, Dorotea Fracchiolla, Eleonora Turco, Christine Abert, Julia Romanov, and Sascha Martens. 2015. “Oligomerization of P62 Allows for Selection of Ubiquitinated Cargo and Isolation Membrane during Selective Autophagy.” *ELife* 4 (September 2015). https://doi.org/10.7554/eLife.08941.

Xie, Xingqiao, Faxiang Li, Yuanyuan Wang, Yingli Wang, Zhijie Lin, Xiaofang Cheng, Jianping Liu, Changbin Chen, and Lifeng Pan. 2015. “Molecular Basis of Ubiquitin Recognition by the Autophagy Receptor CALCOCO2.” *Autophagy* 11 (10): 1775–89. https://doi.org/10.1080/15548627.2015.1082025.

Xing, Li, Xiaolong Tang, Kaikai Wu, Xiong Huang, Yi Yi, and Jinliang Huan. 2020. “TRIM27 Functions as a Novel Oncogene in Non-Triple-Negative Breast Cancer by Blocking Cellular Senescence through P21 Ubiquitination.” *Molecular Therapy - Nucleic Acids* 22 (December): 910–23. https://doi.org/10.1016/j.omtn.2020.10.012.

Yang, Qing, Tian Tian Liu, Heng Lin, Man Zhang, Jin Wei, Wei Wei Luo, Yun Hong Hu, Bo Zhong, Ming Ming Hu, and Hong Bing Shu. 2017. “TRIM32-TAX1BP1-Dependent Selective Autophagic Degradation of TRIF Negatively Regulates TLR3/4-Mediated Innate Immune Responses.” *PLoS Pathogens* 13 (9). https://doi.org/10.1371/journal.ppat.1006600.

Yao, J. Xu, T. Tian, T. Fu, X. Wang, W., Li S. 2016. “Tripartite Motif 16 Suppresses Breast Cancer Stem Cell Properties through Regulation of Gli-1 Degradation via the Ubiquitin-Proteasome Pathway.” *Oncology Reports*. https://doi.org/10.3892/or.2015.4437.

Yao, Feng, Tor Svensjö, Thomas Winkler, Michael Lu, Carl Eriksson, and Elof Eriksson. 1998. "Tetracycline Repressor, TetR, Rather than the TetR-Mammalian Cell Transcription Factor Fusion Derivatives, Regulates Inducible Gene Expression in Mammalian Cells." *Human Gene Therapy* 9 (13): 1939–50. https://doi.org/10.1089/hum.1998.9.13-1939.

Yao, Yangyang, Zhen Liu, Yuan Cao, Hui Guo, Bailing Jiang, Jun Deng, and Jianping Xiong. 2020. "Downregulation of TRIM27 Suppresses Gastric Cancer Cell Proliferation via Inhibition of the Hippo-BIRC5 Pathway." *Pathology Research and Practice* 216 (9): 153048. https://doi.org/10.1016/j.prp.2020.153048.

Yoo, Seung-Min Min, and Yong-Keun Keun Jung. 2018. "A Molecular Approach to Mitophagy and Mitochondrial Dynamics." *Mol. Cells* 41 (1): 18–26. https://doi.org/10.14348/molcells.2018.2277.

Yoshii, Saori R., and Noboru Mizushima. 2017. "Monitoring and Measuring Autophagy." *International Journal of Molecular Sciences*. MDPI AG. https://doi.org/10.3390/ijms18091865.

Yoshizawa, Takuya, Ryu-Suke Nozawa, Tony Z Jia, Tomohide Saio, and Eiichiro Mori. 2020. "Biological Phase Separation: Cell Biology Meets Biophysics The Formation and Regulation of Membrane-Less Cellular Organelles." *Biophysical Reviews*. https://doi.org/10.1007/s12551-020-00680-x.

Young, Andrew R.J., Edmond Y.W. Chan, Xiao Wen Hu, Robert Köchl, Samuel G. Crawshaw, Stephen High, Dale W. Halley, Jennifer Lippincott-Schwartz, and Sharon A. Tooze. 2006. "Starvation and ULK1-Dependent Cycling of Mammalian Atg9 between the TGN and Endosomes." *Journal of Cell Science* 119 (18): 3888–3900. https://doi.org/10.1242/jcs.03172.

Yu, H, and A Matouschek. 2017. "Recognition of Client Proteins by the Proteasome." *Annu Rev Biophys* 46: 149–73. https://doi.org/10.1146/annurev-biophys-070816-033719.

Zachar, István, and · Gergely Boza. 2020. "Endosymbiosis before Eukaryotes: Mitochondrial Establishment in Protoeukaryotes." *Cellular and Molecular Life Sciences* 77: 3503–23. https://doi.org/10.1007/s00018-020-03462-6.

Zaffagnini, Gabriele, and Sascha Martens. 2016. "Mechanisms of Selective Autophagy." *Journal of Molecular Biology*. Academic Press. https://doi.org/10.1016/j.jmb.2016.02.004.

Zaffagnini, Gabriele, Adriana Savova, Alberto Danieli, Julia Romanov, Shirley Tremel, Michael Ebner, Thomas Peterbauer, et al. 2018. "P62 Filaments Capture and Present Ubiquitinated Cargos for Autophagy." *The EMBO Journal* 37 (5). https://doi.org/10.15252/embj.201798308.

Zaman, M M, T Nomura, T Takagi, T Okamura, W Jin, T Shinagawa, Y Tanaka, and S Ishii. 2013. "Ubiquitination-Deubiquitination by the TRIM27-USP7 Complex Regulates Tumor Necrosis Factor Alpha-Induced Apoptosis." *Mol Cell Biol* 33 (24): 4971–84. https://doi.org/10.1128/MCB.00465-13.

Zhang, H X, Z S Xu, H Lin, M Li, T Xia, K Cui, S Y Wang, Y Li, H B Shu, and Y Y Wang. 2018. "TRIM27 Mediates STAT3 Activation at Retromer-Positive Structures to Promote Colitis and Colitis-Associated Carcinogenesis." *Nat Commun* 9 (1): 3441. https://doi.org/10.1038/s41467-018-05796-z.

Zhang, Jing, Ming-Ming Hu, Yan-Yi Wang, and Hong-Bing Shu. 2012. "TRIM32 Protein Modulates Type I Interferon Induction and Cellular Antiviral Response by Targeting MITA/STING Protein for K63-Linked Ubiquitination * □ S." https://doi.org/10.1074/jbc.M112.362608.

Zhang, Y, Y Feng, D Ji, Q Wang, W Qian, S Wang, Z Zhang, et al. 2018. "TRIM27 Functions as an Oncogene by Activating Epithelial-Mesenchymal Transition and p-AKT in Colorectal Cancer." *Int J Oncol* 53 (2): 620–32. https://doi.org/10.3892/ijo.2018.4408.

Zhao, Jinghui, Jeffrey J. Brault, Andreas Schild, Peirang Cao, Marco Sandri, Stefano Schiaffino, Stewart H. Lecker, and Alfred L. Goldberg. 2007. "FoxO3 Coordinately Activates Protein Degradation by the Autophagic/Lysosomal and Proteasomal Pathways in Atrophying Muscle Cells." *Cell Metabolism* 6 (6): 472–83. https://doi.org/10.1016/j.cmet.2007.11.004.

Zhao, Ting Ting, Feng Jin, Ji Guang Li, Ying Ying Xu, Hui Ting Dong, Qun Liu, Peng Xing, et al. 2018. “TRIM32 Promotes Proliferation and Confers Chemoresistance to Breast Cancer Cells through Activation of the NF-KB Pathway.” *Journal of Cancer* 9 (8): 1349–56. https://doi.org/10.7150/jca.22390.

Zheng, Q, J Hou, Y Zhou, Y Yang, B Xie, and X Cao. 2015. “Siglec1 Suppresses Antiviral Innate Immune Response by Inducing TBK1 Degradation via the Ubiquitin Ligase TRIM27.” *Cell Res* 25 (10): 1121–36. https://doi.org/10.1038/cr.2015.108.

Zhou, Changqian, Kaili Ma, Ruize Gao, Chenglong Mu, Linbo Chen, Qiangqiang Liu, Qian Luo, Du Feng, Yushan Zhu, and Quan Chen. 2017. “Regulation of MATG9 Trafficking by Src- and ULK1-Mediated Phosphorylation in Basal and Starvation-Induced Autophagy.” *Cell Research* 27 (2): 184–201. https://doi.org/10.1038/cr.2016.146.

Zhuang, X J, W H Tang, X Feng, C Y Liu, J L Zhu, J Yan, D F Liu, P Liu, and J Qiao. 2016. “Trim27 Interacts with Slx2, Is Associated with Meiotic Processes during Spermatogenesis.” *Cell Cycle* 15 (19): 2576–84. https://doi.org/10.1080/15384101.2016.1174796.

Zimber, Amazia, Quang Dé Nguyen, and Christian Gespach. 2004. “Nuclear Bodies and Compartments: Functional Roles and Cellular Signalling in Health and Disease.” *Cellular Signalling*. Pergamon. https://doi.org/10.1016/j.cellsig.2004.03.020.

Zimmermann, Andreas, Katharina Kainz, Aleksandra Andryushkova, Sebastian Hofer, Frank Madeo, and Didac Carmona-Gutierrez. 2016. “Autophagy: One More Nobel Prize for Yeast.” *Microbial Cell*. Shared Science Publishers OG. https://doi.org/10.15698/mic2016.12.544.

Zong, Zhi, Zhengkui Zhang, Liming Wu, Long Zhang, and Fangfang Zhou. 2021. “The Functional Deubiquitinating Enzymes in Control of Innate Antiviral Immunity.” *Advanced Science* 8 (2): 2002484. https://doi.org/10.1002/advs.202002484.

Zoumpoulidou, G, C Broceno, H Li, D Bird, G Thomas, and S Mittnacht. 2012. “Role of the Tripartite Motif Protein 27 in Cancer Development.” *J Natl Cancer Inst* 104 (12): 941–52. https://doi.org/10.1093/jnci/djs224.

Zurek, B, I Schoultz, A Neerincx, L M Napolitano, K Birkner, E Bennek, G Sellge, et al. 2012. “TRIM27 Negatively Regulates NOD2 by Ubiquitination and Proteasomal Degradation.” *PLoS One* 7 (7): e41255. https://doi.org/10.1371/journal.pone.0041255.

Paper I

TRIM27 is an autophagy substrate implicated in autophagy induction and regulation of LAMP2

Juncal Garcia Garcia[1], Katrine Stange Overå[1], Zambarlal Bhujabal[1], Erik Knutsen[2], Hanne Britt Brenne[1], Gry Evjen[1], Trond Lamark[1], Terje Johansen[1], Eva Sjøttem[1]*

[1]*Molecular Cancer Research Group, Department of Medical Biology, University of Tromsø – The Arctic University of Norway, 9037 Tromsø, Norway*

[2]*RNA and Molecular Pathology Research Group, Department of Medical Biology, University of Tromsø –The Arctic University of Norway, 9037 Tromsø, Norway*

*Corresponding author. Tel: +47 776 46425; E-mail: eva.sjottem@uit.no

Running title: TRIM27 in autophagy and cancer

Keywords: TRIM27, autophagy, breast cancer

ABSTRACT

Cells use autophagy, an evolutionary conserved catabolic process, to maintain proper homeostasis. Defects in autophagy have been associated with cancer, where it modulates cell resistance or sensitivity to therapy, in addition to affecting the migration and invasion capabilities of tumor cells. The tripartite motif-containing 27 (TRIM27) protein is highly expressed in various cancers including breast cancer, shown to be involved in a multitude of processes such as cell proliferation, transcriptional repression, apoptosis, STAT3 activation, inhibition of NF-kB activation, and innate immune response. Here we identify TRIM27 as an autophagic substrate, depending on ATG7 and the sequestosome-like receptors for its lysosomal degradation. We mapped a LIR motif within its coiled-coil regions, with highest specificity towards LC3C. TRIM27 forms small cytoplasmic bodies that colocalizes with early autophagy proteins, and with the autophagy receptors p62/SQSTM1 and NBR1. Ablation of TRIM27 in HEK293 FlpIn cells reduced the starvation induced autophagy response, and resulted in increased levels of the lysosomal protein LAMP2. The increased LAMP2 expression resulted in enhanced formation of large, perinuclear lysosomes. TRIM27 is recognized as an oncogene, and mRNA expression profiling confirmed that TRIM27 is significantly upregulated in breast cancer tissue compared to normal tissue. Importantly, TRIM27 expression levels seemed to be inversely correlated with LAMP2 and LC3B expression levels in various breast cancer cell lines. These results point to TRIM27 as a regulator of autophagy in cancer cells, providing one of the oncogenic mechanisms of TRIM27.

INTRODUCTION

Synthesis and clearance of functional proteins regulate their availability within the cell, adapting the protein pool to the cellular needs. Thus, protein degradation is a crucial element in the maintenance of cellular homeostasis. Such an important process is tightly regulated in a spatially and timely manner through two main systems: the ubiquitin-proteasome system (UPS) and the lysosomal-mediated proteolysis (hereafter autophagy) (Dikic 2017).

The main tag for degradation is a globular protein of 76 amino acids called ubiquitin. Targeted proteins are conjugated to ubiquitin by the mediation of three sequential reactions. The first reaction is the activation of ubiquitin by E1 enzymes. The second reaction consists in the conjugation of ubiquitin to E2 enzymes for its delivery to the next step. The third and last reaction is mediated by E3 ligases that make possible the binding of the activated ubiquitin with the target molecule. While E1 and E2 are highly conserved and do not present much specificity, E3 ligases are in charge of recognizing the substrate, which makes them the main regulator of the pattern of ubiquitylation (Kleiger and Mayor 2014). Ubiquitin is a common denominator for both UPS and autophagy that work coordinately to create an efficient proteolytic network (Ji and Kwon 2017). In the beginning, ubiquitin was identified as a simple tag for protein degradation. However, in the last decades, evidences have shown the important role of ubiquitylation as a posttranslational modification in many cellular processes such as DNA repair response, cell cycle regulation, autophagy, cellular differentiation and cell-mediated immunity (Swatek and Komander 2016; Kwon and Ciechanover 2017; Yu and Matouschek 2017).

Tripartite motif family proteins (TRIMs) are a wide family of proteins involved in the control of several cellular processes such as intracellular signaling, innate immunity, transcription, autophagy and carcinogenesis. To date, there are more than 80 distinct protein members in the TRIM family (Watanabe and Hatakeyama 2017). The vast majority of those TRIMs present E3 ligase activity since they contain a RING finger-domain. Those TRIMs defined as E3 ligases are characterized by the presence of tripartite motif RBCC domain. The RBCC domain contains in the N-terminal a RING-finger domain, one or two B-boxes (B1/B2) and a coiled-coil (CC) domain. In addition, most TRIMs also present domains at the C-terminus, which gives them specificity for their target proteins (Esposito, Koliopoulos, and Rittinger 2017). TRIM proteins play several roles in autophagy, both as regulators and effectors. Some TRIMs, such as TRIM5α, 6, 16, 17, 20, 22, 49 and 55, act as a platform through the assembling of ULK1 and Beclin1. This regulatory complex has been name TRIMosome, which

regulates selective autophagy (M A Mandell et al. 2014). Other TRIMs, such as TRIM5α can also act as autophagy receptors of specific targets (Michael A Mandell et al. 2015). Moreover, some TRIMs regulate autophagy through their interaction with p62/SQSTM1 (hereafter p62/SQSTM1). This interaction often take place under certain cellular conditions, such as TRIM13 during ER stress. This shows the high specificity of this family of E3 ligases. No TRIM homologs have been identified in yeast, which is a well-studied autophagy model organism. Thus, TRIM proteins might add complexity to the mammalian autophagy system, being able to regulate more specific degradation processes.

TRIM27 is an E3 ligase also known as Ret finger protein (RFP protein), which was firstly described as a fusion protein with the tyrosine kinase domain of the c-RET proto-oncogene originated by DNA rearrangement (Cao et al. 1996). This 58-kDa protein can be found in both the cytoplasm and the nucleus of the cells, depending on the cell type (G. Tezel et al. 1999). TRIM27 is involved in the regulation of several cellular processes such as immunity, apoptosis, cell growth, proliferation and endosomal recycling (Nie et al. 2016; Zoumpoulidou et al. 2012; Liu et al. 2014; Zhuang et al. 2016). TRIM27 is reported to have several roles in host defense against pathogens. It acts as a host restriction factor during mycobacterial infection, enhancing immune-inflammatory response and cell apoptosis (Nie et al. 2016). In addition, TRIM27 has been identified as a degradation target of Herpes Simple Virus 1 ICP0 (Conwell et al. 2015), and together with USP7 negatively modulates antiviral type I interferon signaling (Cai et al. 2018). Moreover, TRIM27 plays a role in endosomal recycling when it is in complex with USP7 and MAGE-L2. This complex regulates the activity of the WASH/retromer-mediated endosomal recycling through its ubiquitylation status (Hao et al. 2015). TRIM27 is identified as an oncogene, highly expressed in various cancer types such as breast cancer. TRIM27 promotes proliferation mainly through its nuclear function, participating in transcriptional regulation complexes (Horio et al. 2012; Iwakoshi et al. 2012; Tsukamoto et al. 2009; G. G. Tezel et al. 2009; H. X. Zhang et al. 2018; Cai et al. 2018) It is also shown to promote cell migration and invasion (Y. Zhang et al. 2018). However, whether TRIM27 plays a role in autophagy in cancer cells still need to be fully elucidated.

Here we show that TRIM27 is a cargo for the sequestosome-like receptors p62/SQSTM1 and NDP52, directing it for lysosomal degradation. A LIR motif with specificity towards LC3C was identified in its coiled-coil region. However, TRIM27 did not seem to act as an autophagy receptor itself. TRIM27 is localized in specific structures in the cytoplasm, often together with early autophagy proteins such as ATG9, ATG13 and ULK1, and the

autophagy receptors p62/SQSTM1 and NBR1. Knock out of TRIM27 in HEK293 FlpIn cells reduced the starvation induced autophagy response, and resulted in increased expression of LAMP2 and formation of large LAMP2 rings. Moreover, LAMP2 was identified as an interaction partner of TRIM27.

In line with previous studies, our bioinformatics analysis show that TRIM27 expression is upregulated in breast cancer tissues. Interestingly, the expression of TRIM27 varies substantially in cells representing different breast cancer subtypes, and its expression level seemed to be inversely correlated with the expression of LAMP2 and LC3B. Altogether, these results suggest that TRIM27 may regulate the autophagy process in certain cancer cell lines.

MATERIALS AND METHODS

Antibodies and reagents.

The following primary antibodies were used: rabbit polyclonal antibody for TRIM27 (Proteintech, #122205-1-AP)(1:1000); rabbit polyclonal anti-GFP (Abcam, ab290)(1:5000); rabbit polyclonal anti-LC3B (Sigma, L7543)(1:1000 for WB, 1:500 for IF); LAMP2(Santa Cruz Sc-18822, 1:1000 for WB, 1:500 for IF), ATG13 (Cell signaling 13468S, 1:100 for IF), ULK1 (Cell signaling 8054, 1:100 for IF), GM130 (Abcam Ab 53649, 1:500 for IF), USP7 (Biosite A300-033A, 1:200 for IF), NBR1 (Santa Cruz Sc-130380, 1:1000 for WB, 1:200 for IF), TOM20 (Santa Cruz Sc-11415, 1:500 for IF), FK2 (AH Diagnostics BML-PW8810-0100, 1:1000 for WB, 1:500 for IF); mouse monoclonal anti-p62/SQSTM1 lck ligand (BD Biosciences, 610833)(1:2000) and guinea pig polyclonal anti-p62/SQSTM1 (Progen, GP62/SQSTM1-C)(1:2000); mouse monoclonal anti-PCNA (DAKO, M0879)(1:1000). The following secondary antibodies were used: Horseradish-peroxidase (HRP)-conjugated goat anti-rabbit IgG (BD Biosciences, 554021)(1:2000); HRP-conjugated goat anti-mouse Ig (BD Biosciences, 554002)(1:2000); and HRP-conjugated anti-Biotin antibody (Cell Signalling, #7075)(1:2000). The following fluorescent secondary antibodies were used: Alexa Fluor® 488-conjugated goat anti-mouse IgG (Life Technologies, A-11029)(1:1000); Alexa Fluor® 555-conjugated goat anti-rabbit IgG (Life Technologies, A-11008)(1:5000); Alexa Fluor® 555-conjugated goat anti-mouse IgG (Life Technologies, A-21424)(1:1000); Alexa Fluor® 647-conjugated goat anti-guinea pig IgG (Life Technologies, A-21450)(1:1000). The reagents used were Bafilomycin A1 (Sigma, B1793); MG132 (Sigma, C2759); Tetracycline (Sigma, #87128); Hanks Balanced salt solution (Sigma, H8264).

Construction of Plasmids

All plasmids used in this study are listed in Table 1. Plasmids were made by use of the Gateway recombination system (ThermoFisher). Gateway LR reactions were performed as described in the instruction manual. Point mutations were carried out using the Site-directed-mutagenesis kit from STRATAGENE. Primers for establishment of LIR mutated TRIM27$^{W184A/F186A/L189A}$ 5′-GAAGATTGTTGCGGAGGCTGAGCAGGCGTATCACTCCTTA-3′ were ordered from ThermoFisher. All plasmids were verified by restriction enzyme digestion and DNA sequencing (BigDye, Applied Biosystems, 4337455).

Table 1: Plasmids used in this study

pDONR221 TRIM27	Harvard HsCD00042999
pDest mCherry-EYFP TRIM27	(Overå et al. 2019)
pDest EGFP-C1	(Lamark et al. 2003)
pDest EGFP-TRIM27	This study
pDest Myc-TRIM27	This study
pDest Myc-TRIM27 $^{W184A/F186A/L189A}$	This study
pDest Myc-p62/SQSTM1	(Lamark et al., 2003)
pDestMyc-NDP52	(Abudu et al., 2019)
pDest Myc	(Lamark et al. 2003)
pDest15 LC3A	(Pankiv et al. 2007)
pDest15 LC3B	(Pankiv et al. 2007)
pDest LC3C	(Alemu et al. 2012)
pDest GABARAP	(Pankiv et al. 2007)
pDest GABARAP L1	(Pankiv et al. 2007)
pDest GABARAP L2	(Pankiv et al. 2007)
pSPCas9(BB)-2A-GFP (PX458)	(Ran et al. 2013) Addgene#48138
pDest EGFP FlpIn FRT/TO	(Alemu et al. 2012)
pDest EGFP FlpIn TRIM27	This study

Cell culture and transfections

HeLa (ATCC, CCL2), Hek293 (ATCC, CRL-1573) and Hek293 T-Rex (ThermoFisher, R714-07) cells were cultured in Dulbecco's modified eagle's medium (DMEM) (Sigma, D6046) with

10% fetal bovine serum and 1% streptomycin-penicillin (Sigma, P4333). Hek FlpIn T-Rex cells with integrated EGFP-TRIM27 were grown in the same medium with additional selection marker antibiotics, 200µg/ml Hygromycin B (Invitrogen, #10687010) and 7,5 µg/ml Blasticidin (Gibco, A1113903). The breast cancer cell lines HS578, MDA-MD-231, and MCF7 were cultured in DMEM medium. The breast cancer cell lines BT549, T47D, MDA-MD-468, BT474, HCC1569 and SKBR3 were cultured in RPMI-1640 medium. Sub-confluent cells were transfected using TransIT-LT1 (Mirus, MIR2300) or Metafectene Pro (Biontex, T040) following the manufacturer's instructions. All cell lines were routinely tested for mycoplasma contamination.

Recombinant protein production and GST pulldown analysis

GST or GST-tagged proteins were expressed in *Escherichia coli* strain SoluBL21 (Genlantis, #C700200). Protein expression was induced by treating overnight bacterial culture with 50µg/ml Isopropyl β-D-1-thiogalactopyranoside (IPTG). GST or GST fusion proteins were purified and immobilized on Glutathione-Sepharose 4 Fast Flow beads (GE Healtcare, 17-5132-01). Myc-tagged proteins were *in vitro* translated using the TNT T7 reticulocyte Lysate system (Promega, #14610) in the presence of ^{35}S-methionine. *In vitro* translated protein or total cell lysate was pre-incubated with 10µl glutathione sepharose beads and 100µl of NETN buffer (50mM Tris pH 8.0; 150mM NaCl; 1 mM EDTA; 0.5% Nonidet P-40) with cOmplete Mini EDTA-free protease inhibitor mixture tablets (Roche Applied Science, 11836170001) for 1hr at 4°C to reduce unspecific binding. Pre-incubated lysate was then incubated with the immobilized GST fusion protein for 2hrs at 4°C. Beads were washed five times with NETN buffer, boiled with 2xSDS gel loading buffer (125mM Tris pH 7.5; 4% SDS; 0.04% bromphenol blue; 8% sucrose; 100mM dithiolthreitol) and subjected to SDS-PAGE. Gels were stained with Coomassie Brilliant Blue R-250 Dye (Thermofisher scientific, #20278) to visualize GST fusion proteins and then vacuum-dried. Signals from ^{35}S-labelled proteins were detected by a Fujifilm bioimaging analyzer BAS-5000 (Fujifilm).

Peptide Array

TRIM27 peptide arrays were synthesized on cellulose membranes using MultiPrep peptide synthesizer (INTAVIS Bioanalytical Instruments AG, Germany). Membranes were blocked with 5% non-fat dry milk in TBST and peptide interactions were tested with GST and GST-GABARAP by overlaying the membrane with 1 µg/ml of recombinant proteins and incubation

for 2 h at room temperature. Bound proteins were visualized with HRP-conjugated anti-GST antibody.

Western Blotting

Cells were seeded in 6 well dishes and treated as indicated. Cells were lysed in 1xSDS buffer (50mM Tris pH 7.4; 2% SDS; 10% Glycerol) supplemented with 200mM dithiothreitol (DTT, Sigma, #D0632) and heated at 100°C for 10 minutes. Protein concentration was measured using the Pierce BCA Protein Assay Kit (Thermofisher Scientific, #23227). Equal amounts of protein were resolved by SDS-PAGE and transferred to nitrocellulose membrane (Sigma, GE10600003). The membrane was stained with Ponceau S (Sigma, P3504), blocked with 5% non-fat dry milk in 1% TBS-T (0.2M Tris pH 8; 1.5M NaCl and 0.05% Tween20 (Sigma, P9416)) and then incubated with indicated primary antibodies for 24h. The membrane was washed three times for 10 minutes each with TBS-T followed by incubation with secondary antibody for 1h. The membrane was washed three times for 10 minutes and analyzed by enhanced chemiluminescence using the ImageQuant LAS 4000 (GE Lifescience).

Immunostaining and Fluorescence confocal microscopy

Subconfluent cells grown in 24-well plates on coverslips (VWR, #631-0150) coated with Fibronectin (Sigma, F1141) and treated as indicated. They were fixed in 4% paraformaldehyde for 20 min. The cells were then permeabilized with methanol at RT for 5min, blocked in 5% goat serum/PBS or 5%BSA/PBS and incubated at room temperature with a specific primary antibody followed by Alexa Fluor 488, 555 or 647 conjugated secondary antibody and DAPI. Confocal images were obtained using a 63x/NA1.4 oil immersion objective on an LSM780 (Zeiss). Quantification of cells containing red only dots in the double tagged screen, or large LAMP2 rings, was done manually in three independent experiments.

Generation of TRIM27 knock out in HEK293 FlpIn cell lines

To generate knock out cells for TRIM27, the CRISPR/Cas9 system was exploited as described by (Ran et al. 2013). The Guide RNA sequence 5′-CTTTACCAGTTGGGTCACGT-3′ was ligated into the vector pSpCas9(BB)-2A-GFP (PX458) (Addgene, #48138) using BbsI restriction sites. Subconfluent Hek293 FlpIn T-Rex cells were transfected with the targeting plasmid using Metafectene Pro (Biontex, T020). EGFP-positive cells were sorted by FACS and plated into 96-wells plates three days post transfection. Single colonies were expanded up to 12-well plates

and KO validated by immunoblotting. Confirmed KO clones were further screened by genomic sequencing. The targeted genomic regions were amplified by PCR using the primers 5'-CCGGAGAGAGCGCCGGAGAGTTG-3' and 5'-CAAGGTGAGGGCGCGGATCCGGGAG-3' and the resulting PCR products ligated into the pGEM-T-EASy vector (Promega, A3600). Sequencing were conducted for at least 3 clones for each PCR product.

Generation of tetracycline inducible HEK293 FlpIn cell lines

Stable cell lines were generated using the FlpIn T-Rex system (Thermofisher, R71407). TRIM27 cDNA was transferred to the inducible FlpIn expression vector pDest-EGFP-Flp-In by GATEWAY cloning. FlpIn T-Rex cells were then cotransfected with the TRIM27 FlpIn expression vector and the FlpIn recombinase vector pOG44 in the ratio of 1:3. Cells were selected by treatment with 200µg/ml Hygromycin B (Invitrogen, #10687010) and 7,5 µg ml^{-1} Blasticidin (Gibco, A1113903), and protein expression verified by induction with Tetracycline (Sigma, #87128).

Cell proliferation assay

The cell lines HEK293 T-Rex FlpIn, HEK293 T-Rex FlpIn TRIM27 KO, HEK293 T-Rex FlpIn TRIM27 KO + TRIM27 WT and HEK293 T-Rex FlpIn TRIM27 KO + GFP were harvested with trypsin and seeded into 12-well plates at a density of 100.000 cells per well. Afterwards, cells were incubated in IncuCyte (Essen BioScience, Ann Arbor, MI, USA) at 10x magnification and images were taken in the phase and green channels every 24h. Images were analyzed by Incucyte S3 Live-cell analysis system. The assays were performed in triplicate.

Migration assay

The cell lines HEK293 T-Rex FlpIn, HEK293 T-Rex FlpIn TRIM27 KO, HEK293 T-Rex FlpIn TRIM27 KO + TRIM27 WT and HEK293 T-Rex FlpIn TRIM27 KO + GFP were harvested with trypsin and seeded into 96-well Image-Lock Microplate (Essen BioScience, Ann Arbor, MI, USA) at a density of 8.000 cells per well. Twenty-four hours after seeding, a scratch wound was made by using the Incucyte 96-well WoundMaker tool (Essen BioScience, Ann Arbor, MI, USA) according to the manufacturer's instructions. Cells were incubated at 37 °C with CO2 in the Incucyte (Essen BioScience, Ann Arbor, MI, USA) at 10x magnification and pictures were taken in the phase and green channels every 15h (for figure presentation, quantification ever 24 hours is shown). Images were analyzed by Incucyte S3 Live-cell analysis system. The assay was repeated independently two times.

Bioinformatics

For the analysis of TRIM27 expression in normal versus tumor, two publically available breast cancer datasets, PRJNA399721 and PRJNA172761, were downloaded from the Sequence Read Archive (SRA). PRJNA399721 consist of 22 primary invasive breast cancer carcinoma expressing estrogen receptors and their paired adjacent mammary healthy tissues. Libraries were prepared using the TruSeq® Stranded Total RNA kit and Ribo-Zero rRNA Removal kit (Illumina) and sequencing was performed by strand-specific RNA sequencing on a Illumina HiSeq. PRJNA172761 consist of 53 primary breast cancers and 6 normal breast samples from mammoplasty patients. Single-end Illumina-based RNA-sequencing was performed, using both 29 bp reads (on 29 tumor samples) and 100 bp reads (on 24 tumor samples and 6 normals).

The CLC Genomic workbench (v8.5.1) was used for analyzing the RNA-Seq data. Raw reads were trimmed for quality (Quality limit = 0.05) and adaptor (Illumina TruSeq LT and HT adaptor or Illumina 1.5 Small RNA). Trimmed reads were mapped to GRCh38 with Ensembl annotation v84, using either strand specific mapping (PRJNA399721) or non-strand specific mapping (PRJNA172761), (Mismatch cost = 2, Insertion cost = 3, Deletion cost = 3, Length fraction = 0.9, Similarity fraction = 0.8). Only uniquely mapped reads were included in gene quantification. Reads per million (RPM) normalization was utilized, and gene counts were log2 transformed. Graphpad prism was used for making illustrations and statistical analysis. A paired t-test was used for the comparison of paired tumor versus normal samples, while a non-paired t-test was used for the calculation of normal versus tumor samples.

Statistics

All experiments were repeated at least three times, unless otherwise specified. Error bars represent the s.d. or s.e.m. as indicated in Figure legends. Replicates were not pooled for statistical analyses.

RESULTS

Autophagic degradation of TRIM27 is dependent on ATG7 and the Sequestosome-Like receptors.

In a qualitative screen in HeLa cells using the double tag mCherry-EYFP fused to 22 various members of the TRIM family of ubiquitin E3 ligases, we identified TRIM27 as a potential target for autophagic degradation (Figure 1A) (Overå et al. 2019). Both under normal and starved conditions, RedOnly puncta could be observed in the mCherry-EYFP-TRIM27 expressing cells (Figure 1A), with a slightly increased induction of RedOnly puncta upon starvation (Figure 1B). To pinpoint the autophagy pathway implicated in TRIM27 degradation, the mCherry-EYFP-TRIM27 double tag assay was performed in ATG7 KO cell lines. We were not able to observe any RedOnly dots in the transfected ATG7 KO cell lines (Figure 1A,B). Previously, we have shown that autophagic degradation of TRIM32 is mediated by selective autophagy involving the Sequestosome-Like-Receptors (SLRs) (Overå et al. 2019). To investigate if also TRIM27 is degraded by selective autophagy mediated by the SLRs, the mCherry-EYFP-TRIM27 double tag assay was applied on a cell line knocked out for the five SLRs p62/SQSTM1, NBR1, NDP52, Optineurin and Tax1BP1 (pentaKO) (Lazarou et al. 2015). No RedOnly dots of mCherry-EYFP-TRIM27 could be observed neither under normal nor starved conditions (Figure 1A,B). Together, these results indicate that autophagic degradation of TRIM27 is mediated by selective autophagy.

To measure whether p62/SQSTM1 is sufficient to direct TRIM27 to autophagic degradation, we applied the mCherry-EYFP-TRIM27 double tag assay on the HeLa penta KO cell line reconstituted with EGFP-p62/SQSTM1 (Figure 1A,B) (Overå et al. 2019). Reintroduction of EGFP-p62/SQSTM1 facilitated formation of mCherry-EYFP-TRIM27 RedOnly dots, but not to the same extent as the wild type cells (Figure 1A-B). Similar results were obtained by reintroduction of EGFP-NDP52 (Figure 1A,B). Thus, both SLRs were able to direct autophagic degradation of mCherry-EYFP-TRIM27. To sum up, here we suggest that TRIM27 is a cargo for selective autophagy, and its dependence on the SLRs for autophagic degradation indicates that it does not act as an autophagy receptor itself.

In order to determine if endogenous TRIM27 is degraded by autophagy, we analyzed the TRIM27 protein levels in HeLa ATG9 KO cells (kindly provided by Y. Abudu, unpublished). ATG9 vesicles are required for nucleation of the autophagic isolation membrane, and hence ablation of ATG9 will block the autophagy process (Orsi et al. 2012). Notably, TRIM27 seems to be stabilized and modified in the ATG9 KOs cells. The slower migrating TRIM27 band suggests that ATG9 and inhibition of autophagy has an impact on TRIM27

expression (Fig 1C,D). The autophagy receptors p62/SQSTM1 and NBR1 also display migration differences in HeLa ATG9 KO cells compared to normal HeLa cells (Fig 1C). This further suggests that there is a link between TRIM27 and the autophagy receptors.

TRIM27 has a LIR with specificity towards LC3C.

TRIM27 belongs to the same TRIM family subclass as TRIM5α retroviral restriction factor acting during the early post entry stages of the retroviral life cycle to block infection by a broad range of retroviruses, disrupting reverse transcription and integration (Sawyer et al. 2005). Trim5α was reported to act as a selective autophagy receptor, targeting a restricted virus to the autophagosome for degradation (Michael A Mandell et al. 2015). It was demonstrated that TRIM5α interacts directly with ATG8 proteins via a LIR motif. Later, the LC3 interacting region in TRIM5α was proposed to be located in a helical region within the coiled-coil region, including the residues D192, W196 and E203 (Keown et al. 2018). The similarity of TRIM5α and TRIM27 prompted us to apply a peptide array to identify putative ATG8 interacting regions in TRIM27. In this assay, various 20 amino acid long peptides covering the complete region of TRIM27 were spotted on filter paper and probed against GST-GABARAP proteins expressed and purified from *E. coli*. The spot blot identified a putative LIR located within the W184-F186-L189 region of TRIM27 (Figure 2A). To verify this putative LIR motif, we established the TRIM27$^{W184A/F186A/L189A}$ mutant and compared its ability to bind the ATG8s with the binding ability of wild type TRIM27 in a GST-pulldown assay using GST-ATG8 proteins expressed and purified from *E. coli*, and TRIM27 proteins produced by *in vitro* translation. Figure 2B shows that wild type TRIM27 has high affinity for LC3C, binds with lower affinity to GABARAP and GABARAPL1, and very weakly or not at all to LC3A, LC3B and GABARAPL2.

Introduction of the W184A/F186A/L189A mutations in TRIM27 resulted in strong reduction of the LC3C binding, and some reduction in the binding to GABARAP and GABARAPL1 (Figure 2B). This suggests that TRIM27 contains a LIR with highest specificity against LC3C, located close to or within its coiled-coil region. The specificity for LC3C and partially GABARAP was further verified by GST-pulldown assay using cell extracts from the HEK293 FlpIn EGFP-TRIM27 cell line (Figure 2C). To sum up, here we show that TRIM27 contains a LIR motif with high specificity towards LC3C. The TRIM27 LIR displays strong similarity to the LIR2 of TRIM5α (Figure 2D).

TRIM27 forms cytoplasmic puncta that co-localizes with proteins implicated in the autophagy process

To further address if TRIM27 may impact the autophagy process, we established a HEK293 FlpIn TRIM27 KO cell line by CRISPR/Cas9 (Ran et al. 2013), reconstituted cell line with tetracycline inducible expression of EGFP-TRIM27, and a HEK293 FlpIn TRIM27 KO cell line with inducible expression of EGFP as control cell line (Figure S1A-C). The expression level of EGFP-TRIM27 in the reconstituted TRIM27 KO cell line was close to the endogenous level (Figure S1D), and localized to certain dots/aggregates in the cytoplasm, in addition to a few nuclear dots (Figure S1E). This is in line with the reported localization of endogenous TRIM27 (proteinatlas.org). Next, we compared the proliferation and migration potential of the HEK293 FlpIn TRIM27 KO cells with the reconstituted TRIM27 KO cell lines (Figure S1F). The HEK293 FlpIn TRIM27 KO cell line displays an enhanced proliferation rate compared to the HEK293 FlpIn TRIM27 KO cell line reconstituted with EGFP-TRIM27 (Figure S1F, left graph). This suggests that TRIM27 expression may inhibit cell proliferation in HEK293 FlpIn cells. Conversely, the migration rate of the TRIM27 KO cells was reduced compared to the HEK293 FlpIn cells, while reintroduction of EGFP-TRIM27 restored the migration rate (Figure S1F, right graph). Thus, in HEK293 FlpIn cells TRIM27 seems to facilitate cell migration but not cell proliferation. This is in line with previous studies showing that TRIM27 facilitates cell migration and invasion (H. X. Zhang et al. 2018), and may have a role in Epithelial to Mesenchymal transition in cancer cells.

Since the expression level of induced EGFP-TRIM27 in the HEK293 FlpIn TRIM27 KO cells is similar to the endogenous TRIM27 expression levels (Figure S1D), the physiological effect of the reconstituted EGFP-TRIM27 may be close to the effect of endogenous protein.

Next, we analyzed whether TRIM27 is localized to autophagic structures in the cell. For this purpose, we performed immunostaining of autophagy related proteins in the HEK293 FlpIn TRIM27 KO EGFP-TRIM27 cells. EGFP-TRIM27 formed several cytoplasmic puncta in addition to a few nuclear puncta, and in some cells EGFP-TRIM27 formed larger structures (Figure 3). TRIM27 does not seem to co-localize with GM130 (Golgi marker) and calreticulin (ER marker), suggesting that TRIM27 is not present or migrates to the Golgi or the ER (Figure S2A).

EGFP-TRIM27 co-localizes strongly with the autophagy receptors p62/SQSTM1 and NBR1 (Fig 3). This supports the finding that TRIM27 is a substrate for selective autophagy.

Moreover, TRIM27 co-localizes in multiple dots with the autophagy proteins ATG9, ATG13, and ULK1 (Fig 3). Together these results suggest that TRIM27 is associated with autophagy structures, and hence is a potential regulator of the autophagy process. As controls of the EGFP-TRIM27 localization pattern, we stained the HEK293 FlpIn TRIM27 KO EGFP-TRIM27 cells with antibodies against USP7 and ubiquition (FK2). TRIM27 forms a complex with USP7 that is in charge of the regulation of Tumor necrosis factor alpha induced apoptosis, and together with USP7 and MAGE2, this complex regulates the protein levels of WASH that is involved in vesicles trafficking (Cai et al. 2018; Zaman et al. 2013). In accordance with this, we see that USP7 is present in certain EGFP-TRIM27 dots (Fig 3). Also several of the EGFP-TRIM27 dots are recognized by the ubiquitin antibody (FK2) (Fig 3). Thus, reconstituted EGFP-TRIM27 localization seems to represent the localization pattern of endogenous TRIM27, suggesting that TRIM27 associates with autophagic structures in the cytoplasm.

TRIM27 is associated with several proteins involved in the autophagy process.

To further assess the potential role of TRIM27 in autophagy, we applied mass spectrometry (MS) analysis to identify whether autophagy-related proteins co-precipitated with EGFP-TRIM27 immunoprecipitated from the reconstituted HEK293 FlpIn TRIM27 KO cells. The HEK293 FlpIn TRIM27 KO cells reconstituted with EGFP only were used as a control to discard possible unspecific binding with the EGFP-tag. The MS data identified that TRIM27 co-precipitates the autophagy receptors p62/SQSTM1, NBR1, CALCOCO2 (NDP52) and TAX1BP1 (Fig 4A). This supports that TRIM27 is a substrate for selective autophagy. Additionally, we identified the autophagy protein ATG7, the autophagy regulator TBK1, and the lysosomal protein LAMP2 as putative interaction partners of TRIM27, supporting our findings that TRIM27 co-localizes with autophagy structures in the cell (Fig 3). To verify these interactions further, we performed Western blotting against selected proteins from the MS screen, on immunoprecipitated EGFP-TRIM27 extracts from the reconstituted HEK293 FlpIn TRIM27 KO cells As displayed in Figure 4B, the autophagy receptors p62/SQSTM1 and NBR1 are associated with EGFP-TRIM27, although the NBR1 interaction seems weak. To test whether the interaction with p62/SQSTM1 were directly, a GST-pulldown assay with GST-p62/SQSTM1 expressed and purified from *E. coli* was incubated with in-vitro translated TRIM27 (Figure 4C). This assay was also performed with GST-NDP52, which displayed a very weak interaction with TRIM27 (Figure 4C). Clearly, TRIM27 seems to interact directly with the autophagy receptor p62/SQSTM1. To elucidate whether TRIM27 has the ability to

ubiquitylate p62/SQSTM1, we transfected myc-p62/SQSTM1 expression plasmids into the HEK293 FlpIn TRIM27 KO EGFP-TRIM27 cell lines. Ubiquitylation of myc-p62/SQSTM1 was detected by immunoprecipitation of myc-p62/SQSTM1 and Western Blotting using an antibody recognizing ubiquitin (Figure 4D). EGFP-TRIM27 expression leads to a slower migrating myc-p62/SQSTM1 band that are detected by the ubiquitin antibody, indicating that TRIM27 ubiquitylates p62/SQSTM1. This was further supported by Western blotting of endogenous p62/SQSTM1 in HEK293 FlpIn TRIM27 KO cells and the TRIM27 KO cells reconstituted with EGFP-TRIM27. Our results display a slower migrating band of endogenous p62/SQSTM1 in cells expressing EGFP-TRIM27 (Figure S2B).

Notably, the immunoprecipitation also verified association of TRIM27 with LAMP2 (Figure 4B). Previous reports has linked TRIM27 to subcellular membrane systems, as a MAGE2-USP7-TRIM27 complex regulates the retromer at sorting endosomes (Hao et al. 2015). The interaction of TRIM27 with LAMP2 may suggest a role for TRIM27 in lysosomal pathways, such as autophagy.

TRIM27 facilitates starvation-induced autophagy

Next we set out to analyze whether TRIM27 may impact the autophagy process. It is well recognized that p62/SQSTM1 and LC3B co-localizes in certain cytoplasmic dots indicative of autophagosomes in HEK293 cells, and that the number of dots increases upon starvation due to induction of autophagy. Starvation induced autophagy is initiated by activation of ULK1, leading to phosphorylation of the ULK1 complex members ATG13 and FIP200 (Dossou and Basu 2019). Subsequently, the BECLIN1 complex including the VPS34 lipid kinase is activated and produces a pool of phosphatidylinositol 3-phosphate (PtdIns(3)P) at membrane sites where formation of the omegasome takes place. Generation of PtdIns(3)P facilitates recruitment of WIPI2 (WD-repeat PtdIns(3)P effector protein) which can be observed as specific starvation induced WIPI2 dots by immunostaining. WIPI2 recruits LC3B via the LC3 conjugation system to the forming omegasome (Melia, Lystad, and Simonsen 2020). Co-staining of p62/SQSTM1 and LC3B in the TRIM27 KO cells under normal and starved conditions, indicated that starvation induced initiation of the autophagy process was affected by TRIM27 ablation (Figure 5A,B). In the HEK293 FlpIn cell line, p62/SQSTM1 and LC3B co-localized in certain cytoplasmic dots in the cells cultured in normal medium, and the number of such dots increased by changing the medium with HBSS for 2 hours. In contrast, in HEK293 FlpIn TRIM27 KO cells, the number of p62/SQSTM1 dots did not show an increase upon starvation. Moreover,

the number of LC3B dots decreased upon starvation in the HEK293 FlpIn TRIM27 KO cells. In line with this, the number of WIPI2 dots in the HEK293 FlpIn cells increased upon starvation, while this increase could not be observed in the HEK293 FlpIn TRIM27 KO cells (Figure5C,D). Thus, the starvation induced initiation of autophagy seems to be impaired in the TRIM27 KO cells, suggesting that TRIM27 facilitates the induction of autophagy upon starvation.

Depletion of TRIM27 leads to increased LAMP2 levels and formation of large LAMP2 rings in HEK293 FlpIn cells.

TRIM proteins interacting with the core autophagy machinery have been already identified (T Kimura et al. 2015; T Kimura, Mandell, and Deretic 2016; Tomonori Kimura et al. 2017; M A Mandell et al. 2014), and recently we showed that TRIM32 binds to p62/SQSTM1 and the ATG8s *in vitro*, and co-localizes with p62/SQSTM1 and LC3B in specific puncta in cell cytoplasm (Overå et al. 2019). TRIM27 is an ubiquitin E3 ligase that can direct other proteins for degradation. In order to assess whether TRIM27 and its interaction with autophagy-associated proteins lead to their degradation, we analyzed the protein levels of p62/SQSTM1, NBR1, LC3B, ATG9, LAMIN-B1 (used as nuclear control) and LAMP2 (used as a cytoplasmic control) in the cytoplasmic and nuclear fractions of HEK293 FlpIn, TRIM27 KO and TRIM27 reconstituted with EGFP-TRIM27 (Figure 6A). Surprisingly, the level of LAMP2 seems to increase strongly in the HEK293 TRIM27 KO cell line compared to the HEK293 FlpIn cells, while the levels of the other autophagy proteins remain the same in all cells (Figure 6A). Normal LAMP2 expression was fully recovered in the reconstituted HEK293 FlpIn EGFP-TRIM27 cells (Figure 6A,B). Similar increase in LAMP2 level were seen in HEK293 FlpIn cells treated with TRIM27 siRNA (Figure 7C). To further assess this effect of TRIM27 on LAMP2 levels, we immunostained the HEK293 FlpIn TRIM27 KO cells, HEK293 FlpIn TRIM27 KO EGFP-TRIM27 and HEK293 FlpIn cells treated with TRIM27 siRNA with LAMP2 antibodies. Whereas HEK293 FlpIn cells and HEK293 FlpIn TRIM27 KO cells reconstituted with EGFP-TRIM27 cells showed similar LAMP2 staining, a large proportion of the HEK293 FlpIn TRIM27 KO cells and HEK293 FlpIn TRIM27 KD cells displayed large LAMP2 rings (Figure 6D) often localized in the perinuclear region and close to the EGFP-TRIM27 bodies and the mitochondria (Figure 6E). Together these results indicate that TRIM27 associates with LAMP2 and may have a role in the regulation of the cellular levels of LAMP2.

TRIM27 and LAMP2 expression is inversely correlated in breast cancer cell lines.

Our results suggest that TRIM27 is an autophagy substrate and has a role in the regulation of starvation induced autophagy. TRIM27 is described as an oncogene, and high expression of TRIM27 is associated with increased invasion and migration of cancer cells (H. X. Zhang et al. 2018). It is well recognized that autophagy is an important process for the survival and growth of cancer cells (Hatakeyama 2017; Koukourakis et al. 2015; Alessandrini, Pezzè, and Ciribilli 2017). Upregulated TRIM27 expression has been associated with breast cancer and mechanistically this has been linked to its nuclear role implicated in Estrogen Receptor transcription complexes (G. G. Tezel et al. 2009). In order to investigate if TRIM27 expression is associated with autophagy activity in breast cancer, we first analysed the TRIM27 mRNA expression in tumor tissue and normal tissue from two different patient cohorts (Figure 7A). In both cohorts, TRIM27 mRNA was significantly upregulated in the cancer tissues compared to normal tissue. Next, the amount of TRIM27 and LC3B proteins in various breast cancer cell lines representing various breast cancer subtypes were analysed by Western blotting (Figure 7B). The TRIM27 expression level varies substantially within the the various cell lines, with high expression in the luminal cell lines MCF7 and T47D, and in the basal-like cell ine MDA-MD-468. Moreover, in the MDA-MD-468 cells, the TRIM27 protein migrates slower suggesting that it may represent a TRIM27 fusion protein, or a TRIM27 protein highly modified by post-translational modifications. TRIM27-RET fusions are described in several cancers, however has not been detected in breast cancer (Hameed et al. 2009). In contrast, in the trippel-negative MDA-MD-231 and BT549 cell lines, no TRIM27 expression could be detected. Interestingly, LC3B was highly expressed in the triple-negative breast cancer cell lines, while it was low in luminal and Her2 positive cell lines. Hence, the expression of TRIM27 and LC3B seems to be inversely correlated in the breast cancer cells. Moveover, LAMP2 expression is upregulated in the breast cancer cell lines displaying no or very low expression levels of TRIM27. This correlates well with our analyses in HEK293 cells, suggesting that loss of TRIM27 leads to enhanced LAMP2 expression. Collectively, these results point to TRIM27 as a putative regulator of autophagy, and that one of its oncogenic features is to facilitate the autophagy process in cancer cells. Moveover, breast cancer cell lines with various expression levels of TRIM27 represent promising model systems for further revealing the molecular mechanisms of TRIM27 in autophagy and cancer.

DISCUSSION

This study originated from a double-tag assay of various TRIM proteins, in order to identify TRIMs that were localized inside the lysosomes (Overå et al. 2019). Our hypothesis was that TRIMs that are directed to degradation in the lysosome, may have a role in regulation of the autophagy process. We observed that mCherry-EYFP-TRIM27 formed several RedOnly puncta both in normal conditions and upon starvation. In this work, we show that degradation of TRIM27 can happen via autophagic pathways, and that the core autophagy protein ATG7 and the SLRs family of autophagy receptors are required for this degradation. This indicates that TRIM27 is degraded via selective autophagy.

It is recently shown that the only transmembrane autophagy protein ATG9 plays an important role in the nucleation of the autophagosome (Sawa-Makarska et al. 2020). ATG9 vesicles traffics from Golgi to endosomes in a ULK1-dependent manner under stress conditions (Young et al. 2006), and ULK1 phosphorylation regulates trafficking of ATG9 under autophagy-inducing conditions (Zhou et al. 2017). In this work, we show that depletion of ATG9 leads to increased levels of TRIM27. TRIM27 seems to be modified in the ATG9 KO cells, resulting in a slower migrating band visualized by Western blotting. Moreover, certain EGFP-TRIM27 bodies co-localized with ATG9 in the reconstituted HEK293 FlpIn EGFP-TRIM27 cell line. In addition, the autophagy receptors p62/SQSTM1 and NBR1 displayed increased protein levels in the ATG9 KO cells, and occurred as slower migration bands on the Western blot gels. This clearly points to TRIM27 as an autophagy substrate similarly as NBR1 and p62/SQSTM1. In contrast, the autophagy receptor NDP52 did not display aberrant mobility in the ATG9 KO cell extract, even if its protein level were slightly increased. Protein levels of lipidated LC3B were decreased in the ATG9 KO cells. This is in line with recent reports describing that ATG9 vesicles recruit the autophagy machinery and establish membrane contact sites with membrane donor compartments. ATG2 mediates transfer of lipids from donor membrane to the autophagosome formation sites, leading to PIP3 formation and ATG8 lipidation. Hence, lipidation of LC3 is dependent on ATG9 vesicles (Sawa-Makarska et al. 2020). Interestingly, we observed decreased levels of LC3B dots in the HEK293 FlpIn TRIM27 KO cell lines, indicative of reduced LC3B lipidation in these cells. Moreover, in the breast cancer cell lines, we observed an inverse correlation between TRIM27 expression and the amount of lipidated LC3B. This may suggest that TRIM27 is implicated in the ATG9 regulated pathway for autophagosome formation.

Mass spectrometry analyses revealed that several proteins linked to autophagy associates with EGFP-TRIM27 precipitated from the reconstituted HEK293 FlpIn cells, further suggesting a role for TRIM27 in autophagy. Among the autophagy receptors, p62/SQSTM1 seemed to be the one that associated strongest with TRIM27. Similarly as we have previously shown for TRIM32 (Overå et al., 2019), co-expression of TRIM27 and p62/SQSTM1 in the HEK293 FlpIn TRIM27 KO cells led to ubiquitylation of p62/SQSTM1. Moreover, enhanced ubiquitylation of endogenous p62/SQSTM1 could be detected in HEK293 FlpIn TRIM27 KO cells reconstituted with EGFP-TRIM27, compared to HEK293 FlpIn TRIM27 KO cells. Induction of EGFP-TRIM27 expression in the HEK293 FlpIn TRIM27 KO cells also lead to strong accumulation of p62/SQSTM1 in the EGFP-TRIM27 cytoplasmic bodies. This may be due to a strong interaction between TRIM27 and p62/SQSTM1, or it may be caused by strong ubiquitylation of certain TRIM27 bodies as detected by immunostaining with the ubiquitin antibody FK2. P62/SQSTM1 binds strongly to ubiquitin (Bjørkøy et al. 2005). This aggregation of p62/SQSTM1 in TRIM27 bodies thus may lead to the ubiquitylation of p62/SQSTM1 detected on Western blots.

Surprisingly, we identified LAMP2 as a TRIM27 interaction partner. LAMP2 is a highly glycosylated protein decorating the luminal surface of lysosomal membranes (Eskelinen, Tanaka, and Saftig 2003). It is an important regulator of maturation of autophagosomes, and LAMP2 deficiences leads to accumulation of autophagosomes (Saftig et al., 2008). Ablation of TRIM27 either by genetic KO, or by TRIM27 siRNA treatments, resulted in accumulation of LAMP2 protein levels, and the formation of large LAMP2 rings in HEK293 FlpIn cells. The large LAMP2 rings were often localized in the perinuclear region, in close proximity with TRIM27 bodies and mitochondria. Whether LAMP2 accumulation as such leads to formation of large lysosomes, or whether these large LAMP2 rings indicate that TRIM27 is implicated in the regulation of lysosome biogenesis, is an interesting question to address in further studies. However, we clearly show that TRIM27 deficiency result in accumulation of LAMP2. This accumulation can be due to impaired degradation of LAMP2 in TRIM27 KO cells, since TRIM27 is an E3 ligase that directs proteins to degradation by ubiquitylation. Alternatively, it can also be due to increased expression of LAMP2 at the transcriptional level, since TRIM27 also have a nuclear role.

TRIM27 was originally identified as a gene involved in the oncogenic rearrangements with the RET proto-oncogene (Hasegawa et al. 1996). Later it is shown that TRIM27 is highly expressed in various cancers including breast, endometrial, ovarian, lung, colon and colorectal

cancer, and colitis and colitis-associated carcinogenesis (Ma et al. 2016; Zoumpoulidou et al. 2012). In these studies TRIM27 has been proposed as a oncogene promoting cell proliferation, and the mechanisms have been connected to its nuclear function participating in transcriptional regulation complexes (Zurek et al. 2012). The proliferation and migration studies in the HEK293 FlpIn TRIM27 KO cells suggest that TRIM27 facilitates cell migration,, which is in line with a recent study showning TRIM27 to activate epithelial-mesencymal transition in colorectal cancer and to promote anchorage-independent growth of various cell lines (Y. Zhang et al. 2018).

Breast cancer is the most frequent malignancy in women and is a heterogeneous disease on the molecular level (Harbeck et al. 2019). In our results, TRIM27 mRNA expression in tumor tissue and normal tissue from two different patient cohorts was significantly upregulated in the cancer tissues compared to normal tissue. Moreover, the TRIM27 expression level varies substantially within the the various breast cancer cell lines. LAMP2 expression is upregulated in the breast cancer cell lines displaying no or very low expression levels of TRIM27. This correlates well with our analyses in HEK293 cells, suggesting that loss of TRIM27 leads to enhanced LAMP2 expression. LAMP2 plays a role in the support of early cancer progression, helping cancer cells surviving in acidic enviroments (Mogami et al. 2013). LAMP2 is highly expressed in several cancers, where reduced expression of LAMP2 has been associated with a loss of migration and invasion capabilities (Koukourakis et al. 2015). LAMP2A isoform has shown increased expression in breast tumor tissue, and its inhibition reuslts in sensitation of tumor cells to radioation and doxorubicin therapy (Saha 2012). Autophagy helps cancer cells to survive under nutrient and oxygen stress (Filomeni, De Zio, and Cecconi 2015). TRIM27 seems to facilitate starvation induced autophagy. Hence, this can be one mechanism that TRIM27 uses to facilitate growth of cancer cells. Collectively, these results point to TRIM27 as a putative regulator of autophagy, and that one of its oncogenic features is to facilitate the autophagy process in cancer cells. Moveover, breast cancer cell lines with various expression levels of TRIM27 represent promising model systems for further revealing the molecular mechanisms of TRIM27 in autophagy and cancer.

ACKNOWLEDGEMENT

We thank Richard Youle, National Institutes of Health, Bethesda, MD 20892, USA, for the generous gift of the pentaKO cell line, Yakubu P. Abudu, UiT – The Arctic University of Norway, for the gift of the EGFP-NDP52 and EGFP-p62/SQSTM1 reconstituted pentaKO cell lines and the HeLa ATG9 KO cell line. Thanks to the Advanced Microscopy Core Facility at UiT – The Arctic University of Norway, for the use of instrumentation. Thanks to Jack-Ansgar Bruun at the Tromsø University Proteomics Platform for help with Mass spectrometry analysis. This work was supported by PhD grants to K.S.O and J.G.G from UiT – The Arctic University of Norway, and by the Research Council of Norway (TOPPFORSK program grant #249884 to T.J).

FIGURE LEGENDS

Figure 1. Autophagic degradation of TRIM27 is dependent on ATG7, ATG9 and the Sequestosome-Like receptors. A) Normal HeLa cells and cells that were genetically knocked out for ATG7, the 5 autophagy receptors p62/SQSTM1, NBR1, NDP52, Optineurin and Tax1BP1 (pentaKO), pentaKO cells with reintroduced GFP-p62/SQSTM1 or pentaKO cells with reintroduced GFP-NDP52 as indicated to the right, were transfected with mCherry-EYFP-TRIM27 expression plasmids. One-day post transfection half of the cells were treated with HBSS for 2 hours (SM), before all cells were fixated, stained with DAPI and imaged using a Zeiss780 confocal microscope. FM: Full medium, SM: HBSS 2hrs. Scale bar (10 μm). **B)** The graphs represent the amount of Yellow dots and RedOnly dots in the mCherry-EYFP-TRIM27 transfected cells shown with representative images in (A). The graphs are representative for 3 independent experiments. Normal (FM) and starved (HBSS 2hrs) (SM) conditions. **C)** Western blot analysis of endogenous TRIM27 in HeLa ATG9 KO cells in normal medium (FM) or treated with HBSS (SM) for 4 hours. **D)** Quantitation of Western blot analysis as displayed in (C). The graph represents the average of three independent experiments with standard deviations. *: $p < 0.05$ using student T-test; n.s.: $p>0.05$ using student T-test.

Figure 2. TRIM27 interacts with ATG8s and has a LIR with specificity towards LC3C. A) Schematic representation of the domain architecture of TRIM27 with RING, B-box, Coiled-Coil (CC), LIR, and PRY/SPRY domains indicated. Peptide array with 20-mers spanning the complete region of TRIM27 to define the peptides of TRIM27 able to interact with recombinant GST-GABARAP. The peptide walk was done with steps of three amino acid from one spot to

the next. The peptide arrays were probed with 1μg/ml GST-GABARAP for 2 h, and binding to GST-GABARAP was detected with anti-GST antibodies. The identified putative LIR is highlighted by stars and shadowed background in the amino acid sequence. **B)** GST-pulldown assay using ^{35}S-labeled Myc-TRIM27 or ^{35}S-labeled Myc- TRIM27$^{W184A/F186A/L189A}$ and recombinant GST and GST-ATG8 proteins. The amount of Myc-TRIM27 or Myc-TRIM27$^{W184A/F186A/L189A}$ bound to the various ATG8 proteins was detected by autoradiography. The graph represents the average binding compared to input from three independent experiments. **C)** GST-pulldown assay using cell extracts from HEK293 FlpIn EGFP-TRIM27 cells and GST or GST-ATG8 proteins as indicated, immobilized on Glutathione Sepharose beads. EGFP-TRIM27 was detected using an anti-GFP antibody. GST proteins were visualized by Ponceau staining. **D)** Sequence alignment of LIR in TRIM27 and LIR2 in TRIM5α. The LIRs are indicated by shadowed background, and the residues important for TRIM5α LIR2 interaction with the ATG8s are highlighted in red.

Figure 3: TRIM27 co-localizes with core autophagy proteins and SLRs. Representative images of HEK293 FlpIn TRIM27 KO EGFP-TRIM27 cells fixed and stained with antibodies for p62/SQSTM1, NBR1, ATG9A, ATG13, ULK1, USP7 and FK2 (Ubiquitin). Images were obtained using a ZEISS780 confocal laser scanning microscope, and the co-localization monitored using the ZEN software**.** Scale bar (10 μm), on inserts (2 μm). Arrows indicate colocalisation between EGFP-TRIM27 and the indicated proteins.

Figure 4: TRIM27 associates withthe SLR family of autophagy receptors and core autophagy proteins. A) Results from Mass Spectometry (MS) from GFP trap using HEK293 FlpIn TRIM27 KO reconstituted with EGFP and EGFP-TRIM27 cells. The list represents proteins that precipitated with EGFP-TRIM27 induced in the HEK293 FlpIn TRIM27 KO cells, and not with induced EGFP. The experiment was performed in triplicate.. **B)** HEK293 FlpIn TRIM27 KO reconstituted with EGFP and EGFP-TRIM27 cells were harvested and incubated overnight with GFP trap. The cell extracts were then analyzed by Western blot to detect p62/SQSTM1, NBR1, LAMP2, GFP and TRIM27. **C)** GST-pulldown assays using ^{35}S-labeled Myc-TRIM27 and recombinant GST, GST-p62/SQSTM1 or GST-NDP52 immobilized on Glutathione Sepharose beads. **D)** HEK293 FlpIn TRIM27 KO cells were transfected with EGFP-TRIM27 or EGFP and myc-62/SQSTM1. Then cell extracts were incubated overnight with Myc-trap. Input and IP were analyzed by Western blot using Myc and Ubiquitin (FK2) antibodies. The * indicate ubiquitylated p62/SQSTM1.

Figure 5: Depletion of TRIM27 impairs starvation induced autophagy. A) Representative images of HEK293 FlpIn and HEK293 FlpIn TRIM27 KO cells in full media (FM) or starved with HBSS (2 hrs) (SM) fixed and stained with antibodies for LC3B and p62/SQSTM1. Images were obtained using a ZEISS780 confocal laser scanning microscope**.** Scale bar (10 μm), on inserts (2 μm).. **B)** The graphs display the quantitation of p62/SQSTM1 dots (upper panel) and LC3B dots (lower panel) in the HEK293 FlpIn TRIM27 KO cell line and the HEK293 FlpIn wild type cell line under normal and starved (HBSS 2hrs) conditions using the Volocity software (PerkinElmer). Each graph represents the average of three independent experiments with standard deviations, each including around 100 cells per condition. *: $p < 0.05$ using student T-test; n.s.: $p>0.05$ using student T-test.

C) Representative images of HEK293 FlpIn and HEK293 FlpIn TRIM27 KO cells in full media (FM) or starved with HBSS (2 hrs) (SM) fixed and stained with antibodies for WIPI2. Images were obtained using a ZEISS780 confocal laser scanning microscope Scale bar (10 μm), on inserts (2 μm). **D)** The graph displays the quantitation of WIPI2 dots in the HEK293 FlpIn TRIM27 KO cell line and the HEK293 FlpIn wild type cell line under normal and starved (HBSS 2hrs) conditions using the Volocity software (PerkinElmer). Each graph represents the average of three independent experiments with standard deviations, each including around 100 cells per condition. *: $p < 0.05$ using student T-test; n.s.: $p>0.05$ using student T-test.

Figure 6: TRIM27 KO and KD increase LAMP2 levels and promotes the formation of big LAMP2 rings in HEK293 FlpIn cells. A) Western blot analyses of the nuclear and cytoplasmic fractions of HEK293 FlpIn, HEK293 FlpIn TRIM27 KO and HEK293 FlpIn reconstituted with EGFP-TRIM27 cell lines. LAMP2 antibody and LAMIN B1 antibody were used as cytoplasmic and nuclear controls, respectively. The * indicates an unspecific band detected by the TRIM27 antibody. **B)** Upper panels shows Western blot analyses of extracts from HEK293 FlpIn, HEK293 FlpIn TRIM27 KO and HEK293 FlpIn EGFP-TRIM27 cells incubated in full media (FM) or starved with HBSS 4 hrs (SM). The * indicate an unspecific band detected by the TRIM27 antibody. The graph in the lower panel shows average band intensities with standard deviations quantitated using ImageJ (Fiji) from three independent experiments. **: $p < 0.005$ using student T-test; *: $p < 0.05$ using student T-test; n.s.: $p>0.05$ using student T-test. **C)** Upper panels shows Western blot analyses of extracts from HEK293 FlpIn cells treated with Control siRNA or TRIM27 siRNA, incubated in full media (FM) or

starved with HBSS 4 hrs (SM). The graph in the lower panel shows average band intensities with standard deviations quantitated using ImageJ (Fiji) from three independent experiments. *: $p < 0.05$ using student T-test; n.s.: $p>0.05$ using student T-test. **D)** Representative images of HEK293 FlpIn, HEK293 FlpIn TRIM27 KO, HEK293 FlpIn reconstituted with EGFP-TRIM27 and HEK293 FlpIn transfected with TRIM27 siRNA immunostained with LAMP2 antiodies (red). The nucleus is visualized by DAPI (blue). Images were obtained using a ZEISS780 confocal laser scanning microscope**.** Scale bar (10 μm).. The graph represents the average amount (%) of cells containing large LAMP2 rings for each of the cell lines represented by the images. The quantitations were performed manually in two independent experimens, each containing 50 cells per condition. **E)** Representative image of HEK293 FlpIn reconstituted with EGFP-TRIM27 immunostained with antibodies against LAMP2 and TOM20. Images were obtained using an AiryScan 880 microscope**.** Scale bar (10 μm), on insert (5 μm).

Figure 7: TRIM27 is highly expressed in breast cancer tissues and inversely correlated with LAMP2 and LC3B expression in various breast cancer cell lines. A) Graphs representing the TRIM27 mRNA (log2) expression levels in breast cancer tissues compared to normal tissues. The left graph represents average TRIM27 mRNA expression in breast cancer tissue compared to normal tissue in the same patients (n=23). The right graph represents average TRIM27 mRNA expression in tissue from healthy individuals (n=5) compared to average TRIM27 mRNA expression in breast cancer tissue from patients (n=53). **B)** Western blot analysis of endogenous TRIM27, LC3B, p62/SQSTM1 and LAMP2 in cell extracts from nine different breast cancer cell lines representing different breast cancer subtypes. The blot is representative of three independent experiments.

Supplementary Figure 1: TRIM27 localizes to cytoplasmic bodies and facilitates cell migration of HEK 293T FlpIn cells. A) DNA sequences encompassing the target sequence employed in the CRISPR/Cas9 mediated strategy generation TRIM27 KO cell line. The lower part show the DNA sequences of the PCR products obtained from the genomic loci targeted by CRISPR/Cas9. **B)** Western blot analysis of HEK293 FlpIn cells and the TRIM27 KO cells, showing KO of TRIM27. The * indicates an unspecific band detected by the TRIM27 antibody. **C)** Western blot analysis of HEK293 FlpIn TRIM27 KO cells reconstituted with tetracycline inducible expression of EGFP or EGFP-TRIM27. Expression of EGFP and EGFP was detected by an anti-GFP antibody. Tetracyclin (100 ng) were added where indicated above the blot. **D)** Western blot analysis comparing expression of endogenous TRIM27 in the HEK293 FlpIn cells

and tetracycline (100 ng) induced expression of EGFP-TRIM27 in the reconstituted HEK293 FlpIn TRIM27 KO cell lines. The proteins were detected using an anti-TRIM27 antibody. The * indicate an unspecific band detected by the TRIM27 antibody. **E)** Representative images of EGFP-TRIM27 expressed in the reconstituted HEK293 FlpIn TRIM27 KO cell lines, upon normal (FM) and starved (SM) (HBSS 2 hrs) conditions. Images were obtained using a ZEISS780 confocal laser scanning microscope.Scale bar (10 μm). **F)** Proliferation (left graph) and migration (right graph) curves of HEK293 FlpIn, HEK293 FlpIn TRIM27 KO, and HEK293 FlpIn TRIM27 KO reconstituted with EGFP-TRIM27. The graphs were obtained using the IncuCyte® S3 Live-Cell Analysis System (Sartorius). Error bars indicate s.d. of independent experiments (n=3 for Proliferation, n=2 for migration).

Supplementary Figure 2: A) Representative images of HEK293 FlpIn TRIM27 KO cells reconstituted with EGFP-TRIM27fixed and stained with antibodies for GM130 orCalreticulin as indicated. Images were obtained using a ZEISS780 confocal laser scanning microscope**.** Scale bar (10 μm), on inserts (2 μm). **B)** Western blot analysis showing that a fraction of p62/SQSTM1 is ubiquitylated in HEK293 FlpIn TRIM27 KO cells that are reconstituted with EGFP-TRIM27 compared to HEK293 FlpIn TRIM27 KO cells both in full media (FM) or when starved with HBSS (2 hrs) (SM) for 4h.

REFERENCES

Alemu, Endalkachew Ashenafi, Trond Lamark, Knut Martin Torgersen, Aasa Birna Birgisdottir, Kenneth Bowitz Larsen, Ashish Jain, Hallvard Olsvik, Aud Øvervatn, Vladimir Kirkin, and Terje Johansen. 2012. "ATG8 Family Proteins Act as Scaffolds for Assembly of the ULK Complex: Sequence Requirements for LC3-Interacting Region (LIR) Motifs." *Journal of Biological Chemistry* 287 (47): 39275–90. https://doi.org/10.1074/jbc.M112.378109.

Alessandrini, Federica, Laura Pezzè, and Yari Ciribilli. 2017. "LAMPs: Shedding Light on Cancer Biology." *Seminars in Oncology*. W.B. Saunders. https://doi.org/10.1053/j.seminoncol.2017.10.013.

Bjørkøy, Geir, Trond Lamark, Andreas Brech, Heidi Outzen, Maria Perander, Aud Øvervatn, Harald Stenmark, and Terje Johansen. 2005. "P62/SQSTM1 Forms Protein Aggregates Degraded by Autophagy and Has a Protective Effect on Huntingtin-Induced Cell Death." *The Journal of Cell Biology* 171 (4): 603–14. https://doi.org/10.1083/jcb.200507002.

Cai, J, H Y Chen, S J Peng, J L Meng, Y Wang, Y Zhou, X P Qian, et al. 2018. "USP7-TRIM27 Axis Negatively Modulates Antiviral Type I IFN Signaling." *FASEB J* 32 (10): 5238–49. https://doi.org/10.1096/fj.201700473RR.

Cao, T, M Shannon, M A Handel, and L D Etkin. 1996. "Mouse Ret Finger Protein (Rfp) Proto-Oncogene Is Expressed at Specific Stages of Mouse Spermatogenesis." *Dev Genet* 19 (4): 309–20.

https://doi.org/10.1002/(SICI)1520-6408(1996)19:4<309::AID-DVG4>3.0.CO;2-D.

Conwell, S E, A E White, J W Harper, and D M Knipe. 2015. “Identification of TRIM27 as a Novel Degradation Target of Herpes Simplex Virus 1 ICP0.” *J Virol* 89 (1): 220–29. https://doi.org/10.1128/JVI.02635-14.

Dikic, Ivan. 2017. “Proteasomal and Autophagic Degradation Systems.” *The Annual Review of Biochemestry*. https://doi.org/10.1146/annurev-biochem.

Dossou, Akpedje S, and Alakananda Basu. 2019. “Cancers The Emerging Roles of MTORC1 in Macromanaging Autophagy.” *Cancers*. https://doi.org/10.3390/cancers11101422.

Eskelinen, Eeva Liisa, Yoshitaka Tanaka, and Paul Saftig. 2003. “At the Acidic Edge: Emerging Functions for Lysosomal Membrane Proteins.” *Trends in Cell Biology*. Elsevier Ltd. https://doi.org/10.1016/S0962-8924(03)00005-9.

Esposito, D, M G Koliopoulos, and K Rittinger. 2017. “Structural Determinants of TRIM Protein Function.” *Biochem Soc Trans* 45 (1): 183–91. https://doi.org/10.1042/BST20160325.

Filomeni, G., D. De Zio, and F. Cecconi. 2015. “Oxidative Stress and Autophagy: The Clash between Damage and Metabolic Needs.” *Cell Death and Differentiation*. Nature Publishing Group. https://doi.org/10.1038/cdd.2014.150.

Hameed, Omar, Arie Perry, Ruma Banerjee, Xiaopei Zhu, and John D Pfeifer. 2009. “Papillary Carcinoma of the Breast Lacks Evidence of RET Rearrangements despite Morphological Similarities to Papillary Thyroid Carcinoma.” *Modern Pathology* 22: 1236–42. https://doi.org/10.1038/modpathol.2009.91.

Hao, Y H, M D Fountain Jr., K Fon Tacer, F Xia, W Bi, S H Kang, A Patel, et al. 2015. “USP7 Acts as a Molecular Rheostat to Promote WASH-Dependent Endosomal Protein Recycling and Is Mutated in a Human Neurodevelopmental Disorder.” *Mol Cell* 59 (6): 956–69. https://doi.org/10.1016/j.molcel.2015.07.033.

Harbeck, Nadia, Frédérique Penault-Llorca, Javier Cortes, Michael Gnant, Nehmat Houssami, Philip Poortmans, Kathryn Ruddy, Janice Tsang, and Fatima Cardoso. 2019. “Breast Cancer.” *Nature Reviews Disease Primers* 5 (1): 1–31. https://doi.org/10.1038/s41572-019-0111-2.

Hasegawa, N, T Iwashita, N Asai, H Murakami, Y Iwata, T Isomura, H Goto, T Hayakawa, and M Takahashi. 1996. “A RING Finger Motif Regulates Transforming Activity of the Rfp/Ret Fusion Gene.” *Biochem Biophys Res Commun* 225 (2): 627–31. https://doi.org/10.1006/bbrc.1996.1221.

Hatakeyama, S. 2017. “TRIM Family Proteins: Roles in Autophagy, Immunity, and Carcinogenesis.” *Trends Biochem Sci* 42 (4): 297–311. https://doi.org/10.1016/j.tibs.2017.01.002.

Horio, M, T Kato, S Mii, A Enomoto, M Asai, N Asai, Y Murakumo, K Shibata, F Kikkawa, and M Takahashi. 2012. “Expression of RET Finger Protein Predicts Chemoresistance in Epithelial Ovarian Cancer.” *Cancer Med* 1 (2): 218–29. https://doi.org/10.1002/cam4.32.

Iwakoshi, A, Y Murakumo, T Kato, A Kitamura, S Mii, S Saito, Y Yatabe, and M Takahashi. 2012. “RET Finger Protein Expression Is Associated with Prognosis in Lung Cancer with Epidermal Growth Factor Receptor Mutations.” *Pathol Int* 62 (5): 324–30. https://doi.org/10.1111/j.1440-1827.2012.02797.x.

Ji, C H, and Y T Kwon. 2017. “Crosstalk and Interplay between the Ubiquitin-Proteasome System and Autophagy.” *Mol Cells* 40 (7): 441–49. https://doi.org/10.14348/molcells.2017.0115.

Keown, Jeremy R., Moyra M. Black, Aaron Ferron, Melvyn Yap, Michael J. Barnett, F. Grant Pearce, Jonathan P. Stoye, and David C. Goldstone. 2018. “A Helical LC3-Interacting Region Mediates the Interaction between the Retroviral Restriction Factor Trim5 and Mammalian Autophagy-Related ATG8 Proteins.” *Journal of Biological Chemistry* 293 (47): 18378–86.

https://doi.org/10.1074/jbc.RA118.004202.

Kimura, T, A Jain, S W Choi, M A Mandell, K Schroder, T Johansen, and V Deretic. 2015. "TRIM-Mediated Precision Autophagy Targets Cytoplasmic Regulators of Innate Immunity." *J Cell Biol* 210 (6): 973–89. https://doi.org/10.1083/jcb.201503023.

Kimura, T, M Mandell, and V Deretic. 2016. "Precision Autophagy Directed by Receptor Regulators - Emerging Examples within the TRIM Family." *J Cell Sci* 129 (5): 881–91. https://doi.org/10.1242/jcs.163758.

Kimura, Tomonori, Ashish Jain, Won Choi, and Michael A Mandell. 2017. "TRIM-Directed Selective Autophagy Regulates Immune Activation." https://doi.org/10.1080/15548627.2016.1154254.

Kleiger, G, and T Mayor. 2014. "Perilous Journey: A Tour of the Ubiquitin-Proteasome System." *Trends Cell Biol* 24 (6): 352–59. https://doi.org/10.1016/j.tcb.2013.12.003.

Koukourakis, Michael I., Dimitra Kalamida, Achilleas Mitrakas, Stamatia Pouliliou, Sofia Kalamida, Efthimios Sivridis, and Alexandra Giatromanolaki. 2015. "Intensified Autophagy Compromises the Efficacy of Radiotherapy against Prostate Cancer." *Biochemical and Biophysical Research Communications* 461 (2): 268–74. https://doi.org/10.1016/j.bbrc.2015.04.014.

Kwon, Y T, and A Ciechanover. 2017. "The Ubiquitin Code in the Ubiquitin-Proteasome System and Autophagy." *Trends Biochem Sci* 42 (11): 873–86. https://doi.org/10.1016/j.tibs.2017.09.002.

Lamark, Trond, Maria Perander, Heidi Outzen, Kurt Kristiansen, Aud Øvervatn, Espen Michaelsen, Geir Bjørkøy, and Terje Johansen. 2003. "Interaction Codes within the Family of Mammalian Phox and Bem1p Domain-Containing Proteins*." *Journal of Biological Chemistry* 278: 34568–81. https://doi.org/10.1074/jbc.M303221200.

Lazarou, Michael, Danielle A. Sliter, Lesley A. Kane, Shireen A. Sarraf, Chunxin Wang, Jonathon L. Burman, Dionisia P. Sideris, Adam I. Fogel, and Richard J. Youle. 2015. "The Ubiquitin Kinase PINK1 Recruits Autophagy Receptors to Induce Mitophagy." *Nature* 524 (7565): 309–14. https://doi.org/10.1038/nature14893.

Liu, Y, M Zhu, L Lin, X Fan, Z Piao, and X Jiang. 2014. "Deficiency of Trim27 Protects Dopaminergic Neurons from Apoptosis in the Neurotoxin Model of Parkinson's Disease." *Brain Res* 1588: 17–24. https://doi.org/10.1016/j.brainres.2014.09.018.

Ma, Y, Z Wei, R C Bast Jr., Z Wang, Y Li, M Gao, Y Liu, et al. 2016. "Downregulation of TRIM27 Expression Inhibits the Proliferation of Ovarian Cancer Cells in Vitro and in Vivo." *Lab Invest* 96 (1): 37–48. https://doi.org/10.1038/labinvest.2015.132.

Mandell, M A, A Jain, J Arko-Mensah, S Chauhan, T Kimura, C Dinkins, G Silvestri, et al. 2014. "TRIM Proteins Regulate Autophagy and Can Target Autophagic Substrates by Direct Recognition." *Dev Cell* 30 (4): 394–409. https://doi.org/10.1016/j.devcel.2014.06.013.

Mandell, Michael A, Tomonori Kimura, Ashish Jain, Terje Johansen, and Vojo Deretic. 2015. "TRIM Proteins Regulate Autophagy: TRIM5 Is a Selective Autophagy Receptor Mediating HIV-1 Restriction." https://doi.org/10.4161/15548627.2014.984278.

Melia, Thomas J., Alf H. Lystad, and Anne Simonsen. 2020. "Autophagosome Biogenesis: From Membrane Growth to Closure." *Journal of Cell Biology*. Rockefeller University Press. https://doi.org/10.1083/JCB.202002085.

Mogami, Tae, Naho Yokota, Mikiko Asai-Sato, Roppei Yamada, Shiro Koizume, Yuji Sakuma, Mitsuyo Yoshihara, et al. 2013. "Annexin A4 Is Involved in Proliferation, Chemo-Resistance and Migration and Invasion in Ovarian Clear Cell Adenocarcinoma Cells." Edited by Guan Xin-Yuan. *PLoS ONE* 8 (11): e80359. https://doi.org/10.1371/journal.pone.0080359.

Muhlinen, Natalia von, Masato Akutsu, Benjamin J. Ravenhill, Ágnes Foeglein, Stuart Bloor, Trevor J.

Rutherford, Stefan M.V. Freund, David Komander, and Felix Randow. 2012. “LC3C, Bound Selectively by a Noncanonical LIR Motif in NDP52, Is Required for Antibacterial Autophagy.” *Molecular Cell* 48 (3): 329–42. https://doi.org/10.1016/j.molcel.2012.08.024.

Nie, D, D Zhang, J Dai, M Zhang, X Zhao, W Xu, Z Chen, L Wang, Z Wang, and Z Qiao. 2016. “Nicotine Induced Murine Spermatozoa Apoptosis via Up-Regulation of Deubiquitylated RIP1 by Trim27 Promoter Hypomethylation.” *Biol Reprod* 94 (2): 31. https://doi.org/10.1095/biolreprod.115.131656.

Orsi, A, M Razi, H C Dooley, D Robinson, A E Weston, L M Collinson, and S A Tooze. 2012. “Dynamic and Transient Interactions of Atg9 with Autophagosomes, but Not Membrane Integration, Are Required for Autophagy.” https://doi.org/10.1091/mbc.E11-09-0746.

Overå, Katrine Stange, Juncal Garcia-Garcia, Zambarlal Bhujabal, Ashish Jain, Aud Øvervatn, Kenneth Bowitz Larsen, Vojo Deretic, Terje Johansen, Trond Lamark, and Eva Sjøttem. 2019. “TRIM32, but Not Its Muscular Dystrophy-Associated Mutant, Positively Regulates and Is Targeted to Autophagic Degradation by P62/SQSTM1.” *Journal of Cell Science* 132 (23). https://doi.org/10.1242/jcs.236596.

Pankiv, Serhiy, Terje Høyvarde Clausen, Trond Lamark, Andreas Brech, Jack Ansgar Bruun, Heidi Outzen, Aud Øvervatn, Geir Bjørkøy, and Terje Johansen. 2007. “P62/SQSTM1 Binds Directly to Atg8/LC3 to Facilitate Degradation of Ubiquitylated Protein Aggregates by Autophagy*[S].” *Journal of Biological Chemistry* 282 (33): 24131–45. https://doi.org/10.1074/jbc.M702824200.

Ran, F. Ann, Patrick D. Hsu, Jason Wright, Vineeta Agarwala, David A. Scott, and Feng Zhang. 2013. “Genome Engineering Using the CRISPR-Cas9 System.” *Nature Protocols* 8 (11): 2281–2308. https://doi.org/10.1038/nprot.2013.143.

Saftig, Paul, Wouter Beertsen, and Eeva Liisa Eskelinen. 2008. “LAMP-2: A Control Step Fot Phagosome and Autophagosome Maturation.” *Autophagy* 4 (4): 510–12. https://doi.org/10.4161/auto.5724.

Saha, Tapas. 2012. “LAMP2A Overexpression in Breast Tumors Promotes Cancer Cell Survival via Chaperone-Mediated Autophagy.” *Autophagy* 8 (11): 1643–56. https://doi.org/10.4161/auto.21654.

Sawa-Makarska, Justyna, Verena Baumann, Nicolas Coudevylle, Sören von Bülow, Veronika Nogellova, Christine Abert, Martina Schuschnig, Martin Graef, Gerhard Hummer, and Sascha Martens. 2020. “Reconstitution of Autophagosome Nucleation Defines Atg9 Vesicles as Seeds for Membrane Formation.” *Science* 369 (6508). https://doi.org/10.1126/SCIENCE.AAZ7714.

Sawyer, Sara L., Lily I. Wu, Michael Emerman, and Harmit S. Malik. 2005. “Positive Selection of Primate TRIM5α Identifies a Critical Species-Specific Retroviral Restriction Domain.” *Proceedings of the National Academy of Sciences of the United States of America* 102 (8): 2832–37. https://doi.org/10.1073/pnas.0409853102.

Swatek, Kirby N., and David Komander. 2016. “Ubiquitin Modifications.” *Cell Research*. Nature Publishing Group. https://doi.org/10.1038/cr.2016.39.

Tezel, G G, A Uner, I Yildiz, G Guler, and M Takahashi. 2009. “RET Finger Protein Expression in Invasive Breast Carcinoma: Relationship between RFP and ErbB2 Expression.” *Pathol Res Pract* 205 (6): 403–8. https://doi.org/10.1016/j.prp.2008.12.014.

Tezel, G, T Nagasaka, N Iwahashi, N Asai, T Iwashita, K Sakata, and M Takahashi. 1999. “Different Nuclear/Cytoplasmic Distributions of RET Finger Protein in Different Cell Types.” *Pathol Int* 49 (10): 881–86. https://doi.org/10.1046/j.1440-1827.1999.00957.x.

Tsukamoto, H, T Kato, A Enomoto, N Nakamura, Y Shimono, M Jijiwa, N Asai, et al. 2009. “Expression of Ret Finger Protein Correlates with Outcomes in Endometrial Cancer.” *Cancer Sci* 100 (10): 1895–1901. https://doi.org/10.1111/j.1349-7006.2009.01278.x.

Verlhac, Pauline, Christophe Viret, and Mathias Faure. 2015. “Dual Function of CALCOCO2/NDP52 during Xenophagy.” *Autophagy* 11 (6): 965–66. https://doi.org/10.1080/15548627.2015.1046672.

Watanabe, M, and S Hatakeyama. 2017. “TRIM Proteins and Diseases.” *J Biochem* 161 (2): 135–44. https://doi.org/10.1093/jb/mvw087.

Young, Andrew R.J., Edmond Y.W. Chan, Xiao Wen Hu, Robert Köchl, Samuel G. Crawshaw, Stephen High, Dale W. Halley, Jennifer Lippincott-Schwartz, and Sharon A. Tooze. 2006. “Starvation and ULK1-Dependent Cycling of Mammalian Atg9 between the TGN and Endosomes.” *Journal of Cell Science* 119 (18): 3888–3900. https://doi.org/10.1242/jcs.03172.

Yu, H, and A Matouschek. 2017. “Recognition of Client Proteins by the Proteasome.” *Annu Rev Biophys* 46: 149–73. https://doi.org/10.1146/annurev-biophys-070816-033719.

Zaman, M M, T Nomura, T Takagi, T Okamura, W Jin, T Shinagawa, Y Tanaka, and S Ishii. 2013. “Ubiquitylation-Deubiquitylation by the TRIM27-USP7 Complex Regulates Tumor Necrosis Factor Alpha-Induced Apoptosis.” *Mol Cell Biol* 33 (24): 4971–84. https://doi.org/10.1128/MCB.00465-13.

Zhang, H X, Z S Xu, H Lin, M Li, T Xia, K Cui, S Y Wang, Y Li, H B Shu, and Y Y Wang. 2018. “TRIM27 Mediates STAT3 Activation at Retromer-Positive Structures to Promote Colitis and Colitis-Associated Carcinogenesis.” *Nat Commun* 9 (1): 3441. https://doi.org/10.1038/s41467-018-05796-z.

Zhang, Y, Y Feng, D Ji, Q Wang, W Qian, S Wang, Z Zhang, et al. 2018. “TRIM27 Functions as an Oncogene by Activating Epithelial-Mesenchymal Transition and p-AKT in Colorectal Cancer.” *Int J Oncol* 53 (2): 620–32. https://doi.org/10.3892/ijo.2018.4408.

Zhou, Changqian, Kaili Ma, Ruize Gao, Chenglong Mu, Linbo Chen, Qiangqiang Liu, Qian Luo, Du Feng, Yushan Zhu, and Quan Chen. 2017. “Regulation of MATG9 Trafficking by Src- and ULK1-Mediated Phosphorylation in Basal and Starvation-Induced Autophagy.” *Cell Research* 27 (2): 184–201. https://doi.org/10.1038/cr.2016.146.

Zhuang, X J, W H Tang, X Feng, C Y Liu, J L Zhu, J Yan, D F Liu, P Liu, and J Qiao. 2016. “Trim27 Interacts with Slx2, Is Associated with Meiotic Processes during Spermatogenesis.” *Cell Cycle* 15 (19): 2576–84. https://doi.org/10.1080/15384101.2016.1174796.

Zoumpoulidou, G, C Broceno, H Li, D Bird, G Thomas, and S Mittnacht. 2012. “Role of the Tripartite Motif Protein 27 in Cancer Development.” *J Natl Cancer Inst* 104 (12): 941–52. https://doi.org/10.1093/jnci/djs224.

Zurek, B, I Schoultz, A Neerincx, L M Napolitano, K Birkner, E Bennek, G Sellge, et al. 2012. “TRIM27 Negatively Regulates NOD2 by Ubiquitylation and Proteasomal Degradation.” *PLoS One* 7 (7): e41255. https://doi.org/10.1371/journal.pone.0041255.

Figure 1

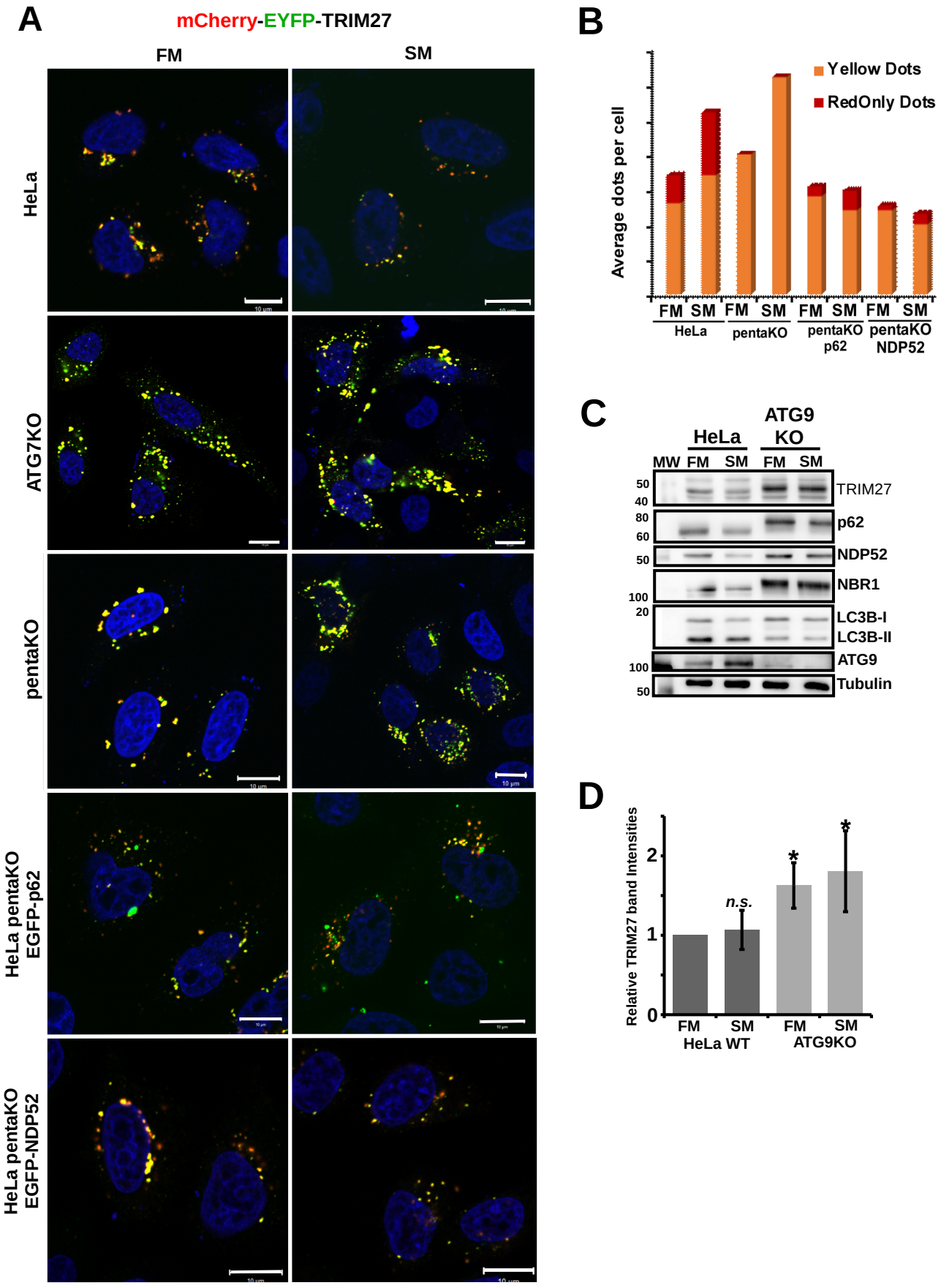
A
mCherry-EYFP-TRIM27
FM
SM
HeLa
ATG7KO
pentaKO
HeLa pentaKO EGFP-p62
HeLa pentaKO EGFP-NDP52
B
Yellow Dots
RedOnly Dots
Average dots per cell
FM SM FM SM FM SM FM SM
HeLa
pentaKO
pentaKO p62
pentaKO NDP52
C
ATG9 KO
HeLa
MW FM SM FM SM
50
40
TRIM27
80
60
p62
50
NDP52
100
NBR1
20
LC3B-I
LC3B-II
100
ATG9
50
Tubulin
D
Relative TRIM27 band Intensities
2
1
0
n.s.
*
*
FM SM FM SM
HeLa WT
ATG9KO

Figure 2

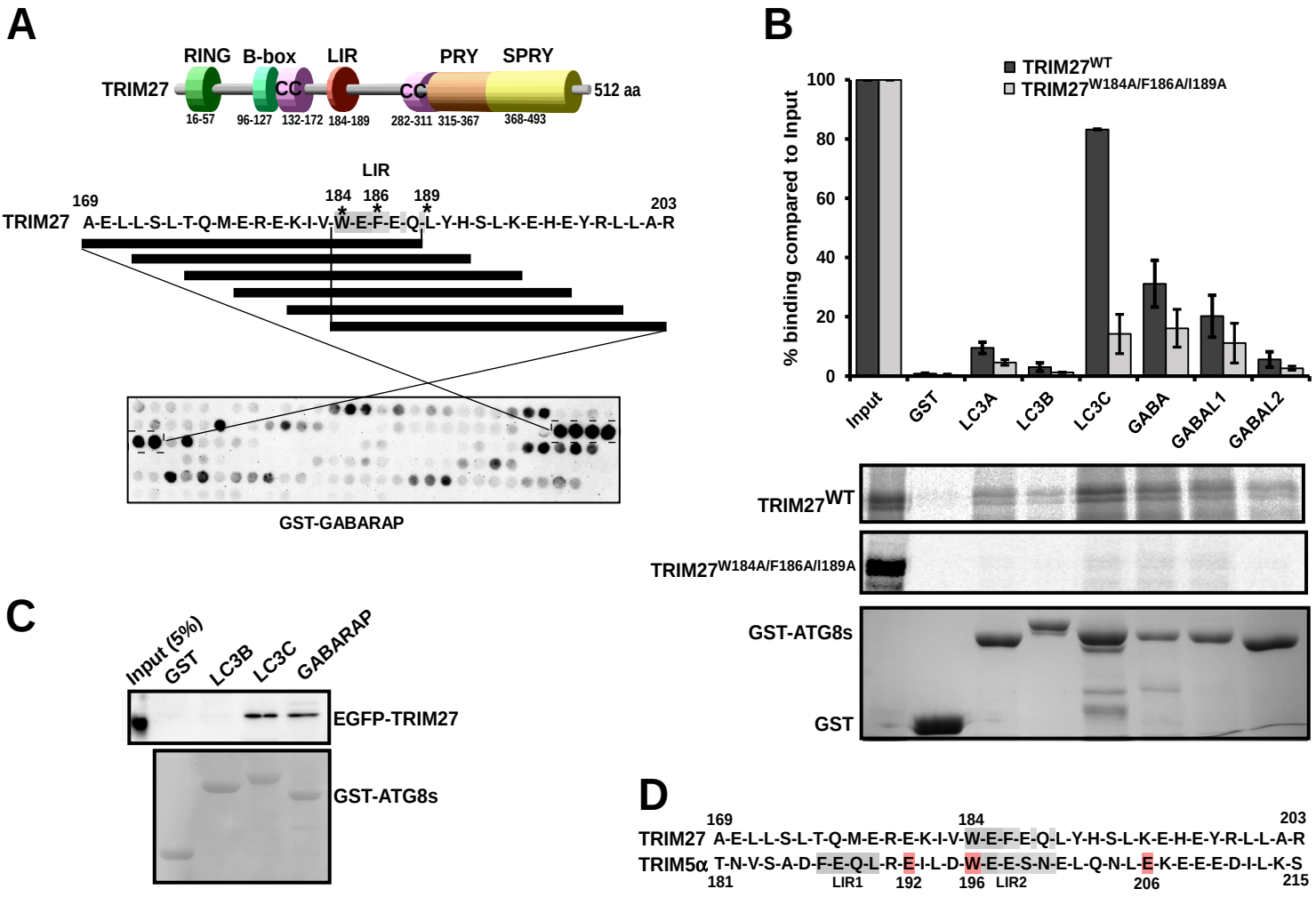
A
RING
B-box
LIR
PRY
SPRY
TRIM27
CC
CC
512 aa
16-57
96-127
132-172
184-189
282-311
315-367
368-493
LIR
169
184
186
189
203
TRIM27 A-E-L-L-S-L-T-Q-M-E-R-E-K-I-V-W-E-F-E-Q-L-Y-H-S-L-K-E-H-E-Y-R-L-L-A-R
GST-GABARAP
B
TRIM27WT
TRIM27W184A/F186A/I189A
% binding compared to Input
100
80
60
40
20
0
Input
GST
LC3A
LC3B
LC3C
GABA
GABAL1
GABAL2
TRIM27WT
TRIM27W184A/F186A/I189A
GST-ATG8s
GST
C
Input (5%)
GST
LC3B
LC3C
GABARAP
EGFP-TRIM27
GST-ATG8s
D
169
184
203
TRIM27 A-E-L-L-S-L-T-Q-M-E-R-E-K-I-V-W-E-F-E-Q-L-Y-H-S-L-K-E-H-E-Y-R-L-L-A-R
TRIM5α T-N-V-S-A-D-F-E-Q-L-R-E-I-L-D-W-E-E-S-N-E-L-Q-N-L-E-K-E-E-E-D-I-L-K-S
181
LIR1
192
196
LIR2
206
215

Figure 3

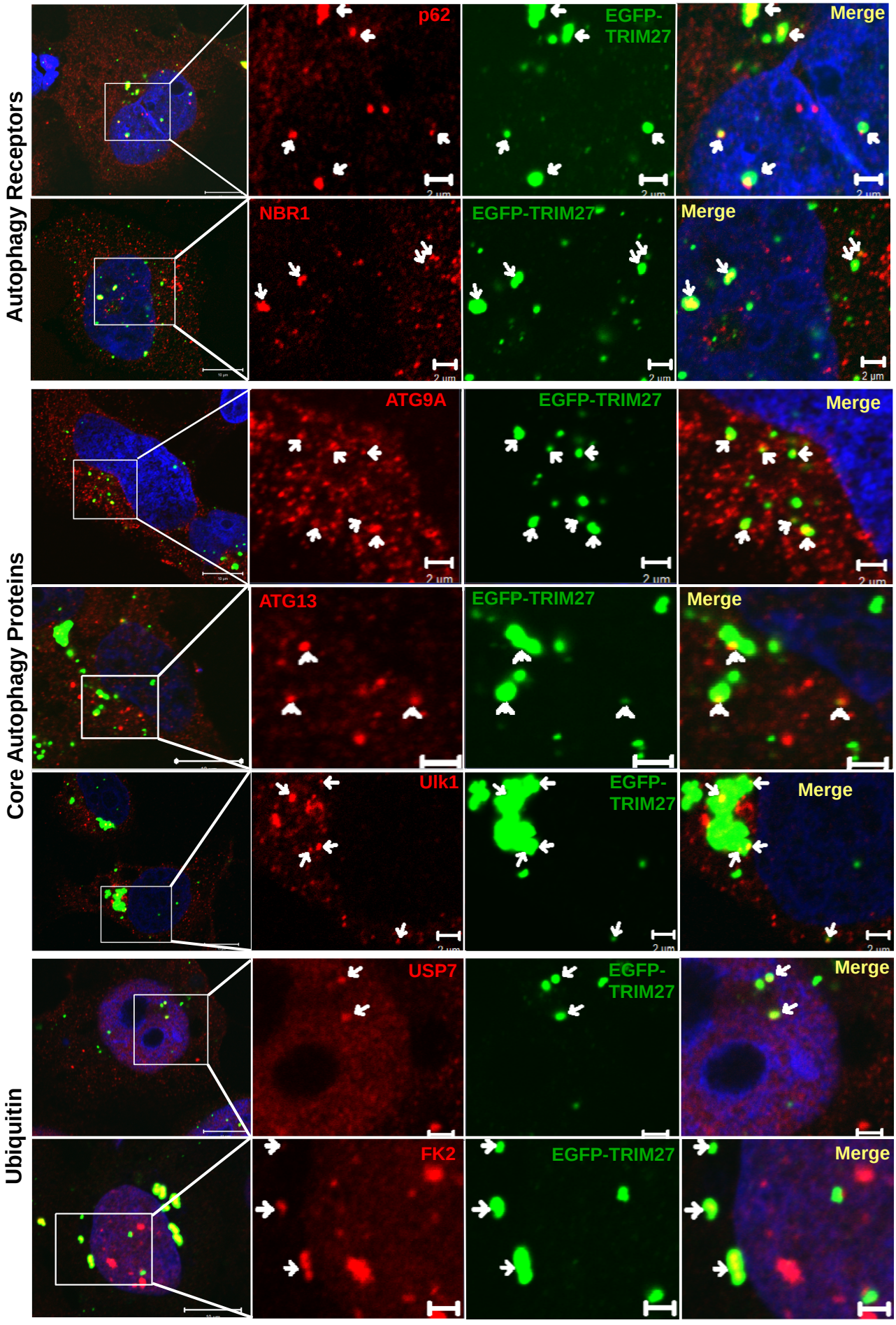
Autophagy Receptors
p62
EGFP-TRIM27
Merge
NBR1
EGFP-TRIM27
Merge
Core Autophagy Proteins
ATG9A
EGFP-TRIM27
Merge
ATG13
EGFP-TRIM27
Merge
Ulk1
EGFP-TRIM27
Merge
Ubiquitin
USP7
EGFP-TRIM27
Merge
FK2
EGFP-TRIM27
Merge
2 µm

Figure 4

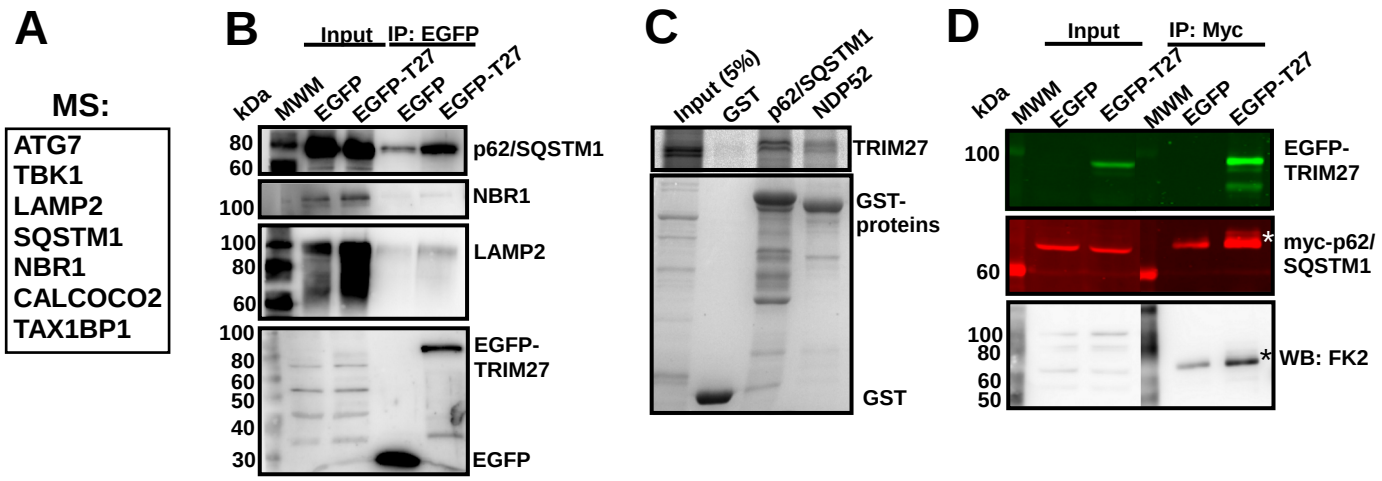
A
MS:
ATG7
TBK1
LAMP2
SQSTM1
NBR1
CALCOCO2
TAX1BP1
B
Input
IP: EGFP
kDa
MWM
EGFP
EGFP-T27
EGFP
EGFP-T27
80
60
p62/SQSTM1
100
NBR1
100
80
60
LAMP2
100
80
60
50
40
30
EGFP-
TRIM27
EGFP
C
Input (5%)
GST
p62/SQSTM1
NDP52
TRIM27
GST-
proteins
GST
D
Input
IP: Myc
kDa
MWM
EGFP
EGFP-T27
MWM
EGFP
EGFP-T27
100
EGFP-
TRIM27
60
*
myc-p62/
SQSTM1
100
80
60
50
*
WB: FK2

Figure 5

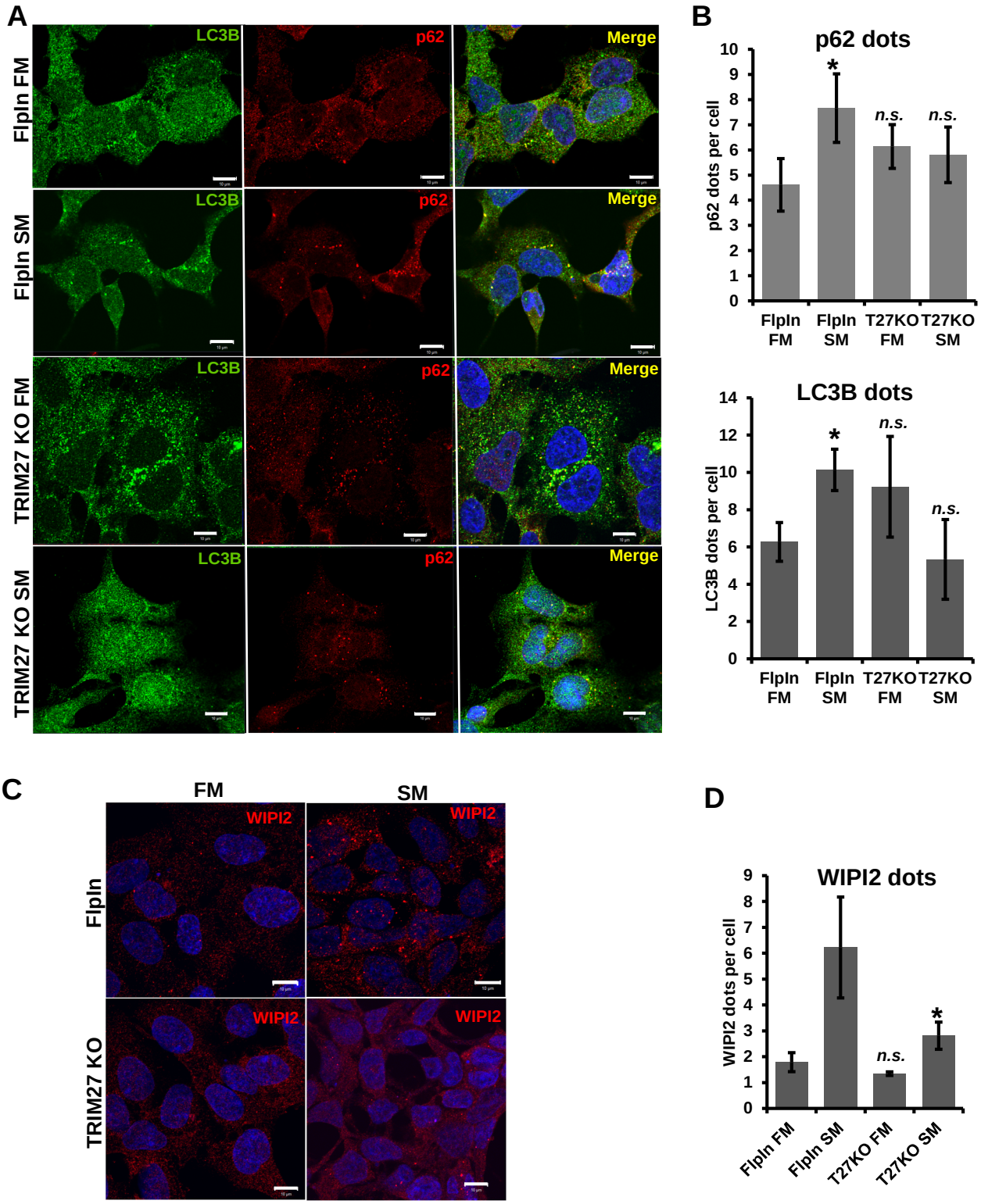
A
LC3B
p62
Merge
FlpIn FM
FlpIn SM
TRIM27 KO FM
TRIM27 KO SM
B
p62 dots
p62 dots per cell
*
n.s.
n.s.
FlpIn FM
FlpIn SM
T27KO FM
T27KO SM
LC3B dots
LC3B dots per cell
*
n.s.
n.s.
C
FM
SM
WIPI2
FlpIn
TRIM27 KO
D
WIPI2 dots
WIPI2 dots per cell
n.s.
*
FlpIn FM
FlpIn SM
T27KO FM
T27KO SM

Figure 6

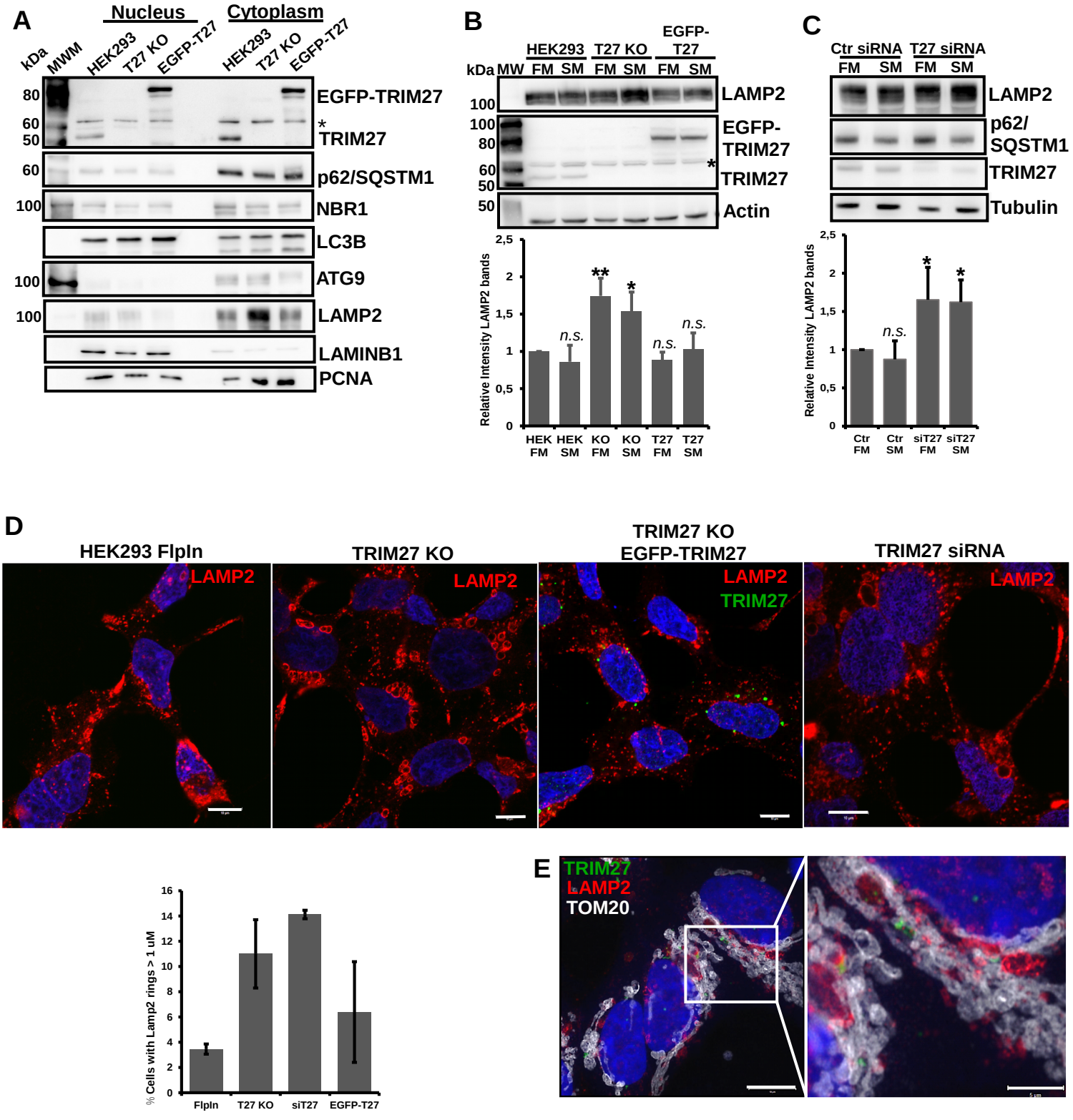
A
Nucleus
Cytoplasm
kDa
MWM
HEK293
T27 KO
EGFP-T27
HEK293
T27 KO
EGFP-T27
80
60
50
EGFP-TRIM27
*
TRIM27
60
p62/SQSTM1
100
NBR1
LC3B
100
ATG9
100
LAMP2
LAMINB1
PCNA
B
kDa MW
HEK293
T27 KO
EGFP-T27
FM SM FM SM FM SM
100
LAMP2
100
80
60
50
EGFP-TRIM27
*
TRIM27
50
Actin
Relative Intensity LAMP2 bands
2,5
2
1,5
1
0,5
0
n.s.
**
*
n.s.
n.s.
HEK FM
HEK SM
KO FM
KO SM
T27 FM
T27 SM
C
Ctr siRNA
T27 siRNA
FM SM FM SM
LAMP2
p62/ SQSTM1
TRIM27
Tubulin
Relative Intensity LAMP2 bands
2,5
2
1,5
1
0,5
0
n.s.
*
*
Ctr FM
Ctr SM
siT27 FM
siT27 SM
D
HEK293 FlpIn
TRIM27 KO
TRIM27 KO EGFP-TRIM27
TRIM27 siRNA
LAMP2
LAMP2
LAMP2
TRIM27
LAMP2
% Cells with Lamp2 rings > 1 uM
16
14
12
10
8
6
4
2
0
FlpIn
T27 KO
siT27
EGFP-T27
E
TRIM27
LAMP2
TOM20

Figure 7

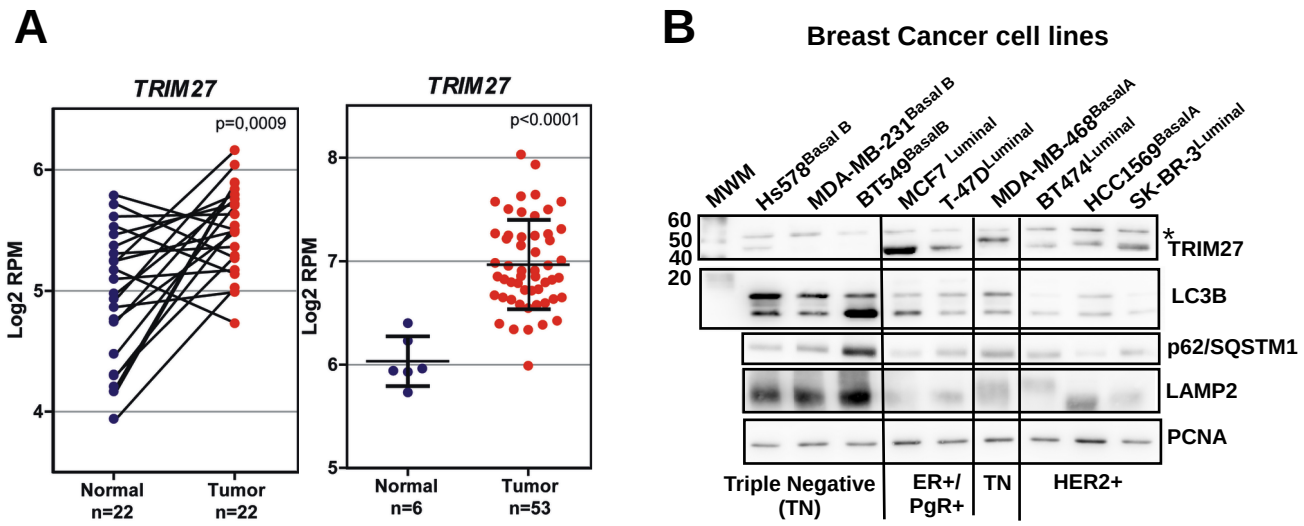
A
TRIM27
p=0,0009
Log2 RPM
6
5
4
Normal
n=22
Tumor
n=22
TRIM27
p<0.0001
Log2 RPM
8
7
6
5
Normal
n=6
Tumor
n=53
B
Breast Cancer cell lines
MWM
Hs578Basal B
MDA-MB-231Basal B
BT549BasalB
MCF7 Luminal
T-47DLuminal
MDA-MB-468BasalA
BT474Luminal
HCC1569BasalA
SK-BR-3Luminal
60
50
40
20
*TRIM27
LC3B
p62/SQSTM1
LAMP2
PCNA
Triple Negative (TN)
ER+/ PgR+
TN
HER2+

Supplemental Figure S1

A

TRIM27 Exon1 (Guide sequence):

```
atggcctccgggagtgtggccgagtgcctgcagcaggagaccacctgccccgtgtgcctgcagtacttcgcagagcccatgatgctcgactgcg
gccataacatctgttgcgcgtgcctcgcccgctgctggggcacggcagagactaacgtgtcgtgcccgcagtgccgggagaccttcccgcagag
gcacatgcggcccaaccggcacctggccaacgtgacccaactggtaaagcagctgcgca
```

A1 (140 nt deletion + 9 nt insertion):

```
atggcctccgggagtgtggccgagtgcctgcagcaggagaccacctgccccgtgtgcctgcagtacttcgcagagcccat.............
.....................aatgctcga.....................................................................
.........................acgtgacccaactggtaaagcagctgcgca
```

A2 (133 nt deletion + 2 nt insertion):

```
Atggcctccgggagtgtggccgagtgcctgcagcaggagaccacctgccccgtgtgcctgcagtacttcgcagagcccatgatgctcgactg..
...................................aa.....................................................
.............................tgacccaactggtaaagcagctgcgca
```

B

C

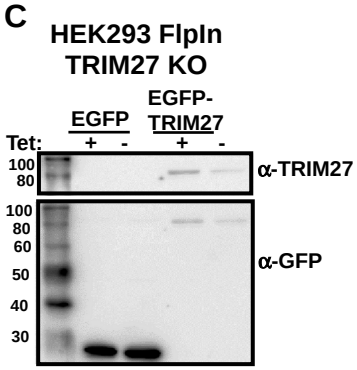

D

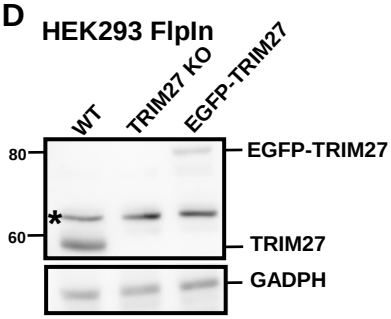

E

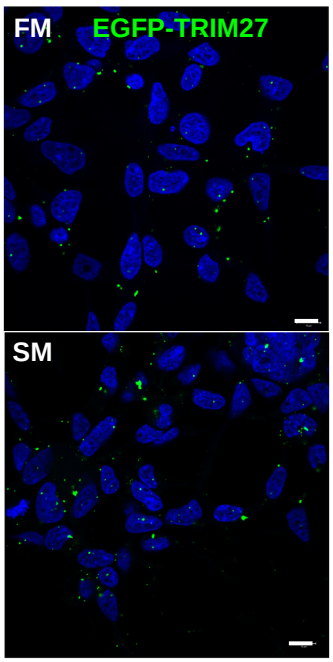

F

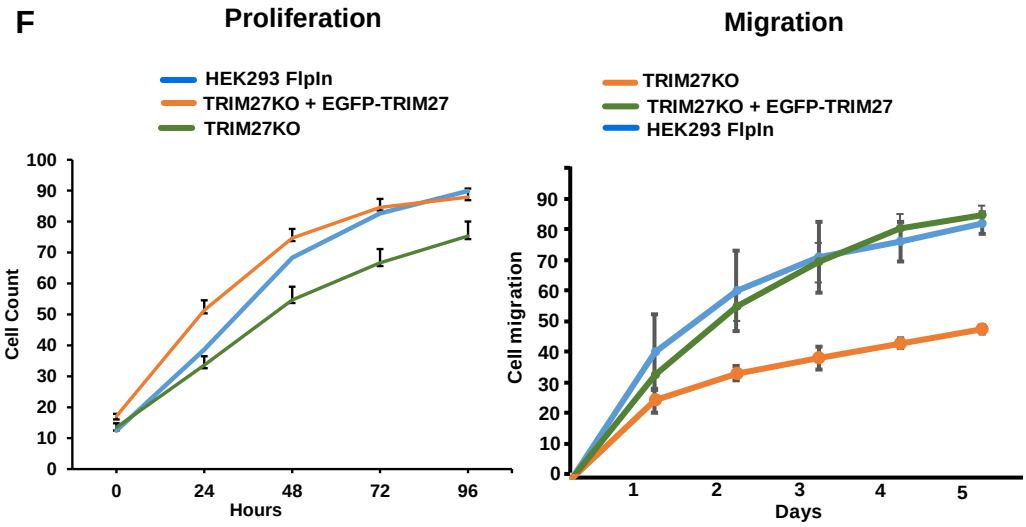

Supplemental Figure S2

A

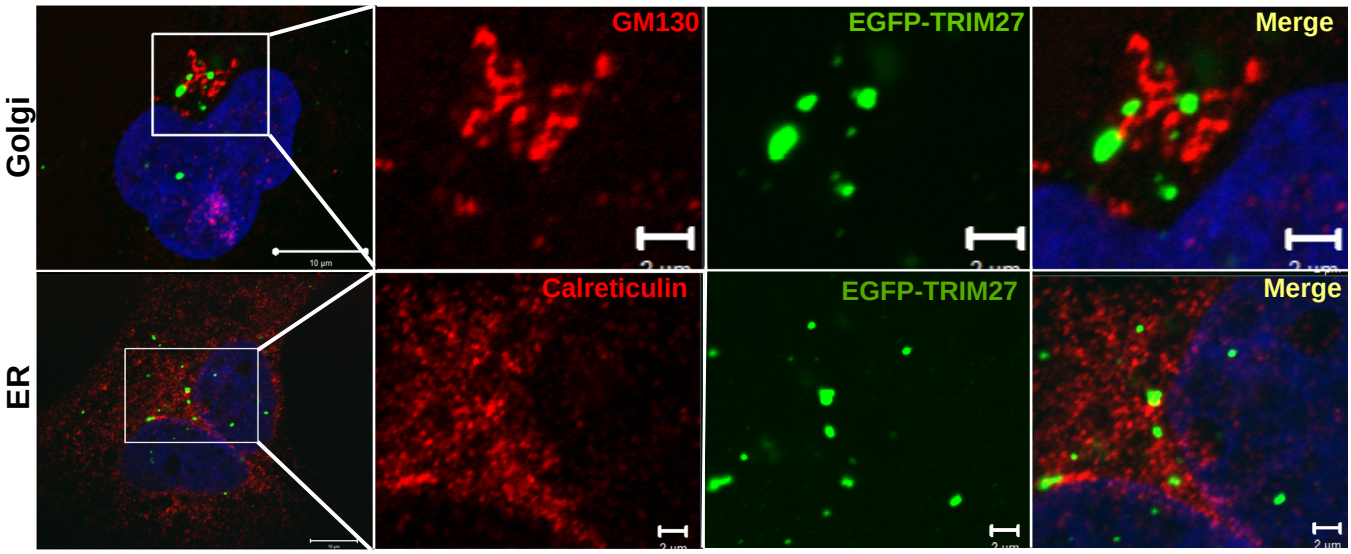

B

Paper II

© 2019. Published by The Company of Biologists Ltd | Journal of Cell Science (2019) 132, jcs236596. doi:10.1242/jcs.236596

RESEARCH ARTICLE

TRIM32, but not its muscular dystrophy-associated mutant, positively regulates and is targeted to autophagic degradation by p62/SQSTM1

Katrine Stange Overå[1], Juncal Garcia-Garcia[1], Zambarlal Bhujabal[1], Ashish Jain[1,*], Aud Øvervatn[1], Kenneth Bowitz Larsen[1], Vojo Deretic[2,3], Terje Johansen[1], Trond Lamark[1] and Eva Sjøttem[1,‡]

ABSTRACT

The tripartite motif (TRIM) proteins constitute a family of ubiquitin E3 ligases involved in a multitude of cellular processes, including protein homeostasis and autophagy. TRIM32 is characterized by six protein–protein interaction domains termed NHL, various point mutations in which are associated with limb-girdle-muscular dystrophy 2H (LGMD2H). Here, we show that TRIM32 is an autophagy substrate. Lysosomal degradation of TRIM32 was dependent on ATG7 and blocked by knockout of the five autophagy receptors p62 (also known as SQSTM1), NBR1, NDP52 (also known as CALCOCO2), TAX1BP1 and OPTN, pointing towards degradation by selective autophagy. p62 directed TRIM32 to lysosomal degradation, while TRIM32 mono-ubiquitylated p62 on lysine residues involved in regulation of p62 activity. Loss of TRIM32 impaired p62 sequestration, while reintroduction of TRIM32 facilitated p62 dot formation and its autophagic degradation. A TRIM32^{LGMD2H} disease mutant was unable to undergo autophagic degradation and to mono-ubiquitylate p62, and its reintroduction into the TRIM32-knockout cells did not affect p62 dot formation. In light of the important roles of autophagy and p62 in muscle cell proteostasis, our results point towards impaired TRIM32-mediated regulation of p62 activity as a pathological mechanisms in LGMD2H.

KEY WORDS: TRIM32, p62/SQSTM1, LGMD2H, Autophagy, BBS11, Ubiquitylation

INTRODUCTION

Protein quality control is crucial for cellular health, especially in tissues containing long-lived cells like the muscles and nervous system. Dysfunctional quality control leads to protein aggregation and development of diseases with increasing prevalence related to age (Dikic and Elazar, 2018). The two most important biological machineries controlling protein degradation are autophagy and the ubiquitin-proteasome system (UPS), where protein ubiquitylation mediated by E3 ubiquitin ligases provide substrate specificity. Based on their structural properties, E3 ubiquitin ligases are classified as RING, HECT or RBR ligases (Morreale and Walden, 2016). TRIM family proteins belong to the RING E3s, which constitute the most-abundant family of ubiquitin ligases (Hatakeyama, 2017). TRIMs are characterized by the highly conserved RING finger–B-box–coiled-coil domains at their N-termini, generally constituting their E3 ligase and oligomerization activity. Human TRIM family proteins comprise 82 members that are classified into 12 different subfamilies according to the domain structure of their C-terminal region (Fig. 1A). They have important functions in development, differentiation, immune responses and carcinogenesis (reviewed in Hatakeyama, 2017). Furthermore, certain TRIM proteins act as regulators of autophagy activity (Pizon et al., 2013; Tomar et al., 2012) and as autophagy receptors (Chauhan et al., 2016; Kimura et al., 2015, 2016; Mandell et al., 2016, 2014). TRIM32 is characterized by six repeats of NHL (NCL-1, HT2A and LIN-41) motifs in its C-terminus, which are thought to mediate protein–protein interactions (Slack and Ruvkun, 1998). TRIM32 is expressed throughout the body, but with high expression levels in the brain and heart (Frosk et al., 2002). The biological roles of TRIM32 are multi-faceted, impacting muscle physiology, cancer and immunity. This is reflected in the many substrates reported to be targeted by its E3 ligase activity, such as the muscular relevant proteins actin, α-actinin, desmin, tropomysin and dysbindin, the cell cycle regulators c-Myc, MYCN and p53, and the innate immunity adaptor STING (also known as TMEM173) (reviewed in Lazzari and Meroni, 2016). The finding that mutations in the NHL domains of TRIM32 can lead to the hereditary muscular disease limb-girdle muscular dystrophy 2H (LGMD2H), identified TRIM32 as an important player in muscular physiology (Frosk et al., 2002). Whether the pathogenic effect of LGMD2H is due to a role for TRIM32 in muscle atrophy (Cohen et al., 2012) or more in muscle homeostasis and regrowth after atrophy (Kudryashova et al., 2012, 2005; Nicklas et al., 2012; Servián-Morilla et al., 2019) is not well understood. However, it has been shown that the LGMD2H mutations lead to impaired self-oligomerization and auto-ubiquitylation, and reduced TRIM32 expression level (Albor et al., 2006; Kudryashova et al., 2011; Locke et al., 2009; Servián-Morilla et al., 2019). Moreover, recent work analyzing muscle biopsies and primary myoblasts from LGMD2H patients, described reduced proliferation and differentiation capacity, diminished satellite cell pool, and enhanced senescence and autophagy activity (Servián-Morilla et al., 2019). In addition, another very recent publication reported that TRIM32 is important for induction of autophagy in atrophic muscle cells, while the LGMD2H mutant was unable to activate autophagy in these cells (Di Rienzo et al., 2019). All mutations associated with LGMD2H are either deletions or point mutations located in the NHL domains, while a point mutation in the B-box of TRIM32 is associated with a completely unrelated disease, multisystemic disorder

[1]Molecular Cancer Research Group, Department of Medical Biology, University of Tromsø –The Arctic University of Norway, 9037 Tromsø, Norway. [2]Autophagy Inflammation and Metabolism Center of Biomedical Research Excellence, University of New Mexico Health Sciences Center, Albuquerque, NM 87131, USA. [3]Department of Molecular Genetics and Microbiology, University of New Mexico Health Sciences Center, Albuquerque, NM 87131, USA.
*Present address: Department of Molecular Cell Biology, Centre for Cancer Biomedicine, University of Oslo and Institute for Cancer Research, The Norwegian Radium Hospital, Oslo, Norway.

‡Author for correspondence (eva.sjottem@uit.no)

E.S., 0000-0003-2668-1708

Received 15 July 2019; Accepted 28 October 2019

Journal of Cell Science (2019) 132, jcs236596. doi:10.1242/jcs.236596

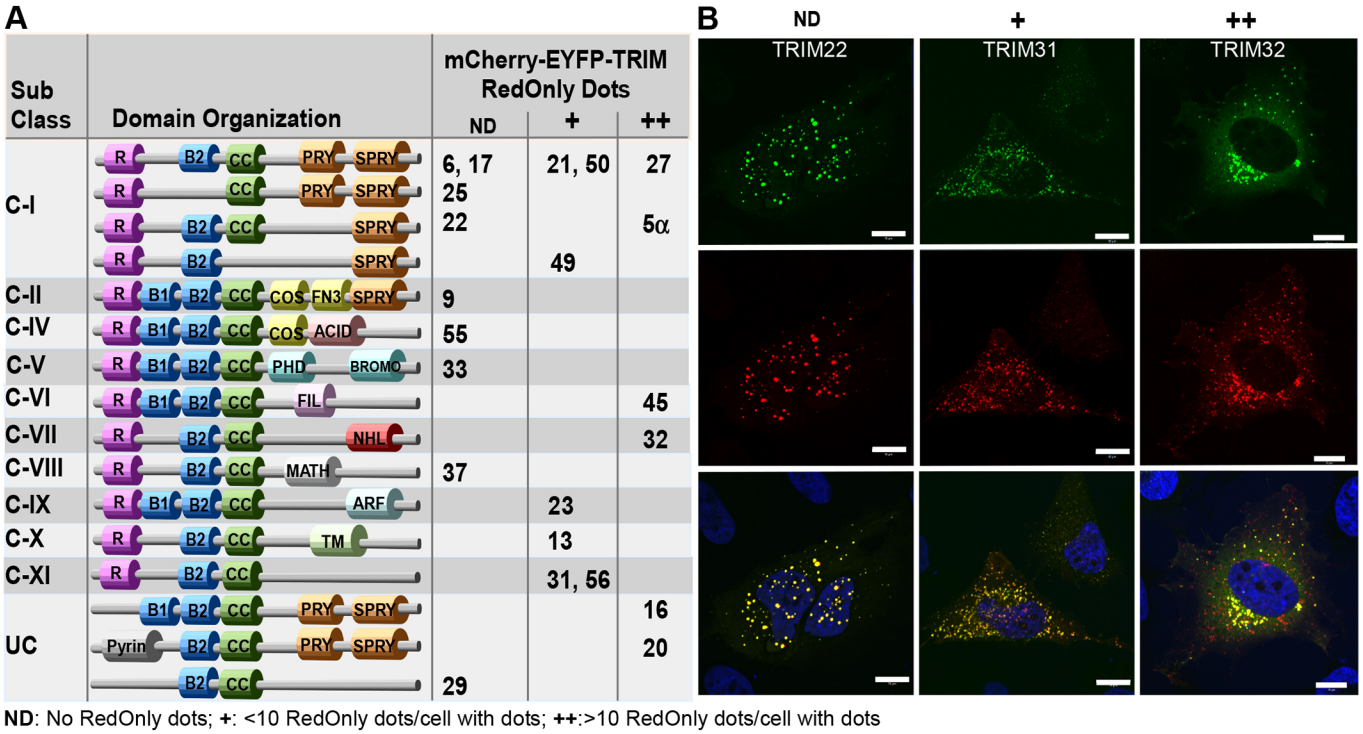

Fig. 1. TRIM proteins from various subclasses are degraded in the lysosome. (A) Subclasses and domain organization of the 22 TRIM proteins analyzed in the double-tag screen. The ability of each mCherry–EYFP–TRIM protein to form RedOnly structures is indicated by ND (no RedOnly structures detected),+(<10 RedOnly structures in cells with fluorescent puncta), **++** (many RedOnly structures in cells with fluorescent puncta). R, Ring finger B1/B2: Bbox1/Bbox2; CC, Coiled coil. (B) Confocal images of mCherry–EYFP-tagged TRIM proteins representing each of the categories ND, + and ++. HeLa cells were transfected with mCherry–EYFP-tagged TRIM22, TRIM31 or TRIM32 1 day before fixation and imaged using a Zeiss780 confocal microscope and the Zen software. Blue, DAPI staining. Scale bars: 10 µm.

Bardet–Biedl syndrome 11 (BBS11) (Chiang et al., 2006). The pathogenic mechanism for the disease is not understood.

Autophagy is a cellular renovation system that uses lysosome-mediated pathways to degrade and recycle almost any type of cell content (Mizushima and Komatsu, 2011). Autophagy is described to act both as a non-selective bulk degradation pathway, and as a selective elimination of components such as aberrant protein aggregates, RNA bodies, lipid droplets, unwanted organelles and invading pathogens in a process termed selective autophagy (reviewed in Rogov et al., 2014). Selective autophagy provides quality control of cellular components, degrading damaged and harmful material during normal cellular conditions. When cells are stressed by hypoxia, ischemia, starvation or infection, selective autophagy is stimulated and specifically targets excess or toxic structures (Johansen and Lamark, 2011; Rogov et al., 2014). This allows the cell to adapt to the unfavorable conditions. Autophagy receptors are instrumental in the process. They bind specifically to the cargo and to ATG8 family proteins (such as LC3B, also known as MAP1LC3B) at the forming autophagosome, directing the cargo for degradation in the lysosome. The first selective autophagy receptor to be identified was p62, also known as sequestosome-1 (SQSTM1) (Bjørkøy et al., 2005). Ubiquitin labeling is one of the signals for cargo degradation via selective types of autophagy. Ubiquitylated protein aggregates containing autophagy receptors are evident in a range of human diseases. p62 contains a C-terminal ubiquitin-binding domain (UBA), a LC3-interacting region (LIR) and an N-terminal Phox and Bem1 (PB1) domain with an oligomerization property (Pankiv et al., 2007). The oligomerization activity of p62 is important for sequestering its cargo and for scaffolding phagophore membrane development (Bjørkøy et al., 2005; Itakura and Mizushima, 2011), described as a p62-mediated phase separation process dependent on ubiquitin (Sun et al., 2018; Zaffagnini et al., 2018). Recent studies have revealed that the autophagy activity of p62 itself is regulated by ubiquitylation (Heath et al., 2016; Jongsma et al., 2016; Lee et al., 2017; Pan et al., 2016; Peng et al., 2017). The UBA domain of unmodified p62 has a strong tendency to form an intermolecular dimer that spatially occludes ubiquitin binding (Isogai et al., 2011; Long et al., 2010). Ubiquitylation of several residues both inside and outside the UBA domain is reported to enhance the ubiquitin-binding activity and autophagy activity of p62 (Lee et al., 2017; Peng et al., 2017). Interestingly, several studies implicate p62 as an important player of protein homeostasis in muscle cells (Arndt et al., 2010; Lee et al., 2018; Rodriguez-Muela et al., 2018). Furthermore, proper regulation of autophagy is fundamental for muscle homeostasis, and dysregulation of autophagy has a pathogenic role in several forms of muscle diseases (Jiao and Demontis, 2017).

By employing a fluorescence-based double-tag screen of 22 TRIM proteins representing each of the TRIM subfamilies, we identified TRIM32 as a potential autophagy cargo protein. Interaction analysis *in vitro* and in cells revealed direct interaction and colocalization of TRIM32 and p62, while autophagy assays showed that p62 was able to mediate autophagic degradation of TRIM32. Conversely, ubiquitylation assays and proteomic analysis identified p62 as a TRIM32 substrate. TRIM32 mediated mono-ubiquitylation of p62 at residues previously shown to be important for the ubiquitin-binding activity of p62. By establishment of TRIM32-knockout (KO) and reconstituted cells, we show that TRIM32 facilitates p62 sequestration and autophagic degradation. Introduction of the LGMD2H disease mutation in TRIM32 inhibited its autophagic degradation, and also its ability to regulate p62

Journal of Cell Science (2019) 132, jcs236596. doi:10.1242/jcs.236596

activity. In contrast, introduction of the BBS11 mutation in TRIM32 strongly facilitated p62 sequestration and degradation. Our results demonstrate a dual role for TRIM32 in autophagy, acting both as a substrate and as a positive regulator of p62. Importantly, the inactivity of the TRIM32 LGMD2H mutant points toward dysfunctional TRIM32 mediated regulation of p62 as a pathological mechanism in LGMD2H.

RESULTS

TRIM proteins from various subclasses are degraded in the lysosome

Recent studies have shown that certain TRIM proteins are implicated in the autophagy process, as regulators and as receptors in selective autophagy (reviewed in Di Rienzo et al., 2019; Hatakeyama, 2017; Kimura et al., 2017, 2016; van Gent et al., 2018). Furthermore, a few TRIM proteins seemingly are degraded by autophagy themselves, including TRIM50 (Fusco et al., 2012), TRIM30 (Choi et al., 2015) and TRIM5α (Mandell et al., 2016). Here, we employed the double-fluorescence-tag strategy (Pankiv et al., 2007) to identify TRIM proteins that could be degraded by autophagy, and hence that are potential as autophagy regulators and receptors. A total of 22 different TRIM proteins, representing 11 subclasses of the TRIM family, were fused to the double fluorescence tag mCherry–EYFP and expressed in HeLa cells. Since EYFP is unstable in acidic milieus with a pH below 6, while mCherry is stable, double-tagged proteins will only have red florescence when they are sequestered in the lysosome (denoted 'RedOnly' structures), which has a pH of ∼4.7. At 24 h after transfection, the cells were exposed to normal medium or were starved for 2 h in Hanks' balanced salt solution (HBSS), before fixation and confocal microscopy imaging. To verify that the RedOnly structures represented lysosomal compartments, we analyzed, in parallel, cells treated with the lysosomal inhibitor Bafilomycin A1 (BafA1) for 4 h before fixation. BafA1 impairs the acidification of the lysosomes, and hence the quenching of EYFP localized in the lysosome. As presented in Fig. 1, 13 of the 22 TRIM proteins tested formed some RedOnly structures. Nine of these have previously been linked to autophagy, namely, TRIM20 and TRIM21 (Kimura et al., 2015), TRIM50 (Fusco et al., 2012), TRIM23 (Sparrer et al., 2017), TRIM13 (Tomar et al., 2012), TRIM31 (Ra et al., 2016), TRIM5α (Mandell et al., 2014), TRIM32 (Di Rienzo et al., 2019; Yang et al., 2017) and TRIM16 (Chauhan et al., 2016; Kimura et al., 2017). The observation that not all TRIM proteins form RedOnly structures may indicate that this is not a general trait of the conserved N-terminal RING finger–B-box–coiled-coil domains, or that degradation of certain TRIMs by autophagy is dependent on factors not present in HeLa cells. Furthermore, RedOnly structures were detected among TRIMs from many different subclasses (Fig. 1A), suggesting that it is not dependent on any specific domains in the C-terminal. However, four of the six TRIM proteins that gave a substantial amount of RedOnly structures both in normal medium and upon starvation conditions contain a SPRY domain in their very C-terminal end. Three of these, TRIM5α, TRIM16 and TRIM20, have been previously identified as autophagy receptors (Chauhan et al., 2016; Kimura et al., 2017; Mandell et al., 2014) and hence confirm our screening strategy. mCherry–EYFP–TRIM32 displayed a strong and reproducible formation of RedOnly dots in both normal and starved conditions (Fig. 1B). Interestingly, TRIM32 is reported to interact with the autophagy receptor TAX1BP1, and thereby mediate autophagic degradation of the TLR3/4 adaptor protein TRIF (Yang et al., 2017) and a recent report suggests autophagic degradation of the TRIM32 LGMD2H disease mutants (Servián-Morilla et al., 2019). However, whether TRIM32 is a substrate for autophagic degradation is unresolved.

TRIM32 interacts and colocalizes with the autophagy marker proteins LC3B and p62

The double tag assay clearly indicated lysosomal degradation of exogenous TRIM32. In order to determine whether endogenous TRIM32 is degraded via lysosomal pathways or via the proteasome, the lysosomal inhibitor BafA1 and the proteasomal inhibitor MG132 were applied on HEK293 cells grown in full medium or starved in HBSS for 4 h. The protein levels of endogenous TRIM32 during the various conditions was analyzed by western blotting and the band intensities quantitated and correlated to the level of PCNA (Fig. 2A). Treatment with the lysosomal inhibitor and the proteasomal inhibitor increased the amount of TRIM32 to a similar degree under starvation conditions, while the proteasomal pathway seems to be most important under normal cellular conditions. The increase of the LC3B II band (representing lipidated LC3B) upon BafA1 treatment, and the phosphorylation status of the mTOR-regulated translation initiation factor 4E (p4E-BP1) verified that the cells responded as expected to the lysosomal inhibitor and to the starvation medium. These data suggest that TRIM32 is degraded via the proteasomal and lysosomal pathways to a similar extent during starvation conditions, while the proteasomal pathway is dominant under normal conditions.

Several TRIM proteins are reported to interact with core components of the autophagy machinery, and to function as autophagy receptors and regulators of autophagosome formation (Kimura et al., 2015, 2016; Mandell et al., 2016, 2014). We applied *in vitro* GST-pulldown assays to determine whether TRIM32 has the ability to bind directly to the ATG8 family proteins. Fig. 2B shows that TRIM32 binds to LC3A (MAP1LC3A), LC3C (MAP1LC3C), GABARAP and GABARAP-L1, and weakly to LC3B and GABARAP-L2. However, we were not able to find any candidate LC3-interacting regions (LIRs) in TRIM32 with bioinformatic tools, and GST-pulldown assays with the N-terminal part of TRIM32 (the RING finger–B-box–coiled-coil domains) and the C-terminal part (NHL-domains) both displayed binding to GST–LC3B and GST–GABARAP (Fig. S1A). Further attempts to identify LIRs in TRIM32 did not give any consistent results (data not shown). We next tried to identify whether the interaction between TRIM32 and the ATG8 protein family was mediated by the newly characterized ubiquitin-interacting motif (UIM) docking site (Marshall et al., 2019). However, we were not able to identify a UIM motif in TRIM32. This suggests that TRIM32 can interact directly with ATG8 proteins in a non-LIR- and non-UIM-dependent way, suggesting that other or more complex interfaces are involved.

To further investigate the lysosomal degradation of the TRIM32 mutants, Flp-In T-Rex 293 cell lines with tetracycline-inducible expression of EGFP–TRIM32^{P130S} and EGFP–TRIM32^{D487N} were established (Fig. S1B). In accordance with previous reports, TRIM32 is normally a cytoplasmic protein forming distinct perinuclear bodies or aggregates (Fig. 2C; Fig. S1B) (Locke et al., 2009). Furthermore, western blots of the expressed EGFP fusion proteins revealed a slower-migrating form of EGFP–TRIM32 and the BBS11 mutant EGFP–TRIM32^{P130S}, but not the LMGD2H mutant EGFP–TRIM32^{D487N} (Fig. S1B). Co-staining the FlpIn EGFP–TRIM32 cells with antibodies against the autophagy marker protein LC3B and the autophagy receptor protein p62 showed that certain TRIM32 bodies colocalized with LC3B-positive p62 bodies (Fig. 2C). This indicates that a subpopulation of the TRIM32 bodies represent autophagosomes. Such bodies were observed both in full medium and in starvation conditions. To further evaluate whether TRIM32 interacts with p62 in cells, the DuoLink proximity ligation assay was employed to detect close colocalization of EGFP–TRIM32 and endogenous p62 in the Flp-In

Journal of Cell Science (2019) 132, jcs236596. doi:10.1242/jcs.236596

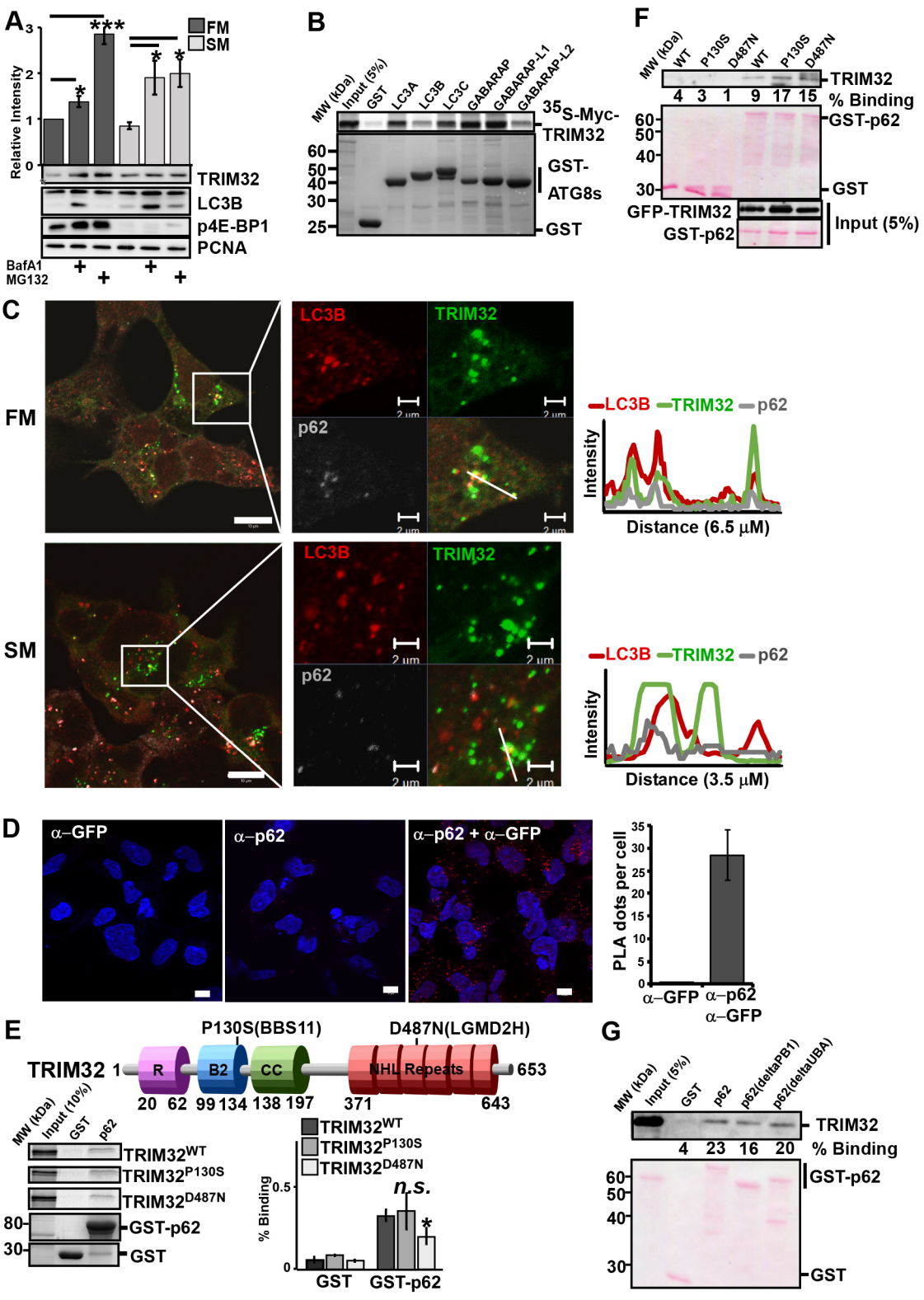

Fig. 2. See next page for legend.

EGFP–TRIM32 cell line. The DuoLink assay revealed close to 30 distinct spots per cell (Fig. 2D). Together, these data show that TRIM32 is recruited to LC3B-positive p62 bodies, and is stabilized by treating cells with the lysosomal inhibitor BafA1. This strongly indicates that a subpopulation of TRIM32 proteins is degraded by autophagy.

Seven various mutations in the NHL repeat region of TRIM32 are associated with the recessive muscular dystrophy disease LGMD2H, with the TRIM32^{D487N} mutation being the most common (Fig. 2E) (Frosk et al., 2002), while a point mutation in the B-Box2, TRIM32^{P130S}, leads to the pleiotropic disorder BBS11 (Fig. 2E) (Chiang et al., 2006). We applied the *in vitro*

Journal of Cell Science

Journal of Cell Science (2019) 132, jcs236596. doi:10.1242/jcs.236596

Fig. 2. TRIM32 interacts and colocalizes with the autophagy marker proteins LC3B and p62. (A) HEK293 FlpIn cells were treated with BafA1 (200 nM) or MG132 (10 µM) for 4 h in HBSS (starvation medium, SM) or full medium (FM), before cell extracts were harvested in 1× SDS. 10 µg of the various cell extracts were separated on SDS-PAGE gels and blotted against the indicated antibodies. The bar graphs on top panel represent the mean± s.e.m. relative band intensities estimated by ImageJ from three independent experiments (n=3). *P<0.05, ***P<0.0005 (Student's t-test). (B) GST-pulldown assay using ^{35}S-labeled Myc–TRIM32 and recombinant GST and GST–ATG8 proteins. The amount of Myc–TRIM32 bound to the various ATG8 proteins was detected by autoradiography. The assay was repeated with similar results. (C) HEK293 FlpIn EGFP-TRIM32 cells in full medium or starved in HBSS (2 h) were fixed and stained with antibodies for LC3B and p62. Images were obtained using a ZEISS780 confocal laser scanning microscope, and the colocalization monitored using the ZEN software. Scale bars: 10 µm (main images), 2 µm (magnifications). Intensity profiles along the indicated line are shown to the right. (D) Representative images of the Flp-In EGFP-TRIM32 cells analyzed by the proximation ligation assay DuoLink using antibodies against GFP and p62. The graph represents the mean±s.d. of colocalization dots using the Volocity software, from three independent experiments. Each experiment includes z-stack images of n=100 cells per condition. Scale bars: 10 µm. (E) The top panel shows a schematic of the TRIM32 domain organization with the localization of the disease point mutations P130S and D487N indicated. R, Ring finger; B2, Bbox2; CC, Coiled coil. The lower panels show GST-pulldown assays using ^{35}S-labeled Myc–TRIM32^{WT}, Myc–TRIM32^{P130S} or Myc–TRIM32^{D487N} and recombinant GST and GST–p62 immobilized on glutathione–Sepharose beads. Quantifications of the binding of wild-type and mutant constructs to GST–p62 are presented as percentage binding relative to input. The bars represent the mean±s.d. band intensities compared to input as quantified using ImageJ of three independent experiments. *P=0.025; n.s., not significant (Student's t-test). (F) GST-pulldown assay using cell extracts from FlpIn EGFP-TRIM32^{WT}, EGFP-TRIM32^{P130S} or EGFP-TRIM32^{D487N} cells and GST–p62 immobilized on glutathione–Sepharose beads. EGFP–TRIM32 was detected using an anti-GFP antibody. GST proteins were visualized by Ponceau staining. Quantifications of the band intensities of the bound proteins compared to 5% input are indicated below the blot. (G) GST-pulldown assays using cell extracts from the FlpIn EGFP–TRIM32 cells and recombinant GST, GST-p62, or various GST-p62 deletion constructs immobilized on glutathione–Sepharose beads. Bound EGFP–TRIM32 was detected using anti-GFP antibody, while the GST proteins were visualized by Ponceau staining. Quantifications of the band intensities of the bound proteins compared to 5% input using ImageJ are indicated below the blot.

GST-pulldown assay to verify the direct interaction between p62 and wild-type TRIM32 and its two disease mutants. p62 expressed in *E.coli* and immobilized on glutathione beads was added to *in-vitro*-translated Myc–TRIM32^{WT}, Myc–TRIM32^{P130S} or Myc–TRIM32^{D487N}. The amount of bound proteins was analyzed by SDS-PAGE (Fig. 2E). Wild-type TRIM32 and both its disease mutants bound weakly to p62. The interaction between TRIM32 and p62 in cells was further confirmed by GST-pulldown assays using cell extracts from HEK293 cell lines expressing EGFP-tagged wild-type TRIM32 and its disease mutants (Fig. 2F), and by co-immunoprecipitation of endogenous p62 (Fig. S1D).

The PB1 domain and the UBA domain of p62 is important for p62 oligomerization and for binding to ubiquitylated proteins (Bjørkøy et al., 2005; Lee et al., 2017). In order to identify whether the PB1 domain or the UBA domain of p62 is implicated in the interaction with TRIM32, we performed GST-pulldown assays using p62 PB1 and UBA deletion constructs fused to GST and cell extracts from cells expressing exogenous EGFP–TRIM32. We found that deletion of the UBA domain or the PB1 domain did not affect the interaction with TRIM32, indicating that the interaction is not mediated by ubiquitin (Fig. 2G). These results show that TRIM32 binds directly to the autophagy receptor p62, and this interaction is not impaired by the LGMD2H and BBS11 disease mutations.

TRIM32 is targeted to autophagic degradation by p62

Next, we evaluated whether the lysosomal degradation of TRIM32 is mediated by macroautophagy. For this purpose, we applied the mCherry–EYFP–TRIM32 double-tag assay in the autophagy-deficient ATG7-KO cells (Mejlvang et al., 2018). ATG7 is an ubiquitin E1-like activating enzyme that is essential for assembly and function of the ubiquitin-like conjugation systems (Nakatogawa et al., 2009). mCherry–EYFP–TRIM32 did not form any RedOnly dots in the ATG7-KO cells (Fig. 3A,C). Furthermore, degradation of endogenous TRIM32 was not stabilized by BafA1 treatment in ATG7-KO cells (Fig. 3B). This clearly indicates that lysosomal degradation of TRIM32 is mediated by the macroautophagy pathway. Next question was whether TRIM32 is degraded by selective autophagy. To this end, the degradation of TRIM32 was assayed in a cell line lacking the five autophagy receptors p62, NBR1, NDP52, TAX1BP1 and OPTN (denoted the 'pentaKO') (Lazarou et al., 2015). Only a few cells with mCherry–EYFP–TRIM32 RedOnly dots were observed in pentaKO cells grown under normal and starvation conditions (Fig. 3A,C). This suggests that TRIM32 is dependent on the autophagy receptors for efficient degradation by autophagy, pointing towards degradation by selective autophagy.

The interaction and colocalization of TRIM32 with p62 prompted us to analyze the degradation of TRIM32 in pentaKO cells reconstituted with EGFP–p62. mCherry–EYFP–TRIM32 formed several RedOnly dots both under normal and starvation conditions in this cell line, indicating that p62 is able to mediate autophagic degradation of TRIM32 (Fig. 3C,D). To evaluate if p62 is essential for autophagic degradation of TRIM32, we employed the double tag assay in a HEK293 FlpIn cell line knocked out for p62. The T-REx HEK293 p62$^{-/-}$ cell line was established by CRISPR/Cas9 as described in the Materials and Methods section (Fig. S1C). Ablation of p62 strongly reduced the number of RedOnly dots in the mCherry–EYFP–TRIM32-transfected cells compared to wild-type cells (Fig. 3C,D), but did not completely abolish lysosomal degradation of mCherry–EYFP–TRIM32. This indicates that p62 can mediate autophagic degradation of TRIM32. However, other autophagy receptors beside p62 may also be involved.

The LGMD2H disease mutant of TRIM32 is not degraded by autophagy

To investigate whether the TRIM32^{P130S} and TRIM32^{D487N} disease mutants were degraded by autophagy, they were fused to the mCherry–EYFP double tag and transfected into HeLa cells. Interestingly, we found that mCherry–EYFP–TRIM32^{P130S} displayed a strong ability to form RedOnly dots, especially under starvation conditions (Fig. 4A). TRIM32^{D487N} on the other hand, was mainly diffuse except from in some cells where it formed several round dots distributed throughout the cell. However, none of these dots were found to be RedOnly (Fig. 4A). Similar results were obtained when we transfected the double-tag constructs into the myoblast cell line C2C12 (Fig. S2A). Around 75% of the C2C12 cells expressing mCherry–EYFP–TRIM32^{WT} and mCherry–EYFP–TRIM32^{P130S} contained RedOnly dots, compared to only 12% of the C2C12 cells expressing mCherry–EYFP–TRIM32^{D487N}. Moreover, double-tag analyses in the C2C12 cells expressing the mutants TRIM32^{R394H} and TRIM32^{V591M}, both of which are within the NHL repeats region and are associated with LGMD2H, revealed that they did not localize in acidic compartments (Fig. S2A). These results clearly indicate that TRIM32 undergoes autophagic degradation in muscle cells, and that this degradation is strongly inhibited by mutations associated with LGMD2H.

Journal of Cell Science (2019) 132, jcs236596. doi:10.1242/jcs.236596

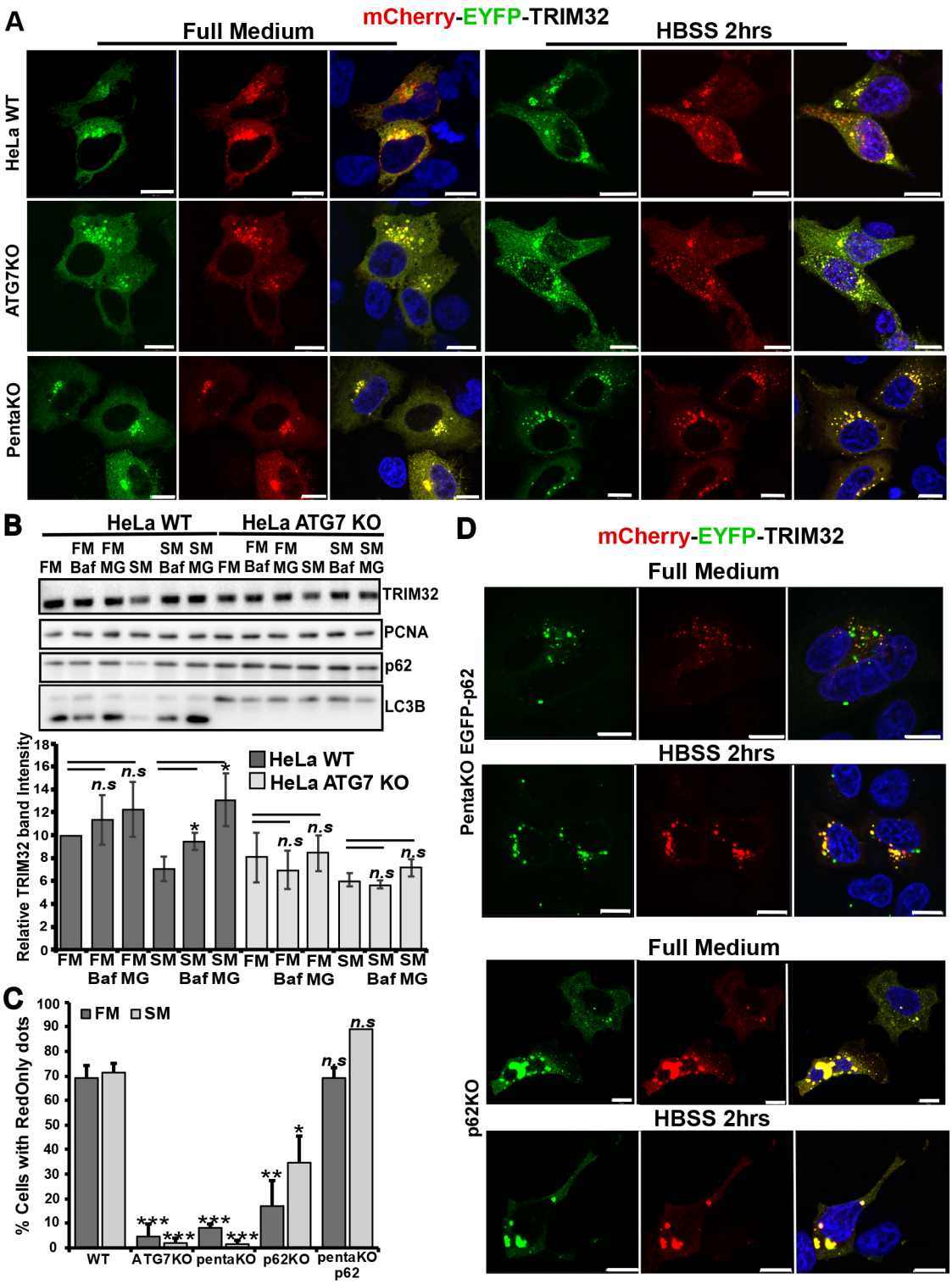

Fig. 3. TRIM32 is targeted to autophagic degradation by p62. (A) Normal HeLa cells and cells that were genetically knocked out for ATG7 or the five autophagy receptors p62, NBR1, NDP52, OPTN or TAX1BP1 (pentaKO) as indicated, were transfected with mCherry–EYFP–TRIM32. At 1 day post transfection, half of the cells were treated with HBSS for 2 h (starvation medium, SM) and half were maintained in full medium (FM), before all cells were fixed, stained with DAPI and imaged using a Zeiss780 confocal microscope. Scale bars: 10 µm. (B) Western blot analysis of endogenous TRIM32 in wild-type HeLa cells and HeLa ATG7-KO cells in normal medium (FM) in HBSS (SM), and treated or not with BafA1 (Baf) and MG132 (MG) for 4 h. The graph represents the mean±s.d. TRIM32 band intensities from three independent experiments quantitated using ImageJ. *P*-values are obtained using Student's *t*-test. n.s.=not significant (*P*-value>0.05). PCNA represents the loading control, while p62 and LC3B are controls of autophagy flux. (C) The graphs represent the amount of mCherry-EYFP-TRIM32 transfected cells that contain RedOnly dots compared to the amount of cells that display mCherry-EYFP-TRIM32 dots (representative images shown in A and D) under normal and starvation (HBSS 2 h) conditions. Each graph represents the mean±s.e.m. of at least three independent experiments (n=25–50 cells). **P*<0.05, ***P*<0.005, ****P*<0.0005, n.s., not significant (Student's *t*-test). (D) PentaKO cells reconstituted with GFP–p62 (green dots) and HEK293 FlpIn cells genetically knocked out for p62 as indicated to the right, were transfected and treated as described in A. Scale bars: 10 µm.

Journal of Cell Science (2019) 132, jcs236596. doi:10.1242/jcs.236596

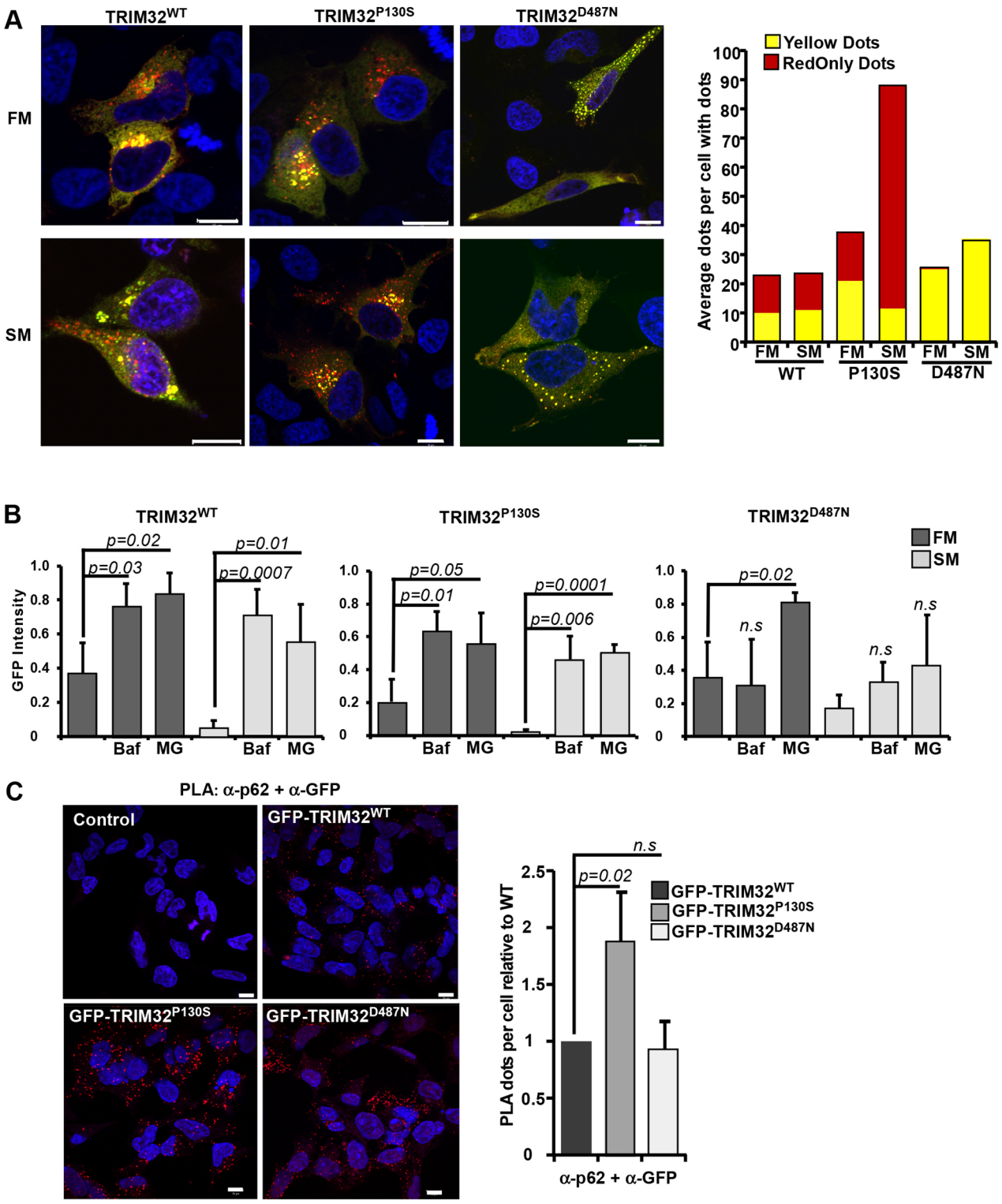

Fig. 4. The LGMD2H disease mutant of TRIM32 is not degraded by autophagy. (A) HeLa cells were transfected with mCherry–EYFP–TRIM32^{WT}, mCherry–EYFP–TRIM32^{P130S} or mCherry–EYFP–TRIM32^{D487N} as indicated, kept in normal medium (full medium, FM) or starved with HBSS for 2 h (starvation medium, SM) at 1 day post transfection and imaged by a Zeiss780 confocal microscope. The graphs to the right display manual quantification of RedOnly dots and yellow dots in *n*=30 cells, and are representative of three independent experiments. Scale bars: 10 µm. (B) GFP fluorescence intensities (arbitrary units) of EGFP–TRIM32^{WT}, EGFP–TRIM32^{P130S} and EGFP–TRIM32^{D487N} as measured by flow cytometry 24 h after promoter shut off in full medium (FM) or HBSS for 6 h (SM), supplemented with BafA1 2 µm (Baf) or MG132 20 µM (MG) as indicated. Bars show average mean±s.d. GFP intensity from three independent experiments (*n*=10,000 cells). *P*-values are as indicated; n.s., not significant (Student's *t*-test). (C) Representative images of the Flp-In EGFP-TRIM32 cells analyzed by the proximation ligation assay DuoLink using antibodies against GFP and p62. The graph represents the mean±s.d. relative number of colocalization dots with from three independent experiments. Each experiment includes *z*-stack images of *n*≈100 cells per condition, and was quantified using the Volocity software. *P*-values are as indicated; n.s., not significant (Student's *t*-test). Scale bars: 10 µm.

Journal of Cell Science (2019) 132, jcs236596. doi:10.1242/jcs.236596

Next, a flow-based reporter cell system (Larsen et al., 2010) was applied on the HEK293 FlpIn EGFP–TRIM32 cell lines, to monitor degradation of EGFP–TRIM32 and the two disease mutants under normal conditions and starvation. Expression of EGFP–TRIM32 or the disease mutants was induced by treatment with tetracycline for 24 h. Thereafter, the expression was shut off by tetracycline wash-out. The cells were starved in HBSS for 6, 12 and 24 h, and the degradation measured by flow cytometry using the mean GFP intensity in the cell population as a read out. BafA1 was applied to determine degradation by lysosomal pathways, while MG132 was included to measure proteasomal degradation. In full medium, EGFP–TRIM32 is stabilized to a similar extent by BafA1 and MG132, implicating both autophagy and the proteasome system in TRIM32 degradation under normal conditions (Fig. 4B). This is in line with the data presented in Fig. 2A, showing that endogenous TRIM32 is degraded both by autophagy and by the proteasome. This shows that EGFP–TRIM32 inducibly expressed in FlpIn cell lines is degraded similarly to the endogenous protein. Upon 6 h starvation, EGFP–TRIM32 expression is reduced by 85% compared to normal conditions. The degradation is inhibited both by BafA1 and MG132, pointing towards involvement of both autophagy and the proteasomal system also under starved conditions. Similar results were obtained when the starvation period was extended to 12 and 24 h (data not shown). However, the expression level of EGFP–TRIM32 did not decline further, indicating that the expression of TRIM32 is stabilized after 6 h starvation. Applying the flow reporter assay on the BBS11 disease mutant EGFP–TRIM32^{P130S} indicated a higher rate of degradation compared to the wild-type protein, with a 90% reduction in the expression after 6 h of starvation (Fig. 4B). The LGMD2H disease mutant EGFP–TRIM32^{D487N}, however, was not stabilized by BafA1 treatment under either normal or starvation conditions (Fig. 4B). The expression level of EGFP–TRIM32^{D487N} upon starvation is reduced by 50%, which indicates a dramatically lower turnover than the wild-type protein and the BBS11 mutant. Hence, as indicated by the double-tag assay in Fig. 4A, EGFP–TRIM32^{D487N} is not an autophagic substrate, suggesting that it shows dependence on its oligomerization and/or auto-mono-ubiquitylation abilities to be recognized as an autophagic substrate. This is in contrast to a recent report showing BafA1-mediated stabilization of a TRIM32 LGMD2H mutant in primary myoblasts isolated from a patient (Servián-Morilla et al., 2019). This discrepancy can be explained by a TRIM32^{V591M} mutation in this patient, while we have analyzed the TRIM32^{D487N} mutation.

Since we found that TRIM32 colocalizes with p62 in punctate structures, and that reintroduction of p62 into the pentaKO cells was sufficient to direct TRIM32 to autophagic degradation, the next question was whether EGFP–TRIM32^{D487N} had lost its ability to interact with endogenous p62. To this end, the Duolink proximation ligation assay was performed on the FlpIn EGFP–TRIM32 wild-type and mutant cell lines (Fig. 4C). Importantly, EGFP–TRIM32^{D487N} colocalized with p62 to a similar extent as EGFP–TRIM32^{WT}. Hence, interaction with p62 is not sufficient to target TRIM32 to autophagic degradation. Interestingly, the BBS11 disease mutant interacted strongly with p62, forming around twice as many dots in the Duolink assay as wild-type TRIM32 (Fig. 4C). This suggests that the P130S mutation in TRIM32 may modulate the colocalization of TRIM32 and p62 in cells.

Wild-type TRIM32, but not the LGMD2H disease mutant, mono-ubiquitylates p62

In order to investigate the role of TRIM32 in selective autophagy, we established HEK293 FlpIn TRIM32-KO cell lines by CRISPR/Cas9. Knockout of TRIM32 expression in the cell lines was verified by western blotting (Fig. S2B) and genomic sequencing (Fig. S2C). Measuring the proliferation curve of the TRIM32-KO cell lines revealed that they had impaired proliferation compared to the mother HEK293 FlpIn cell line (Fig. 2D). This is in line with the reported roles of TRIM32 in tumorigenesis (Liu et al., 2014; Wang et al., 2018; Yin et al., 2018; Zhao et al., 2018), and thus validates the TRIM32-KO cell lines further.

Recent research connects the upregulation of TRIM proteins in tumor cells to enhanced protein quality control and antioxidant defense (Chen et al., 2017). p62 plays important roles both in protein quality control and in antioxidant defense via NRF2 (also known as NFE2L2) (Jain et al., 2010; Pankiv et al., 2007), and ubiquitylation is an important signaling event in these processes. Moreover, reports describing ubiquitin modifications of p62 as a modulator of its activity are emerging (Heath et al., 2016; Jongsma et al., 2016; Lee et al., 2017; Lin et al., 2017; Pan et al., 2016). This prompted us to investigate whether TRIM32 has the ability to ubiquitylate p62. Myc–p62 was immunoprecipitated from a HEK293 p62-KO cell line co-expressing Myc–p62 and EGFP–TRIM32. Western blotting revealed a slow-migrating band both for Myc–p62 and EGFP–TRIM32 (Fig. 5A), indicative of mono-ubiquitylation of both proteins. Whether these slower migrating bands indeed represented ubiquitin modification was verified by coexpressing the de-ubiquitylase USP2 (Fig. 5B). Expressing USP2 removed the slow-migrating band of both p62 and TRIM32. Furthermore, such slower-migrating bands were not detected when Myc–p62 was precipitated from HEK293 cells expressing EGFP–TRIM32^{C44S} (catalytic dead) or EGFP–TRIM32^{D487N} (an LGMD2H disease mutation). This indicates that TRIM32 mediates mono-ubiquitylation of p62, and that this is impaired by mutations in the NHL domains involved in the LGMD2H disease. Mutation in the BBox2 (P130S, a BBS11 disease mutation), however, did not affect mono-ubiquitylation of p62. Both K63- and K48-linked ubiquitylation were responsible for the p62 modification to a similar extent (Fig. 5C). Both wild-type and mutated forms of EGFP–TRIM32 co-precipitated with Myc–p62, which is in line with the GST-pulldown (Fig. 2) and Duolink assay (Fig. 4) results. Hence, the disease mutations do not impair the p62–TRIM32 interaction in cells. Similar ubiquitylation of p62 was obtained when co-transfecting Myc–p62 and wild-type or P130S EGFP–TRIM32 constructs in the HEK293 FlpIn TRIM32-KO cells (Fig. 5C). Myc–p62 also formed a high-molecular-mass band in the SDS gel when co-transfected with the active forms of TRIM32 (Fig. 5D), suggesting that TRIM32-mediated ubiquitylation of p62 leads to the formation of stable p62 oligomers. To identify whether impaired ubiquitylation of p62 is a general trait of LGMD2H disease mutations, the recently described V591M mutant of TRIM32 (Di Rienzo et al., 2019) was co-transfected with Myc–p62 in the HEK293 FlpIn TRIM32-KO cells (Fig. 5E). Introduction of the V591M mutation strongly impaired the p62 ubiquitylation, clearly pointing towards aberrant ubiquitylation of p62 as a general phenotype of LGMD2H. Western blotting of the Myc–p62 precipitates using an antibody against mono-and poly-ubiquitin (FK2) verified that p62 ubiquitylation was strongly reduced upon introduction of the LGMD2H disease mutations D487N and V591M (Fig. 5E).

Next, we undertook mass spectrometry (MS) analysis to identify which lysine residues in p62 were modified by TRIM32. MS analysis of Myc–p62 immunoprecipitated from HEK293 TRIM32-KO cells co-transfected with Myc–p62 and EGFP–TRIM32, or the TRIM32 disease mutants EGFP–TRIM32^{P130S}

Journal of Cell Science (2019) 132, jcs236596. doi:10.1242/jcs.236596

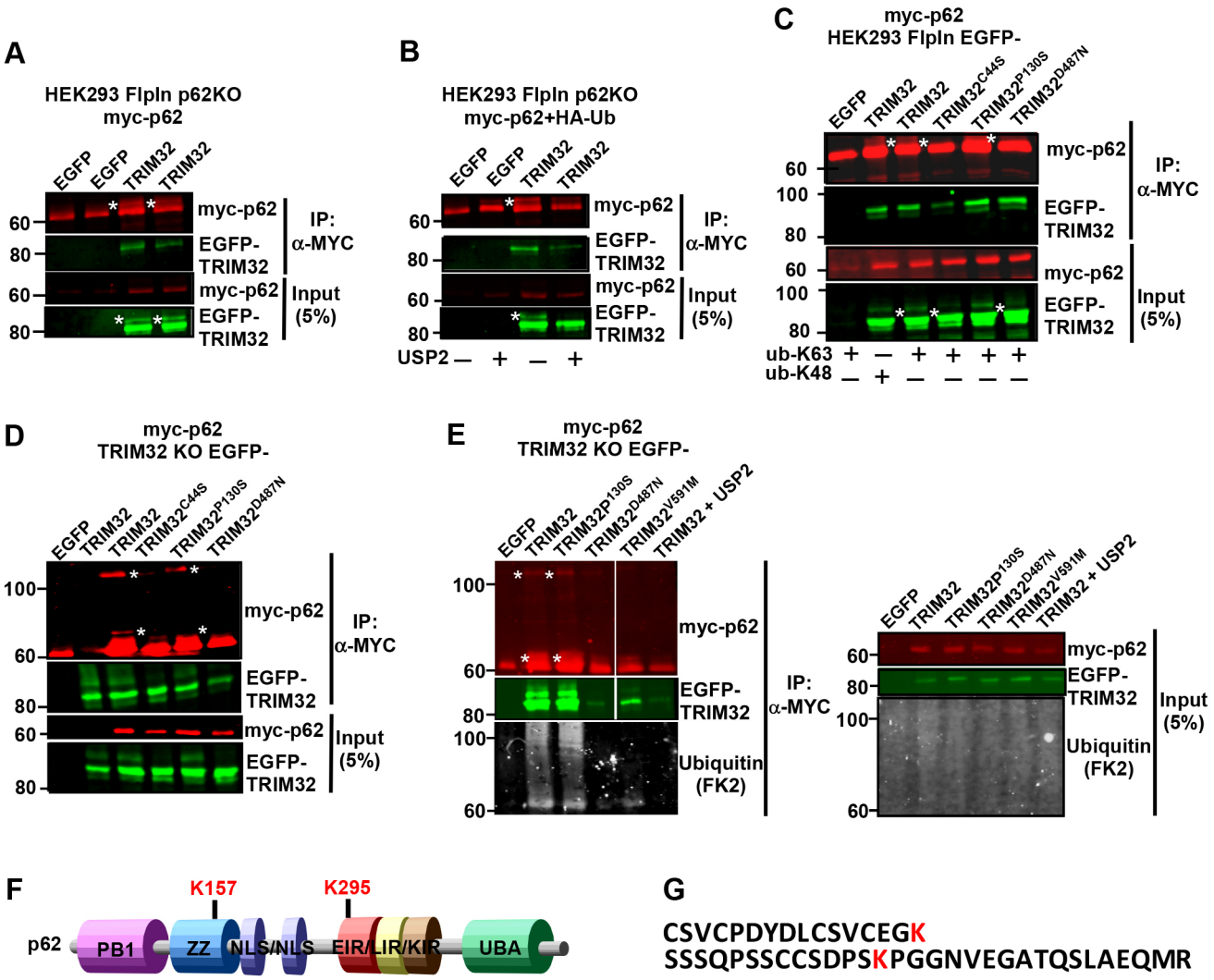

Fig. 5. TRIM32 wild-type, but not the LGMD2H disease mutant, mono-ubiquitylates p62. (A) Western blot of two independent experiments from lysates of HEK293 p62-KO cells co-expressing Myc–p62 with EGFP–TRIM32. Myc–p62 was immunoprecipitated (IP) using a Myc-trap and precipitated p62 detected using an anti-Myc antibody. The EGFP–TRIM proteins were detected using an anti-GFP antibody. * indicates mono-ubiquitylated Myc–p62 and EGFP–TRIM32. (B) Myc–p62 was co-expressed with EGFP–TRIM32 and HA–ubiquitin, and with mCherry–USP2, where indicated, in the HEK293 p62-KO cell line. Myc–p62 was immunoprecipitated using a Myc-trap and precipitated p62 detected using an anti-Myc antibody. The EGFP–TRIM proteins were detected using an anti-GFP antibody. * indicates mono-ubiquitylated Myc–p62 and EGFP–TRIM32. (C) Myc–p62 was co-transfected with HA–Ub-K48 or HA–Ub-K63 in the HEK293 EGFP–TRIM32^{WT}, EGFP–TRIM32^{P130S} and EGFP–TRIM32^{D487N} cell lines and expression induced by tetracyclin (1 µM) for 24 h. Myc–p62 was immunoprecipitated using a Myc-trap and precipitated p62 detected using an anti-Myc antibody. The EGFP–TRIM proteins were detected using an anti-GFP antibody. * indicates mono-ubiquitylated p62 and mono-ubiquitylated EGFP–TRIM32. (D) Myc–p62 was co-transfected with EGFP–TRIM32^{WT}, EGFP–TRIM32^{P130S} or EGFP–TRIM32^{D487N} in the HEK293 TRIM32-KO (#1) cell line. Myc-p62 was immunoprecipitated using a Myc-trap and precipitated p62 detected using an anti-Myc antibody. The EGFP–TRIM proteins were detected using an anti-GFP antibody. * indicates mono-ubiquitylated p62 and a high-molecular-mass form of p62. (E) Myc–p62 was co-transfected with EGFP–TRIM32^{WT}, EGFP–TRIM32^{P130S}, EGFP–TRIM32^{D487N}, EGFP–TRIM32^{V591M}, or EGFP–TRIM32 and mCherry–USP2 in the HEK293 TRIM32-KO (#1) cell line. Myc–p62 was immunoprecipitated using a Myc-trap and precipitated p62 detected using an anti-Myc antibody. Ubiquitin modification of p62 was detected using an antibody recognizing mono- and poly-ubiquitin (FK2) (lower panels). The EGFP–TRIM proteins were detected using an anti-GFP antibody. * indicates mono-ubiquitylated p62 and a high-molecular-mass p62. In all blots, EGFP indicates a control plasmid expressing only EGFP. (F) Schematic of p62 domain organization with location of the two lysine residues mapped to be ubiquitylated by TRIM32 indicated above. ZZ, Zinc finger; NLS, Nuclear localization signal; EIR, E2-interacting region; LIR, LC3-interacting region; KIR, Keap1-interacting region; UBA, Ubiquitin-binding domain. (G) Sequence of the p62 peptides found to be ubiquitylated by TRIM32 by MS analyses.

and EGFP–TRIM32^{D487N}, revealed that co-expression of wild-type TRIM32 and the BBS11 disease mutant lead to ubiquitylation of p62 at two lysine residues, K157 and K295 (Fig. 5F,G). No lysine residue was found to be ubiquitylated when the LGMD2H disease mutant was co-expressed with p62. To verify ubiquitylation on these two residues, we introduced K157R or K295R single and double mutations into p62. However, these mutations did not abolish TRIM32 mediated mono-ubiquitylation (Fig. S3A,B). Mono-ubiquitylation of endogenous p62 under ubiquitin stress is reported to occur on p62^{K157} and p62^{K295}, together with p62^{K313} and p62^{K420} (Peng et al., 2017); in that study, mono-ubiquitylation of p62 at those residues was proposed to inhibit formation of inactive p62 dimers with ‘closed’ UBA domains, and thereby promote p62–polyubiquitin interactions and autophagy activity. Hence, next we established a p62$^{K157R/K295R/K420R}$ triple mutant and subjected it to TRIM32, but still TRIM32 was able to mediate ubiquitylation of

Journal of Cell Science (2019) 132, jcs236596. doi:10.1242/jcs.236596

p62 (Fig. S3B). Neither did introduction of the single K165R or K313R mutations, or the four mutations p62$^{K157R/K295R/K313R/K420R}$ impair ubiquitylation (Fig. S3B). These results indicate that TRIM32-mediated ubiquitylation of p62 may happen at several lysine residues. Interestingly, introducing the D69A mutation in p62, which impairs its ability to undergo oligomerization (Lamark et al., 2003), abolished the TRIM32-mediated mono-ubiquitylation (Fig. S3A,B). This indicates that TRIM32 recognize and ubiquitylate oligomerized p62, but not monomeric p62 molecules.

TRIM32 enhances the formation and turnover of p62 dots

To assess the impact of TRIM32 on the early autophagy events, we assayed WIPI-dot formation in the TRIM32-KO cell lines compared to wild-type cells in normal and starvation conditions. The TRIM32-KO cells did not display any strong effect on the formation of WIPI dots upon starvation (Fig. S3C). However, confocal analysis of p62 in the TRIM32-KO cells showed that the ability of p62 to form dots was significantly reduced (Fig. 6A,B). This suggests that TRIM32-mediated mono-ubiquitylation of p62 stimulates the formation of p62 dots and its autophagic activity, in line with previous studies of the roles of p62 ubiquitylation (Conway and Kirkin, 2017; Lee et al., 2017; Peng et al., 2017). In order to verify this further, we reconstituted the TRIM32-KO cell lines with stably expressing Myc–TRIM32^{WT}, Myc–TRIM32^{P130S} and Myc–TRIM32^{D487N}, and monitored the formation of p62 dots under normal conditions and upon inhibition of autophagy activity by BafA1 treatment (Fig. 6C–F). Conclusively, we found that reintroduction of TRIM32 in the TRIM32-KO cell line strongly facilitated the formation of p62 dots. The number of p62 dots was enhanced upon BafA1 treatment, indicating that TRIM32 augments the autophagic degradation of p62. Importantly, reconstitution with the TRIM32^{P130S} mutant facilitated p62 dot formation nearly as efficiently as TRIM32^{WT}, while reconstitution with the TRIM32^{D487N} mutant had no effect on p62 dot formation (Fig. 6F). This clearly indicates that the E3 ligase activity of TRIM32 is important for its regulatory role on p62. Interestingly, in the TRIM32-KO cells reconstituted with Myc–TRIM32, most cells displayed a diffuse cytoplasmic localization of TRIM32 – with only a few cells containing TRIM32 dots. This was in contrast to the HEK293 FlpIn cells stably overexpressing EGFP–TRIM32. Here, wild-type TRIM32 and the BBS11 disease mutant were found to form cytoplasmic dots in most cells. The more diffuse localization pattern in the reconstituted TRIM32-KO cells suggests that high expression levels of TRIM32 leads to the formation of cytoplasmic dots. However, the dot formation seems to be dependent on TRIM32 ubiquitylation, since the catalytic dead TRIM32 and the LGMD2H disease mutation were mainly diffuse. Importantly, BafA1 treatment of the reconstituted TRIM32-KO cells resulted in formation of several cytoplasmic dots in the cells expressing wild-type Myc–TRIM32 and the BBS11 disease mutant. Myc–TRIM32^{WT} and Myc–TRIM32^{P130S} colocalized with p62 and LC3B in these dots (Fig. 6E). In addition, Myc–TRIM32^{D497N} formed large cytoplasmic dots in some cells. However, these did not colocalize with p62 and LC3B (Fig. 6E). To conclude, our data show that TRIM32 can act as a positive regulator of p62 sequestration and degradation. Concomitantly, TRIM32 itself is a p62 cargo, and thus will be directed to degradation by an active p62. This creates a negative-feedback loop in the TRIM32–p62 interaction pathway (Fig. 6G). Hence, TRIM32-mediated ubiquitylation of p62 seems to regulate its autophagic activity, and thereby cellular proteostasis. One mechanism for the LGMD2H disease can thus be explained by diminished p62 mono-ubiquitylation and lower p62-mediated autophagy activity, resulting in impaired proteostasis.

DISCUSSION

Owing to constant mechanical stress, striated muscle proteins are particularly prone to wear and tear, and require several protein quality-control mechanisms to coordinate protein turnover and removal of damaged proteins. Among these, ubiquitin signaling and the autophagy-lysosomal pathways are important players (reviewed in Dong and Cui, 2018). Here, we identified the E3 ubiquitin ligase TRIM32 as a substrate for the autophagy receptor p62, which targets TRIM32 for degradation by selective autophagy. Interestingly, TRIM32 was identified as one of the proteins rapidly degraded upon starvation together with the autophagy receptor proteins and certain other proteins (Mejlvang et al., 2018). However, the disease mutant of TRIM32 associated with LGMD2H was not degraded by autophagy. Furthermore, we found TRIM32 to bind directly to p62 and mediate mono-ubiquitylation on several lysine residues, among them p62^{K157} and p62^{K295}. In addition, the TRIM32 LGMD2H disease mutant D487N bound directly to p62. However, TRIM32^{D487N} did not mediate ubiquitylation of p62. Mono-ubiquitylation of p62 is proposed to enhance its autophagy receptor potential, which is critical for maintaining proteostasis during cellular stress (Peng et al., 2017). We found the formation of p62 bodies to be reduced in TRIM32-KO cells, while it was strongly facilitated when TRIM32^{WT} or TRIM32^{P130S} was reintroduced into the knockout cells. Importantly, the LGMD2H disease mutation was not able to rescue p62 dot formation in the TRIM32-KO cells. Together, this implicates TRIM32 as a positive regulator of p62-mediated selective autophagy, and suggests that one mechanism for development of LGMD2H in TRIM32^{D487N} muscle cells is due to reduced p62 autophagy activity leading to dysregulated cellular proteostasis.

Several TRIM proteins have been shown to modulate the selective autophagy process (Chauhan et al., 2016; Fusco et al., 2018; Jena et al., 2018; Kimura et al., 2015, 2016; Mandell et al., 2014), and during the completion of this paper Di Rienzo and co-workers (2019) identified TRIM32 as a regulator of ULK1 activity in atrophic muscle cells. Similarly to ULK1, p62 activity during selective autophagy is regulated by ubiquitylation. TRIM21 and NEDD4 are reported to mediate ubiquitylation of p62^{K7} leading to suppressed protein sequestration and induced inclusion body autophagy (Lin et al., 2017; Pan et al., 2016). The E3 ligase RNF166 ubiquitylates p62 at K91 and K189, facilitating the role of p62 in xenophagy (Heath et al., 2016), while RNF26 ubiquitylates p62 within the UBA domain facilitating TOLLIP interaction and vesicular cargo sorting (Jongsma et al., 2016). Keap1–Cullin3 poly-ubiquitylates p62^{K420} leading to diminished p62 sequestration and degradation activity (Lee et al., 2017). The E2 conjugating enzymes UBE2D2 and UBE2D3 are found to bind directly to p62 via the E2-interacting region (EIR) (Fig. 5E), and mediate mono-ubiquitylation of p62 at several lysine residues, among them K157, K295 and K420, upon ubiquitin stress signaling (Peng et al., 2017). This mono-ubiquitylation is proposed to relieve the inhibition of the UBA domain in the p62 UBA dimer, leading to enhanced binding and tethering of ubiquitylated cargoes to ATG8 proteins conjugated to the phagophore (Conway and Kirkin, 2017). Here, we mapped a direct interaction between TRIM32 and p62 that was independent of the PB1 domain and the UBA domain, similar to the p62 interaction with Keap1–Cullin3. However, Keap1–Cullin3 poly-ubiquitylated p62 at K420 in the UBA domain, while we found TRIM32 to mediate mono-ubiquitylation of p62 at K157 and K295. The Keap1–Cullin3-mediated ubiquitylation of p62 increases p62

Journal of Cell Science (2019) 132, jcs236596. doi:10.1242/jcs.236596

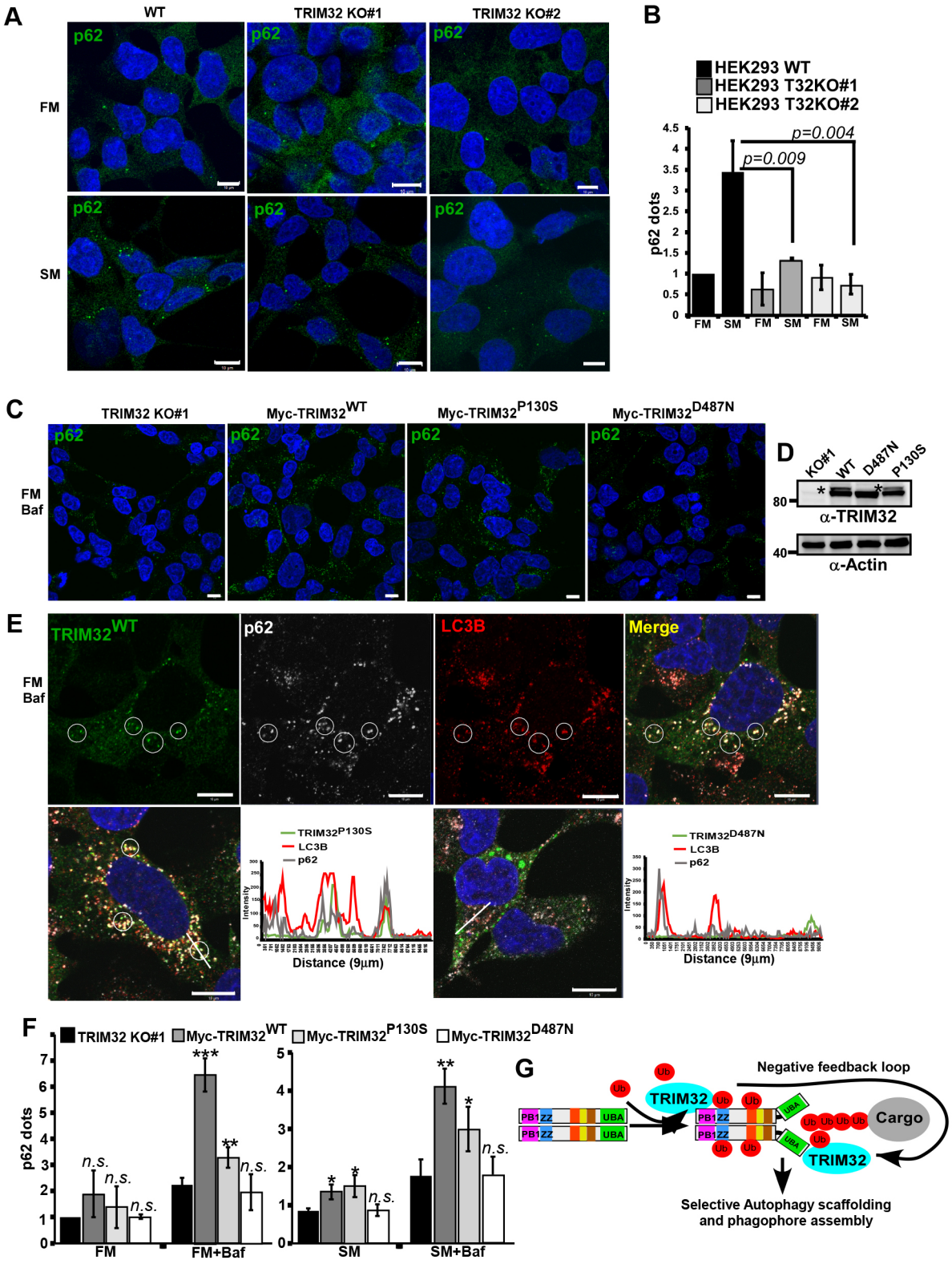

Fig. 6. See next page for legend.

inclusion body formation and subsequent degradation, which is proposed to be a mechanism for Keap1 to release the antagonistic role of p62 and thereby dampen the NRF2-mediated response to oxidative stress (Lee et al., 2017). On the other hand, mono-ubiquitylation of p62 at several residues, including K157, K295 and K420, enhances p62 body formation and p62-mediated autophagy activity. This is proposed to be critical for homeostasis during various cellular stresses.

We show that introduction of the LGMD2H disease mutation in TRIM32 makes it unable to mono-ubiquitylate p62. The D487N

Journal of Cell Science

Journal of Cell Science (2019) 132, jcs236596. doi:10.1242/jcs.236596

Fig. 6. TRIM32 enhances the formation and turnover of p62 dots. (A) Immunostaining of endogenous p62 in HEK293 FlpIn cells and the two TRIM32 KO clones under normal (FM) and starvation (SM) conditions (HBSS 2 h). Scale bars: 10 µm. (B) Quantification of p62 dots in the two TRIM32 KO clones and the HEK293 FlpIn wild type cell line under normal (FM) and starvation (SM) (HBSS 2 h) conditions using the Volocity software (PerkinElmer). Each graph represents the mean±s.d. of the relative number of p62 dots per cell (normalized to the value for FM in wild-type cells). The results are from three independent experiments each including ∼100 cells per condition. *P*-values were obtained using Student's *t*-test. (C) Immunostaining of endogenous p62 in the TRIM32 KO (#1) cell line and TRIM32 KO (#1) cells reconstituted with stable expression of Myc–TRIM32^{WT}, Myc–TRIM32^{P130S} or Myc–TRIM32^{D487N} as indicated. The cells are grown in FM with BafA1 (2 µM, 7 h). Scale bars: 10 µm. (D) Western blot showing the expression of Myc–TRIM32, Myc–TRIM32^{P130S} and Myc–TRIM32^{D487N} in the reconstituted HEK293 TRIM32-KO cell lines, grown in FM. * indicates mono-ubiquitylated TRIM32. (E) Upper panels show immunostaining of Myc–TRIM32^{WT}, p62 and LC3B in the reconstituted HEK293 TRIM32-KO cells grown in normal medium supplemented with BafA1 (2 µM) for 7 h. The circles exemplify colocalization of all three proteins in BafA1 dots. The lower panels show merged images of similar immunostainings in the TRIM32-KO cell line reconstituted with Myc–TRIM32^{P130S} or Myc–TRIM32^{D487N}. Images were obtained using a ZEISS780 confocal laser scanning microscope, and the colocalization line plots to the right obtained using the ZEN software. Scale bars: 10 µm. (F) Quantification of p62 dots in the cell lines represented in C, under normal (FM) and normal plus BafA1 (7 h) conditions, and starvation (SM) (HBSS 4 h) and starvation plus BafA1 conditions. The graphs represent the mean±s.d. of the relative number of p62 dots per cell (normalized to the value for FM in TRIM32-KO cells) quantified using Volocity software (PerkinElmer). The results are from three independent experiments each including *n*>100 cells per condition. **P*<0.05, ***P*<0.005, ****P*<0.0005; n.s., not significant (Student's *t*-test). (G) A model depicting the roles of TRIM32 both as a p62 activator and a p62 substrate in selective autophagy. ZZ, zinc finger; UBA, ubiquitin-binding domain; Ub, Ubiquitin.

mutation located in the evolutionarily conserved NHL region of TRIM32 does not inhibit binding to p62. Previously, the LGMD2H mutant is reported to have impaired oligomerization and E3 ligase activity and to display a more diffuse cytoplasmic localization than TRIM32 WT and TRIM32^{P130S} that are enriched in puncta/aggregates in most cells (Locke et al., 2009). Also, the LGMD2H disease mutants seem to be less expressed in muscle tissues from affected patients (Servián-Morilla et al., 2019). Apart from that, the molecular mechanisms of TRIM32 mutants causing the LGMD2H and BBS11 diseases are far from being understood. It is not known if the self-mono-ubiquitylation is important for activation of TRIM32. Our results suggest that this may be the case, and also that this mono-ubiquitylation is important for degradation of TRIM32 via selective autophagy. Several reports connect TRIM32 ubiquitylation activity to substrates whose deregulation might influence the onset and progression of muscular dystrophy, including actin, tropomyosin, troponins, α-actinin, dysbindin and c-Myc (reviewed in Tocchini and Ciosk, 2015). Interestingly, p62 is strongly implicated in chaperone-assisted selective autophagy (CASA), which is essential for muscle maintenance (Arndt et al., 2010). Dysregulated CASA resulted in Z-disk disintegration and progressive muscle weakness. Here, we found that the TRIM32 mutation implicated in muscle dystrophy is unable to ubiquitylate p62 at lysine residues that are linked to p62-mediated substrate sequestration and autophagy activity. Furthermore, TRIM32-KO cells displayed a reduced capacity for p62 sequestration upon cellular stress induced by starvation. Hence, LGMD2H mutations in TRIM32 lead to impaired substrate ubiquitylation and impaired degradation via p62-mediated selective autophagy, both important players in cellular proteostasis. These findings contribute to the understanding of the pathological mechanisms of LMGD2H.

The TRIM32-mediated ubiquitylation site p62^{K157} is located in the zinc-finger (ZZ) domain (Fig. 5E), and this lysine residue is evolutionarily conserved from zebrafish to human. Recently the small non-coding RNA molecule Vault RNA1-1 was found to bind to the ZZ domain of p62 and thereby modulate its dimerization and autophagy activity (Horos et al., 2019). Hence, post-translational modifications in the ZZ domain could impact such interactions and thereby p62-mediated autophagy activity. The p62^{K295} site lies at the border of the EIR and of a previously predicted PEST sequence. Thus, it can be speculated that this modification can regulate interactions with ubiquitin E2 enzymes, but also have an impact on p62 stability. The latter can thereby explain the reduced expression level of p62 detected in muscle tissue isolated from LGMD2H patients (Servián-Morilla et al., 2019).

In addition to being a positive regulator of p62 activity, this study revealed that TRIM32 is a p62 substrate in selective autophagy (Fig. 6G). TRIM32 first facilitates p62-mediated autophagy activity. This, after a certain period, leads to a reduced TRIM32 expression caused by p62-mediated degradation. Diminished TRIM32 expression will in turn lead to declined p62 activity, creating a negative-feedback loop. This negative-feedback mechanism may be a potential target for therapeutic intervention.

MATERIALS AND METHODS

Antibodies and reagents

The following primary antibodies were used: rabbit polyclonal antibody for TRIM32 (Proteintech, 10326-1-AP; 1:2000); rabbit polyclonal anti-GFP (Abcam, ab290; 1:5000); mouse monoclonal Myc-Tag (9B11) [Cell Signaling Technologies, #2276; 1:2000 for western blotting (WB), 1:200 for immunofluorescence (IF)]; rabbit polyclonal anti-LC3B (Sigma, L7543; 1:1000 for WB, 1:500 for IF); rabbit polyclonal antibody for phospho-4E-BP1 (Cell Signaling Technologies, #9451; 1:1000); rabbit polyclonal anti-actin (Sigma, A2066; 1:1000); mouse monoclonal anti-p62 lck ligand (BD Biosciences, 610833; 1:2000); guinea pig polyclonal anti-p62 (Progen, GP62-C; 1:2000); mouse monoclonal anti-ubiquitin (FK2) (BIOMOL, PW8810, 1:1000) and mouse monoclonal anti-PCNA (DAKO, M0879; 1:1000). The following secondary antibodies were used: horseradish-peroxidase (HRP)-conjugated goat anti-rabbit-IgG (BD Biosciences, 554021; 1:2000); HRP-conjugated goat anti-mouse-Ig (BD Biosciences, 554002; 1:2000); and HRP-conjugated anti-biotin antibody (Cell Signaling Technologies, #7075; 1:2000). The following fluorescent secondary antibodies were used: Alexa Fluor® 488-conjugated goat anti-mouse-IgG (Life Technologies, A-11029; 1:1000); Alexa Fluor® 488-conjugated goat anti-rabbit-IgG (Life Technologies, A-11008; 1:1000); Alexa Fluor® 555-conjugated goat anti-rabbit-IgG (Life Technologies, A-11008; 1:5000); Alexa Fluor® 555-conjugated goat anti-guinea-pig-IgG (Life Technologies, A-21435; 1:1000); Alexa Fluor® 555-conjugated goat anti-mouse-IgG (Life Technologies, A-21424; 1:1000); Alexa Fluor® 647-conjugated goat anti-guinea pig IgG (Life Technologies, A-21450; 1:1000). The reagents used were: BafA1 (Sigma, B1793); MG132 (Sigma, C2759); tetracycline (Sigma, #87128); doxycycline (Sigma, D9891); and Hanks balanced salt solution (Sigma, H8264).

Cell culture and transfections

HeLa (ATCC, CCL2), HEK293 (ATCC, CRL-1573) and Hek293 T-Rex (Thermo Fisher Scientific, R714-07) cells were cultured in Dulbecco's modified Eagle's medium (DMEM) (Sigma, D6046) with 10% fetal bovine serum and 1% streptomycin-penicillin (Sigma, P4333). Hek FlpIn T-Rex cells with integrated TRIM32, TRIM32 C44S, TRIM32 P130S or TRIM32 D487N were grown in the same medium with additional selection marker antibiotics, 200 µg/ml hygromycin B (Invitrogen, #10687010) and 7.5 µg/ml blasticidin (Gibco, A1113903). Sub-confluent cells were transfected using TransIT-LT1 (Mirus, MIR2300) or Metafectene Pro (Biontex, T040) following the manufacturer's instructions. All cell lines were routinely tested for mycoplasma contamination.

Journal of Cell Science (2019) 132, jcs236596. doi:10.1242/jcs.236596

Construction of plasmids

All plasmids used in this study are listed in Table S1. Plasmids were made by conventional restriction enzyme-based cloning or by use of the Gateway recombination system (Thermo Fisher Scientific). Gateway LR reactions were performed as described in the instruction manual. Point mutation was carried out using the site-directed-mutagenesis kit from Stratagene. PCR and sequencing oligonucleotides (Table S2) were ordered from Thermo Fisher Scientific. All plasmids were verified by restriction enzyme digestion and DNA sequencing (BigDye, Applied Biosystems, 4337455). All TRIM proteins were cloned into the pDest mCherry-EYFP (Bhujabal et al., 2017) double tag vector.

Recombinant protein production and GST-pulldown analysis

GST or GST-tagged proteins were expressed in *Escherichia coli* strain SoluBL21 (Genlantis, #C700200). Protein expression was induced by treating overnight bacterial culture with 50 µg/ml isopropyl β-D-1-thiogalactopyranoside (IPTG). GST or GST fusion proteins were purified and immobilized on glutathione–Sepharose 4 Fast Flow beads (GE Healtcare, 17-5132-01). Myc-tagged proteins were *in vitro* translated using the TNT T7 reticulocyte Lysate system (Promega, #14610) in the presence of [^{35}S]methionine. *In vitro* translated protein or total cell lysate was pre-incubated with 10 µl glutathione–Sepharose beads and 100 µl of NETN buffer (50 mM Tris-HCl pH 8.0, 150 mM NaCl, 1 mM EDTA and 0.5% Nonidet P-40) with cOmplete Mini EDTA-free protease inhibitor mixture tablets (Roche Applied Science, 11836170001) for 1 h at 4°C to reduce unspecific binding. Pre-incubated lysate was then incubated with the immobilized GST fusion protein for 2 h at 4°C. Beads were washed five times with NETN buffer, boiled with 2× SDS gel loading buffer (125 mM Tris-HCl pH 7.5, 4% SDS, 0.04% Bromophenol Blue, 8% sucrose and 100 mM dithiolthreitol) and subjected to SDS-PAGE. Gels were stained with Coomassie Brilliant Blue R-250 Dye (Thermo Fisher Scientific, #20278) to visualize GST fusion proteins and then vacuum dried. Signals from ^{35}S-labeled proteins were detected with a Fujifilm bioimaging analyzer BAS-5000 (Fujifilm).

Immunoblotting and immunoprecipitation

Cells were seeded in 6-cm plates and treated as indicated. Cells were lysed in 1× SDS buffer (50 mM Tris-HCl pH 7.4, 2% SDS and 10% glycerol) supplemented with 200 mM dithiothreitol (DTT, Sigma, #D0632) and heated at 100°C for 10 min. Protein concentration was measured using the Pierce BCA protein assay kit (Thermo Fisher Scientific, #23227). Equal amounts of protein were resolved by SDS-PAGE and transferred to nitrocellulose membrane (Sigma, GE10600003). The membrane was stained with Ponceau S (Sigma, P3504), blocked with 5% non-fat dry milk in 1% TBS-T [0.2 M Tris-HCl pH 8, 1.5 M NaCl and 0.05% Tween 20 (Sigma, P9416)] and then incubated with indicated primary antibodies for 24 h. The membrane was washed three times for 10 min each with TBS-T followed by incubation with secondary antibody for 1 h. The membrane was washed three times for 10 min and analyzed by enhanced chemiluminescence using the ImageQuant LAS 4000 (GE Lifescience). For immunoprecipitation, cells were lysed in modified radioimmunoprecipitation assay (RIPA) buffer (50 mM Tris pH 7.5; 150 mM NaCl; 1 mM EDTA; 1% NP40; 0.25% Triton-X-100) supplemented with cOmplete Mini EDTA-free protease inhibitor cocktail tablets (Roche, #11836170001) and phosphatase inhibitor cocktail (Merck Millipore, #524625) by shaking at 4°C for 30 min. The cell lysate was centrifuged at 10,000 ***g*** for 10 min. The resulting supernatant was incubated with antibody to endogenous protein for endogenous immunoprecipitation or with Myc-TRAP (Chromotek, yta-20) for cells stably expressing, or transiently transfected, with Myc-tagged proteins. They were washed five times in RIPA buffer before boiling in 2× SDS gel loading buffer. This was followed by protein identification by immunoblotting as previously described but on Immobilon-FL PVDF membrane (Millipore, IPFL00010), blocked with Odyssey® blocking buffer (PBS) (LI-COR Biosciences, #927-40000) and scanned on Odyssey CLx Imager (LI-COR).

Mass spectrometry

Cells were directly lysed in lysis buffer (Myc-TRAP®_A; Chromotek) supplemented with cOmplete Mini EDTA-free protease inhibitor (Roche), 5 mM NAM (N-Arachidonylmaleimide; Sigma) and 10 mM NEM (*N*-ethylmaleimide; Sigma). Immunoprecipitation of Myc-tagged proteins was performed according to the supplier's protocol (Chromotek). The samples were fractionated by SDS-PAGE followed by SimplyBlue™ SafeStain (Thermo Fisher Scientific) staining. The lanes representing proteins of molecular masses within 55–80 kDa were cut from the gel. In-gel trypsin digestion was performed before analysis by high-performance liquid chromatography–tandem mass spectrometry (HPLC-MS/MS). Gel pieces were subjected to in-gel reduction, alkylation and tryptic digestion using 6 ng µl^{-1} trypsin (V511A; Promega). OMIX C18 tips (Varian) were used for sample cleanup and concentration. Peptide mixtures containing 0.1% formic acid were loaded onto a Thermo Fisher Scientific EASY-nLC1200 system. Samples were injected to a trap column (Acclaim PepMap 75 µm×2 cm, C18, 3 µm, 100 Å; Thermo Fisher Scientific) for desalting before elution to the separation column (EASY-Spray column, C18, 2 µm, 100 Å, 50 µm, 50 cm; Thermo Fisher Scientific). Peptides were fractionated using a 4–40% gradient of increasing amounts of 80% acetonitrile in water over 60 min at a flow rate of 300 nl/min. The mobile phases contained 0.1% formic acid. Separated peptides were analyzed using an Orbitrap Fusion Lumos mass spectrometer. The mass spectrometer was operated in a data-dependent mode with the precursor scan in the orbitrap over the range *m*/*z* 350–1500. The most-intense ions were selected for electron-transfer dissociation (ETD) or collision-induced dissociation (CID) fragmentation using 3 s between each master scan. Dynamic exclusion was set to 30 s. The Orbitrap AGC target was set to 4E5, and the MS2 scans in the Ion Trap were set to 1E4 with maximum injection times 50 and 100 ms, respectively. Precursor ions with charge 3+ in the *m*/*z* range 350–650 and 4+ or 5+ ions in the *m*/*z* range 350–900 were fragmented with ETD. All ions with 6+ or higher were also fragmented using ETD. The rest of the precursor ions were fragmented using CID. Protein identification and post-translational modification mapping was performed using the Proteome Discoverer 2.2 software (Thermo Fisher Scientific).

Immunostaining and fluorescence confocal microscopy

Subconfluent cells grown in 24-well plates on coverslips (VWR, #631-0150) coated with fibronectin (Sigma, F1141) and treated as indicated. They were fixed in 4% paraformaldehyde for 20 min to allow visualization of acidic structures after the staining procedure. The cells were then permeabilized with methanol at room temperature for 5 min, blocked in 5% goat serum in PBS or 5% BSA in PBS and incubated at room temperature with a specific primary antibody followed by Alexa Fluor 488-, 555- or 647-conjugated secondary antibody and DAPI. Confocal images were obtained using a 63× NA 1.4 oil immersion objective on an LSM780/LSM800 system. Quantification of p62 dots were performed using the Volocity software (Perkin Elmer) on 10 images per condition, in three independent experiments. Each image contained 10–20 cells, and was generated using the *z*-stack function in the ZEN software (Zeiss). The line-profile tool in the ZEN software was exploited to plot colocalization of EGFP–TRIM32 and immunostained p62 and LC3B. Quantification of cells containing red only dots in the double-tagged screen was done manually by two independent researchers in three independent experiments.

Generation of TRIM32- and p62-KO HEK293 FlpIn cell lines

To generate a knockout cell line for TRIM32, the CRISPR/Cas9 system was exploited. The knockout was generated as described by Ran et al. (2013). Guide RNAs (gRNA) as described in Table S2 were annealed and ligated into the vector pSpCas9(BB)-2A-GFP (PX458) (Addgene, #48138) using BbsI restriction sites. Subconfluent Hek293 FlpIn T-Rex cells were transfected with the targeting plasmids using Metafectene Pro (Biontex, T020). EGFP-positive cells were sorted by FACS and plated into 96-well plates at 3 days post transfection. Single colonies were expanded up to 12-well plates and knockout validated by immunoblotting. Confirmed knockout clones were further screened by genomic sequencing. The targeted genomic regions were amplified by PCR using the primers TRIM32 PCRfw and TRIM32 PCRrv, or p62 PCRfw and p62PCRrv (Table S2) and the resulting PCR products ligated into the pGEM-T-EASy vector (Promega, A3600). Sequencing were conducted for at least three clones for each PCR product.

Reconstitution of TRIM32-KO cell lines

The TRIM32-KO cell lines were transduced using the lentiviral-based GATEWAY destination vector pCDH-EF1a-Myc-IRES conferring puromycine resistance. This vector enables constitutive expression of Myc–TRIM32^{WT}, Myc–TRIM320^{P130S} or Myc–TRIM32^{D487N} under control of an EF1α promoter.

Generation of stable cell lines

Stable cell lines were generated using the FlpIn T-Rex system (Thermo Fisher Scientific, R71407). cDNAs were PCR amplified and ligated into the inducible FlpIn expression vector, pDest-EGFP-Flp-In (Alemu et al., 2012). FlpIn T-Rex cells were then co-transfected with the cDNA-containing FlpIn expression vector and the FlpIn recombinase vector pOG44 in the ratio of 1:3. Cells were selected by treatment with 200 µg/ml hygromycin B (Invitrogen, #10687010) and 7.5 µg ml^{-1} blasticidin (Gibco, A1113903), and protein expression verified by induction with tetracycline (Sigma, #87128) or doxycycline (Sigma, D9891).

Flow cytometry

Hek293 FlpIn TRIM32 WT, P130S and D487N cells in 12-well plates were trypsinized (Sigma, T4049) and passed through cell strainer caps (BD Biosciences, 352235) to obtain single-cell suspensions. Cells were analyzed on a FACSAria cell sorter running FACSDiva software version 5.0 (BD Biosciences) using the blue laser for excitation of GFP. GFP fluorescence was collected through a 530/30 nm bandpass filter in the E detector. Data was collected from a minimum of 10,000 singlet events per tube, and the median GFP-A value was used for quantification. All bar graphs show the mean±s.d. of the GFP-A median values from three independent experiments.

Proximity ligation assay

Subconfluent HEK293 FlpIn EGFP-TRIM32 cells were fixed with 4% paraformaldehyde. Colocalization of EGFP–TRIM32 and endogenous p62 was detected by performing a Duolink® PLA (Sigma; DUO92101) according to the manufacturer's protocol. The primary antibodies rabbit polyclonal anti-GFP (1:2000, Abcam, ab290) and mouse monoclonal anti-p62 lck ligand (1:200, BD Biosciences, 610833) were incubated at 4°C overnight. The signals were detected using a 63× NA 1.4 oil immersion objective on an LSM780 system. Quantification of dots was performed using the Volocity software (Perkin Elmer) on 10 images per condition, in three independent experiments. Each image contained 10–20 cells, and was generated using the *z*-stack function in the ZEN software (Zeiss).

Cell proliferation assay

Hek FlpIn TRIM32 KO Clone #1, KO Clone #2 and FlpIn T-Rex control cells were seeded with four different concentrations (2000, 4000, 6000 and 8000 cells) in 100 µl DMEM (Sigma, D6046) on E-Plate L16 PET readers (ACEA Biosciences Inc, #2801185). xCELLigence® Real-Time Cell Analysis (RTCA) (ACEA Biosciences) were used to measure the cell proliferation over a time of 96 h with recording at 1 h intervals.

Statistics

All experiments were repeated at least three times, unless otherwise specified. Error bars represent the s.d. or s.e.m. as indicated in figure legends, and two-sided unpaired, homoscedastic Student's *t*-tests were performed to assess significant differences between populations. Replicates were not pooled for statistical analyses. *P<0.05, **P<0.005 and ***P<0.0005; n.s. denotes not signififcant (P>0.05). Sample sizes are denoted in the figure legends.

Acknowledgements

We thank Richard Youle, National Institutes of Health, Bethesda, MD 20892, USA, for the generous gift of the pentaKO cell line, and Yakubu P. Abudu, UiT, The Arctic University of Norway, for the gift of the EGFP–p62, reconstituted pentaKO cell line. Thanks to Jack-Ansgar Bruun at the Tromsø University Proteomics Platform for help with mass spectrometry analysis, and the Advanced Microscopy Core Facility at UiT, The Arctic University of Norway, for the use of instrumentation.

Competing interests

The authors declare no competing or financial interests.

Author contributions

Conceptualization: T.J., T.L., E.S.; Methodology: K.S.O., J.G.G., Z.B., E.S.; Validation: J.G.G., E.S.; Formal analysis: E.S.; Investigation: K.S.O., J.G.G., Z.B., A.J., A.Ø., K.B.L., E.S.; Writing - original draft: K.S.O., E.S.; Writing - review & editing: V.D., T.J., T.L., E.S.; Visualization: K.S.O., E.S.; Supervision: T.J., T.L., E.S.; Project administration: E.S.; Funding acquisition: V.D., T.J., E.S.

Funding

This work was supported by PhD grants to K.S.O. and J.G.G. from UiT – The Arctic University of Norway, by the Research Council of Norway (Norges Forskningsråd) (TOPPFORSK program grant #249884 to T.J.), and by the National Institutes of Health (R37AI042999, R01AI042999, and NIH center grant P20GM121176 to V.D.). Deposited in PMC for release after 12 months.

Supplementary information

Supplementary information available online at
http://jcs.biologists.org/lookup/doi/10.1242/jcs.236596.supplemental

References

Albor, A., El-Hizawi, S., Horn, E. J., Laederich, M., Frosk, P., Wrogemann, K. and Kulesz-Martin, M. (2006). The interaction of Piasy with Trim32, an E3-ubiquitin ligase mutated in limb-girdle muscular dystrophy type 2H, promotes Piasy degradation and regulates UVB-induced keratinocyte apoptosis through NFkappaB. *J. Biol. Chem.* **281**, 25850-25866. doi:10.1074/jbc.M601655200

Alemu, E. A., Lamark, T., Torgersen, K. M., Birgisdottir, A. B., Larsen, K. B., Jain, A., Olsvik, H., Øvervatn, A., Kirkin, V. and Johansen, T. (2012). ATG8 family proteins act as scaffolds for assembly of the ULK complex: sequence requirements for LC3-interacting region (LIR) motifs. *J. Biol. Chem.* **287**, 39275-39290. doi:10.1074/jbc.M112.378109

Arndt, V., Dick, N., Tawo, R., Dreiseidler, M., Wenzel, D., Hesse, M., Fürst, D. O., Saftig, P., Saint, R., Fleischmann, B. K. et al. (2010). Chaperone-assisted selective autophagy is essential for muscle maintenance. *Curr. Biol.* **20**, 143-148. doi:10.1016/j.cub.2009.11.022

Bhujabal, Z., Birgisdottir, A. B., Sjøttem, E., Brenne, H. B., Øvervatn, A., Habisov, S., Kirkin, V., Lamark, T. and Johansen, T. (2017). FKBP8 recruits LC3A to mediate Parkin-independent mitophagy. *EMBO Rep.* **18**, 947-961. doi:10.15252/embr.201643147

Bjørkøy, G., Lamark, T., Brech, A., Outzen, H., Perander, M., Øvervatn, A., Stenmark, H. and Johansen, T. (2005). p62/SQSTM1 forms protein aggregates degraded by autophagy and has a protective effect on huntingtin-induced cell death. *J. Cell Biol.* **171**, 603-614. doi:10.1083/jcb.200507002

Chauhan, S., Kumar, S., Jain, A., Ponpuak, M., Mudd, M. H., Kimura, T., Choi, S. W., Peters, R., Mandell, M., Bruun, J.-A. et al. (2016). TRIMs and galectins globally cooperate and TRIM16 and galectin-3 co-direct autophagy in endomembrane damage homeostasis. *Dev. Cell* **39**, 13-27. doi:10.1016/j.devcel.2016.08.003

Chen, L., Brewer, M. D., Guo, L., Wang, R., Jiang, P. and Yang, X. (2017). Enhanced degradation of misfolded proteins promotes tumorigenesis. *Cell Rep.* **18**, 3143-3154. doi:10.1016/j.celrep.2017.03.010

Chiang, A. P., Beck, J. S., Yen, H.-J., Tayeh, M. K., Scheetz, T. E., Swiderski, R. E., Nishimura, D. Y., Braun, T. A., Kim, K.-Y. A., Huang, J. et al. (2006). Homozygosity mapping with SNP arrays identifies TRIM32, an E3 ubiquitin ligase, as a Bardet-Biedl syndrome gene (BBS11). *Proc. Natl. Acad. Sci. USA* **103**, 6287-6292. doi:10.1073/pnas.0600158103

Choi, U. Y., Choi, W. Y., Hur, J. Y. and Kim, Y.-J. (2015). Polyubiquitin chain-dependent protein degradation in TRIM30 cytoplasmic bodies. *Exp. Mol. Med.* **47**, e159. doi:10.1038/emm.2015.12

Cohen, S., Zhai, B., Gygi, S. P. and Goldberg, A. L. (2012). Ubiquitylation by Trim32 causes coupled loss of desmin, Z-bands, and thin filaments in muscle atrophy. *J. Cell Biol.* **198**, 575-589. doi:10.1083/jcb.201110067

Conway, O. and Kirkin, V. (2017). Love laughs at Locksmiths: ubiquitylation of p62 unlocks its autophagy receptor potential. *Cell Res.* **27**, 595-597. doi:10.1038/cr.2017.56

Di Rienzo, M., Antonioli, M., Fusco, C., Liu, Y., Mari, M., Orhon, I., Refolo, G., Germani, F., Corazzari, M., Romagnoli, A. et al. (2019). Autophagy induction in atrophic muscle cells requires ULK1 activation by TRIM32 through unanchored K63-linked polyubiquitin chains. *Sci. Adv.* **5**, eaau8857. doi:10.1126/sciadv.aau8857

Dikic, I. and Elazar, Z. (2018). Mechanism and medical implications of mammalian autophagy. *Nat. Rev. Mol. Cell Biol.* **19**, 349-364. doi:10.1038/s41580-018-0003-4

Dong, Z. and Cui, H. (2018). The autophagy-lysosomal pathways and their emerging roles in modulating proteostasis in tumors. *Cells* **8**, 4. doi:10.3390/cells8010004

Frosk, P., Weiler, T., Nylen, E., Sudha, T., Greenberg, C. R., Morgan, K., Fujiwara, T. M. and Wrogemann, K. (2002). Limb-girdle muscular dystrophy type

2H associated with mutation in TRIM32, a putative E3-ubiquitin-ligase gene. *Am. J. Hum. Genet.* **70**, 663-672. doi:10.1086/339083

Fusco, C., Micale, L., Egorov, M., Monti, M., D'Addetta, E. V., Augello, B., Cozzolino, F., Calcagni, A., Fontana, A., Polishchuk, R. S. et al. (2012). The E3-ubiquitin ligase TRIM50 interacts with HDAC6 and p62, and promotes the sequestration and clearance of ubiquitinated proteins into the aggresome. *PLoS ONE* **7**, e40440. doi:10.1371/journal.pone.0040440

Fusco, C., Mandriani, B., Di Rienzo, M., Micale, L., Malerba, N., Cocciadiferro, D., Sjøttem, E., Augello, B., Squeo, G. M., Pellico, M. T. et al. (2018). TRIM50 regulates Beclin 1 proautophagic activity. *Biochim. Biophys. Acta Mol. Cell Res.* **1865**, 908-919. doi:10.1016/j.bbamcr.2018.03.011

Hatakeyama, S. (2017). TRIM family proteins: roles in autophagy, immunity, and carcinogenesis. *Trends Biochem. Sci.* **42**, 297-311. doi:10.1016/j.tibs.2017.01.002

Heath, R. J., Goel, G., Baxt, L. A., Rush, J. S., Mohanan, V., Paulus, G. L. C., Jani, V., Lassen, K. G. and Xavier, R. J. (2016). RNF166 determines recruitment of adaptor proteins during antibacterial autophagy. *Cell Rep.* **17**, 2183-2194. doi:10.1016/j.celrep.2016.11.005

Horos, R., Büscher, M., Kleinendorst, R., Alleaume, A.-M., Tarafder, A. K., Schwarzl, T., Dziuba, D., Tischer, C., Zielonka, E. M., Adak, A. et al. (2019). The small non-coding vault RNA1-1 acts as a riboregulator of autophagy. *Cell* **176**, 1054-1067.e1012. doi:10.1016/j.cell.2019.01.030

Isogai, S., Morimoto, D., Arita, K., Unzai, S., Tenno, T., Hasegawa, J., Sou, Y.-S., Komatsu, M., Tanaka, K., Shirakawa, M. et al. (2011). Crystal structure of the ubiquitin-associated (UBA) domain of p62 and its interaction with ubiquitin. *J. Biol. Chem.* **286**, 31864-31874. doi:10.1074/jbc.M111.259630

Itakura, E. and Mizushima, N. (2011). p62 Targeting to the autophagosome formation site requires self-oligomerization but not LC3 binding. *J. Cell Biol.* **192**, 17-27. doi:10.1083/jcb.201009067

Jain, A., Lamark, T., Sjøttem, E., Larsen, K. B., Awuh, J. A., Øvervatn, A., McMahon, M., Hayes, J. D. and Johansen, T. (2010). p62/SQSTM1 is a target gene for transcription factor NRF2 and creates a positive feedback loop by inducing antioxidant response element-driven gene transcription. *J. Biol. Chem.* **285**, 22576-22591. doi:10.1074/jbc.M110.118976

Jena, K. K., Kolapalli, S. P., Mehto, S., Chauhan, S. and Chauhan, S. (2018). TRIM16 controls turnover of protein aggregates by modulating NRF2, ubiquitin system, and autophagy: implication for tumorigenesis. *Mol. Cell. Oncol.* **5**, e1532251. doi:10.1080/23723556.2018.1532251

Jiao, J. and Demontis, F. (2017). Skeletal muscle autophagy and its role in sarcopenia and organismal aging. *Curr. Opin. Pharmacol.* **34**, 1-6. doi:10.1016/j.coph.2017.03.009

Johansen, T. and Lamark, T. (2011). Selective autophagy mediated by autophagic adapter proteins. *Autophagy* **7**, 279-296. doi:10.4161/auto.7.3.14487

Jongsma, M. L. M., Berlin, I., Wijdeven, R. H. M., Janssen, L., Janssen, G. M. C., Garstka, M. A., Janssen, H., Mensink, M., van Veelen, P. A., Spaapen, R. M. et al. (2016). An ER-associated pathway defines endosomal architecture for controlled cargo transport. *Cell* **166**, 152-166. doi:10.1016/j.cell.2016.05.078

Kimura, T., Jain, A., Choi, S. W., Mandell, M. A., Schroder, K., Johansen, T. and Deretic, V. (2015). TRIM-mediated precision autophagy targets cytoplasmic regulators of innate immunity. *J. Cell Biol.* **210**, 973-989. doi:10.1083/jcb.201503023

Kimura, T., Mandell, M. and Deretic, V. (2016). Precision autophagy directed by receptor regulators - emerging examples within the TRIM family. *J. Cell Sci.* **129**, 881-891. doi:10.1242/jcs.163758

Kimura, T., Jia, J., Kumar, S., Choi, S. W., Gu, Y., Mudd, M., Dupont, N., Jiang, S., Peters, R., Farzam, F. et al. (2017). Dedicated SNAREs and specialized TRIM cargo receptors mediate secretory autophagy. *EMBO J.* **36**, 42-60. doi:10.15252/embj.201695081

Kudryashova, E., Kudryashov, D., Kramerova, I. and Spencer, M. J. (2005). Trim32 is a ubiquitin ligase mutated in limb girdle muscular dystrophy type 2H that binds to skeletal muscle myosin and ubiquitinates actin. *J. Mol. Biol.* **354**, 413-424. doi:10.1016/j.jmb.2005.09.068

Kudryashova, E., Struyk, A., Mokhonova, E., Cannon, S. C. and Spencer, M. J. (2011). The common missense mutation D489N in TRIM32 causing limb girdle muscular dystrophy 2H leads to loss of the mutated protein in knock-in mice resulting in a Trim32-null phenotype. *Hum. Mol. Genet.* **20**, 3925-3932. doi:10.1093/hmg/ddr311

Kudryashova, E., Kramerova, I. and Spencer, M. J. (2012). Satellite cell senescence underlies myopathy in a mouse model of limb-girdle muscular dystrophy 2H. *J. Clin. Invest.* **122**, 1764-1776. doi:10.1172/JCI59581

Lamark, T., Perander, M., Outzen, H., Kristiansen, K., Øvervatn, A., Michaelsen, E., Bjørkøy, G. and Johansen, T. (2003). Interaction codes within the family of mammalian Phox and Bem1p domain-containing proteins. *J. Biol. Chem.* **278**, 34568-34581. doi:10.1074/jbc.M303221200

Larsen, K. B., Lamark, T., Øvervatn, A., Harneshaug, I., Johansen, T. and Bjørkøy, G. (2010). A reporter cell system to monitor autophagy based on p62/SQSTM1. *Autophagy* **6**, 784-793. doi:10.4161/auto.6.6.12510

Lazarou, M., Sliter, D. A., Kane, L. A., Sarraf, S. A., Wang, C., Burman, J. L., Sideris, D. P., Fogel, A. I. and Youle, R. J. (2015). The ubiquitin kinase PINK1 recruits autophagy receptors to induce mitophagy. *Nature* **524**, 309-314. doi:10.1038/nature14893

Lazzari, E. and Meroni, G. (2016). TRIM32 ubiquitin E3 ligase, one enzyme for several pathologies: From muscular dystrophy to tumours. *Int. J. Biochem. Cell Biol.* **79**, 469-477. doi:10.1016/j.biocel.2016.07.023

Lee, Y. J., Chou, T.-F., Pittman, S. K., Keith, A. L., Razani, B. and Weihl, C. C. (2017). Keap1/Cullin3 modulates p62/SQSTM1 activity via UBA domain ubiquitination. *Cell Rep.* **20**, 1994. doi:10.1016/j.celrep.2017.08.019

Lee, Y. J., Jonson, P. H., Sarparanta, J., Palmio, J., Sarkar, M., Vihola, A., Evilä, A., Suominen, T., Penttilä, S., Savarese, M. et al. (2018). TIA1 variant drives myodegeneration in multisystem proteinopathy with SQSTM1 mutations. *J. Clin. Invest.* **128**, 1164-1177. doi:10.1172/JCI97103

Lin, Q., Dai, Q., Meng, H., Sun, A., Wei, J., Peng, K., Childress, C., Chen, M., Shao, G. and Yang, W. (2017). The HECT E3 ubiquitin ligase NEDD4 interacts with and ubiquitylates SQSTM1 for inclusion body autophagy. *J. Cell Sci.* **130**, 3839-3850. doi:10.1242/jcs.207068

Liu, J., Zhang, C., Wang, X. L., Ly, P., Belyi, V., Xu-Monette, Z. Y., Young, K. H., Hu, W. and Feng, Z. (2014). E3 ubiquitin ligase TRIM32 negatively regulates tumor suppressor p53 to promote tumorigenesis. *Cell Death Differ.* **21**, 1792-1804. doi:10.1038/cdd.2014.121

Locke, M., Tinsley, C. L., Benson, M. A. and Blake, D. J. (2009). TRIM32 is an E3 ubiquitin ligase for dysbindin. *Hum. Mol. Genet.* **18**, 2344-2358. doi:10.1093/hmg/ddp167

Long, J., Garner, T. P., Pandya, M. J., Craven, C. J., Chen, P., Shaw, B., Williamson, M. P., Layfield, R. and Searle, M. S. (2010). Dimerisation of the UBA domain of p62 inhibits ubiquitin binding and regulates NF-kappaB signalling. *J. Mol. Biol.* **396**, 178-194. doi:10.1016/j.jmb.2009.11.032

Mandell, M. A., Kimura, T., Jain, A., Johansen, T. and Deretic, V. (2014). TRIM proteins regulate autophagy: TRIM5 is a selective autophagy receptor mediating HIV-1 restriction. *Autophagy* **10**, 2387-2388. doi:10.4161/15548627.2014.984278

Mandell, M. A., Jain, A., Kumar, S., Castleman, M. J., Anwar, T., Eskelinen, E.-L., Johansen, T., Prekeris, R. and Deretic, V. (2016). TRIM17 contributes to autophagy of midbodies while actively sparing other targets from degradation. *J. Cell Sci.* **129**, 3562-3573. doi:10.1242/jcs.190017

Marshall, R. S., Hua, Z., Mali, S., McLoughlin, F. and Vierstra, R. D. (2019). ATG8-binding UIM proteins define a new class of autophagy adaptors and receptors. *Cell* **177**, 766-781.e724. doi:10.1016/j.cell.2019.02.009

Mejlvang, J., Olsvik, H., Svenning, S., Bruun, J.-A., Abudu, Y. P., Larsen, K. B., Brech, A., Hansen, T. E., Brenne, H., Hansen, T. et al. (2018). Starvation induces rapid degradation of selective autophagy receptors by endosomal microautophagy. *J. Cell Biol.* **217**, 3640-3655. doi:10.1083/jcb.201711002

Mizushima, N. and Komatsu, M. (2011). Autophagy: renovation of cells and tissues. *Cell* **147**, 728-741. doi:10.1016/j.cell.2011.10.026

Morreale, F. E. and Walden, H. (2016). Types of ubiquitin ligases. *Cell* **165**, 248-248.e241. doi:10.1016/j.cell.2016.03.003

Nakatogawa, H., Suzuki, K., Kamada, Y. and Ohsumi, Y. (2009). Dynamics and diversity in autophagy mechanisms: lessons from yeast. *Nat. Rev. Mol. Cell Biol.* **10**, 458-467. doi:10.1038/nrm2708

Nicklas, S., Otto, A., Wu, X., Miller, P., Stelzer, S., Wen, Y., Kuang, S., Wrogemann, K., Patel, K., Ding, H. et al. (2012). TRIM32 regulates skeletal muscle stem cell differentiation and is necessary for normal adult muscle regeneration. *PLoS ONE* **7**, e30445. doi:10.1371/journal.pone.0030445

Pan, J.-A., Sun, Y., Jiang, Y.-P., Bott, A. J., Jaber, N., Dou, Z., Yang, B., Chen, J.-S., Catanzaro, J. M., Du, C. et al. (2016). TRIM21 ubiquitylates SQSTM1/p62 and suppresses protein sequestration to regulate redox homeostasis. *Mol. Cell* **62**, 149-151. doi:10.1016/j.molcel.2016.03.015

Pankiv, S., Clausen, T. H., Lamark, T., Brech, A., Bruun, J.-A., Outzen, H., Øvervatn, A., Bjørkøy, G. and Johansen, T. (2007). p62/SQSTM1 binds directly to Atg8/LC3 to facilitate degradation of ubiquitinated protein aggregates by autophagy. *J. Biol. Chem.* **282**, 24131-24145. doi:10.1074/jbc.M702824200

Peng, H., Yang, J., Li, G., You, Q., Han, W., Li, T., Gao, D., Xie, X., Lee, B.-H., Du, J. et al. (2017). Ubiquitylation of p62/sequestosome1 activates its autophagy receptor function and controls selective autophagy upon ubiquitin stress. *Cell Res.* **27**, 657-674. doi:10.1038/cr.2017.40

Pizon, V., Rybina, S., Gerbal, F., Delort, F., Vicart, P., Baldacci, G. and Karsenti, E. (2013). MURF2B, a novel LC3-binding protein, participates with MURF2A in the switch between autophagy and ubiquitin proteasome system during differentiation of C2C12 muscle cells. *PLoS ONE* **8**, e76140. doi:10.1371/journal.pone.0076140

Ra, E. A., Lee, T. A., Won Kim, S., Park, A., Choi, H. J., Jang, I., Kang, S., Hee Cheon, J., Cho, J. W., Eun Lee, J. et al. (2016). TRIM31 promotes Atg5/Atg7-independent autophagy in intestinal cells. *Nat. Commun.* **7**, 11726. doi:10.1038/ncomms11726

Ran, F. A., Hsu, P. D., Wright, J., Agarwala, V., Scott, D. A. and Zhang, F. (2013). Genome engineering using the CRISPR-Cas9 system. *Nat. Protoc.* **8**, 2281-2308. doi:10.1038/nprot.2013.143

Rodriguez-Muela, N., Parkhitko, A., Grass, T., Gibbs, R. M., Norabuena, E. M., Perrimon, N., Singh, R. and Rubin, L. L. (2018). Blocking p62-dependent SMN degradation ameliorates spinal muscular atrophy disease phenotypes. *J. Clin. Invest.* **128**, 3008-3023. doi:10.1172/JCI95231

Rogov, V., Dötsch, V., Johansen, T. and Kirkin, V. (2014). Interactions between autophagy receptors and ubiquitin-like proteins form the molecular basis for selective autophagy. *Mol. Cell* **53**, 167-178. doi:10.1016/j.molcel.2013.12.014

Servián-Morilla, E., Cabrera-Serrano, M., Rivas-Infante, E., Carvajal, A., Lamont, P. J., Pelayo-Negro, A. L., Ravenscroft, G., Junckerstorff, R., Dyke, J. M., Fletcher, S. et al. (2019). Altered myogenesis and premature senescence underlie human TRIM32-related myopathy. *Acta Neuropathol. Commun.* **7**, 30. doi:10.1186/s40478-019-0683-9

Slack, F. J. and Ruvkun, G. (1998). A novel repeat domain that is often associated with RING finger and B-box motifs. *Trends Biochem. Sci.* **23**, 474-475. doi:10.1016/S0968-0004(98)01299-7

Sparrer, K. M. J., Gableske, S., Zurenski, M. A., Parker, Z. M., Full, F., Baumgart, G. J., Kato, J., Pacheco-Rodriguez, G., Liang, C., Pornillos, O. et al. (2017). TRIM23 mediates virus-induced autophagy via activation of TBK1. *Nat. Microbiol.* **2**, 1543-1557. doi:10.1038/s41564-017-0017-2

Sun, D., Wu, R., Zheng, J., Li, P. and Yu, L. (2018). Polyubiquitin chain-induced p62 phase separation drives autophagic cargo segregation. *Cell Res.* **28**, 405-415. doi:10.1038/s41422-018-0017-7

Tocchini, C. and Ciosk, R. (2015). TRIM-NHL proteins in development and disease. *Semin. Cell Dev. Biol.* **47-48**, 52-59. doi:10.1016/j.semcdb.2015.10.017

Tomar, D., Singh, R., Singh, A. K., Pandya, C. D. and Singh, R. (2012). TRIM13 regulates ER stress induced autophagy and clonogenic ability of the cells. *Biochim. Biophys. Acta* **1823**, 316-326. doi:10.1016/j.bbamcr.2011.11.015

van Gent, M., Sparrer, K. M. J. and Gack, M. U. (2018). TRIM proteins and their roles in antiviral host defenses. *Annu. Rev. Virol.* **5**, 385-405. doi:10.1146/annurev-virology-092917-043323

Wang, C., Xu, J., Fu, H., Zhang, Y., Zhang, X., Yang, D., Zhu, Z., Wei, Z., Hu, Z., Yan, R. et al. (2018). TRIM32 promotes cell proliferation and invasion by activating beta-catenin signalling in gastric cancer. *J. Cell. Mol. Med.* **22**, 5020-5028. doi:10.1111/jcmm.13784

Yang, Q., Liu, T.-T., Lin, H., Zhang, M., Wei, J., Luo, W.-W., Hu, Y.-H., Zhong, B., Hu, M.-M. and Shu, H.-B. (2017). TRIM32-TAX1BP1-dependent selective autophagic degradation of TRIF negatively regulates TLR3/4-mediated innate immune responses. *PLoS Pathog.* **13**, e1006600. doi:10.1371/journal.ppat.1006600

Yin, H., Li, Z., Chen, J. and Hu, X. (2018). Expression and the potential functions of TRIM32 in lung cancer tumorigenesis. *J. Cell. Biochem.* **120**, 5232-5243. doi:10.1002/jcb.27798

Zaffagnini, G., Savova, A., Danieli, A., Romanov, J., Tremel, S., Ebner, M., Peterbauer, T., Sztacho, M., Trapannone, R., Tarafder, A. K. et al. (2018). Phasing out the bad-How SQSTM1/p62 sequesters ubiquitinated proteins for degradation by autophagy. *Autophagy* **14**, 1280-1282. doi:10.1080/15548627.2018.1462079

Zhao, T.-T., Jin, F., Li, J.-G., Xu, Y.-Y., Dong, H.-T., Liu, Q., Xing, P., Zhu, G.-L., Xu, H., Yin, S.-C. et al. (2018). TRIM32 promotes proliferation and confers chemoresistance to breast cancer cells through activation of the NF-kappaB pathway. *J. Cancer* **9**, 1349-1356. doi:10.7150/jca.22390

Paper III

TRIM32 – a putative regulator of NDP52 mediated selective autophagy

Juncal Garcia-Garcia[#], Zambarlal Bhujabal[#], Katrine Stange Overå, Eva Sjøttem*

Molecular Cancer Research Group, Department of Medical Biology, University of Tromsø – The Arctic University of Norway, 9037 Tromsø, Norway

*Corresponding author. Tel: +47 776 46425; E-mail: eva.sjottem@uit.no

#The authors contributed equally

Running title: TRIM32 regulates NDP52 activity?

Keywords: TRIM32, NDP52, Mitophagy, ULK1, Ubiquitylation

ABSTRACT

Several members of the tripartite motif (TRIM) family proteins are identified as regulators of autophagy. They associate with autophagy factors and serve as platforms for recruitment of activated ULK1 and BECLIN1, promoting phagophore formation and expansion. TRIM32 acts both as regulator and cargo of the autophagy receptor p62/SQSTM1, and is identified as an activator of ULK1 in atrophic muscle cells. Mutations in the C-terminal NHL domains of TRIM32 is linked to Limb-Girdle-Muscular-Dystrophy 2H, while a mutation in its BBox causes Bardet-Biedl-syndrome type 11. The autophagy receptor NDP52 is important for recruiting ULK1 and the autophagic machinery to damaged mitochondria. Here we show that TRIM32 is a potential cargo and a regulator of NDP52. TRIM32 mediates ubiquitylation of NDP52. Reintroduction of TRIM32 in TRIM32 KO cells leads to ULK1 stabilisation and increased TBK1 autophosphorylation. Conversely, the LGMD2H mutated version of TRIM32 does not affect NDP52 and ULK1 expression, or facilitate TBK1 autophosphorylation. Moreover, our data show that mitophagy is impaired in TRIM32 KO cells compared to normal cells and TRIM32 KO cells reconstituted with TRIM32. Collectively, this study identify TRIM32 as a potential regulator of NDP52, ULK1 and TBK1, facilitating selective degradation of mitochondria.

INTRODUCTION

Selective autophagy is a catabolic process that plays an important role in the maintenance of cellular homeostasis. It identifies and recycles unwanted or dysfunctional components, such as protein aggregates, damaged mitochondria, ferritin and intracellular pathogens (Rogov et al., 2014). In this way, selective autophagy protects from diseases such as cancer, neurodegeneration, and uncontrolled infections (Levine and Kroemer, 2019). Recent studies have revealed that selective autophagy is induced by cargo receptors that bind to their substrates and orchestrate the autophagy machinery to initiate phagophore assembly (Vargas et al., 2019, Turco et al., 2019, Agudo-Canalejo et al., 2020, Fujioka et al., 2020). The most extensive studied cargo receptors are the family of sequestosome-like-receptors (SLRs); sequestosome-1 (p62/SQSTM1), nuclear dot protein 52 kDa (NDP52); neighbor of BRCA1 gene 1 (NBR1); Optineurin and Tax1-binding protein 1 (Tax1BP1) (Johansen and Lamark, 2011, Rogov et al., 2014). The SLRs seem to have at least partly overlapping functions, in which they recognize ubiquitylated cargo via their ubiquitin binding domains, oligomerize and interacts directly with the autophagy machinery via FIP200 and the ATG8s (Khaminets et al., 2016, Turco et al., 2019).

One of the main cargo receptors of damaged mitochondria is NDP52, which is recruited to depolarized mitochondria by the ubiquitin ligase PINK1 (Lazarou et al., 2015). Tethering of NDP52 to the mitochondria leads to positioning of the autophagy initiation complex including FIP200 and ULK1 on the mitochondria (Vargas et al., 2019). The process is facilitated by TBK1, and leads to activation of ULK1 and induction of mitophagy. A similar scenario takes place upon cellular infection of cytosol-invading bacteria (Ravenhill et al., 2019). Here, NDP52 recognizes Galectin-8 on the damaged bacterial-containing vacuole. This leads to recruitment of ULK1 and TBK1 via the ULK1 complex subunit FIP200 and the TBK1 adaptor SINTBAD, which promotes phagophore formation and xenophagy

Several members of the tripartite motif (TRIM) protein family of E3 ligases function as autophagy receptors, acting in precision autophagy (Kimura et al., 2015). They recruit the autophagy initiation complexes ULK1 and PI3Kc1 to their substrates to facilitate autophagic degradation (Mandell et al., 2014). TRIM proteins are characterized by a RING-domain which constitutes the E3 ligase activity, one or two BBox domains, a coiled-coil domain and a variable C-terminal region (Reymond et al., 2001). The C-terminal domain of TRIM32 encompasses six NHL-repeats which are involved in dimerization and cargo recognition (Koliopoulos et al., 2016). Genetic mutations in the NHL domains cause the muscle disorder Limb Girdle Muscular

Dystrophy 2H (LGMD2H), and is associated with impaired auto-oligomerization and self-ubiquitylation, and reduced TRIM32 expression level (Zhao et al., 2019, Locke et al., 2009). A missense-mutation in the BBox domain results in the disease Bardet-Biedl syndrome 11 (BBS11) which has a pleiotropic phenotype (Chiang et al., 2006). A recent study demonstrates that TRIM32 activates ULK1 and thereby facilitates autophagy in muscle cells upon atrophy induction (Di Rienzo et al., 2019). TRIM32 was linked to ULK1 via the autophagy cofactor AMBRA1. Importantly, the LGMD2H disease mutant of TRIM32 was unable to associate with ULK1 and induce autophagy. In another study, we show that TRIM32 mediates ubiquitylation of p62/SQSTM1, leading to enhanced p62/SQSTM1 sequestration and degradation (Overa et al., 2019).

Here we show that TRIM32 downregulates the protein levels of all SLR proteins, without affecting their expression at the RNA level. Conversely, autophagic degradation of TRIM32 is dependent on the SLRs, and beside p62/SQSTM1 both NDP52 and NBR1 are able to direct TRIM32 to degradation in the lysosome. We reveal that TRIM32 interacts directly with and ubiquitylates NDP52. Furthermore, mitophagy induced by co-overexpression of FKBP8 and LC3A is significantly reduced in TRIM32 KO cells compared to normal HEK293 cells. Reintroduction of myc-TRIM32 into the KO cells restored the mitophagy activity. In line with this, TRIM32 enhances ULK1 stability and TBK1 autophosphorylation, both shown to facilitate NDP52 mediated mitophagy.

MATERIALS AND METHODS

Antibodies and reagents

The following primary antibodies were used: rabbit polyclonal antibody for TRIM32 (Proteintech, 10326-1-AP); rabbit polyclonal anti-GFP (Abcam, ab290); mouse monoclonal Myc-Tag (9B11) (Cell Signalling, #2276); rabbit polyclonal anti-LC3B (Sigma, L7543); rabbit polyclonal anti-Actin (Sigma, A2066); mouse monoclonal anti-p62 lck ligand (BD Biosciences, 610833); rabbit polyclonal anti-CALCOCO2/NDP52 (Sigma, HPA023195); rabbit polyclonal anti-TAX1BP1 (Sigma, HPA024432); mouse monoclonal mono- and polyubiquitinylated conjugates FK2 (Enzo, BML-PW8810); rabbit monoclonal anti-ULK1 (D8H5) (Cell Signalling, #8054); rabbit polyclonal anti-GABARAP (MBL, PM037); rabbit monoclonal anti-TBK1 (Millipore, 108A429); rabbit monoclonal anti-Phsopho-TBK1/NAK (Cell Signalling, #5483); mouse monoclonal anti-NBR1 (Santa Cruz, sc-130380). The following secondary

antibodies were used: Horseradish-peroxidase (HRP)-conjugated goat anti-rabbit IgG (BD Biosciences, 554021); HRP-conjugated goat anti-mouse Ig (BD Biosciences, 554002); HRP-conjugated anti-Biotin antibody (Cell Signalling, #7075); IRDye 800CW Goat anti-Rabbit IgG (Li-Cor, 925-32211); IRDye 680RD Goat anti-Mouse IgG (Li-Cor, 925-68070). The following fluorescent secondary antibodies were used: Alexa Fluor® 488-conjugated goat anti-mouse IgG (Life Technologies, A-11029); Alexa Fluor® 555-conjugated goat anti-rabbit IgG (Life Technologies, A-11008). The reagents used were Hanks Balanced salt solution (Sigma, H8264).

Plasmids

Plasmids used in this study are listed in Table 1.

Table 1: Plasmids used in this study

pDest Myc	(Lamark et al., 2003)
pDest Myc TRIM32	(Overå et al., 2019)
pDest Myc TRIM32 D487N	(Overå et al., 2019)
pDest Myc TRIM32 P130S	(Overå et al., 2019)
pDest Myc NDP52	(Abudu et al., 2019)
pDest mCherry-EYFP TRIM32	(Overå et al., 2019)
pDest EGFP-C1	(Lamark et al., 2003)
pDest EGFP TRIM32	(Overå et al., 2019)
pDest EGFP TRIM32 D487N	(Overå et al., 2019)
pDest EGFP TRIM32 P130S	(Overå et al., 2019)
pDest EGFP ULK1	(Alemu et al., 2012)
pDest Myc FKBP8	(Bhujabal et al., 2017)
mCherry-EGFP-OMP25-TM	(Wang et al., 2015)
pDest-3XFlag-LC3A	(Bhujabal et al., 2017)

Cell culture and transfections

HeLa (ATCC, CCL2), HEK293 (ATCC, CRL-1573), HEK293 FlpIn T-Rex (ThermoFisher, R714-07), HEK293 FlpIn TRIM32 KO (Overå et al., 2019); HEK293 FlpIn TRIM32 KO myc-TRIM32^{WT} (Overå et al., 2019) , HEK293 FlpIn TRIM32 KO myc-TRIM32^{P130S} (Overå et al., 2019), HEK293 FlpIn TRIM32 KO myc-TRIM32^{D487N} (Overå et al., 2019), HeLa Penta KO (Lazarou et al., 2015), HeLa Penta KO EGFP-NDP52 and HeLa Penta KO EGFP-NBR1 cells were cultured in Dulbecco's modified eagle's medium (DMEM) (Sigma, D6046) with 10% fetal bovine serum and 1% streptomycin-penicillin (Sigma, P4333). Sub-confluent cells were

transfected using TransIT-LT1 (Mirus, MIR2300) or Metafectene Pro (Biontex, T040) following the manufacturer's instructions.

Recombinant protein production and GST pulldown analysis

GST or GST-tagged proteins were expressed in *Escherichia coli* strain SoluBL21 (Genlantis, #C700200). Protein expression was induced by treating overnight bacterial culture with 50µg/ml Isopropyl β-D-1-thiogalactopyranoside (IPTG). GST or GST fusion proteins were purified and immobilized on Glutathione-Sepharose 4 Fast Flow beads (GE Healtcare, 17-5132-01). Myc-tagged proteins were *in vitro* translated using the TNT T7 reticulocyte Lysate system (Promega, #14610) in the presence of ^{35}S-methionine. *In vitro* translated protein or total cell lysate was pre-incubated with 10µl glutathione sepharose beads and 100µl of NETN buffer (50mM Tris pH 8.0; 150mM NaCl; 1 mM EDTA; 0.5% Nonidet P-40) with cOmplete Mini EDTA-free protease inhibitor mixture tablets (1 tablet/10ml) (Roche Applied Science, 11836170001) for 1hr at 4°C to reduce unspecific binding. Pre-incubated lysate was then incubated with the immobilized GST fusion protein for 2hrs at 4°C. Beads were washed five times with NETN buffer, boiled with 2xSDS gel loading buffer (125mM Tris pH 7.5; 4% SDS; 0.04% bromphenol blue; 8% sucrose; 100mM dithiolthreitol) and subjected to SDS-PAGE. Gels were stained with Coomassie Brilliant Blue R-250 Dye (Thermofisher scientific, #20278) to visualize GST fusion proteins and then vacuum-dried. Signals from ^{35}S-labelled proteins were detected by a Fujifilm bioimaging analyzer BAS-5000 (Fujifilm).

Western Blotting

Cells were seeded in 6 well dishes and treated as indicated. Cells were lysed in 1xSDS buffer (50mM Tris pH 7.4; 2% SDS; 10% Glycerol) supplemented with 200mM dithiothreitol (DTT, Sigma, #D0632) and heated at 100°C for 10 minutes. Protein concentration was measured using the Pierce BCA Protein Assay Kit (Thermofisher Scientific, #23227). Equal amounts of protein were resolved by SDS-PAGE and transferred to nitrocellulose membrane (Sigma, GE10600003). The membrane was stained with Ponceau S (Sigma, P3504), blocked with 5% non-fat dry milk in 1% TBS-T (0.2M Tris pH 8; 1.5M NaCl and 0.05% Tween20 (Sigma, P9416)) and then incubated with indicated primary antibodies for 24h. The membrane was washed three times for 10 minutes each with TBS-T followed by incubation with secondary antibody for 1h. The membrane was washed three times for 10 minutes and analyzed by enhanced chemiluminescence using the ImageQuant LAS 4000 (GE Lifescience).

Ubiquitylation Assay

Subconfluent HEK293 FlpIn TRIM32 KO cells seeded in 6-well dishes were transiently co-transfected with pDEST myc-NDP52 (500 ng) and pDEST EGFP-TRIM32^{WT} (500 ng), pDEST EGFP-TRIM32^{P130S}(500 ng), or pDEST EGFP-TRIM32^{D487N}(500 ng) using Metafecten Pro (Biontex, T040). Subconfluent TRIM32 KO cells and reconstituted TRIM32 KO with Myc-TRIM32 WT, Myc-TRIM32 P130S or Myc-TRIM32 D487N cells were transfected with pDEST EGFP-ULK1 (500 ng) using Metafectene Pro. One day post transfection, the cells were lysed in modified Radioimmunoprecipitation assay (RIPA) buffer (50mM Tris pH 7.5; 150mM NaCl; 1mM EDTA; 1% NP40; 0.25% Triton-X-100) supplemented with cOmplete Mini EDTA-free protease inhibitor cocktail tablets (Roche, #11836170001) and phosphatase inhibitor cocktail (Merck Millipore, #524625) by shaking at 4°C for 30 min. The cell lysate was centrifuged at 10.000 x g for 10 min. The resulting supernatant was incubated with Myc-TRAP (Chromotek, yta-20) or GFP-TRAP (Chromotek, gta-20). They were washed five times in RIPA buffer before boiling in 2X SDS gel loading buffer. This was followed by protein identification by immunoblotting as previously described but on Immobilon-FL PVDF membrane (Millipore, IPFL00010), blocked with Odyssey® blocking buffer (PBS) (LI-COR Biosciences, #927-40000) and scanned on Odyssey CLx Imager (LI-COR).

Immunostaining and Fluorescence confocal microscopy

Subconfluent cells were grown on coverslips (VWR, #631-0150) coated with Fibronectin (Sigma, F1141) and treated as indicated. They were fixed in 4% formaldehyde for 20min at R.T., permeabilized with methanol at RT for 5min, blocked in 5% goat serum/PBS or 5%BSA/PBS and incubated at room temperature with a specific primary antibody followed by Alexa Fluor 488 or 555 conjugated secondary antibody and DAPI. Confocal images were obtained using a 63x/NA1.4 oil immersion objective on an LSM780 system or LSM800 system and the ZEN software (Zeiss). Quantification of cells containing red only dots in the mCherry-EYFP-double tag assay was done manually in three independent experiments.

RT-PCR/QPCR

Total RNA was extracted from HEK 293T FlpIn cells TRIM32 KO cells reconstituted with TRIM32 WT, TRIM32 P130S mutant and TRIM32 D487N mutant using the Gene Elute Mammalian Total RNA Miniprep kit (Sigma). The RNA quality was checked by 260/280 nm absorption using a NanoDrop 2000 spectrophotometer (Thermo Fisher scientific). First-strand cDNA was prepared using the High Capacity RNA-to-cDNA Kit according to the

manufacturer's instruction. Amplification was performed with SYBR green kit FastStart Essential DNA Green Master (Roche) in a 20 µl reaction. Reactions were run with the following cycling parameters temperatures (58 degrees aneling temperature for Actin, GAPDH, NDP52 and Optineurin and 60 for p62 and NBR1) and 45 cycles by Lightcycler 96 (Roche). All reactions were performed in triplicate. Relative expression levels were calculated after correction for the expression of Actin and GAPDH as an endogenous reference. The primer sequences used for p62 fw and reverse were 5'-ggagaagagcagctcacagcca-3' and 5'-ccttcagccctgtgggtccct-3', NBR1 forward and reverse 5'-ggaagcagaagaagacctgagtg-3' and 5'-ccagagtctgtgaggtcgtgag-3', and NDP52 fw and reverse 5'-accatggaggagaccatcaa-3' and 5'-ttctggacggaattggaaag-3', and standards (Actin and GAPDH) fw and reverse Actin 5'-tgacggtcaggtcatcactatcggcaatga-3' and 5'-ttgatcttcatggtgataggagcgagggca-3', gapdh 5'-ggcactgtcaaggctgaaaacg-3' and 5'-ggagatgagatgataccacgcttag-3'.

Mitophagy assay

HEK293 FlpIn T-Rex cells, TRIM32 KO cells and TRIM32 KO cells reconstituted with Myc-TRIM32 were seeded on fibronectin-coated coverslips two days before transient co-transfection with the plasmids mCherry-EGFP-OMP25-TM (100 ng), pDEST-3xFlag-LC3A (100 ng) and pDEST-myc-FKBP8 (100 ng) using the Trans-IT (Mirus) transfection reagent. One day post transfection, the cells were fixated in 4% Formaldehyde, 15 minutes at R.T., stained with DAPI (5 min). The cells were imaged using a Zeiss800 confocal microscope, and z-stack images of at least 100 cells per condition per experiment were manually quantitated for RedOnly stuctures using the ZEN software (Zeiss).

Statistics

All experiments were repeated at least three times, unless otherwise specified. Error bars represent the standard deviation, or standard error of the mean as indicated in the Figure legends. Two-sided unpaired, homoscedastic Student T-Tests, were performed to assess significant differences between populations. Replicates were not pooled for statistical analyses.

RESULTS AND DISCUSSION

Recently we showed that TRIM32 is an autophagy substrate (Overa et al., 2019). Its lysosomal degradation was mediated by selective autophagy, dependent on ATG7 and the sequestosome-like receptors (SLRs). Reintroduction of p62/SQSTM1 in a cell line lacking the SLRs was

sufficient to direct autophagic degradation of TRIM32. However, knock out of p62/SQSTM1 did not abolish lysosomal degradation of TRIM32, suggesting that other SLRs may direct TRIM32 to autophagic degradation. Furthermore, we identified TRIM32 as an activator of p62/SQSTM1, facilitation p62/SQSTM1 sequestration and degradation. Here we set out to identify the effect of TRIM32 expression on the protein levels of other SLRs than p62/SQSTM1. Cell extracts from two different TRIM32 knock-out clones, KO#1 and KO#2 (Overa et al., 2019), reconstituted with myc-TRIM32 wild type or the disease mutants TRIM32^{D487N} and TRIM32^{P130S}, were exposed to antibodies against the SLRs p62/SQSTM1, NBR1, NDP52 and TAX1BP1 (Fig. 1A). Consistently, reintroduction of myc-TRIM32^{WT} or myc-TRIM32^{P130S} reduced the protein levels of the SLRs, suggesting that TRIM32 enhances SLR mediated selective autophagy (Fig. 1A, B). In contrast, reintroduction of the LGMD2H disease mutant form of TRIM32, TRIM32^{D487N}, did not affect the protein levels of the SLRs. As shown previously (Frosk et al., 2002, Overa et al., 2019), TRIM32^{WT} and TRIM32^{P130S} contain ubiquitylation activity and are themselves degraded by autophagy. TRIM32^{D487N} is not found to ubiquitylate itself or any target proteins, suggesting that mutations in the NHL-repeat region abolish its enzymatic activity and its ability to be degraded by autophagy. Western blot analyses of LC3B and Gabarap in the same cell extracts did not display a reproducible change of their protein level or lipidation (Fig. 1A). Moreover, exposure of the TRIM32 KO and the TRIM32 KO myc-TRIM32^{WT} cell lines to starvation conditions, followed by additions of the lysosome and proteasome inhibitors Bafilomycin A1 and MG132, respectively, showed that the autophagy flux is not severe inhibited in the TRIM32 KO cells (Fig. S1). This is in line with previous data showing that TRIM32 does not display any prominent effect on global autophagy, but instead on SLR mediated selective autophagy (Overa et al., 2019). In order to investigate whether the TRIM32 induced reduction of SLR expression was due to reduced transcription of the SLR genes, we analysed RNA expression by QPCR of representative SLRs in the same cell lines (Fig. 1C). Comparing SLR RNA levels in the reconstituted cell lines with the SLR RNA levels in the TRIM32 KO#1 cell line revealed no significant change in RNA expression. Together, our results show that expression of catalytic active TRIM32 reduces the protein levels of the SLRs. For p62/SQSTM1 we have shown that this is due to TRIM32 mediated ubiquitylation of p62/SQSTM1 leading to enhanced p62/SQSTM1 autophagic activity. An interesting question to address is whether this is a general mechanism for all SLRs, pointing towards an important regulatory role of TRIM32 in selective autophagy.

We have previously shown that autophagic degradation of TRIM32 is strongly inhibited in a HeLa pentaKO cell line (Lazarou et al., 2015) lacking expression of the five SLRs (Overa et al., 2019). To identify if any of the SLRs beside p62/SQSTM1 were able to direct autophagic degradation of TRIM32, we established pentaKO cell lines stably expressing each of the SLRs. Transfection of mCherry-EYFP-tagged TRIM32 into these cell lines revealed that reintroduction of NDP52 or NBR1 facilitated autophagic degradation of TRIM32 (Fig. 2). This suggests that each of the SLRs mediates autophagic degradation of TRIM32, and that they are independent of each other for facilitating this process.

The very consistent downregulation of NDP52 protein levels in the TRIM32 KO cells reconstituted with catalytic active TRIM32 (Fig. 1A), prompted us to investigate whether there is a direct interaction between TRIM32 and NDP52. GST-pulldown assays using immobilised GST-NDP52 or GST-p62/SQSTM1 expressed and purified from *E. coli* together with *in vitro* translated EGFP-TRIM32^{WT} or the disease mutants EGFP-TRIM32^{P130S} and EGFP-TRIM32^{D487N}, showed that there is a direct interaction between NDP52 and TRIM32 *in vitro* (Fig. 3A). The interaction is weak, but stronger than the previously reported interaction between TRIM32 and p62/SQSTM1 (Overa et al., 2019). Both TRIM32^{WT} and the two disease mutants bound to NDP52, suggesting that the *in vitro* interaction is independent on the E3 ligase activity of TRIM32. Next, we applied immunofluorescence assays to determine if TRIM32 colocalizes with endogenous NDP52 in cells. TRIM32 KO cells, and TRIM32 KO cells reconstituted with myc-TRIM32^{WT} or the disease mutants myc-TRIM32^{P130S} and myc-TRIM32^{D487N}, were grown in normal medium or normal medium supplemented with Bafilomycin A1, fixated and exposed to an NDP52 antibody (Fig. 3B). TRIM32^{WT} and both disease mutants colocalised with NDP52 in certain dots under normal conditions (Fig. 3B). Inhibition of the lysosome resulted in accumulation of larger NDP52 dots that colocalised with TRIM32^{WT} and TRIM32P^{130S}. However, the LGMD2H disease mutant TRIM32^{D487N}, which displays augmented E3 ligase activity and is not a substrate for autophagic degradation, did not accumulate in larger NDP52 dots upon BafA1 treatment. These results indicate that TRIM32, both WT and disease mutants, are enriched in certain NDP52 dots in cells under normal conditions. However, accumulation of TRIM32^{WT} and TRIM32^{P130S} but not TRIM32^{D487N} in NDP52 dots upon lysosomal inhibition, suggest that NDP52 mediated lysosomal degradation of TRIM32 is dependent on the E3 ligase activity of TRIM32. We therefore went on to test if NDP52 is a TRIM32 substrate. Immunoprecipitation of myc-NDP52 co-expressed with EGFP-TRIM32 WT and disease mutants in TRIM32 KO cells, revealed several slow-migrating myc-NDP52 forms in the cells

expressing TRIM32^{WT} or TRIM32^{P130S}. In the precipitate from the TRIM32^{D487N} expressing cells, no such slow migrating NDP52 forms was observed (Fig. 3C). To identify if these slow-migrating NDP52 could represent mono and poly-ubiquitylation NDP52, the immonoprecipitates were blotted against an antibody recognising mono- and poly-ubiquitin (Fig. 3C, lower panels). Clearly, NDP52 immunoprecipitated from cells expressing the E3 ligase active forms of TRIM32, TRIM32^{WT} and TRIM32^{P130S}, is modified by ubiquitin. On the other hand, NDP52 precipitated from the cells expressing the E3 ligase inhibited form of TRIM32, TRIM32^{D487N}, is not recognised by the ubiquitin antibody. The upper panel in Figure 3C show that TRIM32^{WT} and TRIM32^{P130S} co-precipitate very well NDP52, while the association between TRIM32^{D487N} and NDP52 is weaker. Together, these data show that NDP52 interacts with TRIM32 *in vitro* and in cells, and that they colocalise in certain dots in cells. Furthermore, TRIM32 mediates ubiquitylation of NDP52, and this ubiquitylation seems to be important for regulation of NDP52 protein levels.

Recent reports have demonstrated that NDP52 plays an important role in selective degradation of depolarized mitochondria (mitophagy) (Lazarou et al., 2015, Vargas et al., 2019, Heo et al., 2015). Tethering of NDP52 to the mitochondria recruited the ULK1 complex via FIP200 interactions, and the authors suggested that this recruitment initiated autophagosome biogenesis directly on the mitochondria (Vargas et al., 2019). TRIM proteins are reported to control autophagy by modulating the activity of BECLIN1 and ULK1 (Mandell et al., 2014). Moreover, in atrophic muscle cells TRIM32 mediates induction of autophagy via ULK1 activation. This activation of ULK1 requires TRIM32 E3 ligase activity, and is impaired in atrophic muscle cells expressing the LGMD2H disease mutant TRIM32^{D487N} (Di Rienzo et al., 2019). These reports prompted us to investigate whether ULK1 and TBK1 were aberrantly expressed in the HEK293 FlpIn TRIM32 KO and reconstituted cell lines. Western Blot analyses of ULK1 expression levels in the TRIM32 KO cells, and TRIM32 KO cells reconstituted with myc-TRIM32^{WT}, myc-TRIM32^{P130S} or myc-TRIM32^{D487N}, revealed that ULK1 is strongly stabilised in the cells expressing myc-TRIM32^{WT} and myc-TRIM32^{P130S} (Fig. 4 A, B). In contrast, reintroduction of the LGMD2H disease mutant TRIM32^{D487N}, did not affect ULK1 protein levels (Fig. 4 A, B). K63-linked ubiquitylation of ULK1 stimulates its kinase activity (Nazio et al., 2013). To assess if TRIM32 mediated stabilization of ULK1 is due to ubiquitylation of ULK1, ULK1 was immunoprecipitated from HEK293 cells co-expressing TRIM32 and EGFP-ULK1. However, no increased ubiquitylation of ULK1 could be detected (Fig. 4C). This is in line with the work of Di Rienzo et al. (Di Rienzo et al., 2019), where they

found that ULK1 is not a direct substrate of TRIM32 in their system. Instead, they showed that ULK1 associated with unanchored K63-linked polyubiquitin chains synthesized by TRIM32 in an AMBRA1 dependent manner, and this binding to polyubiquitin chains stimulated ULK1 activity, monitored as increased phosphorylation of VPS34(S249) and BECLIN1 (S15). TBK1 facilitates the association of NDP52 with the ULK1 complex on mitochondria leading to mitophagy, while a kinase-dead TBK1 does not (Vargas et al., 2019). Recruiting TBK1 to the mitochondria induced TBK1 S172 autophosphorylation. Furthermore, selective autophagy of cytosol-invading bacteria involves NDP52 meditated recruitment of the TBK1-SINTBAD and ULK1-FIP200 complexes to the bacteria containing vacuole, promoting phagophore formation (Ravenhill et al., 2019). Assessing the TBK1 S172 phosphorylation in the TRIM32 KO and reconstituted cell lines, revealed that the amount of S172 phosphorylated TBK1 is highly upregulated in the cells reconstituted with TRIM32 compared to the TRIM32 KO cells (Fig. 4 D, E). Since TBK1 undergoes autophosphorylation at S172 when TBK1 is enriched at subcellular structures, this suggests that TRIM32 facilitates TBK1 recruitment and activation which is important for efficient mitophagy and xenophagy.

Next question was if TRIM32 could facilitate mitophagy. For this purpose, we induced mitophagy in HEK293 FlpIn cells, and the TRIM32 KO and reconstituted cell line. Mitophagy induction was obtained by overexpression of FKBP8 and LC3A, and autophagic degradation of mitochondria measured using the double-tag mCherry-EGFP-OMP25TM (Bhujabal et al., 2017) (Fig. 4F). In the HEK293 FlpIn cells, co-overexpression of FKBP8 and LC3A induced mitophagy in 10-12% of the cells (Fig. 4G). However, in the HEK293 FlpIn TRIM32 KO cells, the amount of cells undergoing mitophagy by FKBP8 and LC3A overexpression was reduced to 5%. Importantly, reintroduction of myc-TRIM32 in the TRIM32 KO cells restored the mitophagy activity (Fig. 4G).

To sum up, here we show that TRIM32 affect the protein expression levels of the SLRs. Focusing on autophagy receptor NDP52, we reveal that TRIM32 interacts with NDP52 and subjects it for ubiquitylation. NDP52 is an important receptor for mitophagy, and in congruence with this we find that mitophagy is downregulated in TRIM32 KO cells compared to normal HEK293 FlpIn cells and TRIM32 KO cells reconstituted with myc-TRIM32. Furthermore, ULK1 is stabilised and TBK1 autophosphorylation upregulated in cells expressing active TRIM32, but not in cells expressing the LGMD2H disease version of TRIM32 shown to have impaired E3 ligase activity (Fig. 4H). An important question to address in future study is

whether the TRIM32 mediated ubiquitylation of NDP52 directly facilitates its role as a mitophagy and xenophagy receptor.

FIGURE LEGENDS

Figure 1: E3 ligase active TRIM32 downregulates the protein levels of the sequestosome-like cargo receptors. A) Western blots showing the protein levels of the autophagy cargo receptors p62/SQSTM1, NBR1, NDP52 and TAX1BP1, and the autophagy marker proteins LC3B and GABARAP, in TRIM32 KO cells, and TRIM32 KO cells reconstituted with stable expression of myc-TRIM32^{WT}, myc-TRIM32^{P130S}, and myc-TRIM32^{D487N}. Actin serves as loading control, and the blot against TRIM32 shows the expression levels of the various TRIM32 proteins in the reconstituted cells. A biotinylated molecular weight marker is shown to the left. **B)** Quantitation of the band intensities from three independent experiments as represented in A. The bar graphs represent the average band intensities normalized to the corresponding actin band from three independent experiments with s.e.m. The band intensities were quantitated by the use of ImageJ. *: $p<0.05$; ***: $p<0.0005$; *n.s.*: $p>0.05$; **C)** RNA levels of the SLRs p62/SQSTM1, NBR1 and NDP52 in the reconstituted TRIM32^{WT}, TRIM32^{P130S} and TRIM32^{D487N} expressing cell lines relative to the RNA levels in the TRIM32 KO cell line. The graphs represent the average relative RNA levels with s.e.m. obtained by QPCR in three independent experiments, each performed in triplicate.

Figure 2: The cargco receptors NDP52 and NBR1 direct TRIM32 to autophagic degradation. A) Normal HeLa cells and cells that were genetically knocked out for the 5 SLRs (pentaKO), or pentaKO cells reconstituted with stable expression of EGFP-NDP52 or EGFP-NBR1 as indicated to the right, were transfected with mCherry-EYFP-TRIM32 expression plasmids. One day post transfection the cells were fixated, stained with DAPI and imaged using a Zeiss780 confocal microscope. Scale bar (10 μm). **B)** Quantitation of the number of yellow dots and red-only dots in the cells transfected as described in A. The graphs display the average number of yellow and RedOnly dots with S.D. in cells with mCherry-EYFP-TRIM32 dots, obtained in three independent experiments.

Figure 3: TRIM32 associates with and ubiquitylates NDP52. A) GST-pulldown assays using ^{35}S-labeled Myc-TRIM32, Myc-TRIM32^{P130S}, or Myc-TRIM32^{D487N} and recombinant GST, GST-p62 and GST-NDP52 immobilized on Glutathione Sepharose beads. Quantifications of the binding of wild type and mutant constructs to the GST proteins are presented as percentage binding relative to the 5% input. The bars represent the average band intensities with s.d. quantitated using ImageJ, of three independent experiments. **B)** Representative images of HEK293 FlpIn TRIM32 KO cells, and the TRIM32 KO cells reconstituted with myc-TRIM32^{WT}, myc-TRIM32^{P130S} or myc-TRIM32^{D487N} cells in full media (FM) or full media added the lysosomal inhibitor Bafilomycin A1 (BafA1) (4 hrs) fixed and stained with antibodies for NDP52. Images were obtained using a ZEISS780 confocal laser scanning microscope, and monitored using the ZEN software**.** Scale bar (10 μm). **C)** Myc-NDP52 expression plasmid was cotransfected with EGFP-TRIM32, EGFP-TRIM32^{P130S} or EGFP-TRIM32^{D487N} expression constructs in the HEK293 FlpIn TRIM32 KO cell line. Myc-NDP52 was immunoprecipitated using a myc-trap and precipitated NDP52 detected using an anti-myc antibody. The EGFP-TRIM proteins were detected using an anti-GFP antibody, and ubiquitin by using an FK2 antibody recognizing both mono-and poly-ubiquitin chains. * indicates ubiquitylated NDP52.

Figure 4: TRIM32 stabilizes ULK1 and facilitates TBK1 phosphorylation and mitophagy. A) Western blots showing the protein levels of ULK1 in HEK293 FlpIn TRIM32 KO cells, and HEK293 FlpIn TRIM32 KO cells reconstituted with stable expression of myc-TRIM32^{WT}, myc-TRIM32^{P130S}, and myc-TRIM32^{D487N}. Actin serves as loading control, and the blot against TRIM32 shows the expression levels of the various TRIM32 proteins in the reconstituted cells. A biotinylated molecular weight marker is shown to the left. **B)** Quantitation of the band intensities from three independent Western blots as represented in C. The bar graphs represent the average band intensities normalized to the corresponding actin band from three independent experiments with s.e.m. The band intensities were quantitated by the use of ImageJ. **: $p<0.005$; *: $p<0.05$; *n.s.:* $p>0.05$. **C)** EGFP-ULK1 expression plasmid was transfected into TRIM32KO cell lines reconstituted with myc-TRIM32, myc-TRIM32^{P130S} or myc-TRIM32^{D487N}. EGFP-ULK1 was immunoprecipitated using a GFP-trap and precipitated EGFP-ULK1 detected using an anti-GFP antibody. The myc-TRIM proteins were detected using an anti-myc antibody, and ubiquitin by using an FK2 antibody recognizing both mono-and poly-ubiquitin chains. **D)** Western blots showing the protein levels of phosphorylated TBK1 and

TBK1 as indicated to the right, in TRIM32 KO cells, and TRIM32 KO cells reconstituted with stable expression of myc-TRIM32^{WT}, myc-TRIM32^{P130S}, and myc-TRIM32^{D487N}. The extracts are from cells exposed to normal medium and cells starved in HBSS for two hours, as indicated above. Tubulin serves as loading control. **E)** Quantitation of the band intensities from three independent Western blots as represented in D. The bar graphs represent the average band intensities normalized to the corresponding tubulin band from three independent experiments with s.e.m. The band intensities were quantitated by the use of ImageJ. *: $p<0.05$; *n.s.:* $p>0.05$. **F)** HEK293 FlpIn cells, HEK293 TRIM32 KO cells, or HEK293 TRIM32 KO cells reconstituted with myc-TRIM32 were transiently transfected with expression plasmids for the mitochondria marker mCherry-EGFP-OMP25TM, 3xFlag LC3A and mitophagy receptor myc-FKBP8. The appearance of RedOnly structures indicates acidified mitochondria. **G)** Quantitation of the cells represented in A displaying RedOnly dots indicative of mitophagy activity. The bars represent the average with s.e.m. of three independent experiments, each including > 100 cells per condition. *: $p<0.05$; *n.s.:* $p>0.05$. **H)** TRIM32 induces ubiquitylation of NDP52, enhances TBK1 phosphorylation and ULK1 expression that are important for phagophore formation on the mitochondria, and facilitates mitophagy.

Supplementary Figure S1: Loss of TRIM32 does not impair autophagic degradation of the SLRs. A) Western blots showing the protein levels of the autophagy cargo receptors NBR1, TAX1BP1, p62/SQSTM1 and NDP52, and the autophagy marker protein LC3B, in TRIM32 KO cells, and TRIM32 KO cells reconstituted with stable expression of myc-TRIM32^{WT}. The cells were exposed to full medium (FM) or starvation medium (SM, HBSS 2 hrs), and treated with lysosomal inhibitor (Baf, 4 hrs) or proteasomal inhibitor (MG, 4 hrs) where indicated above. Actin serves as loading control, and the blot against TRIM32 shows the expression levels of the TRIM32 in the reconstituted cells. A biotinylated molecular weight marker is shown to the left. * indicate an unspecific band recognized by the TRIM32 antibody.

ACKNOWLEDGEMENT

We thank Richard Youle, National Institutes of Health, Bethesda, MD 20892, USA, for the generous gift of the pentaKO cell line, and Yakubu P. Abudu, UiT – The Arctic University of Norway, for the gift of the EGFP-NDP52 and EGFP-NBR1 reconstituted pentaKO cell lines. Thanks to the Advanced Microscopy Core Facility at UiT – The Arctic University of Norway,

for the use of instrumentation. This work was supported by PhD grants to K.S.O and J.G.G from UiT – The Arctic University of Norway.

REFERENCES

ABUDU, Y. P., PANKIV, S., MATHAI, B. J., LAMARK, T., JOHANSEN, T. & SIMONSEN, A. 2019. NIPSNAP1 and NIPSNAP2 act as "eat me" signals to allow sustained recruitment of autophagy receptors during mitophagy. *Autophagy,* 15**,** 1845-1847.

AGUDO-CANALEJO, J., SCHULTZ, S. W., CHINO, H., MIGLIANO, S. M., SAITO, C., KOYAMA-HONDA, I., STENMARK, H., BRECH, A., MAY, A. I., MIZUSHIMA, N. & KNORR, R. L. 2020. Wetting regulates autophagy of phase-separated compartments and the cytosol. *Nature*.

ALEMU, E. A., LAMARK, T., TORGERSEN, K. M., BIRGISDOTTIR, A. B., LARSEN, K. B., JAIN, A., OLSVIK, H., OVERVATN, A., KIRKIN, V. & JOHANSEN, T. 2012. ATG8 family proteins act as scaffolds for assembly of the ULK complex: sequence requirements for LC3-interacting region (LIR) motifs. *J Biol Chem,* 287**,** 39275-90.

BHUJABAL, Z., BIRGISDOTTIR, A. B., SJOTTEM, E., BRENNE, H. B., OVERVATN, A., HABISOV, S., KIRKIN, V., LAMARK, T. & JOHANSEN, T. 2017. FKBP8 recruits LC3A to mediate Parkin-independent mitophagy. *EMBO Rep,* 18**,** 947-961.

CHIANG, A. P., BECK, J. S., YEN, H. J., TAYEH, M. K., SCHEETZ, T. E., SWIDERSKI, R. E., NISHIMURA, D. Y., BRAUN, T. A., KIM, K. Y., HUANG, J., ELBEDOUR, K., CARMI, R., SLUSARSKI, D. C., CASAVANT, T. L., STONE, E. M. & SHEFFIELD, V. C. 2006. Homozygosity mapping with SNP arrays identifies TRIM32, an E3 ubiquitin ligase, as a Bardet-Biedl syndrome gene (BBS11). *Proc Natl Acad Sci U S A,* 103**,** 6287-92.

DI RIENZO, M., ANTONIOLI, M., FUSCO, C., LIU, Y., MARI, M., ORHON, I., REFOLO, G., GERMANI, F., CORAZZARI, M., ROMAGNOLI, A., CICCOSANTI, F., MANDRIANI, B., PELLICO, M. T., DE LA TORRE, R., DING, H., DENTICE, M., NERI, M., FERLINI, A., REGGIORI, F., KULESZ-MARTIN, M., PIACENTINI, M., MERLA, G. & FIMIA, G. M. 2019. Autophagy induction in atrophic muscle cells requires ULK1 activation by TRIM32 through unanchored K63-linked polyubiquitin chains. *Sci Adv,* 5**,** eaau8857.

FROSK, P., WEILER, T., NYLEN, E., SUDHA, T., GREENBERG, C. R., MORGAN, K., FUJIWARA, T. M. & WROGEMANN, K. 2002. Limb-girdle muscular dystrophy type 2H associated with mutation in TRIM32, a putative E3-ubiquitin-ligase gene. *Am J Hum Genet,* 70**,** 663-72.

FUJIOKA, Y., ALAM, J. M., NOSHIRO, D., MOURI, K., ANDO, T., OKADA, Y., MAY, A. I., KNORR, R. L., SUZUKI, K., OHSUMI, Y. & NODA, N. N. 2020. Phase separation organizes the site of autophagosome formation. *Nature,* 578**,** 301-305.

HEO, J. M., ORDUREAU, A., PAULO, J. A., RINEHART, J. & HARPER, J. W. 2015. The PINK1-PARKIN Mitochondrial Ubiquitylation Pathway Drives a Program of OPTN/NDP52 Recruitment and TBK1 Activation to Promote Mitophagy. *Mol Cell,* 60**,** 7-20.

JOHANSEN, T. & LAMARK, T. 2011. Selective autophagy mediated by autophagic adapter proteins. *Autophagy,* 7**,** 279-96.

KHAMINETS, A., BEHL, C. & DIKIC, I. 2016. Ubiquitin-Dependent And Independent Signals In Selective Autophagy. *Trends Cell Biol,* 26**,** 6-16.

KIMURA, T., JAIN, A., CHOI, S. W., MANDELL, M. A., SCHRODER, K., JOHANSEN, T. & DERETIC, V. 2015. TRIM-mediated precision autophagy targets cytoplasmic regulators of innate immunity. *J Cell Biol,* 210**,** 973-89.

KOLIOPOULOS, M. G., ESPOSITO, D., CHRISTODOULOU, E., TAYLOR, I. A. & RITTINGER, K. 2016. Functional role of TRIM E3 ligase oligomerization and regulation of catalytic activity. *EMBO J,* 35**,** 1204-18.

LAMARK, T., PERANDER, M., OUTZEN, H., KRISTIANSEN, K., OVERVATN, A., MICHAELSEN, E., BJORKOY, G. & JOHANSEN, T. 2003. Interaction codes within the family of mammalian Phox and Bem1p domain-containing proteins. *J Biol Chem,* 278**,** 34568-81.

LAZAROU, M., SLITER, D. A., KANE, L. A., SARRAF, S. A., WANG, C., BURMAN, J. L., SIDERIS, D. P., FOGEL, A. I. & YOULE, R. J. 2015. The ubiquitin kinase PINK1 recruits autophagy receptors to induce mitophagy. *Nature,* 524**,** 309-314.

LEVINE, B. & KROEMER, G. 2019. Biological Functions of Autophagy Genes: A Disease Perspective. *Cell,* 176**,** 11-42.

LOCKE, M., TINSLEY, C. L., BENSON, M. A. & BLAKE, D. J. 2009. TRIM32 is an E3 ubiquitin ligase for dysbindin. *Hum Mol Genet,* 18**,** 2344-58.

MANDELL, M. A., KIMURA, T., JAIN, A., JOHANSEN, T. & DERETIC, V. 2014. TRIM proteins regulate autophagy: TRIM5 is a selective autophagy receptor mediating HIV-1 restriction. *Autophagy,* 10**,** 2387-8.

NAZIO, F., STRAPPAZZON, F., ANTONIOLI, M., BIELLI, P., CIANFANELLI, V., BORDI, M., GRETZMEIER, C., DENGJEL, J., PIACENTINI, M., FIMIA, G. M. & CECCONI, F. 2013. mTOR inhibits autophagy by controlling ULK1 ubiquitylation, self-association and function through AMBRA1 and TRAF6. *Nat Cell Biol,* 15**,** 406-16.

OVERA, K. S., GARCIA-GARCIA, J., BHUJABAL, Z., JAIN, A., OVERVATN, A., LARSEN, K. B., DERETIC, V., JOHANSEN, T., LAMARK, T. & SJOTTEM, E. 2019. TRIM32, but not its muscular dystrophy-associated mutant, positively regulates and is targeted to autophagic degradation by p62/SQSTM1. *J Cell Sci,* 132.

RAVENHILL, B. J., BOYLE, K. B., VON MUHLINEN, N., ELLISON, C. J., MASSON, G. R., OTTEN, E. G., FOEGLEIN, A., WILLIAMS, R. & RANDOW, F. 2019. The Cargo Receptor NDP52 Initiates Selective Autophagy by Recruiting the ULK Complex to Cytosol-Invading Bacteria. *Mol Cell,* 74**,** 320-329 e6.

REYMOND, A., MERONI, G., FANTOZZI, A., MERLA, G., CAIRO, S., LUZI, L., RIGANELLI, D., ZANARIA, E., MESSALI, S., CAINARCA, S., GUFFANTI, A., MINUCCI, S., PELICCI, P. G. & BALLABIO, A. 2001. The tripartite motif family identifies cell compartments. *EMBO J,* 20**,** 2140-51.

ROGOV, V., DOTSCH, V., JOHANSEN, T. & KIRKIN, V. 2014. Interactions between autophagy receptors and ubiquitin-like proteins form the molecular basis for selective autophagy. *Mol Cell,* 53**,** 167-78.

TURCO, E., FRACCHIOLLA, D. & MARTENS, S. 2019. Recruitment and Activation of the ULK1/Atg1 Kinase Complex in Selective Autophagy. *J Mol Biol*.

VARGAS, J. N. S., WANG, C., BUNKER, E., HAO, L., MARIC, D., SCHIAVO, G., RANDOW, F. & YOULE, R. J. 2019. Spatiotemporal Control of ULK1 Activation by NDP52 and TBK1 during Selective Autophagy. *Mol Cell,* 74**,** 347-362 e6.

WANG, Y., SERRICCHIO, M., JAUREGUI, M., SHANBHAG, R., STOLTZ, T., DI PAOLO, C. T., KIM, P. K. & MCQUIBBAN, G. A. 2015. Deubiquitinating enzymes regulate PARK2-mediated mitophagy. *Autophagy,* 11**,** 595-606.

ZHAO, M., SONG, K., HAO, W., WANG, L., PATIL, G., LI, Q., XU, L., HUA, F., FU, B., SCHWAMBORN, J. C., DORF, M. E. & LI, S. 2019. Non-proteolytic ubiquitination of OTULIN regulates NF-kappaB signaling pathway. *J Mol Cell Biol*.

Figure 1

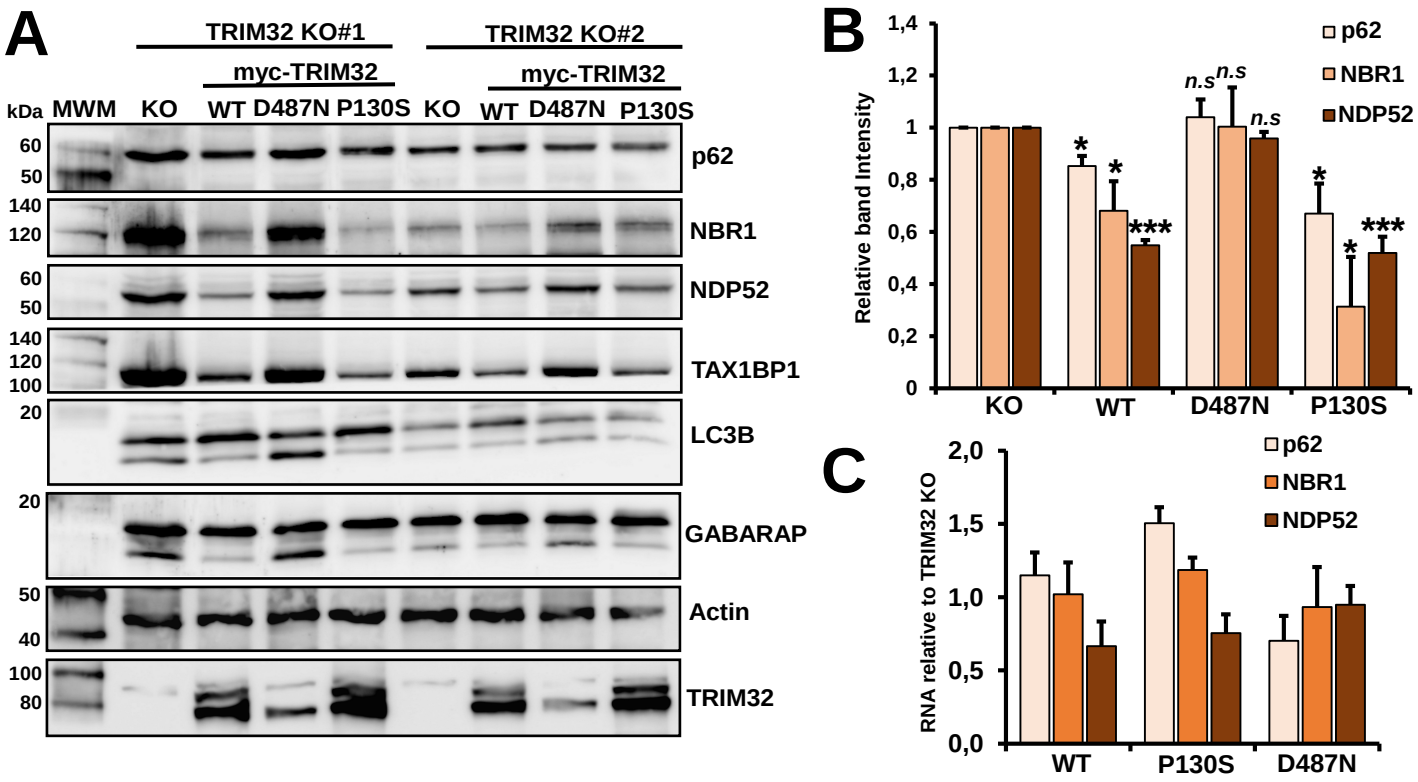
A
TRIM32 KO#1
TRIM32 KO#2
myc-TRIM32
myc-TRIM32
kDa MWM KO WT D487N P130S KO WT D487N P130S
60
50
p62
140
120
NBR1
60
50
NDP52
140
120
100
TAX1BP1
20
LC3B
20
GABARAP
50
40
Actin
100
80
TRIM32
B
Relative band Intensity
1,4
1,2
1
0,8
0,6
0,4
0,2
0
p62
NBR1
NDP52
n.s
n.s
n.s
*
*
***
*
*
***
KO
WT
D487N
P130S
C
RNA relative to TRIM32 KO
2,0
1,5
1,0
0,5
0,0
p62
NBR1
NDP52
WT
P130S
D487N

Figure 2

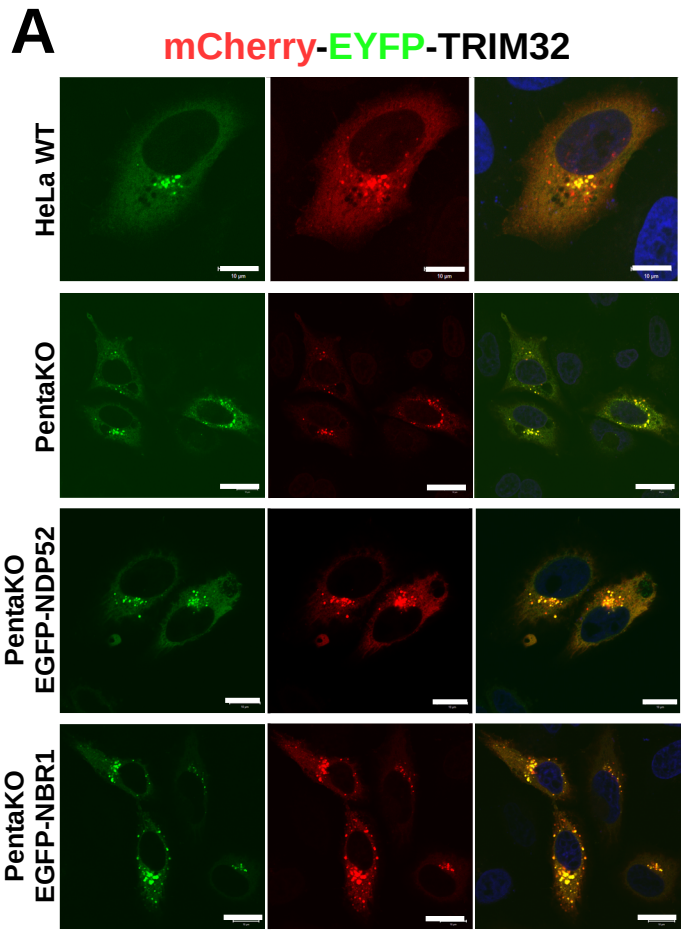
A
mCherry-EYFP-TRIM32
HeLa WT
PentaKO
PentaKO EGFP-NDP52
PentaKO EGFP-NBR1

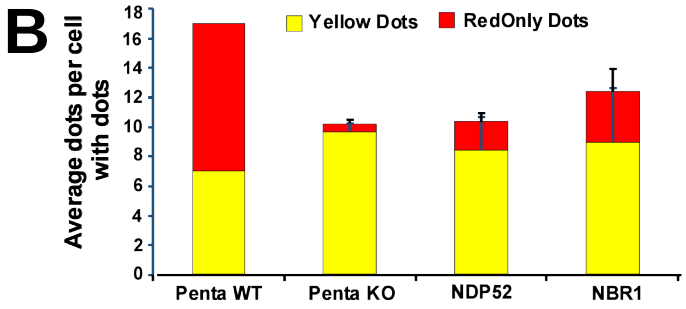
B
Average dots per cell with dots
Yellow Dots
RedOnly Dots
0
2
4
6
8
10
12
14
16
18
Penta WT
Penta KO
NDP52
NBR1

Figure 3

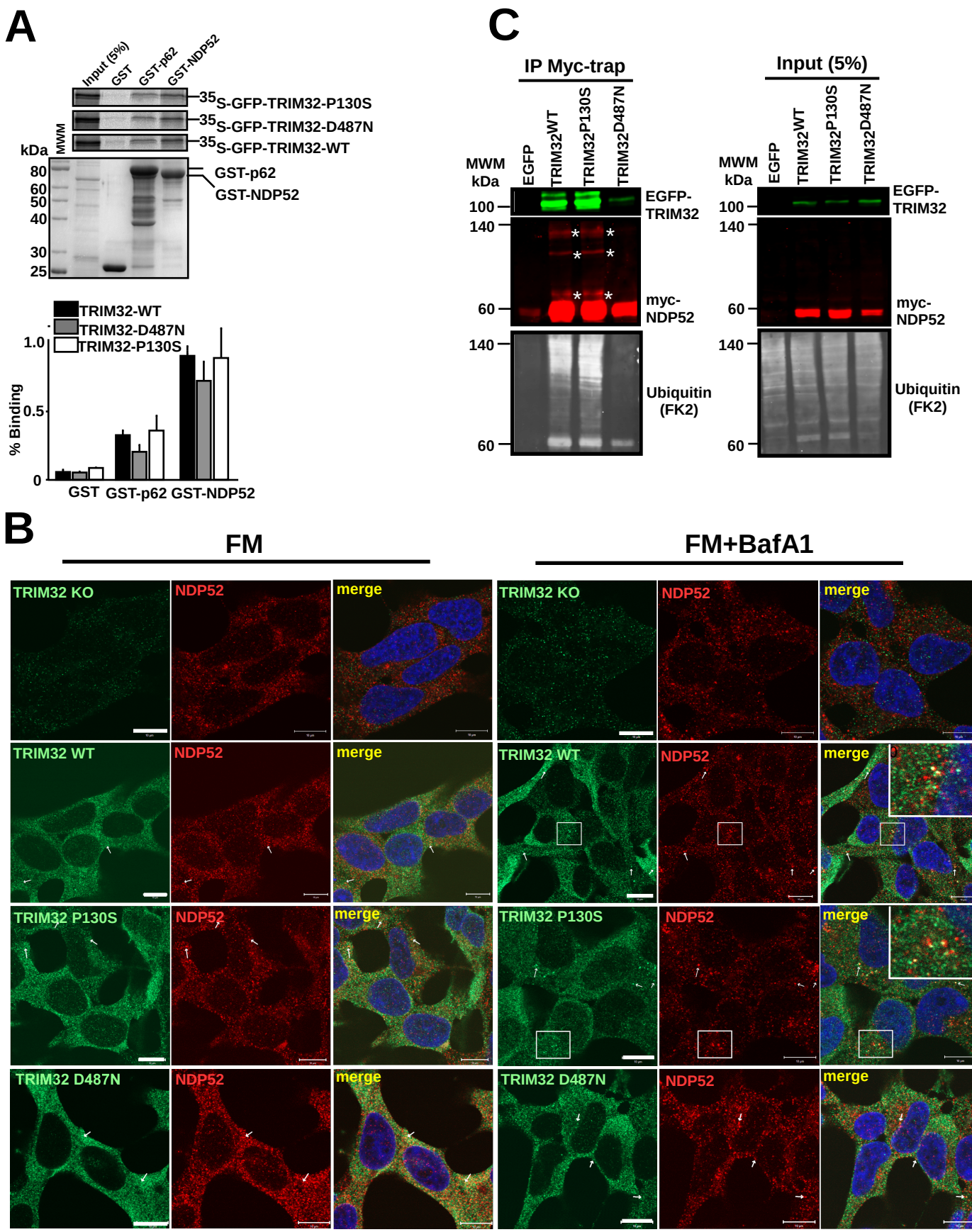
A
Input (5%)
GST
GST-p62
GST-NDP52
MWM
kDa
80
60
50
40
30
25
35S-GFP-TRIM32-P130S
35S-GFP-TRIM32-D487N
35S-GFP-TRIM32-WT
GST-p62
GST-NDP52
TRIM32-WT
TRIM32-D487N
TRIM32-P130S
% Binding
1.0
0.5
0
GST
GST-p62
GST-NDP52
C
IP Myc-trap
Input (5%)
MWM
kDa
EGFP
TRIM32WT
TRIM32P130S
TRIM32D487N
100
140
60
EGFP-
TRIM32
myc-
NDP52
Ubiquitin
(FK2)
B
FM
FM+BafA1
TRIM32 KO
TRIM32 WT
TRIM32 P130S
TRIM32 D487N
NDP52
merge

Figure 4

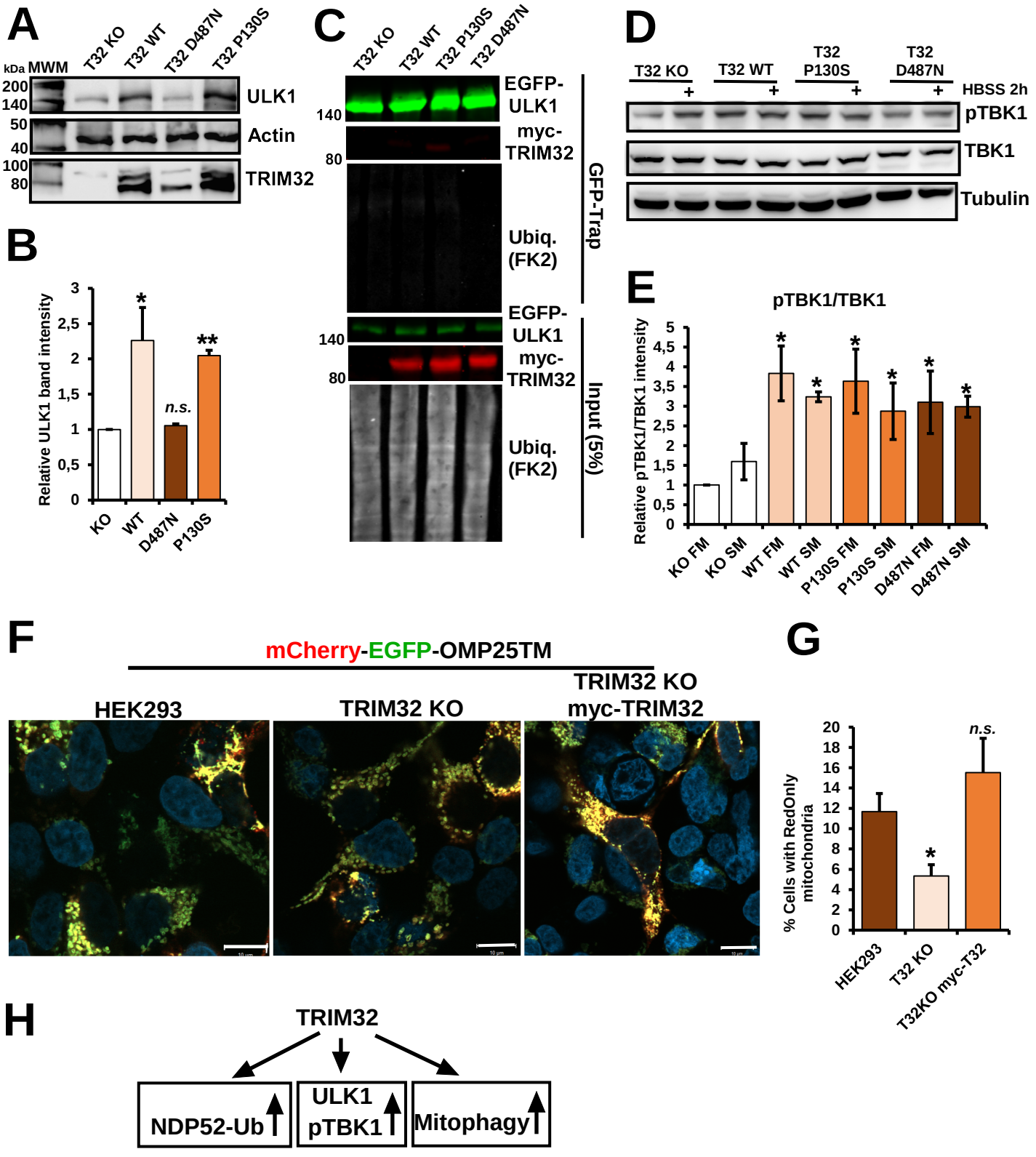
A
kDa MWM
T32 KO
T32 WT
T32 D487N
T32 P130S
200
140
50
40
100
80
ULK1
Actin
TRIM32
B
Relative ULK1 band intensity
3
2,5
2
1,5
1
0,5
0
*
**
n.s.
KO
WT
D487N
P130S
C
T32 KO
T32 WT
T32 P130S
T32 D487N
140
80
EGFP-ULK1
myc-TRIM32
Ubiq. (FK2)
GFP-Trap
EGFP-ULK1
myc-TRIM32
Ubiq. (FK2)
Input (5%)
D
T32 KO
T32 WT
T32 P130S
T32 D487N
HBSS 2h
+
pTBK1
TBK1
Tubulin
E
pTBK1/TBK1
Relative pTBK1/TBK1 intensity
5
4,5
4
3,5
3
2,5
2
1,5
1
0,5
0
KO FM
KO SM
WT FM
WT SM
P130S FM
P130S SM
D487N FM
D487N SM
F
mCherry-EGFP-OMP25TM
HEK293
TRIM32 KO
TRIM32 KO myc-TRIM32
G
% Cells with RedOnly mitochondria
20
18
16
14
12
10
8
6
4
2
0
n.s.
*
HEK293
T32 KO
T32KO myc-T32
H
TRIM32
NDP52-Ub
ULK1 pTBK1
Mitophagy

Supplementary
Figure S1

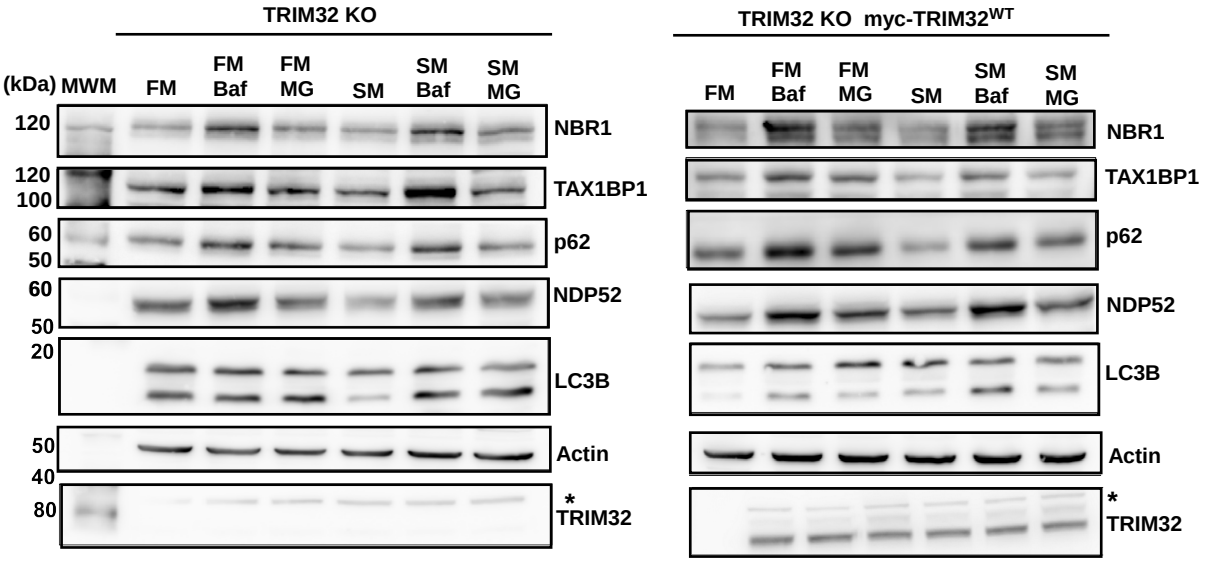

Paper IV

Generation of the short TRIM32 isoform is regulated by Lys 247 acetylation and a PEST sequence

Juncal Garcia-Garcia, Katrine Stange Overå, Waqas Khan, Eva Sjøttem*

Molecular Cancer Research Group, Department of Medical Biology, University of Tromsø – The Arctic University of Norway, 9037 Tromsø, Norway

*Corresponding author: Eva Sjøttem

E-mail: eva.sjottem@uit.no

Phone: 0047 77646425

Running title: PTMs and a PEST region regulating TRIM32

Keywords: TRIM32, LGMD2H, PEST, acetylation, ubiquitylation

Abstract

TRIM32 is an E3 ligase implicated in diverse biological pathways and pathologies such as muscular dystrophy and cancer. TRIM32 are expressed both as full-length proteins, and as a truncated protein. The mechanisms for regulating these isoforms are poorly understood. Here we identify a PEST sequence in TRIM32 located in the unstructured region between the RING-BBox-CoiledCoil domains and the NHL repeats. The PEST sequence directs cleavage of TRIM32, generating a truncated protein similarly to the short isoform. We map three lysine residues that regulate PEST mediated cleavage and auto-ubiquitylation activity of TRIM32. Mimicking acetylation of lysine K247 completely inhibits TRIM32 cleavage, while the lysines K50 and K401 are implicated in auto-ubiquitylation activity. We show that the short isoform of TRIM32 is catalytic inactive, suggesting a dominant negative role. These findings uncover that TRIM32 is regulated by post-translational modifications of three lysine residues, and a conserved PEST sequence.

Introduction

Tripartite motif (TRIM) proteins have emerged as a large family of ubiquitin E3 ligases that are involved in a wide range of cellular processes such as development, differentiation, immunity and carcinogenesis [1]. As a member of the TRIM family, TRIM32 shows the common RBCC domain organization in its N-terminal, consisting of a "Really interesting New gene" (RING) domain, followed by one B-box domain, and a Coiled Coil (CC) region [2]. TRIM32 is characterized by six NHL repeats in its C-terminus. The RING domain is essential for the E3 ligase activity, while the BBOX domain is necessary to modulate chain assembly rate of ubiquitin units. The CC domain assumes an α-helix structure that allows the formation of anti-parallel dimers [3]. To date, the NHL repeats are found to be involved in dimerization and cargo recognition [4]. TRIM32 oligomerization is a pre-requisite for its catalytic activity.

TRIM32 has multiple target proteins involved in innate immunity, carcinogenesis and muscle physiology [5]. TRIM32 is linked to two different genetic diseases [4]. Mutations in the NHL domains result in the muscle disorders Limb Girdle Muscular Dystrophy 2H (LGMD2H) and Sarcotubular myopathy (STM). These mutants display impaired oligomerization and auto-ubiquitylation activity, as well as reduced overall TRIM32 expression. A missense mutation in the BBOX domain causes Bardet-Biedl Syndrome 11 (BBS11), which has a pleiotropic phenotype [6]. TRIM32 can be degraded both by the proteasome and by selective autophagy, and auto-ubiquitylation activity is required for its autophagic degradation [7]. The autophagy receptor p62/SQSTM1 can direct ubiquitylated TRIM32 to autophagic degradation, but is at the same time a TRIM32 substrate, uncovering a role for TRIM32 in the regulation of selective autophagy.

Post-translational modifications (PTMs) such as phosphorylation, acetylation, ubiquitylation and SUMOylation are essential for the function and fate of most proteins. The attachment of these small molecules can modulate greatly the properties of a protein, affecting its stability, function, intracellular distribution and interaction with other proteins [8]. Acetylation is the most common PTM, playing important roles in cell signaling, and in the regulation of protein localization, stability and functionality. The addition of the acetyl group from an Acetyl coenzyme A (Ac-CoA) can occur in two different

positions, in their N^{α}-termini of the amino acid or in the ε-amino group of a lysine amino acid. Lysine acetylation is a reversible modification that is tightly controlled by multiple acetyltransferases and deacetylases [9]. This repertoire of addition and removal of molecules allow the cell to control fast and efficiently the different changes in the environment.

Ubiquitylation of proteins are implicated as a regulatory mechanism of many cellular processes. The addition of ubiquitin moieties is a reversible process that occur on lysine residues. Ubiquitin itself contains seven lysine residues that can be ubiquitylated, forming ubiquitin chains. This allows multiple combinations, which adds a high degree of complexity to this cellular regulation mechanism [10]. As acetylation, ubiquitylation processes are controlled by a balance between ubiquitin E3 ligases and de-ubiquitin enzymes.

A PEST sequence is a region rich in proline (P), glutamic acid (E), serine (S) and threonine (T). This sequence of amino acids acts as a proteolytic signal to control the rapid turnover of the protein [11]. Originally PEST sequences were attributed to short-lived proteins, but later PEST sequences are also identified in some long-lived proteins. Moreover, alternative functions have been linked to PEST domains, hence their function is not limited to proteolytic signaling [12]. PEST regions are generally unstructured and flexible, and the 26S Proteasome and other proteases such as calpains are in charge of the degradation of PEST containing proteins. PEST sequences can lead to constitutive degradation of the protein, but they can also behave as conditional degradation signals depending on the cellular needs [13].

In this work we identify a PEST sequence in the unstructured region between the RBCC region and the NHL domains of the ubiquitin E3 ligase TRIM32. The PEST sequence directs cleavage of TRIM32, leading to a truncated TRIM32 protein lacking the C-terminal NHL-repeat, resembling isoform 3 of TRIM32. The existence of TRIM32 isoform 3 is experimental evidenced at protein level, but a corresponding transcript is not verified. We uncover that PEST mediated cleavage of TRIM32 is regulated by post-translational modifications of three lysine residues, K50, K247 and K401. Mimicking acetylation on K247 completely protects TRIM32 from PEST mediated cleavage. K50 and K401 were found to be important for TRIM32 auto-ubiquitylation activity, which is reported to be necessary for its tetramerization and cytoplasmic body formation. This is the first time that a PEST sequence has been

described in a TRIM protein, as well as the regulation of a PEST sequence by acetylation of an adjacent lysine residue.

Results

PTMs of the lysine residues K50, K247 and K401 regulate TRIM32 cleavage

It is well recognized that TRIM32 has auto-ubiquitylation activity in addition to conventional ubiquitin-protein ligase activity [14, 15]. Auto-ubiquitylation seems to regulate its expression level, E3 ligase activity and ability to form cytoplasmic bodies [7, 16-18]. We and others have shown that the missense mutation TRIM32^{D487N} causing LGMD2H does not undergo auto-ubiquitylation [7, 18]. Auto-ubiquitylated TRIM32 can be detected as a slower-migrating band on Western Blots, as indicated in Fig 1A where the slower migrating band is detected approximately 10 kDa above the band of the catalytic active EGFP-TRIM32^{WT} and EGFP-TRIM32^{P130S} [7]. The EGFP-TRIM32^{D487N} mutant which do not contain auto-ubiquitylation activity[7], does not display this slow migrating band. Auto-ubiquitylation seems to be a prerequisite for the catalytic activity of TRIM32, as the LGMD2H mutant is unable to ubiquitylate the substrate protein p62/SQSTM1 [7]. Moreover, PKA mediated phosphorylation of TRIM32^{S651}, which impairs its ability to undergo auto-ubiquitylation, leads to repression of its E3 ligase activity. The PKA phosphorylation was shown to be regulated by 14-3-3 protein binding to soluble TRIM32, trapping it in a soluble and functionally latent complex [17]. In an attempt to better understand the regulation of TRIM32, we started out to identify which lysine residues in TRIM32 are targeted by its auto-ubiquitylation activity. For this purpose we applied Mass Spectroscopy (MS) analyses of the catalytic inactive disease mutant myc-TRIM32^{D487N}, and compared it to immunoprecipitated catalytic active myc-TRIM32^{WT} and myc-TRIM32^{P130S}. All proteins were stably expressed in the HEK293 FlpIn TRIM32 knock out cells described previously [7]. No lysine residues of the catalytic inactive TRIM32^{LGMD2H} disease mutant were detected as ubiquitylated, while peptides with K50 and K401 ubiquitylation were found in precipitates of the catalytic active enzymes myc-TRIM32^{WT} and myc-

TRIM32^{P130S} (Figs 1B and 1C). However, peptides with acetylation of lysine K247 were identified in precipitates of the myc-TRIM32 disease mutants, but not in the TRIM32^{WT} precipitates (Figs 1B and 1C). In order to determine if these lysine residues are targets for TRIM32 auto-ubiquitylation activity, the constructs EGFP-TRIM32^{K50R}, EGFP-TRIM32^{K247R}, and EGFP-TRIM32^{K401R} were established by site-directed mutagenesis and transiently transfected into a HEK293 FlpIn TRIM32 KO cells [7]. Western Blot analysis of the transfected proteins revealed that none of these single lysine to arginine mutations impaired auto-ubiquitylation activity of TRIM32 (S1 Fig 1A). Next, we introduced double and triple K to R mutations in EGFP-TRIM32, generating EGFP-TRIM32$^{K247R/K401R}$, EGFP-TRIM32$^{K50R/K247R}$, EGFP-TRIM32$^{K50R/K401R}$ and EGFP-TRIM32$^{K50R/K247R/K401R}$, respectively. These mutants along with EGFP-TRIM32^{WT}, were transiently transfected into the TRIM32 KO cells and their auto-ubiquitylation activity investigated by Western blotting (Fig 1 D). Surprisingly, introduction of the double mutation EGFP-TRIM32$^{K247R/K401R}$ resulted in a partially cleaved protein (Fig 1D and Fig 1E, lane 3), while the triple EGFP-TRIM32$^{K50R/K247R/K401R}$ mutation resulted in a completely cleaved protein (Fig 1D and Fig 1E, lane 6). Co-transfection of the broad specificity de-ubiquitinase USP2 verified that the slower-migrating band on the Western blots are due to ubiquitylated TRIM32 (Fig 1D, Fig 1E and S1 Fig 1B). Since mutations in TRIM32 is associated with muscular dystrophy, similar experiment was performed in the myoblast C2C12 cell line. Introduction of the K247R/K401R and K50/K247R/K401R mutations were exposed to cleavage also in this cell line (Fig 1E). Moreover, the polyclonal TRIM32 antibody displayed the same protein pattern on the Western blot as the GFP antibody, indicating that cleavage of EGFP-TRIM32$^{K50R/K247R/K401R}$ generates a stable N-terminal cleavage product of around 55 kDa. In contrast, any C-terminal cleavage products can not be detected in the gel, suggesting that this part of TRIM32 is exposed to further degradation.

Fig 1. PTMs of TRIM32^{K50}, TRIM32^{K247} and TRIM32^{K401} regulate its cleavage. (A) Western blot analysis of cell extracts from HEK293 FlpIn cells with tetracycline inducible expression of EGFP-TRIM32^{WT}, the BBS11 associated mutant EGFP-TRIM32^{P130S}, or the LGMD2H causing mutant EGFP-TRIM32^{D487N} shows auto-ubiquitylation activity of TRIM32^{WT} and TRIM32^{P130S}, but not the LGMD2H mutant. (B) Sequence of the TRIM32 peptides identified by MS to display PTMs on lysine residues that

differed between the TRIM32 proteins with auto-ubiquitylation activity (TRIM32^{WT} and TRIM32^{P130S}) and the LGMD2H disease variant lacking auto-ubiquitylation activity (TRIM32^{D487N}). (C) Schematic of TRIM32 domain organization. The D487N mutation in the NHL repeats that is associated with LGMD2H and the P130S mutation in the BBox causing BBS11 are indicated above. The three lysine residues that are focused in this paper are indicated in red, while the PTMs of these residues identified by MS are indicated above. Ub: Ubiquitylation. Ac: acetylation (D) Western Blot analysis of HEK293 FlpIn TRIM32 KO cells transiently transfected with expression plasmids for EGFP-TRIM32^{WT}, the double mutants EGFP-TRIM32$^{K247R/K401R}$, EGFP-TRIM32$^{K50R/K247R}$, or EGFP-TRIM32$^{K247R/K401R}$, or the triple mutant EGFP-TRIM32$^{K50R/K247R/K401R}$. The last lane represents cotransfection of EGFP-TRIM32^{WT} and mCherry-USP2 expression vectors. The bands representing EGFP-TRIM32, auto-ubiquitylated EGFP-TRIM32, and cleaved EGFP-TRIM32 are indicated to the right. PCNA represents the loading control. (E) Western blot analysis of a similar experiment as in (D), except that the myoblast C2C12 cell line is used instead of the HEK293 FlpIn TRIM32 KO cell line, and the antibody used is an anti-TRIM32 antibody instead of an anti-GFP antibody.

Acetylation of K247 is sufficient to inhibit cleavage of TRIM32

According to ENSEMBL genome browser (ensemble.org) and UniProt protein database (uniprot.org) there are two variants of the TRIM32 protein in humans. The main variant (Uniprot.org Q13049) is a 653 amino acid protein of 72 kDa. Additional, there is clear experimental evidence for the existence of a short 172 amino acid long variant of TRIM32 (Uniprot.org Q5JVY0) (Fig 2A). However, the existence of a transcript encoding the short protein variant is not validated, since a transcript with a 3'UTR is unrecognized so far (ensemble.org). The short isoform contains the N-terminal RBCC domains, but lack the NHL-repeats and the unstructured region between RBCC and the NHL-domain. The short isoform is around 20 kDa, and hence has a size very similar to the 55 kDa TRIM32 N-terminal cleavage product that we observed above (20 kDa plus the EGFP-tag of 32.7 kDa). This prompted us to ask whether the short TRIM32 protein may be generated by proteolytic cleavage of the long form, and if this cleavage could be regulated by post-translational modifications of the lysine residues identified above (K50,

K247, K401)(Fig 1C). De-ubiquitylation of TRIM32 by USP2 over-expression did not result in TRIM32 cleavage (Fig 1D and Fig 1E). Therefore, we asked whether acetylation of the lysine residues K50, K247 and K401 would affect TRIM32 cleavage. Each of these lysine residues were replaced by the acetylation mimicking amino acid glutamine (Q) in the EGFP-TRIM32$^{K50R/K247R/K401R}$ construct. The constructs were transfected into the HEK293 FlpIn TRIM32 KO cell line, and their expression monitored by Western blotting (Fig 2B). Clearly, introduction of the acetylation mimicking mutant at position K247 completely inhibited cleavage of TRIM32 (Fig 2B, lane 5), while the K50Q and K401Q mutations did not (Fig 2B, lanes 4 and 6). This suggests that acetylation of K247 in TRIM32 is implicated in regulation of TRIM32 cleavage. The subcellular localization of the TRIM32 lysine mimicking mutants were examined by transient transfection of wild type EGFP-TRIM32 and the mutant constructs into HEK293 FlpIn TRIM32 KO cells. In line with previous reports, EGFP-TRIM32^{WT} is enriched in small round cytoplasmic bodies in addition to diffuse cytoplasmic localization. Co-staining with the Golgi marker GM130 showed that many of the TRIM32 bodies localize close to the Golgi apparatus (Fig 2C). The EGFP-TRIM32 mutants that generate the cleaved TRIM32 product (TRIM32$^{K50Q/k247R/K401R}$ and TRIM32$^{K50R/K247R/K401Q}$) formed mainly a few large bodies or aggregates localized in or close to the Golgi region. In contrast, the TRIM32$^{K50R/K247Q/K401R}$ mutant that inhibits TRIM32 cleavage, displays a subcellular localization very similar to the wild type protein (Fig 2C). Hence, the short TRIM32 protein seem to have a strong tendency to form large aggregates compared to full-length TRIM32 isoform.

Fig 2. K247 acetylation inhibits TRIM32 cleavage and facilitates its subcellular distribution. (A) Western Blot analysis of HEK293 FlpIn TRIM32 KO cells transiently transfected with expression plasmids for EGFP-TRIM32^{WT}, EGFP-TRIM32$^{K50R/K247R/K401R}$, EGFP-TRIM32$^{K50Q/K247R/K401R}$, TRIM32$^{K50R/K247Q/K401R}$ or EGFP-TRIM32$^{K50R/K247R/K401Q}$. The bands representing EGFP-TRIM32 and cleaved EGFP-TRIM32 are indicated to the right. Ponceau staining of the membrane represents the loading control. (B) Confocal images of HEK293 FlpIn TRIM32 KO cells transiently transfected with expression plasmids for EGFP-TRIM32^{WT}, EGFP-TRIM32$^{K50R/K247R/K401R}$, EGFP-TRIM32$^{K50Q/K247R/K401R}$, TRIM32$^{K50R/K247Q/K401R}$ or EGFP-TRIM32$^{K50R/K247R/K401Q}$, and immunostained

with anti-GM130 antibodies, a Golgi marker. The cell nuclei is visualized by DAPI staining. Scale bars: 10 μM.

Autophagic degradation of TRIM32 is dependent on K50, K247 and K401 modifications

We have recently shown that TRIM32 is a substrate for selective autophagy [7]. Our next question was whether the short TRIM32 isoform is a target for selective autophagy. For this purpose, the double fluorescent tag mCherry-EYFP was cloned in front of the TRIM32 constructs TRIM32^{WT}, TRIM32$^{K247R/K401R}$, TRIM32^{K247Q}, TRIM32$^{K50R/K247Q/K401R}$, and TRIM32$^{K50R/K247R/K401R}$ and transiently transfected into the HEK293 FlpIn TRIM32 KO cells. Since EYFP is unstable in acidic environments while mCherry is stable, double-tagged TRIM32 constructs targeted to the lysosome will be visualized as RedOnly dots in the fluorescence microscope, while TRIM32 bodies in the cytoplasm will occur as yellow. The mCherry-EYFP-TRIM32$^{K247R/K401R}$ and mCherry-EYFP-TRIM32^{K247Q} constructs formed RedOnly dots, but to a lesser extent than mCherry-EYFP-TRIM32^{WT} (Fig 3). However, when all three lysine residues were substituted with Arginine, giving rise to the cleaved TRIM32 product, or when K50 and K401 were substituted with arginine and K247 with glutamine, giving rise to a full length TRIM32 product, no red only dots was observed in the transfected cells (Fig 3). This suggests that PTMs on the lysine residues K50, K247 and K401 regulate autophagic degradation of TRIM32.

Fig 3. PTMs on TRIM32^{K50}, TRIM32^{K247}, TRIM32^{K401} regulate autophagic degradation of TRIM32. (A) Confocal images of mCherry-EYFP-TRIM32^{WT}, mCherry-EYFP-TRIM32$^{K247R/K401R}$, mCherry-EYFP-TRIM32^{K247Q}, mCherry-EYFP-TRIM32$^{K50R/K247Q/K401R}$ or mCherry-EYFP-TRIM32$^{K50R/K247R/K401R}$ transiently expressed in HEK293 FlpIn TRIM32 KO cells and exposed to normal or starved conditions. Scale bars: 10 μM. (B) The graphs represent the number of cells with RedOnly dots in the mCherry-EYFP-TRIM32 transfected cells shown with representative images in A. The

graphs represent the average of three independent experiments with s.d. (n>20 cells). **P< 0.005; ***P<0.0005 (Student's *t*-test).

TRIM32 cleavage is directed by a PEST sequence

The complete cleavage of the EGFP-TRIM32$^{K50R/K247R/K401R}$ construct prompted us to investigate whether TRIM32 encodes specific sequences that are exposed for proteolytic cleavage. Sequence analysis using the PEST prediction tool EMBOSS:epestfind (https://emboss.bioinformatics.nl/cgi-bin/emboss/epestfind), identified a putative PEST sequence with PEST score 7.4 located from amino acid 248 to 270 (Fig 4A). The predicted PEST sequence is 100% conserved in mammals, and interestingly it is located adjacent to lysine K247 which acetylation inhibits TRIM32 cleavage. To examine if the predicted PEST sequence directs TRIM32 cleavage, specific glutamate and threonine residues within the PEST sequence were mutated to valine or isoleucine, respectively, in the EGFP-TRIM32^{WT} construct. Additionally, a partial deletion of the PEST sequence was introduced in EGFP-TRIM32^{WT} and EGFP-TRIM32$^{K50R/K247R/K401R}$ (Fig 4A). The PEST mutation and deletion constructs were transiently transfected into the HEK293 FlpIn TRIM32 KO cell line, and their expression monitored by Western blotting (Fig 4B). Clearly, partial deletion of the PEST sequence in the EGFP-TRIM32$^{K50R/K247R/K401R}$ constructs completely inhibits TRIM32 cleavage (Fig 4B, lane 6). Partial deletion or mutation of the PEST sequence in wild type TRIM32 did not compromise TRIM32 expression (Fig 4B, lanes 3 and 4). This identifies the 248-270 region of TRIM32 to be a PEST sequence that directs cleavage of TRIM32 that is unable to be modified on K50, K247 and K401. Clearly, mimicking of acetylation on lysine K247, which is localized adjacent to the PEST sequence, completely protects TRIM32 from the PEST directed cleavage (Fig 4B, last lane).

The cleaved TRIM32 protein contains the RBCC domains, and hence may have the ability to undergo auto-ubiquitylation and thereby gain catalytic activity. To examine this, the auto-ubiquitylation activity of the triple mutant TRIM32$^{K50R/K247R/K401R}$ was compared to the auto-ubiquitylation activity of TRIM32^{WT} and TRIM32^{D487N}, which is known to be catalytic inactive. Clearly, no auto-ubiquitylation activity was detected for the cleaved TRIM32 product (Fig 4C, lane 5). Auto-ubiquitylation activity of

TRIM32$^{K50R/K247R/K401R}$ with a partial deleted PEST sequence, and the acetylation mimicking mutant TRIM32$^{K50R/K247Q/K401R}$ were analyzed in parallel. Both these mutations inhibit cleavage of TRIM32 (Fig 4C, lanes 6,7). Notably, none of these mutant forms of TRIM32 displayed auto-ubiquitylation activity. In contrast, TRIM32^{WT} with a partial deleted PEST sequence (Fig 4C, lane 4) and the TRIM32^{K247Q} construct (Fig 4B, last lane) both display auto-ubiquitylation activity.

Together, these results show that the short isoform of TRIM32 can be generated by proteolytic cleavage directed by a PEST sequence located between the RBCC region and the NHL domains. Acetylation of K247 located adjacent to the PEST sequence, completely protects TRIM32 from PEST mediated cleavage. The short TRIM32 isoform and TRIM32 proteins containing K50, K247 and K401 mutations are catalytic inactive, showing the importance of these lysines for TRIM32 activity.

Fig 4. Acetylation of K247 protects TRIM32 from cleavage directed by the adjacent PEST sequence. (A) Schematic of TRIM32 domain organization with the three regulatory Lysine residues identified in this work indicated above, and the sequence of the mapped PEST sequ.ence indicated below. MutPEST and ΔPEST display the modifications introduced to the predicted PEST sequence. (B) Western Blot analysis of cell extracts from HEK293 FlpIn TRIM32 KO cells transiently transfected with expression plasmids for EGFP-TRIM32^{WT}, EGFP-TRIM32^{mutPEST}, EGFP-TRIM32$^{\Delta PEST}$, EGFP-TRIM32$^{K50R/K247R/K401R}$ (3KR), TRIM32$^{K50R/K247R/K401R/\Delta PEST}$ (3KR ΔPEST) or EGFP-TRIM32^{K247Q}. The bands representing EGFP-TRIM32 are indicated to the right. The band representing cleaved EGFP-TRIM32 is indicated to the right. Tubulin represents the loading control. (C) Western Blot analysis of cell extracts from HEK293 FlpIn TRIM32 KO cells transiently transfected with expression plasmids for EGFP-TRIM32^{WT}, EGFP-TRIM32^{WT} and mCherry-USP2, EGFP-TRIM32$^{\Delta PEST}$, EGFP-TRIM32$^{K50R/K247R/K401R}$ (3KR), TRIM32$^{K50R/K247R/K401R/\Delta PEST}$ (3KR ΔPEST) or EGFP-TRIM32$^{K50R/247Q/K401R}$ or EGFP-TRIM32^{D487N}. The bands representing ubiquitylated EGFP-TRIM32, EGFP-TRIM32 and cleaved EGFP-TRIM32 are indicated to the right. Actin represents the loading control.

Discussion

In this study we aimed at gaining insight in how TRIM32 auto-ubiquitylation regulates its activity and stability. TRIM32 is implicated in diverse biological and physiological processes such as muscle physiology, neuronal differentiation, immunity and cancer [5]. TRIM32 is reported to act both as an oncogene and as tumor suppressor, depending on the specific organ and cellular context [5]. TRIM32 overexpression promotes cell proliferation, transforming activity, cell motility and prevents apoptosis [15, 19], but it is also shown to promote asymmetric cell division of neuroblastoma cells and to enhance TNFα-induced apoptosis [20, 21]. Abnormal expression of TRIM32 has been demonstrated in various human cancer cells [22-26], and in the occipital lobe of Alzheimer's disease patients [27]. Reduced TRIM32 expression in lung epithelial and tracheal cells increases their susceptibility to infection of influenza A virus [28]. Thus, regulating TRIM32 activity is of critical importance for healthy cell physiology.

Our data reveal that TRIM32 contains a conserved PEST sequence located in the unstructured region between the N-terminal RBCC domains and the C-terminal NHL-domains. This is the first time a PEST sequence is identified in a TRIM protein. Inhibition of PTMs of the K50, K247 and K401 residues by substitution of these lysine residues with arginine, resulted in exposure of the PEST to proteolytic enzymes, leading to TRIM32 cleavage. However, mimicking acetylation of K247 by glutamine substitution but keeping the K50R and K401R mutations, completely protected TRIM32 from proteolytic degradation. The acetylation also facilitated distribution of TRIM32 bodies throughout the cytoplasm, and protected it from autophagic degradation. Importantly, K247 is located immediately upstream of the PEST region. Thus, our data indicate that reversible acetylation of K247 regulates PEST mediated cleavage of TRIM32.

Research over the past decades have revealed that lysine acetylation is a common mechanism for regulation of protein stability, and can regulate both proteasome-dependent and lysosome-dependent protein degradation (recently reviewed [29]). Acetylation mediated stabilization of proteins can be due to direct competition between acetylation and ubiquitylation of the same lysine residue, such as described for SMAD7 [30] and TRIM50 [31]. However, acetylation is also reported to promote protein

degradation by enhancing ubiquitylation leading to degradation in the proteasome [32, 33] or the lysosome [34, 35]. However, lysine acetylation regulating PEST mediated cleavage is to our knowledge not previously described, and hence presents a new mechanism for lysine acetylation mediating protein expression. Originally, PEST domains were identified in short living proteins [36], and later they are shown to function as an anchor site of E3 ubiquitin ligases required for ubiquitin dependent protein degradation [37, 38]. TRIM32 degradation can be mediated both via proteasomal and lysosomal pathways [7]. Here we applied inhibitors of the proteasome, the lysosome and the calpain proteases (data not shown), but we were not able to pinpoint which pathway is implicated in the PEST mediated cleavage of TRIM32. We may speculate that the K247 acetylation inhibits binding of proteolytic enzymes, since acetylation of proteins is a well known mechanism for inhibiting (or promoting) protein-protein interactions [29].

TRIM32 activity is regulated by tetramerization via its coiled-coil domain [39]. Tetramerization leads to formation of RING domain dimers on each side of the two antiparallel TRIM32 dimers. RING domain dimerization is a common pre-requisite for E3 ligase activity of TRIM proteins [40, 41]. TRIM32 tetramerization induces auto-ubiquitylation, which seems to be necessary for its conventional ubiquitin ligase activity and formation of cytoplasmic bodies. The scaffold 14-3-3 protein binds TRIM32 proteins phosphorylated at S651 in its very C-terminal end, and thereby inhibits TRIM32 tetramerization and cytoplasmic body formation [17]. HSP70, on the other hand, is reported to bind TRIM32 and promote formation of cytoplasmic bodies in an ATP-consuming process [42]. Apart from that, very little is known on how TRIM32 tetramerization and catalytic activity is regulated. The TRIM32^{LGMD2H} disease mutants lack ubiquitylation activity and display a diffuse cytoplasmic localization [7, 18]. This is in line with the MS analysis of PTMs on the TRIM32^{LGMD2H} mutant in this study, where no lysine residues were found to be ubiquitylated. However, lysine K247 in the mutant protein was found to be acetylated, indicating that TRIM32 acetylation is not dependent on tetramerization. Mutation of the lysine residues K50, K247 and K401 to arginine, lead to cleavage of TRIM32 generating an around 20 kDa protein containing the N-terminal RBCC domains. This cleavage product resemble the short TRIM32 isoform, suggesting that isoform 3 of TRIM32 are generated by proteolytic cleavage. This finding is supported by the lack of a transcript that corresponds to isoform 3 (ensembl.org). Mimicking acetylation of lysine

K247, but keeping the K50R and K401R mutations, protected TRIM32 from cleavage but did not restore its auto-ubiquitylation activity. This was in line with our MS results showing that the catalytic inactive $TRIM32^{LGMD2H}$ mutant can undergo K247 acetylation. Mimicking acetylation of K50 or K401 did not protect TRIM32 from PEST mediated cleavage and our MS data indicated that these residues are targets for ubiquitylation and not acetylation. Our results indicate that these two lysine residues are important for auto-ubiquitylation activity, and hence the E3 ligase activity of TRIM32.

Our study uncover that TRIM32 isoform 3 may be generated by PEST mediated cleavage of full-length TRIM32 isoform1/2, and that acetylation of lysine K247 localized adjacent to the PEST sequence protects TRIM32 isoform 1/2 from cleavage. We show that the short TRIM32 isoform is catalytic inactive, and hence may function as a dominant negative mutant regulating TRIM32 E3 ligase activity. Moreover, we find that auto-ubiquitylation activity of full-length TRIM32 is dependent on the lysine residues K50 and K401. K50 is located in the RING domain, and hence may directly affect the formation of a functional catalytic unit. K401 is located in the NHL repeats. Various mutations in the NHL repeats cause LGMD2H, and we have previously shown that $TRIM32^{LGMD2H}$ mutants are catalytic inactive [7].

Identification of a functional PEST sequence in a TRIM family protein is a novel finding, and also that acetylation of a lysine residue adjacent to the PEST region regulates the exposure of the PEST. These findings may contribute to the understanding of cellular mechanisms leading to dysregulated TRIM32 expression observed in pathological conditions.

Materials and Methods

Antibodies

The following primary antibodies were used: rabbit polyclonal antibody for TRIM32 (Proteintech, 10326-1-AP); rabbit polyclonal anti-GFP (Abcam, ab290); rabbit polyclonal anti-Actin (Sigma, A2066); mouse monoclonal anti-PCNA (DAKO, M0879); rabbit monoclonal anti-GM130 (Abcam, #52649). The following secondary antibodies were used: Horseradish-peroxidase (HRP)-conjugated goat anti-rabbit IgG (BD 5 Biosciences, 554021); HRP-conjugated goat anti-mouse Ig (BD Biosciences,

554002); HRPconjugated anti-Biotin antibody (Cell Signalling, #7075), and Alexa FluorR 555-conjugated goat anti-rabbit IgG (Life Technologies, A-11008).

Cell culture and transfections

HEK293 FlpIn T-Rex (ThermoFisher, R714-07), HEK293 FlpIn T-Rex TRIM32 KO [7], C2C12 (ATCC® CRL-1772™) were cultured in Dulbecco's modified eagle's medium (DMEM) (Sigma, D6046) with 10% fetal bovine serum and 1% streptomycin-penicillin (Sigma, P4333). Sub-confluent cells in 6-well plates were transfected using Metafectene Pro (Biontex, T040) following the manufacturer's instructions.

Immunostaining

Subconfluent cells were grown on coverslips (VWR, #631-0150) coated with Fibronectin (Sigma, F1141). They were fixed in 4% formaldehyde for 20min at R.T., permeabilized with methanol at RT for 5min, blocked in 5% goat serum/PBS or 5%BSA/PBS and incubated at room temperature with a specific primary antibody followed by Alexa Fluor 555 conjugated secondary antibody and DAPI. Confocal images were obtained using a 63x/NA1.4 oil immersion objective on an LSM780 system and the ZEN software (Zeiss). Quantification of cells containing red only dots in the mCherry- EYFP-double tag assay was done manually in three independent experiments, each including at least 30 cells.

Plasmids

All plasmids used in this study are listed in Table 1. Plasmids were made by conventional restriction enzyme based cloning or by use of the Gateway recombination system (ThermoFisher). Gateway LR reactions were performed as described in the instruction manual. Point mutations and deletion were carried out using the Site-directed-mutagenesis kit from STRATAGENE, using the primers described in Table 2. The oligonucleotides were ordered from ThermoFisher. All plasmids were verified by DNA sequencing (BigDye, Applied Biosystems, 4337455).

Table 1: Plasmids used in this study

pDest EGFP TRIM32	[7]
pDest EGFP TRIM32 D487N	[7]
pDest EGFP TRIM32 P130S	[7]
pDest EGFP TRIM32 K50R	This study
pDest EGFP TRIM32 K247R	This study
pDest EGFP TRIM32 K401R	This study
pDest EGFP TRIM32 K247R/K401R	This study
pDest EGFP TRIM32 K50R/K247R	This study
pDest EGFP TRIM32 K50Q/K401R	This study
pDest EGFP TRIM32 K50R/K247R/K401R	This study
pDest EGFP TRIM32 K50Q/K247R/K401R	This study
pDest EGFP TRIM32 K50R/K247Q/K401R	This study
pDest EGFP TRIM32 K50R/K247R/K401Q	This study
pDest EGFP TRIM32 ΔPEST	This study
pDest EGFP TRIM32 K50R/K247R/K401R ΔPEST	This study
pDest EGFP TRIM32 mutPEST	This study
pDest EGFP TRIM32 K247Q	This study
pDest mCherry USP2	This study
pDest mCherry-EYFP-TRIM32	[7]
pDest mCherry-EYFP-TRIM32 K247R/K401R	This study
pDest mCherry-EYFP-TRIM32 K247Q	This study
PDest mCherry-EYFP-TRIM32 K50R/K247Q/K401R	This study
pDEST mCherry-EYFP-TRIM32 K50R/K247R/K401R	This study
pDest EGFP-C1	[43]
pDest mCherry-EYFP	[44]

Table 2: Oligonucleotides used in this study

$TRIM32^{K50R}$	5'-TGCCGCCAGTGCCTGGAGCGCCTATTGGCCAGTAGCATC- 3'
$TRIM32^{K247R}$	5'-TACTTCCTGGCCAAGATCCGCCAGGCAGATGTAGCACTA- 3'
$TRIM32^{K401R}$	5'-ATACAAGTCTTTACCCGCCGCGGCTTTTTGAAGGAAATC- 3'
$TRIM32^{K50Q}$	5'-TGCCGCCAGTGCCTGGAGCAGCTATTGGCCAGTAGCATC- 3'
$TRIM32^{K247Q}$	5'-TACTTCCTGGCCAAGATCCAGCAGGCAGATGTAGCACTA- 3'
$TRIM32^{K401Q}$	5'-ATACAAGTCTTTACCCGCCAAGGCTTTTTGAAGGAAATC- 3'
$TRIM32^{\Delta PEST}$	5'-AGGCAGATGTAGCACTACTGCTCACTGCCAGCTTGCCTCG -3'
$TRIM32^{mutPEST}$	5'- CACTACTGGTGGTGATAGCTGATGTGGTGGTGCCAGAGCT- 3'

Western Blotting

Cells were seeded in 6-well dishes and treated as indicated. Cells were lysed in 1xSDS buffer (50mM Tris pH 7.4; 2% SDS; 10% Glycerol) supplemented with 200mM dithiothreitol (Sigma, #D0632) and heated at 100°C for 10 minutes. The lysates were resolved by SDS-PAGE and transferred to

nitrocellulose membrane (Sigma, GE10600003). The membrane was stained with Ponceau S (Sigma, P3504), blocked with 5% non-fat dry milk in 1% TBS-T (0.2M Tris pH 8; 1.5M NaCl and 0.05% Tween20 (Sigma, P9416)) and then incubated with indicated primary antibodies for 24h. The membrane was washed three times for 10 minutes each with PBS-T followed by incubation with secondary antibody for 1h. The membrane was washed three times for 10 minutes and analyzed by enhanced chemiluminescence using the ImageQuant LAS 4000 (GE Lifescience).

Statistics

All experiments were repeated at least three times, unless otherwise specified. Error bars represent the standard deviation. Two-sided unpaired, homoscedastic Student T-Tests, were performed to assess significant differences between populations. Replicates were not pooled for statistical analyses.

Acknowledgements

We thank the Tromsø University Proteomics Platform for help with mass spectrometry analysis and the Advanced Microscopy Core Facility, UiT-The Arctic University of Norway, for the use of instrumentation.

Conflict of interest

The authors declare that they have no conflicts of interest with the contents of this article.

Author Contributions

ES conceived and supervised the study; JGG and ES designed experiments; JGG, KSO, WK an ES performed experiments, JGG and ES analyzed the data and wrote the manuscript.

References

1. Hatakeyama S. TRIM Family Proteins: Roles in Autophagy, Immunity, and Carcinogenesis. Trends Biochem Sci. 2017;42(4):297-311. Epub 2017/01/26. doi: 10.1016/j.tibs.2017.01.002. PubMed PMID: 28118948.
2. Esposito D, Koliopoulos MG, Rittinger K. Structural determinants of TRIM protein function. Biochem Soc Trans. 2017;45(1):183-91. Epub 2017/02/17. doi: 10.1042/BST20160325. PubMed PMID: 28202672.
3. Lazzari E, El-Halawany MS, De March M, Valentino F, Cantatore F, Migliore C, et al. Analysis of the Zn-Binding Domains of TRIM32, the E3 Ubiquitin Ligase Mutated in Limb Girdle Muscular Dystrophy 2H. Cells. 2019;8(3). Epub 2019/03/20. doi: 10.3390/cells8030254. PubMed PMID: 30884854; PubMed Central PMCID: PMCPMC6468550.
4. Tocchini C, Ciosk R. TRIM-NHL proteins in development and disease. Semin Cell Dev Biol. 2015;47-48:52-9. Epub 2015/10/31. doi: 10.1016/j.semcdb.2015.10.017. PubMed PMID: 26514622.
5. Lazzari E, Meroni G. TRIM32 ubiquitin E3 ligase, one enzyme for several pathologies: From muscular dystrophy to tumours. Int J Biochem Cell Biol. 2016;79:469-77. Epub 2016/07/28. doi: 10.1016/j.biocel.2016.07.023. PubMed PMID: 27458054.
6. Servian-Morilla E, Cabrera-Serrano M, Rivas-Infante E, Carvajal A, Lamont PJ, Pelayo-Negro AL, et al. Altered myogenesis and premature senescence underlie human TRIM32-related myopathy. Acta Neuropathol Commun. 2019;7(1):30. Epub 2019/03/03. doi: 10.1186/s40478-019-0683-9. PubMed PMID: 30823891; PubMed Central PMCID: PMCPMC6396567.
7. Overa KS, Garcia-Garcia J, Bhujabal Z, Jain A, Overvatn A, Larsen KB, et al. TRIM32, but not its muscular dystrophy-associated mutant, positively regulates and is targeted to autophagic degradation by p62/SQSTM1. J Cell Sci. 2019;132(23). Epub 2019/11/07. doi: 10.1242/jcs.236596. PubMed PMID: 31685529; PubMed Central PMCID: PMCPMC6918758.
8. Duan G, Walther D. The roles of post-translational modifications in the context of protein interaction networks. PLoS Comput Biol. 2015;11(2):e1004049. Epub 2015/02/19. doi: 10.1371/journal.pcbi.1004049. PubMed PMID: 25692714; PubMed Central PMCID: PMCPMC4333291.
9. Drazic A, Myklebust LM, Ree R, Arnesen T. The world of protein acetylation. Biochim Biophys Acta. 2016;1864(10):1372-401. Epub 2016/06/15. doi: 10.1016/j.bbapap.2016.06.007. PubMed PMID: 27296530.
10. Swatek KN, Komander D. Ubiquitin modifications. Cell Res. 2016;26(4):399-422. Epub 2016/03/26. doi: 10.1038/cr.2016.39. PubMed PMID: 27012465; PubMed Central PMCID: PMCPMC4822133.
11. Rechsteiner M, Rogers SW. PEST sequences and regulation by proteolysis. Trends Biochem Sci. 1996;21(7):267-71. Epub 1996/07/01. PubMed PMID: 8755249.
12. Qile M, Ji Y, Houtman MJC, Veldhuis M, Romunde F, Kok B, et al. Identification of a PEST Sequence in Vertebrate KIR2.1 That Modifies Rectification. Front Physiol. 2019;10:863. Epub 2019/07/25. doi: 10.3389/fphys.2019.00863. PubMed PMID: 31333502; PubMed Central PMCID: PMCPMC6624654.
13. Belizario JE, Alves J, Garay-Malpartida M, Occhiucci JM. Coupling caspase cleavage and proteasomal degradation of proteins carrying PEST motif. Curr Protein Pept Sci. 2008;9(3):210-20. Epub 2008/06/10. doi: 10.2174/138920308784534023. PubMed PMID: 18537676.
14. Kudryashova E, Kudryashov D, Kramerova I, Spencer MJ. Trim32 is a ubiquitin ligase mutated in limb girdle muscular dystrophy type 2H that binds to skeletal muscle myosin and ubiquitinates actin. J Mol Biol. 2005;354(2):413-24. Epub 2005/10/26. doi: 10.1016/j.jmb.2005.09.068. PubMed PMID: 16243356.
15. Albor A, El-Hizawi S, Horn EJ, Laederich M, Frosk P, Wrogemann K, et al. The interaction of Piasy with Trim32, an E3-ubiquitin ligase mutated in limb-girdle muscular dystrophy type 2H, promotes

Piasy degradation and regulates UVB-induced keratinocyte apoptosis through NFkappaB. J Biol Chem. 2006;281(35):25850-66. Epub 2006/07/04. doi: 10.1074/jbc.M601655200. PubMed PMID: 16816390.
16. Kudryashova E, Struyk A, Mokhonova E, Cannon SC, Spencer MJ. The common missense mutation D489N in TRIM32 causing limb girdle muscular dystrophy 2H leads to loss of the mutated protein in knock-in mice resulting in a Trim32-null phenotype. Hum Mol Genet. 2011;20(20):3925-32. Epub 2011/07/22. doi: 10.1093/hmg/ddr311. PubMed PMID: 21775502; PubMed Central PMCID: PMCPMC3177646.
17. Ichimura T, Taoka M, Shoji I, Kato H, Sato T, Hatakeyama S, et al. 14-3-3 proteins sequester a pool of soluble TRIM32 ubiquitin ligase to repress autoubiquitylation and cytoplasmic body formation. J Cell Sci. 2013;126(Pt 9):2014-26. Epub 2013/02/28. doi: 10.1242/jcs.122069. PubMed PMID: 23444366.
18. Locke M, Tinsley CL, Benson MA, Blake DJ. TRIM32 is an E3 ubiquitin ligase for dysbindin. Hum Mol Genet. 2009;18(13):2344-58. Epub 2009/04/08. doi: 10.1093/hmg/ddp167. PubMed PMID: 19349376; PubMed Central PMCID: PMCPMC2694686.
19. Kano S, Miyajima N, Fukuda S, Hatakeyama S. Tripartite motif protein 32 facilitates cell growth and migration via degradation of Abl-interactor 2. Cancer Res. 2008;68(14):5572-80. Epub 2008/07/18. doi: 10.1158/0008-5472.CAN-07-6231. PubMed PMID: 18632609.
20. Ryu YS, Lee Y, Lee KW, Hwang CY, Maeng JS, Kim JH, et al. TRIM32 protein sensitizes cells to tumor necrosis factor (TNFalpha)-induced apoptosis via its RING domain-dependent E3 ligase activity against X-linked inhibitor of apoptosis (XIAP). J Biol Chem. 2011;286(29):25729-38. Epub 2011/06/02. doi: 10.1074/jbc.M111.241893. PubMed PMID: 21628460; PubMed Central PMCID: PMCPMC3138287.
21. Izumi H, Kaneko Y. Trim32 facilitates degradation of MYCN on spindle poles and induces asymmetric cell division in human neuroblastoma cells. Cancer Res. 2014;74(19):5620-30. Epub 2014/08/08. doi: 10.1158/0008-5472.CAN-14-0169. PubMed PMID: 25100564.
22. Zhao TT, Jin F, Li JG, Xu YY, Dong HT, Liu Q, et al. TRIM32 promotes proliferation and confers chemoresistance to breast cancer cells through activation of the NF-kappaB pathway. J Cancer. 2018;9(8):1349-56. Epub 2018/05/04. doi: 10.7150/jca.22390. PubMed PMID: 29721043; PubMed Central PMCID: PMCPMC5929078.
23. Ito M, Migita K, Matsumoto S, Wakatsuki K, Tanaka T, Kunishige T, et al. Overexpression of E3 ubiquitin ligase tripartite motif 32 correlates with a poor prognosis in patients with gastric cancer. Oncol Lett. 2017;13(5):3131-8. Epub 2017/05/20. doi: 10.3892/ol.2017.5806. PubMed PMID: 28521418; PubMed Central PMCID: PMCPMC5431222.
24. Cui X, Lin Z, Chen Y, Mao X, Ni W, Liu J, et al. Upregulated TRIM32 correlates with enhanced cell proliferation and poor prognosis in hepatocellular carcinoma. Mol Cell Biochem. 2016;421(1-2):127-37. Epub 2016/08/31. doi: 10.1007/s11010-016-2793-z. PubMed PMID: 27573002.
25. Yin H, Li Z, Chen J, Hu X. Expression and the potential functions of TRIM32 in lung cancer tumorigenesis. J Cell Biochem. 2019;120(4):5232-43. Epub 2018/11/01. doi: 10.1002/jcb.27798. PubMed PMID: 30378152.
26. Wang M, Luo W, Zhang Y, Yang R, Li X, Guo Y, et al. Trim32 suppresses cerebellar development and tumorigenesis by degrading Gli1/sonic hedgehog signaling. Cell Death Differ. 2020;27(4):1286-99. Epub 2019/09/19. doi: 10.1038/s41418-019-0415-5. PubMed PMID: 31527798; PubMed Central PMCID: PMCPMC7206143.
27. Yokota T, Mishra M, Akatsu H, Tani Y, Miyauchi T, Yamamoto T, et al. Brain site-specific gene expression analysis in Alzheimer's disease patients. Eur J Clin Invest. 2006;36(11):820-30. Epub 2006/10/13. doi: 10.1111/j.1365-2362.2006.01722.x. PubMed PMID: 17032350.
28. Fu B, Wang L, Ding H, Schwamborn JC, Li S, Dorf ME. TRIM32 Senses and Restricts Influenza A Virus by Ubiquitination of PB1 Polymerase. PLoS Pathog. 2015;11(6):e1004960. Epub 2015/06/10. doi: 10.1371/journal.ppat.1004960. PubMed PMID: 26057645; PubMed Central PMCID: PMCPMC4461266.
29. Narita T, Weinert BT, Choudhary C. Functions and mechanisms of non-histone protein acetylation. Nat Rev Mol Cell Biol. 2019;20(3):156-74. Epub 2018/11/24. doi: 10.1038/s41580-018-0081-3. PubMed PMID: 30467427.

30. Gronroos E, Hellman U, Heldin CH, Ericsson J. Control of Smad7 stability by competition between acetylation and ubiquitination. Mol Cell. 2002;10(3):483-93. Epub 2002/11/01. doi: 10.1016/s1097-2765(02)00639-1. PubMed PMID: 12408818.
31. Fusco C, Micale L, Augello B, Mandriani B, Pellico MT, De Nittis P, et al. HDAC6 mediates the acetylation of TRIM50. Cell Signal. 2014;26(2):363-9. Epub 2013/12/07. doi: 10.1016/j.cellsig.2013.11.036. PubMed PMID: 24308962.
32. Jiang W, Wang S, Xiao M, Lin Y, Zhou L, Lei Q, et al. Acetylation regulates gluconeogenesis by promoting PEPCK1 degradation via recruiting the UBR5 ubiquitin ligase. Mol Cell. 2011;43(1):33-44. Epub 2011/07/06. doi: 10.1016/j.molcel.2011.04.028. PubMed PMID: 21726808; PubMed Central PMCID: PMCPMC3962309.
33. Du Z, Song J, Wang Y, Zhao Y, Guda K, Yang S, et al. DNMT1 stability is regulated by proteins coordinating deubiquitination and acetylation-driven ubiquitination. Sci Signal. 2010;3(146):ra80. Epub 2010/11/04. doi: 10.1126/scisignal.2001462. PubMed PMID: 21045206; PubMed Central PMCID: PMCPMC3116231.
34. Lv L, Li D, Zhao D, Lin R, Chu Y, Zhang H, et al. Acetylation targets the M2 isoform of pyruvate kinase for degradation through chaperone-mediated autophagy and promotes tumor growth. Mol Cell. 2011;42(6):719-30. Epub 2011/06/28. doi: 10.1016/j.molcel.2011.04.025. PubMed PMID: 21700219; PubMed Central PMCID: PMCPMC4879880.
35. Zhao D, Zou SW, Liu Y, Zhou X, Mo Y, Wang P, et al. Lysine-5 acetylation negatively regulates lactate dehydrogenase A and is decreased in pancreatic cancer. Cancer Cell. 2013;23(4):464-76. Epub 2013/03/26. doi: 10.1016/j.ccr.2013.02.005. PubMed PMID: 23523103; PubMed Central PMCID: PMCPMC3885615.
36. Rogers S, Wells R, Rechsteiner M. Amino acid sequences common to rapidly degraded proteins: the PEST hypothesis. Science. 1986;234(4774):364-8. Epub 1986/10/17. doi: 10.1126/science.2876518. PubMed PMID: 2876518.
37. Xing H, Hong Y, Sarge KD. PEST sequences mediate heat shock factor 2 turnover by interacting with the Cul3 subunit of the Cul3-RING ubiquitin ligase. Cell Stress Chaperones. 2010;15(3):301-8. Epub 2009/09/22. doi: 10.1007/s12192-009-0144-7. PubMed PMID: 19768582; PubMed Central PMCID: PMCPMC2866995.
38. Meyer RD, Srinivasan S, Singh AJ, Mahoney JE, Gharahassanlou KR, Rahimi N. PEST motif serine and tyrosine phosphorylation controls vascular endothelial growth factor receptor 2 stability and downregulation. Mol Cell Biol. 2011;31(10):2010-25. Epub 2011/03/16. doi: 10.1128/MCB.01006-10. PubMed PMID: 21402774; PubMed Central PMCID: PMCPMC3133358.
39. Koliopoulos MG, Esposito D, Christodoulou E, Taylor IA, Rittinger K. Functional role of TRIM E3 ligase oligomerization and regulation of catalytic activity. EMBO J. 2016;35(11):1204-18. Epub 2016/05/08. doi: 10.15252/embj.201593741. PubMed PMID: 27154206; PubMed Central PMCID: PMCPMC4864278.
40. Plechanovova A, Jaffray EG, Tatham MH, Naismith JH, Hay RT. Structure of a RING E3 ligase and ubiquitin-loaded E2 primed for catalysis. Nature. 2012;489(7414):115-20. Epub 2012/07/31. doi: 10.1038/nature11376. PubMed PMID: 22842904; PubMed Central PMCID: PMCPMC3442243.
41. Streich FC, Jr., Ronchi VP, Connick JP, Haas AL. Tripartite motif ligases catalyze polyubiquitin chain formation through a cooperative allosteric mechanism. J Biol Chem. 2013;288(12):8209-21. Epub 2013/02/15. doi: 10.1074/jbc.M113.451567. PubMed PMID: 23408431; PubMed Central PMCID: PMCPMC3605639.
42. Kawaguchi Y, Taoka M, Takekiyo T, Uekita T, Shoji I, Hachiya N, et al. TRIM32-Cytoplasmic-Body Formation Is an ATP-Consuming Process Stimulated by HSP70 in Cells. PLoS One. 2017;12(1):e0169436. Epub 2017/01/05. doi: 10.1371/journal.pone.0169436. PubMed PMID: 28052117; PubMed Central PMCID: PMCPMC5215751.
43. Lamark T, Perander M, Outzen H, Kristiansen K, Overvatn A, Michaelsen E, et al. Interaction codes within the family of mammalian Phox and Bem1p domain-containing proteins. J Biol Chem. 2003;278(36):34568-81. Epub 2003/06/19. doi: 10.1074/jbc.M303221200. PubMed PMID: 12813044.

44. Bhujabal Z, Birgisdottir AB, Sjottem E, Brenne HB, Overvatn A, Habisov S, et al. FKBP8 recruits LC3A to mediate Parkin-independent mitophagy. EMBO Rep. 2017;18(6):947-61. Epub 2017/04/07. doi: 10.15252/embr.201643147. PubMed PMID: 28381481; PubMed Central PMCID: PMCPMC5452039.

Supporting Information

S1 Fig 1. Inhibition of proteolytic enzymes does not stabilize the TRIM32$^{K50R/K247R/K401R}$ mutant or the TRIM32$^{K247R/K401R}$ mutant. **A.** Western Blot analysis of HEK293 FlpIn TRIM32 KO cells transiently transfected with expression plasmids for TRIM32$^{K50R/K247R/K401R}$, EGFP-TRIM32^{WT}, or TRIM32$^{K247R/K401R}$. The bands representing EGFP-TRIM32 are indicated to the right. The arrow indicates the band representing cleaved/partial degraded EGFP-TRIM32. The cells are treated with lysosomal inhibitor BafA1 (0.5 μM), proteasomal inhibitor MG132 (5μM), and calpain inhibitor E64D (5 μg/ml) for 18 hours where indicated. Actin represents the loading control. **B.** Western Blot analysis of cell extracts from HEK293 FlpIn TRIM32 KO cells transiently co-transfected with expression plasmids for EGFP-TRIM32^{WT} and mCherry-USP2, or EGFP-TRIM32^{WT} and myc-HDAC6, or EGFP-TRIM32^{WT} and mCherry-USP2 and myc-HDAC6, as indicated above. The CBP/p300 inhibitor C646 was added where indicated. The intensities of the TRIM32 bands relative to the intensities of the actin bands are indicated by the numbers below the blot. Actin represents the loading control. EV: Co-transfection with empty vector.

Figure 1

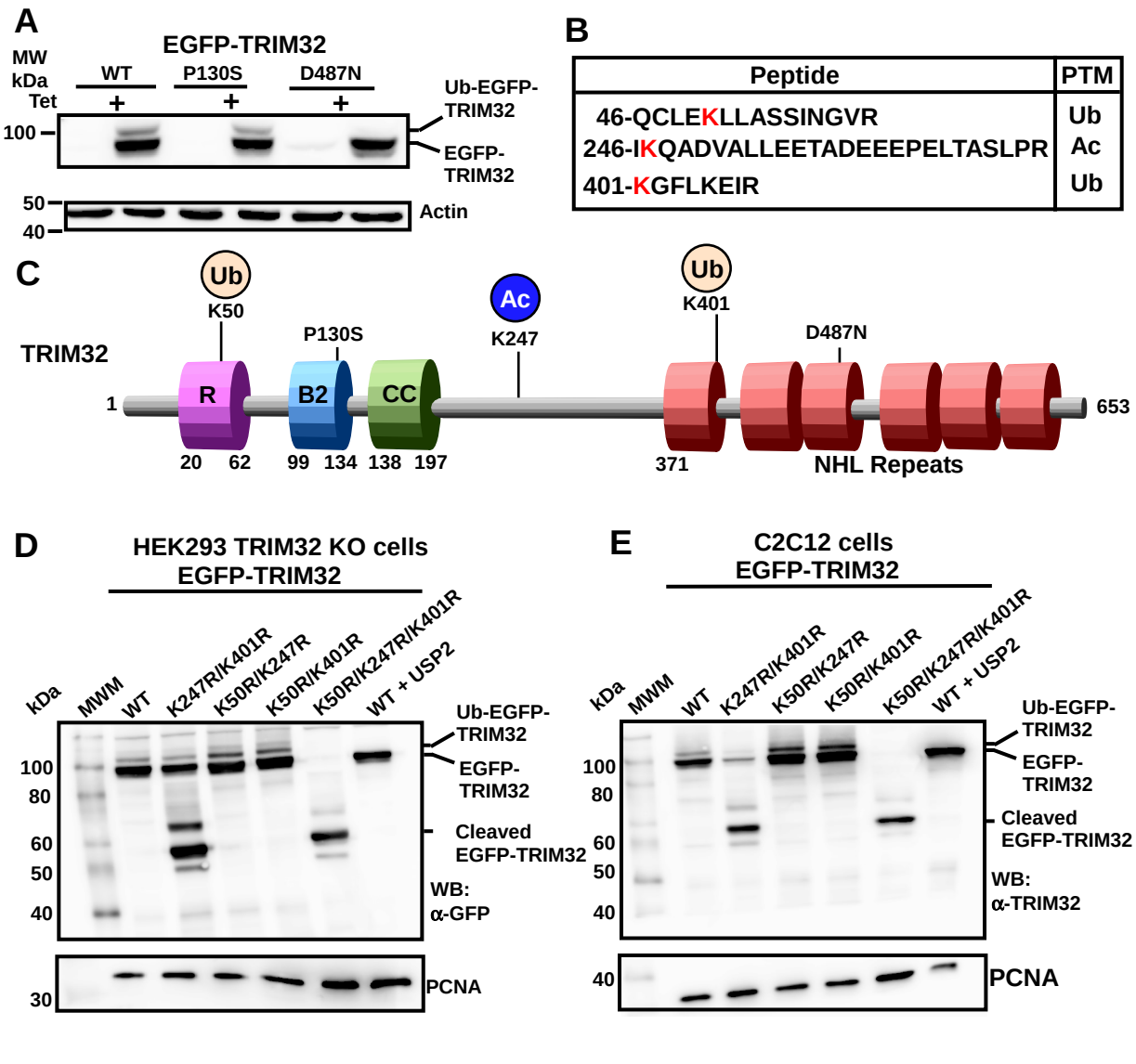
A
EGFP-TRIM32
MW
kDa
Tet
WT
P130S
D487N
+
+
+
100
Ub-EGFP-TRIM32
EGFP-TRIM32
50
40
Actin
B
Peptide
PTM
46-QCLEKLLASSINGVR
Ub
246-IKQADVALLEETADEEEPELTASLPR
Ac
401-KGFLKEIR
Ub
C
TRIM32
Ub
K50
P130S
Ac
K247
Ub
K401
D487N
R
B2
CC
1
653
20
62
99
134
138
197
371
NHL Repeats
D
HEK293 TRIM32 KO cells
EGFP-TRIM32
kDa
MWM
WT
K247R/K401R
K50R/K247R
K50R/K401R
K50R/K247R/K401R
WT + USP2
100
80
60
50
40
Ub-EGFP-TRIM32
EGFP-TRIM32
Cleaved EGFP-TRIM32
WB:
α-GFP
30
PCNA
E
C2C12 cells
EGFP-TRIM32
kDa
MWM
WT
K247R/K401R
K50R/K247R
K50R/K401R
K50R/K247R/K401R
WT + USP2
100
80
60
50
40
Ub-EGFP-TRIM32
EGFP-TRIM32
Cleaved EGFP-TRIM32
WB:
α-TRIM32
40
PCNA

Figure 2

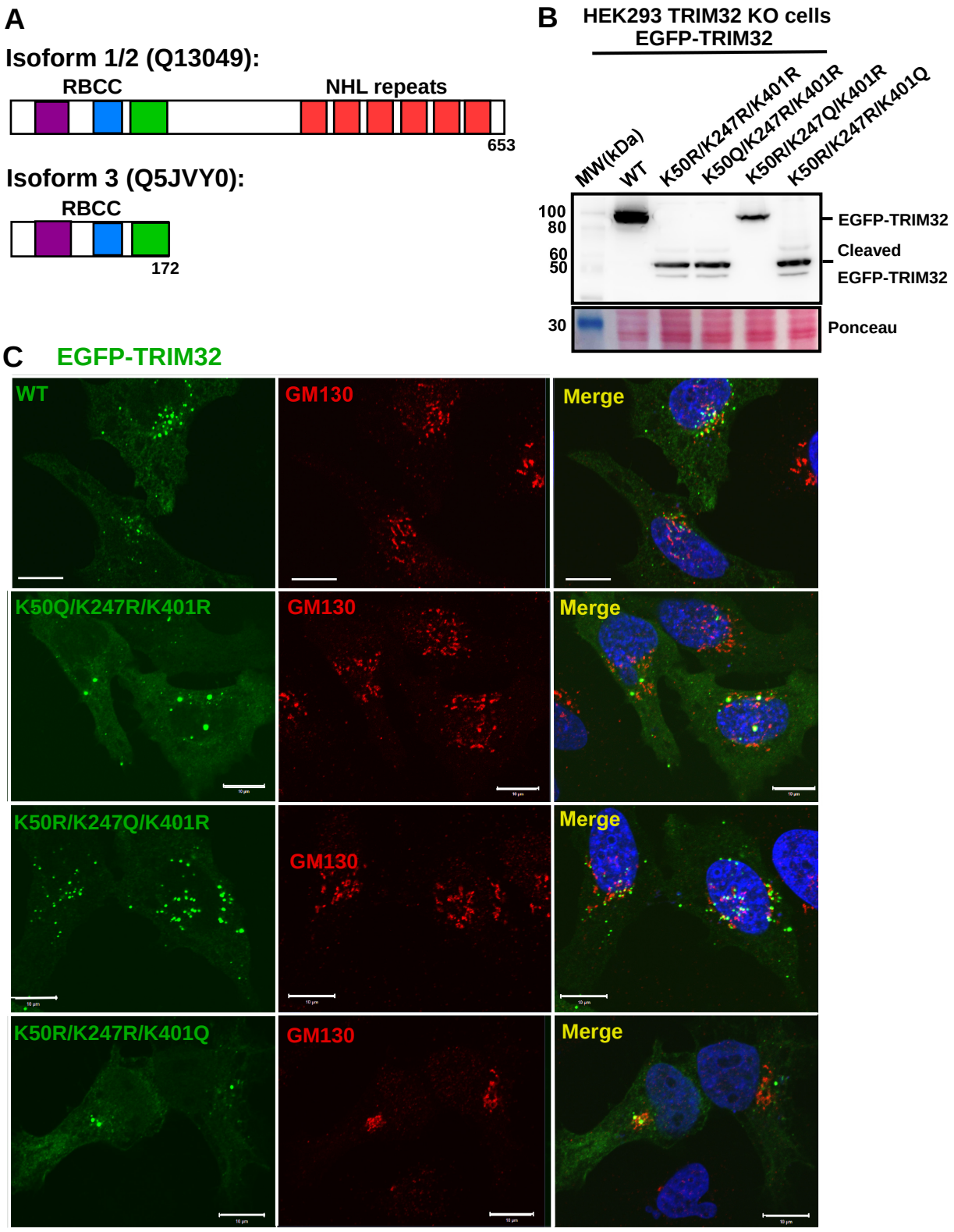
A
Isoform 1/2 (Q13049):
RBCC
NHL repeats
653
Isoform 3 (Q5JVY0):
RBCC
172
B
HEK293 TRIM32 KO cells
EGFP-TRIM32
MW(kDa)
WT
K50R/K247R/K401R
K50Q/K247R/K401R
K50R/K247Q/K401R
K50R/K247R/K401Q
100
80
60
50
30
EGFP-TRIM32
Cleaved
EGFP-TRIM32
Ponceau
C
EGFP-TRIM32
WT
GM130
Merge
K50Q/K247R/K401R
GM130
Merge
K50R/K247Q/K401R
GM130
Merge
K50R/K247R/K401Q
GM130
Merge

Figure 3

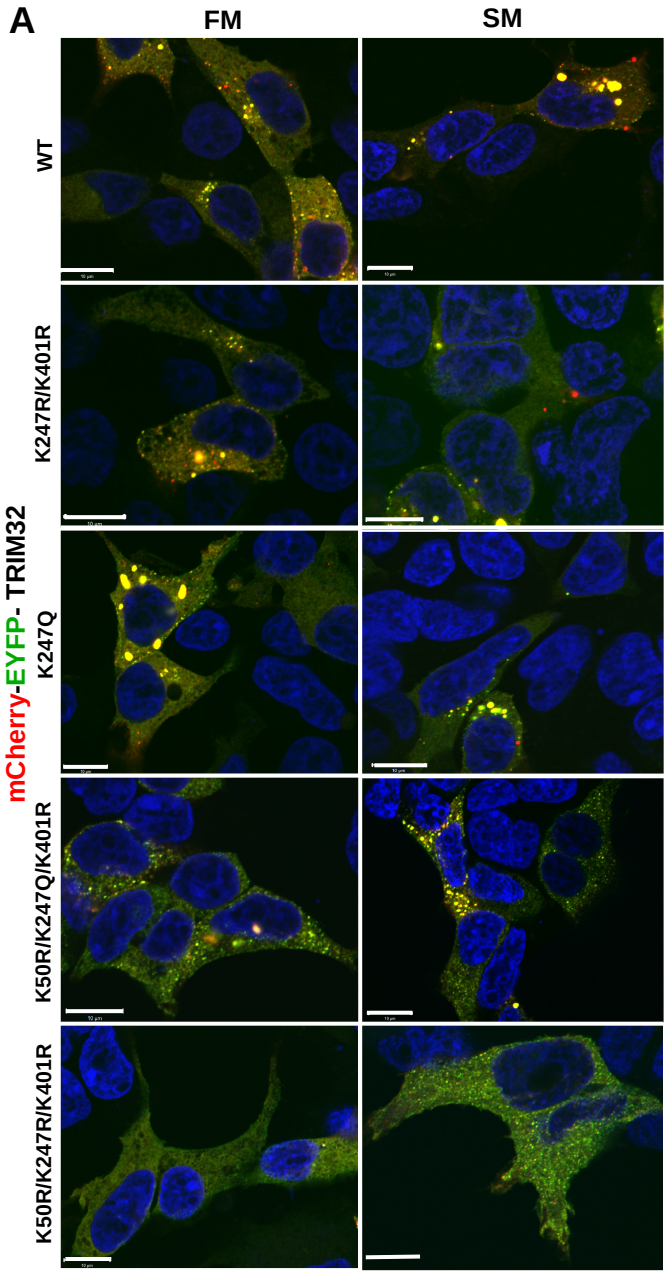
A
FM
SM
mCherry-EYFP- TRIM32
WT
K247R/K401R
K247Q
K50R/K247Q/K401R
K50R/K247R/K401R

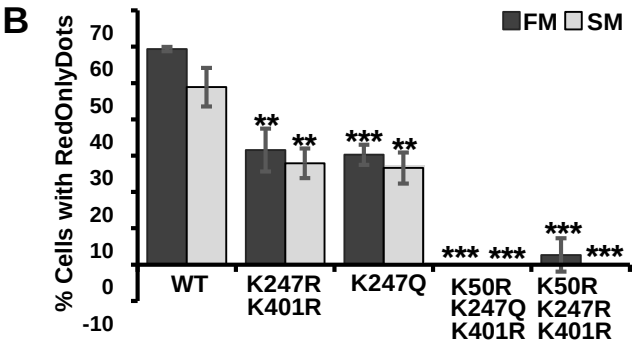
B
FM
SM
% Cells with RedOnlyDots
70
60
50
40
30
20
10
0
-10
**
**
***
**
***
***
***
WT
K247R K401R
K247Q
K50R K247Q K401R
K50R K247R K401R

Figure 4

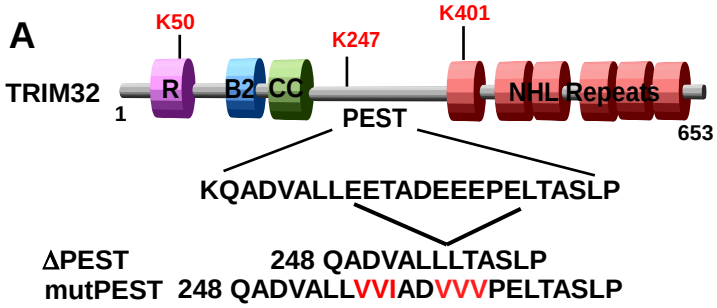
A
K50
K247
K401
TRIM32
R
B2
CC
NHL Repeats
1
PEST
653
KQADVALLEETADEEEPELTASLP
ΔPEST
248 QADVALLLTASLP
mutPEST
248 QADVALLVVIADVVVPELTASLP

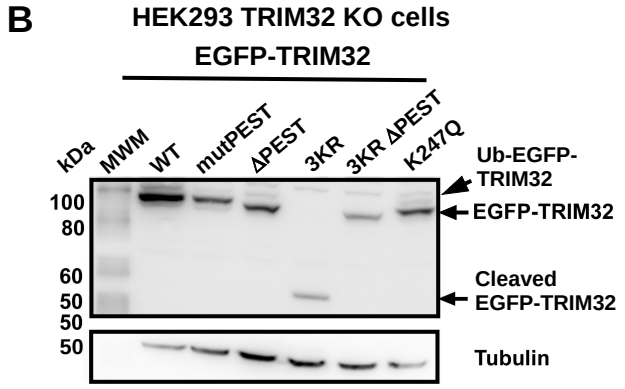
B
HEK293 TRIM32 KO cells
EGFP-TRIM32
kDa
MWM
WT
mutPEST
ΔPEST
3KR
3KR ΔPEST
K247Q
Ub-EGFP-TRIM32
EGFP-TRIM32
Cleaved EGFP-TRIM32
Tubulin
100
80
60
50
50
50

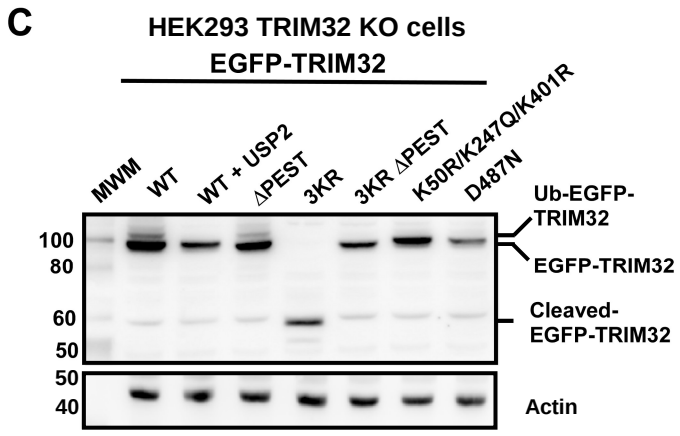
C
HEK293 TRIM32 KO cells
EGFP-TRIM32
MWM
WT
WT + USP2
ΔPEST
3KR
3KR ΔPEST
K50R/K247Q/K401R
D487N
Ub-EGFP-TRIM32
EGFP-TRIM32
Cleaved-EGFP-TRIM32
Actin
100
80
60
50
50
40

Supporting Information S1 Fig 1